STANFORD UNIVERSITY
ENGINEERING IN MEDICINE AND BIOLOGY

EFFECTS OF VISCOSITY AND EXTERNAL CONSTRAINTS ON WAVE TRANSMISSION IN BLOOD VESSELS

EVERETT JONES

I-DEE CHANG

MAX ANLIKER

BIOMECHANICS LABORATORY
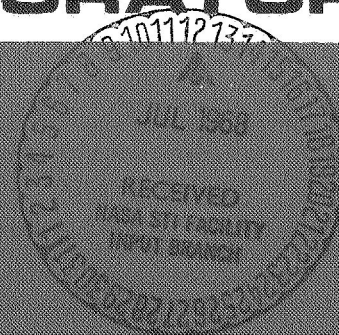
Department of Aeronautics and Astronautics
Stanford University
Stanford, California

EFFECTS OF VISCOSITY AND EXTERNAL CONSTRAINTS ON WAVE TRANSMISSION IN BLOOD VESSELS

by

Everett Jones, I-Dee Chang and Max Anliker

SUDAAR NO. 344
May 1968

SUMMARY

The propagation of sounds and pulse waves within the cardiovascular system is subject to strong dissipative mechanisms. To investigate the effects of viscosity on dissipation as well as dispersion of small pressure signals in arteries and veins, a parametric study has been carried out. A linearized analysis of pressure waves in a cylindrical membrane that contains a viscous fluid and whose wall is isotropically viscoelastic indicates that there are two families of axisymmetric waves--a family of slow waves and one of fast waves. The family of slow waves has been studied earlier by Womersley[10] and others, while the fast waves have only recently been examined theoretically to some extent by Atabek and Lew.[11] Experimental evidence of the existence of the two families was given by Van Citters[14] for rubber tubes and Anliker et al. [13] for arteries and veins under in-vivo conditions.

It is shown that the faster waves are more sensitive to variations in the elastic properties of the medium surrounding the blood vessels. At high Reynolds numbers the attenuation due to fluid viscosity over a fixed length is found to be substantially greater for the fast waves than for the slow waves. At very low Reynolds numbers the effects of attenuation are reversed--that is, the family of slow waves is much more strongly attenuated than the family of fast waves.

The radial displacements are generally much larger for the slow waves than for the fast waves, while conversely the axial displacements are much larger for the faster waves than for the slow waves. For the family of slow waves the axial wall displacements are larger than the radial displacements for sufficiently low frequencies. The presence of external constraints modifies these results.

For the slow waves the phase angle between pressure and radial wall displacement is virtually negligible for mild external constraints, while the phase angles between pressure and fluid velocity are at most 45°. The corresponding phase angles for the fast waves exhibit much larger variations with changes in the elastic properties of the surrounding medium.

The theoretical predictions for an elastic membrane are in good agreement with the limited quantitative experimental results of Van Citters[14] for a latex rubber tube. A comparison with the in-vivo data of Anliker et al.[13] shows clearly that the dissipation due to fluid viscosity alone can not account for the

observed attenuation and does not have the proper frequency dependence. For physiologically meaningful parameter values and high frequencies, the theoretical analysis confirms that the damping due to blood viscosity is much less than that due to the viscoelasticity of the wall material for both families of waves.

TABLE OF CONTENTS

v

LIST OF FIGURES

viii

NOMENCLATURE

a	– Displaced wall radius given by Equation (II-9)
A_1, A_2, A_3, A_4	– Parameters defined by Equations (III-17) to (III-20)
A_5, A_6, A_7	– Parameters defined by Equation (III-23)
A_{5R}	– Parameter defined by Equation (V-33) or (V-46)
A_8	– Parameter defined by Equation (III-24)
A_9	– Parameter defined by Equation (III-25)
$A_\pm$	– Parameter defined by Equation (V-19) or (V-37)
b	– Parameter defined by Equation (III-3)
B_1, B_2	– Parameters defined by Equation (III-27)
$B_\pm$	– Parameter defined by Equation (V-20) or (V-38)
C_o	– Moens-Korteweg wave speed defined by Equation (III-16)
C_{oR}	– Wave speed defined by Equation (V-18)
C_1	– Wave speed for first type of wave given in Equation (III-33)
C_2	– Wave speed for second type of wave given in Equation (III-33)
C_1' to C_6'	– Parameters defined by Equations (III-83) to (III-87)
$C_\pm$	– Parameter defined by Equation (V-21) or (V-39)
D_1 to D_4	– Arbitrary constants defined by Equation (III-26), (III-90), (III-92), (III-100) or (III-111)
E	– Modulus of elasticity for the tube wall
E_m	– Modulus of elasticity for the surrounding medium
E_R	– Modulus of elasticity defined by Equation (V-4)
E_v	– Modulus of elasticity defined by Equation (V-4)
f	– Frequency
$F(z)$	– An arbitrary function of z
$F_1(z)$	– An arbitrary function of z
F_2	– An arbitrary constant in Equation (III-6)

F_3	– An arbitrary constant in Equation (III-21)
G_{5R}, G_{51}, G_{52}	– Parameters defined by Equations (V-27) to (V-29) or (V-46) to (V-48)
h	– Wall thickness
$\vec{i}_m$	– Unit vector normal to wall
$\vec{i}_r$	– Unit vector in radial direction
$\vec{i}_z$	– Unit vector in axial direction
J_0	– Bessel function of first kind of order zero
J_1	– Bessel function of first kind of order one
K_1	– Proportionality factor for radial constraint
K_2	– Proportionality factor for axial constraint
K_1', K_2'	– Parameters defined by Equation (III-63)
K_3 to K_{10}	– Parameters defined by Equations (III-64) to (III-71)
$K_{31}, K_{32}, K_{1R}', K_{2R}', K_{3R}$	– Parameters defined by Equations (V-22) to (V-26)
K_{5R}, K_{51}, K_{52}	– Parameters defined by Equations (V-30) to (V-32) or (V-49) and (V-50)
K_{7R}, K_{8R}	– Parameters defined by Equations (III-68) and (III-69)
K_{9R}, K_{91}, K_{92}	– Parameters defined by Equations (V-34) to (V-36) or (V-49) and (V-51)
L	– Characteristic axial dimension
M_1 to M_8	– Mode shapes defined in Equations (III-40) to (III-47)
M_A	– Magnitude defined in Equation (III-96)
p	– Pressure
P	– Characteristic pressure
P_1 to P_4	– Arbitrary constants in Equation (III-31)
P_1' to P_4'	– Arbitrary constants in Equations (IV-35) to (IV-38)

P_{ij}	–	Parameters defined in Equations (IV-39) to (IV-45) or (IV-54) to (IV-61)
Q	–	Fluid mass flow rate
r	–	Radial coordinate
R_o	–	Mean radius of the tube
R_e	–	Reynolds number defined by Equation (III-48)
$R(r)$	–	Arbitrary function of radius
$R_{3R}, R_{3Z}, R_{4R}, R_{7R}, R_{8R}$	–	Defined by Equations (V-40) to (V-44)
S	–	Defined by Equation (III-3)
S_1, S_2	–	Functions defined by Equation (III-30)
S_1', S_2'	–	Functions defined by Equation (IV-28)
t	–	Time
T	–	Characteristic time
T_θ, T_z	–	Membrane forces per unit length
u	–	Radial velocity component
U	–	Characteristic radial velocity
$\vec{V}_f$	–	Velocity vector for the fluid
$\vec{V}_w$	–	Velocity vector for the wall
w	–	Axial velocity component
W	–	Characteristic axial velocity
$\mathcal{W}$	–	Function defined in Equation (V-53)
X, Y	–	Functions defined by Equation (V-53)
Y_o	–	Bessel function of second kind of order zero
Y_1	–	Bessel function of second kind of order one
z	–	Axial coordinate
$Z(z), Z_1(z)$	–	Arbitrary functions of z

α – Parameter defined by Equation (III-16)

β_1, β_2 – Parameters defined by Equation (III-15)

β_{2R} – Parameter defined by Equation (V-18)

β_3 – Parameter defined by Equation (III-16)

β_{3R} – Parameter defined by Equation (V-18)

Γ_1 – Radial constraint parameter defined by Equation (III-15)

Γ_2 – Axial constraint parameter defined by Equation (III-15)

δ_1, δ_2 – Dissipation coefficients defined by Equation (III-33)

ϕ_A – Phase angle defined by Equation (III-96)

ε_θ – Circumferential strain

ε_z – Axial strain

ς – Axial wall displacements

ς_R – Characteristic axial wall displacements

θ – Circumferential angle

κ_1, κ_2 – Constraint parameters defined in Equation (IV-4)

λ_1 – Wave length for first type of wave

λ_2 – Wave length for second type of wave

μ – Coefficient of viscosity of fluid

ν – Kinematic viscosity of fluid

ξ – Radial wall displacement

ξ_R – Characteristic radial wall displacement

π_1 – Defined by Equations (IV-23) or (IV-49)

π_2 – Defined by Equation (IV-23)

π_3 – Defined by Equations (IV-30) or (IV-49)

$\underline{\underline{\pi}}$ – Stress dyadic in Equation (II-28)

ρ – Fluid density

ρ_w – Wall density

σ – Poisson's ratio for the elastic wall

σ_R, σ_V – Defined in Equation (V-4)

$\tau_{rr}, \tau_{rz}, \tau_{\theta\theta}, \tau_{zz}$ – Stress components

ϕ_1 to ϕ_8 – The phase angles defined by Equations (III-40) to (III-47)

ϕ_B – Angle defined by Bergel and given in Equation (V-58)

ω – Circular frequency

$(\ )_R$ – System quantity for only radial waves

$(\ )_S$ – Steady state quantity

$(\ )_A$ – System quantity for only axial waves

$\underline{(\ )}$ – Nondimensional value of a system quantity

$(\ )'$ – Unsteady component of a system quantity

I. INTRODUCTION

A. Physiological Considerations

The circulatory system performs the vital logistic function of transporting blood throughout the body. Investigation and research of the circulatory system is basically motivated by humanitarian goals but such research has certainly been enhanced and stimulated by the manned space program.

The circulatory system is a complex network of distensible, tapered, and branching tubes with the heart as a pump. Blood pressure and pulse rate are just two of the basic parameters which indicate the operational capabilities of such a mechanical system and which have become basic parameters in clinical medicine.

A quantitative analysis of the dynamics of the circulatory system is considerably more formidable than similar investigations of most engineering systems. The blood itself is a non-Newtonian fluid that exhibits the characteristics of solutions and colloidal and particle suspensions. The apparent viscosity of blood varies with hematocrit and strain rate. The hematocrit is a measure of the relative volume of the blood in particle form. Controlled experiments[1] have shown that the apparent viscosity increases with hematocrit, decreases with strain rate and has a viscosity coefficient that ranges from 1 centipoise to 10 poise. However, McDonald[2] reports that blood in the larger arteries and veins behaves like a Newtonian fluid and normally has a viscosity coefficient of approximately 4 to 7 centipoise. No marked manifestations of non-Newtonian behavior are observed in large blood vessels. Even though blood exhibits compressibility, it has negligible effects on the transmission properties of the usual types of waves that may occur in blood vessels[3].

The experiments of Bergel[4] and those of McDonald and Gessner[5] show that the blood vessel walls are viscoelastic with material properties that depend more strongly on strain than strain rate. Also, blood vessels are essentially incompressible and, therefore, have a Poisson's ratio of approximately 0.5[2]. Experimental data[2] further indicates that the modulus of elasticity for the artery varies from about 10^6 dynes/cm^2 to 10^8 dynes/cm^2. The viscoelastic modulus can be of the order of 25% of the elastic modulus[4,5]. Geometrically, the blood vessels are tapered tubes with the ratio of wall thickness to radius ranging from about 0.05 to 0.30 for arteries and about 0.01 to 0.05 for veins.

The blood vessels are imbedded in tissues, muscle or bone and are usually constrained by these surroundings. The effects of this surrounding medium upon the wave transmission characteristics of blood vessels have not yet been studied quantitatively and qualitative data are fragmentary.

1

B. Previous Theoretical Investigations

Numerous theoretical studies of the dynamic behavior of blood vessels have been reported in the literature. Comprehensive reviews of such investigations have been made by McDonald[2], Rudinger[6], Skalak[7] and Fung[8]. The complexities of the physical and geometric features of blood vessels necessitate an approximate approach in any analysis of their motion. By introducing simplifying yet realistic assumptions and a mathematical model for the mechanical behavior of the vessels, it is possible to arrive at a tractable analytical formulation of dynamic problems such as the prediction of the dispersion and attenuation of waves.

The theoretical analyses of dynamic problems of blood vessels can be separated into two major groups on the basis of the relative rigor with which the solid or fluid mechanics aspects have been treated. Recent contributions emphasizing a realistic formulation of the fluid-dynamic aspects were made by Morgan and Kiely[9], Womersley[10] and Atabek and Lew[11]. The work presented here is an extension of these efforts and is based on a similar mathematical model.

The analytical model introduced by Morgan and Kiely[9] for studying the motion of the vessel and the blood contained in it treats the vessel wall as a linear elastic, homogeneous, isotropic, cylindrical membrane with circular cross section and assumes that the blood behaves like an incompressible, Newtonian fluid in laminar motion. With this model the vessel wall does not resist local bending and therefore its motion should be restricted to one involving small changes in the radii of curvature. They also neglected the constraints of the surrounding medium, and further simplified the boundary value problem by linearization and order of magnitude estimates. Assuming a solution form which requires a wave travelling along the tube, they obtained a quadratic equation for wave speed and attenuation. This equation was solved for the limiting cases of very low frequencies and for very low or very high fluid viscosity. One root of the quadratic equation produced an infinite wave speed in the inviscid limit and was therefore rejected as physically unrealistic. Furthermore, Morgan and Kiely demonstrated that the dynamic behavior of viscoelastic materials, which are dominantly elastic and subjected to a wave motion, can be obtained from the corresponding elastic analysis by interpreting the elastic modulus and Poisson's ratio as complex quantities. They thus demonstrated the applicability of the correspondence principle for linear viscoelastic materials to their wave propagation problem.

2

Womersley[10] also used this model but added a distributed, axial, elastic constraint acting on the outside surface of the vessel to approximate the effects of the surrounding medium. He also assumed a travelling wave solution and obtained a quadratic equation for the wave speed and attenuation. The solution corresponding to the root retained by Morgan and Kiely[9] was investigated numerically without restriction to limiting cases.

The analyses by Morgan and Kiely[9] and by Womersley[10] have become key references. In both studies the wave reflections were neglected and, since one of the roots of the quadratic equation was rejected, only one type of wave was considered. Therefore, only one boundary condition at one axial location is required to determine the solution. However, this solution is not sufficiently general to accommodate additional constraints such as those enforced by branches and bifurcations or by the application of instruments such as electromagnetic flowmeters.

A further inadequacy of the Womersley solution[10] manifests itself whenever distributed radial constraints are present. Womersley's results[10] predict at most a 15% change in the speed of the wave studied for arbitrary variations in the axial constraint and for all Reynolds numbers. By contrast, the addition of an infinite radial constraint besides an infinite axial constraint produces a rigid tube incapable of transmitting waves when filled with an incompressible fluid. It appears, therefore, that radial constraint may play an important role and should be taken into consideration.

Atabek and Lew[11] investigated the wave propagation characteristics of two types of waves corresponding to each of the two roots of the quadratic equation using the basic model above. Aside from considering two types of waves, they also examined the effects of initial stresses upon the transmission characteristics of the waves. However, they disregarded the presence of external constraints.

In a recent parametric study of waves in blood vessels, Maxwell and Anliker[3] treated the blood as an inviscid, compressible fluid and assumed the vessel wall to behave like a cylindrical shell with viscoelastic wall properties. In contrast to a membrane model, the shell model exhibits resistance to local bending in the vessel wall and thus allows the study of a wider class of motions by relaxing the restriction to very small changes in the radii of curvature. The effects of initial stresses are taken into account but external constraints are disregarded. Three wave types were predicted. For both axially symmetric and non-axially symmetric mode shapes, the waves were characterized by the dominant displacement component that an

arbitrary point of the middle surface exhibits at higher frequencies. Accordingly, these waves can be referred to as radial, circumferential, and axial waves. The characteristics of the axially symmetric radial waves are in agreement with Womersley's results[10] for very small fluid viscosity, and the basic properties of axially symmetric radial and axial waves are in partial agreement with the results of Atabek and Lew[11] for the inviscid limit.

In contrast to earlier theoretical investigations, Maxwell and Anliker[3] also presented a detailed parametric study of the mode shapes associated with each wave type in addition to the corresponding dispersion and attenuation. The mode shapes are useful features that facilitate the identification of different waves in experiments.

C. Experimental Studies of Radial and Axial Waves

Most of the experimental data on dispersion and attenuation of radial waves (pressure waves) given in the literature has been derived from a harmonic analysis of the natural pulse wave generated by the heart. These data may have to be reassessed since there is increasing evidence that the transmission of the natural pulse is affected by nonlinear phenomena[12,13]. By utilizing artifically induced pressure signals in the form of finite trains of sine waves[13], it was shown that the aortae of anesthetized dogs are only mildly dispersive for frequencies between 40 and 200 cps. Also, in this frequency range radial waves exhibit strong attenuation that is primarily due to dissipative mechanisms in the vessel wall. Moreover, the amplitude of the radial waves portrays the same experimental decay pattern with distance measured in wave lengths.

Experimental evidence of the presence of axial and radial waves in fluid filled, thin walled latex rubber tubes simulating blood vessels was given by Van Citters[14]. Both types of waves were simultaneously generated by a step variation in pressure at one end of the tube. The axial wave had much larger axial wall displacements and a higher speed than the radial wave. Moreover, the axial wave could easily be attenuated by manually gripping the tube. The observations made by Van Citters have since been partially corroborated in References 3 and 11.

The literature to date does not report the natural occurrence of axial waves in arteries and veins. Systematic experimental data on the dispersion and attenuation of induced axial waves have only now become available[15]. A comparison of these results with theoretical predictions will be given in the body of the report.

D. Intent and Scope of this Analysis

The main objective of the present theoretical analysis is a parametric study of the effects of blood viscosity, distributed external constraints, and visco-elastic properties of the vessel on the transmission characterisitcs of radial and axial waves. To this end, a mathematical model is introduced, which is similar to those in References 9 to 11. It differs from them by the inclusion of radial constraints and by considering the vessel wall to be viscoelastic.

The arrangement of this report reflects the actual sequence of the studies conducted. In Section II, the boundary value problem is derived and linearized with emphasis upon the main conditions of linearization. Section III is devoted to the general solution and specific results corresponding to limiting cases for infinite radial and/or axial constraint and for large or small Reynolds number. The results of the parametric analysis for the transmission characteristics, including velocity profiles and numerical examples are described in Section IV. A comparison of experimental results with theoretical predictions is given in Section V. Finally, the conclusions are presented in Section VI.

II. THE LINEARIZED BOUNDARY VALUE PROBLEM

A. Statement of Boundary Value Problem

The basic problem of interest is the motion of a blood vessel and the blood it contains when this system is subjected to an oscillatory perturbation. However, only the motion of a model of this system is actually analyzed. A steady-state configuration (Figure 1) consisting of a long, cylindrical tube containing a steaming Newtonian fluid is perturbed such that axially symmetric motion with no circumferential velocity is obtained. The perturbation is assumed to be sufficiently small to justify linearization. Therefore, all dependent variables can be expressed in the form

$$( ) = ( )_s + ( )' \tag{II-1}$$

where

$( ) = $ the value of a variable in the perturbed state

$( )_s = $ the value of a variable in the steady state

$( )' = $ the perturbation to the variable.

Since the desired boundary value problem is linear, harmonic solutions for a given frequency can be obtained and more general motions can be studied using Fourier analysis.

The wall material is assumed to be isotropic, homogeneous and elastic in the initial part of the analysis. Furthermore, the tube is assumed to have a wall thickness to radius ratio

$$\frac{h}{R_\bullet} \ll 1 \tag{II-2}$$

and to behave like a membrane with constant strains and stresses across the wall. Since the problem is axially symmetric, the wall displacements, stresses and strains are functions only of axial distance and time. To render the membrane assumption realistic, the displacements will be limited to those producing very small changes in the radii of curvature. This is achieved with the restriction

$$\frac{L}{R_o} \gg 1 \tag{II-3}$$

where L is any characteristic axial dimension.

B. Equations of Motion and Kinematic Boundary Conditions for the Fluid

In cylindrical coordinates the equations for conservation of mass and momentum for an incompressible Newtonian fluid are

$$\frac{\partial(ru)}{\partial r} + \frac{\partial(rw)}{\partial z} = 0 \qquad \text{(II-4)}$$

$$\rho\left(\frac{\partial u}{\partial t} + u\frac{\partial u}{\partial r} + w\frac{\partial u}{\partial z}\right) = -\frac{\partial p}{\partial r} + \mu\left(\frac{\partial^2 u}{\partial r^2} + \frac{1}{r}\frac{\partial u}{\partial r} - \frac{u}{r^2} + \frac{\partial^2 u}{\partial z^2}\right) \qquad \text{(II-5)}$$

$$\rho\left(\frac{\partial w}{\partial t} + u\frac{\partial w}{\partial r} + w\frac{\partial w}{\partial z}\right) = -\frac{\partial p}{\partial z} + \mu\left(\frac{\partial^2 w}{\partial r^2} + \frac{1}{r}\frac{\partial w}{\partial r} + \frac{\partial^2 w}{\partial z^2}\right) \qquad \text{(II-6)}$$

where the radial and axial velocity components (u and w) and the pressure (p)
are the dependent variables.

The kinematic boundary condition for a viscous fluid postulates no relative
motion between the fluid and its boundaries (the no-slip boundary condition).
Therefore,

$$u(a, z, t) = \frac{D\xi(z,t)}{Dt} = \frac{\partial\xi(z,t)}{\partial t} + w(a,z,t)\frac{\partial\xi(z,t)}{\partial z} \qquad \text{(II-7)}$$

$$w(a,z,t) = \frac{D\varsigma(z,t)}{Dt} = \frac{\partial\varsigma(z,t)}{\partial t} + w(a,z,t)\frac{\partial\varsigma(z,t)}{\partial z} \qquad \text{(II-8)}$$

where ξ and ς are respectively the radial and axial displacements of the middle
surface of the membrane and

$$a = R_0 + \xi(z,t) \qquad \text{(II-9)}$$

is the radial coordinate for the membrane displaced from its steady state equil-
ibrium position (r = R_0).

The linearization of these equations and the conditions for the applicability of
the resulting solutions can be simplified by means of an order of magnitude
analysis. The equations (II-4) to (II-8) are expressed in a nondimensional form
such that all variables and derivatives are of order one. To this end the mean
tube radius, R_0, and an average axial velocity, W, are chosen as nondimensional-
izing parameters for r and w, respectively. Nondimensionalizing parameters
for the other variables (T, L, U, P, ξ_R, and ς_R) are obtained on the basis of
physical arguments and the conservation equations. Therefore, the underlined,
nondimensional variables

$$\underline{r} = \frac{r}{R_0} \quad , \quad \underline{z} = \frac{z}{L} , \quad \underline{t} = \frac{t}{T} \quad , \quad \underline{u} = \frac{u}{U} \qquad \text{(II-10)}$$

7

$$\underline{w} = \frac{w}{W}, \quad \underline{p} = \frac{p}{P}, \quad \underline{\xi} = \frac{\xi}{\xi_R}, \quad \underline{\zeta} = \frac{\zeta}{\zeta_R} \tag{II-11}$$

will be assumed to be of order one.

Substitution of (II-10) and (II-11) into (II-4) yields

$$\frac{UL}{R_o W} \frac{1}{\underline{r}} \frac{\partial(\underline{r}\,\underline{u})}{\partial \underline{r}} + \frac{\partial \underline{w}}{\partial \underline{z}} = 0$$

The steady state solution satisfies this equation identically. In the unsteady case the equation requires that both terms be of equal order and, therefore,

$$U = \frac{R_o}{L} W \tag{II-12}$$

$$\frac{1}{\underline{r}} \frac{\partial \underline{r}\,\underline{u}}{\partial \underline{r}} + \frac{\partial \underline{w}}{\partial \underline{z}} = 0 \tag{II-13}$$

Substitution of (II-10), (II-11) and (II-12) into (II-5) and (II-6) yields

$$\frac{\partial \underline{u}}{\partial \underline{t}} + \frac{WT}{L}\left(\underline{u}\frac{\partial \underline{u}}{\partial \underline{r}} + \underline{w}\frac{\partial \underline{u}}{\partial \underline{z}}\right) = -\left(\frac{L}{R_o}\right)^2\left(\frac{P}{\rho W^2}\right)\left(\frac{WT}{L}\right)\frac{\partial \underline{p}}{\partial \underline{r}} +$$
$$+ \frac{\upsilon T}{R_o^2}\left[\frac{\partial^2 \underline{u}}{\partial \underline{r}^2} + \frac{1}{\underline{r}}\frac{\partial \underline{u}}{\partial \underline{r}} - \frac{\underline{u}}{\underline{r}^2} + \left(\frac{R_o}{L}\right)^2\frac{\partial^2 \underline{u}}{\partial \underline{z}^2}\right] \tag{II-14}$$

and

$$\frac{\partial \underline{w}}{\partial \underline{t}} + \frac{WT}{L}\left(\underline{u}\frac{\partial \underline{w}}{\partial \underline{r}} + \underline{w}\frac{\partial \underline{w}}{\partial \underline{z}}\right) = -\left(\frac{P}{\rho W^2}\right)\left(\frac{WT}{L}\right)\frac{\partial \underline{p}}{\partial \underline{z}} +$$
$$+ \frac{\upsilon T}{R_o^2}\left[\frac{\partial^2 \underline{w}}{\partial \underline{r}^2} + \frac{1}{\underline{r}}\frac{\partial \underline{w}}{\partial \underline{r}} + \left(\frac{R_o}{L}\right)^2\frac{\partial^2 \underline{w}}{\partial \underline{z}^2}\right] \tag{II-15}$$

The linearization of (II-14) and (II-15) requires the assumption

$$\frac{WT}{L} \ll 1 \tag{II-16}$$

Application of (II-3) and (II-16) in (II-14) and (II-15) and retention of the lowest order terms for the inertial and viscous forces leads to

$$\frac{\partial \underline{u}}{\partial \underline{t}} = -\left(\frac{L}{R_o}\right)^2\left(\frac{P}{\rho W^2}\right)\left(\frac{WT}{L}\right)\frac{\partial \underline{p}}{\partial \underline{r}} + \frac{\upsilon T}{R_o^2}\left(\frac{\partial^2 \underline{u}}{\partial \underline{r}^2} + \frac{1}{\underline{r}}\frac{\partial \underline{u}}{\partial \underline{r}} - \frac{\underline{u}}{\underline{r}^2}\right) \tag{II-17}$$

8

$$\frac{\partial \underline{w}}{\partial \underline{t}} = -\left(\frac{P}{\rho W^2}\right)\left(\frac{WT}{L}\right)\frac{\partial \underline{P}}{\partial \underline{z}} + \frac{\nu T}{R_0^2}\left(\frac{\partial^2 \underline{w}}{\partial \underline{r}^2} + \frac{1}{\underline{r}}\frac{\partial \underline{w}}{\partial \underline{r}}\right) \qquad \text{(II-18)}$$

In each of these two equations, the inertial and viscous terms have the same ratio. However, the ratio of the pressure gradient term to either the inertia or viscous term is larger in (II-17) than in (II-18). Since the axial pressure gradient induces the flow, the pressure gradient term in (II-18) must be the same order as either the inertia or viscous terms. Therefore, equation (II-17) requires that the radial pressure gradients must vanish and thus, (II-17) and (II-18) can be reduced to

$$\frac{\partial \underline{w}}{\partial \underline{t}} = -\left(\frac{P}{\rho W^2}\right)\left(\frac{WT}{L}\right)\frac{\partial \underline{P}}{\partial \underline{z}} + \frac{\nu T}{R_0^2}\left(\frac{\partial^2 \underline{w}}{\partial \underline{r}^2} + \frac{1}{\underline{r}}\frac{\partial \underline{w}}{\partial \underline{r}}\right) \qquad \text{(II-19)}$$

$$0 = \frac{\partial \underline{P}}{\partial \underline{r}} \qquad \text{(II-20)}$$

In dimensional form equations (II-13), (II-19) and (II-20) can be written as

$$\frac{1}{r}\frac{\partial (r u)}{\partial r} + \frac{\partial w}{\partial z} = 0 \qquad \text{(II-21)}$$

$$\frac{\partial w}{\partial t} = -\frac{1}{\rho}\frac{\partial P}{\partial z} + \frac{\nu}{r}\frac{\partial}{\partial r}\left(r \frac{\partial w}{\partial r}\right) \qquad \text{(II-22)}$$

$$0 = \frac{\partial P}{\partial r} \qquad \text{(II-23)}$$

and constitute the lowest order system defining the motion of the fluid. It is of interest to note that the solution to the well known Poiseuille flow problem

$$u_s(r, z) = 0 \quad , \quad \frac{d P_s(z)}{dz} = \text{constant} \qquad \text{(II-24)}$$

and

$$w_s(r, z) = -\frac{1}{4\mu}\frac{dP_s(z)}{dz}\left(R_0^2 - r^2\right) \qquad \text{(II-25)}$$

also is the steady state solution of the lowest order system (II-21) to (II-23).

The assumption of small displacements of the membrane about the steady state position requires

9

$$\frac{\xi_R}{R_o} << 1 \qquad \text{and} \qquad \frac{\zeta_R}{R_o} << 1 \qquad \text{(II-26)}$$

With (II-26) the fluid velocity components at each point of the membrane wall can then be expanded about the corresponding equilibrium position of the point. The substitution of these expansions into the boundary conditions (II-7) and (II-8) yields after nondimensionalization the relations

$$\underline{u}(1,\underline{z},\underline{t}) + \frac{\xi_R}{R_o}\frac{\partial\underline{u}}{\partial\underline{r}}(1,\underline{z},\underline{t})\,\underline{\xi}(\underline{z},\underline{t}) +\cdots = \frac{\xi_R}{UT}\left\{\frac{\partial\underline{\xi}}{\partial\underline{t}}(\underline{z},\underline{t}) \right.$$

$$\left. + \frac{WT}{L}\left[\underline{w}(1,\underline{z},\underline{t}) + \frac{\xi_R}{R_o}\frac{\partial\underline{w}}{\partial\underline{r}}(1,\underline{z},\underline{t})\,\underline{\xi}(\underline{z},\underline{t}) +\cdots\right]\frac{\partial\underline{\xi}}{\partial\underline{z}}(\underline{z},\underline{t})\right\}$$

and

$$\underline{w}(1,\underline{z},\underline{t}) + \frac{\xi_R}{R_o}\frac{\partial\underline{w}}{\partial\underline{r}}(1,\underline{z},\underline{t})\,\underline{\xi}(\underline{z},\underline{t}) +\cdots = \frac{\zeta_R}{WT}\left\{\frac{\partial\underline{\zeta}}{\partial\underline{t}}(\underline{z},\underline{t}) + \right.$$

$$\left. + \frac{WT}{L}\left[\underline{w}(1,\underline{z},\underline{t}) + \frac{\xi_R}{R_o}\frac{\partial\underline{w}}{\partial\underline{r}}(1,\underline{z},\underline{t})\,\underline{\xi}(\underline{z},\underline{t}) +\cdots\right]\frac{\partial\underline{\zeta}}{\partial\underline{z}}(\underline{z},\underline{t})\right\}$$

Application of the assumptions (II-3) and (II-16) to these equations produces

$$\underline{u}(1,\underline{z},\underline{t}) = \frac{\xi_R}{UT}\frac{\partial\underline{\xi}}{\partial\underline{t}}(\underline{z},\underline{t})$$

and

$$\underline{w}(1,\underline{z},\underline{t}) = \frac{\zeta_R}{WT}\frac{\partial\underline{\zeta}}{\partial\underline{t}}(\underline{z},\underline{t})$$

as the nondimensional lowest order equations for the no-slip boundary condition. The corresponding lowest order equations in dimensional form are

$$u(R_o,z,t) = \frac{\partial\xi}{\partial t}(z,t) \quad , \quad w(R_o,z,t) = \frac{\partial\zeta}{\partial t}(z,t) \qquad \text{(II-27)}$$

C.   The Equations of Motion for the Wall

The equations of motion for the wall are determined by the conditions of dynamic equilibrium for a wall element extending from z to $z+dz$ and Θ to $\Theta+d\Theta$, as shown in Figure 1. The element is subjected to constraint forces

10

acting on the outer surface, viscous shearing stresses acting on the inner surface, inertia forces, hoop tension, and axial tension.

The stress dyadic for the interior fluid is

$$\underline{\Pi} = \tau_{rr}\,\vec{\imath}_r\vec{\imath}_r + \tau_{rz}\,\vec{\imath}_r\vec{\imath}_z + \tau_{\theta\theta}\,\vec{\imath}_\theta\vec{\imath}_\theta + \tau_{rz}\,\vec{\imath}_z\vec{\imath}_r + \tau_{zz}\,\vec{\imath}_z\vec{\imath}_z \qquad \text{(II-28)}$$

where

$$\tau_{rr} = -p + 2\mu\frac{\partial u}{\partial r} \qquad , \qquad \tau_{\theta\theta} = -p + 2\mu\frac{u}{r} \qquad \text{(II-29)}$$

$$\tau_{zz} = -p + 2\mu\frac{\partial w}{\partial z} \qquad , \qquad \tau_{rz} = \mu\left(\frac{\partial u}{\partial z} + \frac{\partial w}{\partial r}\right) \qquad \text{(II-30)}$$

Substitution of (II-9) and (II-10 into (II-29) and (II-30) yields

$$\tau_{rr} = P\left[-p + 2\frac{\rho W^2}{P}\frac{\upsilon}{WL}\frac{\partial u}{\partial r}\right] \quad , \quad \tau_{\theta\theta} = P\left[-p + 2\frac{\rho W^2}{P}\frac{\upsilon}{WL}\frac{u}{r}\right]$$

$$\tau_{zz} = P\left[-p + 2\frac{\rho W^2}{P}\frac{\upsilon}{WL}\frac{\partial w}{\partial z}\right] , \quad \tau_{rz} = \mu\frac{W}{R_o}\left[\frac{\partial w}{\partial r} + \left(\frac{R_o}{L}\right)^2\frac{\partial u}{\partial z}\right]$$

From (II-19), the ratio of viscous forces to pressure forces is

$$\left(\frac{\upsilon T}{R_o^2}\right)\Big/\left[\left(\frac{P}{\rho W^2}\right)\frac{WT}{L}\right] = \frac{\rho W^2}{P}\frac{\upsilon}{WL}\left(\frac{L}{R_o}\right)^2$$

This ratio cannot be greater than one for this problem, therefore,

$$\frac{\rho W^2}{P}\frac{\upsilon}{WL} \ll 1$$

and, to lowest order, the fluid stress components are

$$\tau_{rr} = \tau_{\theta\theta} = \tau_{zz} = -p \qquad , \qquad \tau_{rz} = \mu\frac{\partial w}{\partial r} \qquad \text{(II-31)}$$

For the assumed small displacements, the slope of the surface element is small, which implies that the angle subtended by the normal of the surface element and the radial direction, Θ_s, as shown in Figure 1, is also small. Under such conditions one can make the approximations

11

$$\text{SIN } \Theta_S = \frac{\partial \xi}{\partial z} = \text{TAN } \Theta_S \quad , \quad \cos \Theta_S = 1 \qquad \text{(II-32)}$$

and

$$\vec{\tau}_m = \vec{\tau}_\lambda \cos \Theta_S - \vec{\tau}_z \text{SIN } \Theta_S = \vec{\tau}_\lambda - \vec{\tau}_z \frac{\partial \xi}{\partial z} \qquad \text{(II-33)}$$

By combining (II-28), (II-31), and (II-33) one obtains the linearized form of the viscous force exerted on the inner surface of the membrane element:

$$[(-\vec{\tau}_m) \cdot \underline{\pi}](a \, d\Theta \frac{dz}{\cos \Theta_S}) = \left\{ \vec{\tau}_\lambda \left[(p_s + p')R_0 + p_s \xi + \mu \frac{dw_s}{d\lambda} R_0 \frac{d\xi}{dz} \right] \right.$$
$$\left. - \vec{\tau}_z \left[\mu \frac{dw_s}{d\lambda} R_0 + \mu \frac{dw_s}{d\lambda} \xi + \mu \frac{\partial w'}{\partial \lambda} R_0 + p_s R_0 \frac{\partial \xi}{\partial z} \right] \right\} d\Theta \, dz \qquad \text{(II-34)}$$

Adhering to (II-1) can express the axial and circumferential membrane forces per unit length as:

$$T_\Theta = T_{\Theta_S} + T_\Theta' \quad , \quad T_z = T_{z_S} + T_z' \qquad \text{(II-35)}$$

Also, with axial symmetry and linear wall behavior, the unsteady strain components are

$$\varepsilon_\Theta = \frac{1}{R_0} \xi \quad , \quad \varepsilon_z = \frac{\partial S}{\partial z}$$

The application of Hooke's law yields the relations

$$T_z' = \frac{E h}{1 - \sigma^2} (\varepsilon_z + \sigma \varepsilon_\Theta) = \frac{E h}{1 - \sigma^2} \left(\frac{\partial S}{\partial z} + \frac{\sigma}{R_0} \xi \right) \qquad \text{(II-36)}$$

$$T_\Theta' = \frac{E h}{1 - \sigma^2} (\varepsilon_\Theta + \sigma \varepsilon_z) = \frac{E h}{1 - \sigma^2} \left(\frac{\xi}{R_0} + \sigma \frac{\partial S}{\partial z} \right) \qquad \text{(II-37)}$$

Since the mechanical properties of the biological tissue surrounding the blood vessels are not well defined, Womersley introduced an elastic axial constraint which is applied to the external surface of the membrane and which exerts an axial force $-(a \, d\Theta \frac{dz}{\cos \Theta_S}) K_z S$ that inhibits axial displacements. In addition to this constraint force, an independent, elastic, radial constraint force $-(a \, d\Theta \frac{dz}{\cos \Theta_S}) K_1 \xi$ that opposes the radial displacements was introduced in this analysis. Here K_1 and K_z are stresses per unit displacement in the corresponding directions. With this model for the surface stresses on the outside

12

of the membrane element, the fluid pressure must be referred to the pressure in the surrounding medium.

The force balance on the element of Figure 1 in the presence of the constraints introduced above requires

$$\rho_w \left(a \, d\theta \, \frac{dz}{\cos\theta_s}\right) h \left(\vec{\iota}_\lambda \frac{\partial^2 \xi}{\partial t^2} + \vec{\iota}_z \frac{\partial^2 \varsigma}{\partial t^2}\right) = -a \, d\theta \, \frac{dz}{\cos\theta_s} (\vec{\iota}_\lambda K_1 \xi$$

$$+ \vec{\iota}_z K_2 \varsigma) + (-\vec{\iota}_n) \cdot (\Pi)_{\lambda=a} \, a \, d\theta \, \frac{dz}{\cos\theta_s} +$$

$$+ 2 \left[T_\theta \frac{dz}{\cos\theta_s} \sin\left(\frac{d\theta}{2}\right) \right] [-\vec{\iota}_\lambda \cos\theta_s + \vec{\iota}_z \sin\theta_s] +$$

$$+ \left\{ \left[T_z \, a \, (\vec{\iota}_\lambda \sin\theta_s + \vec{\iota}_z \cos\theta_s) \right]_{z+dz} \right.$$

$$\left. - \left[T_z \, a \, (\vec{\iota}_\lambda \sin\theta_s + \vec{\iota}_z \cos\theta_s) \right]_z \right\} d\theta$$

Expanding the last term into a Taylor series, making use of (II-32) and (II-34) to (II-37), and retaining only linear terms in ξ and ς one obtains

$$\rho_w h \frac{\partial^2 \xi}{\partial t^2} = \left\{ P_s - T_{\theta_s}/R_0 \right\} + \left\{ -K_1 \xi + (p')_{\lambda=R_0} \right.$$

$$+ P_s \frac{\xi}{R_0} + \mu \left(\frac{dw_s}{d\lambda}\right)_{\lambda=R_0} \frac{\partial \xi}{\partial z} - T_\theta' \frac{1}{R_0}$$

$$\left. + T_{z_s} \frac{\partial^2 \xi}{\partial z^2} + \frac{dT_{z_s}}{dz} \frac{\partial \xi}{\partial z} \right\} \qquad \text{(II-38)}$$

$$\rho_w h \frac{\partial^2 \varsigma}{\partial t^2} = \left\{ -\mu \left(\frac{dw_s}{d\lambda}\right)_{\lambda=R_0} + \frac{dT_{z_s}}{dz} \right\} + \left\{ -\mu \left(\frac{dw_s}{d\lambda}\right)_{\lambda=R_0} \frac{\xi}{R_0} \right.$$

$$-K_2 \varsigma - \mu \left(\frac{\partial w'}{\partial\lambda}\right)_{\lambda=R_0} - P_s \frac{\partial\xi}{\partial z} + \frac{T_{\theta_s}}{R_0} \frac{\partial\xi}{\partial z}$$

$$\left. + \frac{T_{z_s}}{R_0} \frac{\partial\xi}{\partial z} + \frac{dT_{z_s}}{dz} \frac{\xi}{R_0} + \frac{\partial T_z'}{\partial z} \right\} \qquad \text{(II-39)}$$

These relations must be true for zero wall displacements which requires

$$T_{\theta_s} = R_0 \, P_s \qquad \text{(II-40)}$$

and

13

$$\frac{dT_{z_s}}{dz} = \mu \left(\frac{dw_s}{d\lambda} \right)_{\lambda=R_0} = \frac{R_0}{2} \frac{dp_s}{dz} \tag{II-41}$$

Substitution of (II-36), (II-37), (II-40) and (II-41) into (II-38) and (II-39) yields

$$\rho_w \, h \, \frac{\partial^2 \xi}{\partial t^2} = -K_1 \xi + (p')_{\lambda=R_0} - \frac{E\,h}{1-\sigma^2} \left(\frac{1}{R_0} \xi \right.$$
$$+ \sigma \frac{\partial S}{\partial z} \left. \right) \frac{1}{R_0} + \left\{ p_s \frac{\xi}{R_0} + \right.$$
$$+ R_0 \frac{dp_s}{dz} \frac{\partial \xi}{\partial z} + T_{z_s} \frac{\partial^2 \xi}{\partial z^2} \left. \right\} \tag{II-42}$$

$$\rho_w \, h \, \frac{\partial^2 S}{\partial t^2} = -K_2 S - \mu \left(\frac{\partial w'}{\partial \lambda} \right)_{\lambda=R_0} + \frac{E\,h}{1-\sigma^2} \left(\frac{\partial^2 S}{\partial z^2} \right.$$
$$+ \frac{\sigma}{R_0} \frac{\partial \xi}{\partial z} \left. \right) + \left\{ \frac{T_{z_s}}{R_0} \frac{\partial \xi}{\partial z} \right\} \tag{II-43}$$

These equations differ from those given by Womersley by the inclusion of a
radial constraint term, $-K_1 \xi$, and by the expansions within the brackets represent-
ing the effects of a mean transmural pressure, an initial axial tension, and a shear-
ing force due to the mean flow. With the exception of both constraint terms, the
difference between (II-42) and (II-43) and the equations derived by Atabeck and Lew
is more subtle. These authors considered perturbations about a steady-state
equilibrium configuration defined by a constant axial tension, T_{z_s}, and by a con-
stant internal pressure causing a circumferential tension, T_{θ_s}. They did not
include the effects of a mean flow. However, they accounted for the rotation of the
hoop stress acting on a surface element during its displacement by the addition of a
term $-(d\xi/dz)(T_{\theta_s}/R_0)$ but they fail to note that this term is actually cancelled
by the identical rotation of the pressure force acting on the internal surface of the
element.

D. Summary of the Linearized Boundary Value Problem

As a first step, the effects of radial and axial constraints on the transmission
characteristics of waves in blood vessels are being investigated for zero mean flow

14

and no initial stresses. Therefore, the bracketed terms in (II-42) and (II-43) may be dropped and the equations of motion for the wall can be reduced to

$$\rho_w \, h \, \frac{\partial^2 \xi}{\partial t^2} = -K_1 \, \xi + (p')_{\lambda=R_0} - \frac{E h}{R_0(1-\sigma^2)} \left(\frac{\xi}{R_0} + \sigma \, \frac{\partial \varsigma}{\partial z} \right) \qquad \text{(II-44)}$$

$$\rho_w \, h \, \frac{\partial^2 \varsigma}{\partial t^2} = -K_2 \, \varsigma - \mu \left(\frac{\partial w'}{\partial \lambda} \right)_{\lambda=R_0} + \frac{E h}{1-\sigma^2} \left(\frac{\partial^2 \varsigma}{\partial z^2} + \frac{\sigma}{R_0} \, \frac{\partial \xi}{\partial z} \right) \qquad \text{(II-45)}$$

With the substitution of (II-1), (II-24) and (II-25) into (II-21) to (II-23) and (II-27), the differential equations for the fluid velocity and pressure perturbations become

$$\frac{1}{\lambda} \, \frac{\partial \lambda u'}{\partial \lambda} + \frac{\partial w'}{\partial z} = 0 \qquad \text{(II-46)}$$

$$\frac{\partial w'}{\partial t} = -\frac{1}{\rho} \, \frac{\partial p'}{\partial z} + \frac{v}{\lambda} \, \frac{\partial}{\partial \lambda} \left(\lambda \, \frac{\partial w'}{\partial \lambda} \right) \qquad \text{(II-47)}$$

$$0 = \frac{\partial p'}{\partial \lambda} \qquad \text{(II-48)}$$

and the boundary conditions can be expressed as

$$u'(R_0, z, t) = \frac{\partial \xi}{\partial t} (z, t) \quad , \quad w'(R_0, z, t) = \frac{\partial \varsigma}{\partial t} (z, t) \qquad \text{(II-49)}$$

III. SOLUTION OF THE LINEARIZED BOUNDARY VALUE PROBLEM

A. The General Solution

The complete linearized boundary value problem is given by Equations
(II-44) to (II-49). By differentiating (II-47) with respect to r and making use of
(II-48) one obtains

$$\rho \frac{\partial}{\partial t}\left(\frac{\partial w'}{\partial r}\right) = \mu \frac{\partial}{\partial r}\left[\frac{1}{r}\frac{\partial}{\partial r}\left(r \frac{\partial w'}{\partial r}\right)\right] \tag{III-1}$$

For the axially-symmetric case $(\partial w'/\partial r)_{r=R_0} = 0$, which means that no purely
oscillatory term in $\partial w'/\partial r$ is possible. Therefore, a separable harmonic solution
can be given in the form

$$\frac{\partial w'}{\partial r} = R(r)\, Z_1(z)\, e^{i\omega t} \tag{III-2}$$

The substitution of (III-2) into (III-1) yields

$$\frac{i\omega}{\upsilon} R(r) = \frac{d}{dr}\left[\frac{1}{r}\frac{d}{dr}\left(r R(r)\right)\right]$$

Changing the independent variable using

$$b s = r \qquad \text{where} \qquad \frac{1}{b} = \sqrt{-i\frac{\omega}{\upsilon}} = i^{3/2}\sqrt{\frac{\omega}{\upsilon}} \tag{III-3}$$

leads to

$$\frac{d^2 R(r)}{ds^2} + \frac{1}{s}\frac{dR(r)}{ds} + \left(1 - \frac{1}{s^2}\right) R(r) = 0$$

which is Bessel's equation for functions of order one. The general solution of this
equation is

$$R(r) = A\, J_1\left(\frac{r}{b}\right) + B\, Y_1\left(\frac{r}{b}\right)$$

However, substitution of this into (III-2) and application of the symmetry requirement,
$(\partial w'/\partial r)_{r=0} = 0$, yields $B = 0$ and

$$\frac{\partial w'}{\partial r} = Z_1(z)\, J_1\left(\frac{r}{b}\right) e^{i\omega t} \tag{III-4}$$

or, after integration,

16

$$w'(\hbar, z, t) = \left\{ Z_1(z) b \left[1 - J_0\left(\frac{\hbar}{b}\right) \right] + i\omega F_1(z) \right\} e^{i\omega t} \qquad \text{(III-5)}$$

Substitution of (III-5) into (II-47) gives an oscillatory expression for $\frac{\partial \rho'}{\partial z}$ which can also be integrated and expressed in the form

$$p'(z,t) = \frac{\mu}{b} \left[Z_1(z) + \frac{i\omega}{b} F(z) + F_z \right] e^{i\omega t} \qquad \text{(III-6)}$$

where

$$Z_1(z) = Z'(z) = \frac{d\, Z(z)}{dz} \quad , \quad F_1(z) = F'(z) = \frac{d\, F(z)}{dz} \qquad \text{(III-7)}$$

From (III-5) and (III-7), if follows that

$$w'(\hbar, z, t) = \left\{ \left[1 - J_0\left(\frac{\hbar}{b}\right) \right] Z'(z) + \frac{i\omega}{b} F'(z) \right\} b\, e^{i\omega t} \qquad \text{(III-8)}$$

By substituting (III-8) into (II-46) and integrating with respect to $\hbar$ one obtains

$$u'(\hbar, z, t) = b \left\{ \left[b\, J_1\left(\frac{\hbar}{b}\right) - \frac{\hbar}{2} \right] Z''(z) - \frac{\hbar}{2} \frac{i\omega}{b} F''(z) \right\} e^{i\omega t} \qquad \text{(III-9)}$$

where the function of z and t generated by this integration must vanish since $u'(\hbar, z, t)$ vanishes for $\hbar = 0$.

The expressions for $\partial \xi/\partial t$ and $\partial \zeta/\partial t$ given by (II-49), (III-8) and (III-9) can be integrated with respect to time to yield the oscillatory solution

$$\xi(z, t) = R_0 \left\{ \frac{b}{i\omega} \left[\frac{b}{R_0} J_1\left(\frac{R_0}{b}\right) - \frac{1}{2} \right] Z''(z) - \frac{1}{2} F''(z) \right\} e^{i\omega t} \qquad \text{(III-10)}$$

$$\zeta(z, t) = \left\{ \frac{b}{i\omega} \left[1 - J_0\left(\frac{R_0}{b}\right) \right] Z'(z) + F'(z) \right\} e^{i\omega t} \qquad \text{(III-11)}$$

According to (III-8), the unsteady mass flux can be written in first approximation

$$Q'(z,t) = \int_0^{R_o} \rho\, w'(r,z,t)\, 2\pi r\, dr = \left\{ \left[\frac{1}{2} - \frac{b}{R_o} J_1\left(\frac{R_o}{b}\right) \right] Z'(z) \right.$$

$$\left. + \frac{1}{2}\, \frac{iw}{b}\, F'(z) \right\} 2\pi R_o^2 \rho\, b\, e^{iwt} \tag{III-12}$$

Substitution of (III-6), (III-8), (III-10) and (III-11) into (II-44) and (II-45) leads to

$$\frac{iw}{b}\left[A_4 R_o^2 F''(z) - \beta_1 F(z) \right] = A_3 R_o^2 Z''(z) + \beta_1 Z(z) + \beta_1 F_z \tag{III-13}$$

$$\frac{iw}{b}\left[\beta_3\left(1 - \frac{\sigma}{2}\right) R_o^2 F''(z) + (1 - \Gamma_z') F(z) \right] = A_2 R_o^2 Z'''(z) - A_1 Z'(z) \tag{III-14}$$

where

$$\Gamma_1 = \frac{K_1}{\rho_w h w^2}, \quad \Gamma_2 = \frac{K_2}{\rho_w h w^2}, \quad \beta_1 = \frac{\rho R_o}{\rho_w h}, \quad \beta_2 = \frac{C_o}{R_o w} \tag{III-15}$$

$$\beta_3 = \frac{E}{\rho_w R_o^2 w^2 (1-\sigma^2)} = \frac{2\beta_1 \beta_2^2}{(1-\sigma^2)}, \quad \alpha = \sqrt{\frac{w}{\nu}}\, R_o, \quad C_o^2 = \frac{E h}{2\rho R_o} \tag{III-16}$$

$$A_1 = (1 - \Gamma_2)\left[1 - J_o\left(i^{3/2}\alpha \right) \right] - \beta_1 \frac{i^{-3/2}}{\alpha} J_1\left(i^{3/2}\alpha \right) \tag{III-17}$$

$$A_2 = -\beta_3 \left\{ \left[1 - J_o\left(i^{3/2}\alpha \right) \right] + \sigma \left[\frac{i^{-3/2}}{\alpha} J_1\left(i^{3/2}\alpha \right) - \frac{1}{2} \right] \right\} \tag{III-18}$$

$$A_3 = (1 - \Gamma_1 - \beta_3)\left[\frac{i^{-3/2}}{\alpha} J_1\left(i^{3/2}\alpha \right) - \frac{1}{2} \right] - \beta_3 \sigma\left[1 - J_o\left(i^{3/2}\alpha \right) \right] \tag{III-19}$$

$$A_4 = \frac{1}{2}(1 - \Gamma_1) - \beta_3\left(\frac{1}{2} - \sigma \right) \tag{III-20}$$

Elimination of $F'''(z)$ from (III-13) and (III-14) and integration of the resulting equation gives

$$\frac{iw}{b} F(z) = -\frac{A_6}{A_5} R_o^2 Z''(z) - \frac{A_7}{A_5} Z(z) + F_3 \tag{III-21}$$

where

18

$$A_5 = \beta_1 + \frac{A_4(1-\Gamma_2)}{\beta_3(1-\sigma/2)} \quad , \quad A_6 = A_3 - \frac{A_2 A_4}{\beta_3(1-\sigma/2)} \quad , \quad A_7 = \beta_1 + \frac{A_1 A_4}{\beta_3(1-\sigma/2)} \qquad \text{(III-22)}$$

By combining (III-21) and (III-13) one obtains

$$R_0^4\, Z''''(z) + A_8 R_0^2\, Z''(z) + A_9\, Z(z) = -(F_2+F_3)\frac{\beta_1 A_5}{A_4 A_6} \qquad \text{(III-23)}$$

where

$$A_8 = \left[A_7 + \frac{A_3(1-\Gamma_2) + \beta_1 A_2}{\beta_3(1-\sigma/2)} \right] \Big/ A_6 \qquad \text{(III-24)}$$

$$A_9 = \frac{1-\Gamma_2 - A_1}{\beta_3(1-\sigma/2)}\, \frac{\beta_1}{A_6} \qquad \text{(III-25)}$$

Equation (III-23) then has the general solution

$$Z(z) = \left[D_1\, e^{-\sqrt{B_1}\, z/R_0} + D_2\, e^{\sqrt{B_1}\, z/R_0} \right] + \left[D_3\, e^{-\sqrt{B_2}\, z/R_0} + \right.$$
$$\left. + D_4\, e^{\sqrt{B_2}\, z/R_0} \right] - (F_2 + F_3)\frac{\beta_1 A_5}{A_4 A_6 A_9} \qquad \text{(III-26)}$$

where B_1 and B_2 are the roots of the equation

$$B^2 + A_8 B + A_9 = 0$$

$$B_1 = \tfrac{1}{2}\left\{ -A_8 + (A_8^2 - 4A_9)^{1/2} \right\} \quad , \quad B_2 = -\tfrac{1}{2}\left\{ A_8 + (A_8^2 - 4A_9)^{1/2} \right\} \qquad \text{(III-27)}$$

From (III-26) and (III-21) one finds

$$\frac{i\omega}{b} F(z) = -\frac{(A_6 B_1 + A_7)}{A_5}\left[D_1\, e^{-\sqrt{B_1}\, z/R_0} + D_2\, e^{\sqrt{B_1}\, z/R_0} \right]$$
$$- \frac{(A_6 B_2 + A_7)}{A_5}\left[D_3\, e^{-\sqrt{B_2}\, z/R_0} + D_4\, e^{\sqrt{B_2}\, z/R_0} \right]$$
$$+ (F_2 + F_3)\frac{\beta_1 A_7}{A_4 A_6 A_9} + F_3 \qquad \text{(III-28)}$$

19

Substitution of (III-26) and (III-28) into (III-6), (III-8), (III-9), (III-10) and (III-11) completes the formal solution. The resulting expression for ρ' can be given as

$$\rho'(z,t) = \frac{\mu}{b} \left\{ S_1 \left[D_1 \, e^{-\sqrt{B_1}\, z/R_0} + D_2 \, e^{\sqrt{B_1}\, z/R_0} \right] \right.$$
$$\left. + S_2 \left[D_3 \, e^{-\sqrt{B_2}\, z/R_0} + D_4 \, e^{\sqrt{B_2}\, z/R_0} \right] \right\} e^{i\omega t} \qquad \text{(III-29)}$$

where

$$S_1 = 1 - \left(\frac{A_6 B_1 + A_7}{A_5} \right) \quad , \quad S_2 = 1 - \left(\frac{A_6 B_2 + A_7}{A_5} \right) \qquad \text{(III-30)}$$

The pressure pulse is often resolved into its Fourier components in studying wave motion. Therefore, it is most convenient to write ρ' in the form

$$\rho'(z,t) = \rho_1(z,t) + \rho_2(z,t) + \rho_3(z,t) + \rho_4(z,t)$$

$$\rho_1(z,t) = P_1 e^{i\omega(t-\frac{z}{C_1})} e^{-\delta_1 z/R_0} \quad , \quad \rho_2(z,t) = P_2 e^{i\omega(t+\frac{z}{C_1})} e^{\delta_1 z/R_0}$$

$$\rho_3(z,t) = P_3 e^{i\omega(t-\frac{z}{C_2})} e^{-\delta_2 z/R_0} \quad , \quad \rho_4(z,t) = P_4 e^{i\omega(t+\frac{z}{C_2})} e^{\delta_2 z/R_0} \qquad \text{(III-31)}$$

where

$$\frac{P_1}{D_1} = \frac{\mu}{b} S_1 = \frac{P_2}{D_2} \quad , \quad \frac{P_3}{D_3} = \frac{\mu}{b} S_2 = \frac{P_4}{D_4} \qquad \text{(III-32)}$$

$$\frac{C_0}{C_1} = \beta_2 \, \mathrm{Im}(\sqrt{B_1}), \; \delta_1 = R_e(\sqrt{B_1}), \; \frac{C_0}{C_2} = \beta_2 \mathrm{Im}(\sqrt{B_2}), \; \delta_2 = R_e(\sqrt{B_2}) \qquad \text{(III-33)}$$

It is also convenient to express the other quantities such that the phase relationship with respect to the pressure waves is exhibited. Substitution of (III-26), (III-28), (III-32) and (III-33) into (III-8), (III-9), (III-10), (III-11) and (III-12) yields

$$w'(r,z,t) = -\frac{i}{\rho \omega R_0} \left\{ \frac{\sqrt{B_1}}{S_1} \left[S_1 - J_0(i^{3/2} \propto \frac{r}{R_0}) \right] \left[\rho_1(z,t) \right. \right.$$
$$\left. - \rho_2(z,t) \right] + \frac{\sqrt{B_2}}{S_2} \left[S_2 - J_0(i^{3/2} \propto \frac{r}{R_0}) \right] \left[\rho_3(z,t) \right.$$
$$\left. \left. - \rho_4(z,t) \right] \right\} \qquad \text{(III-34)}$$

20

$$u'(r,z,t) = \frac{i}{\rho \omega R_0} \left\{ \frac{B_1}{S_1} \left[\frac{i^{-3/2}}{\alpha} J_1(i^{3/2}\alpha \frac{r}{R_0}) - \frac{S_1}{2} \frac{r}{R_0} \right] [p_1(z,t) \right.$$

$$+ p_2(z,t)] + \frac{B_2}{S_2} \left[\frac{i^{-3/2}}{\alpha} J_1(i^{3/2}\alpha \frac{r}{R_0}) \right.$$

$$\left. \left. - \frac{S_2}{2} \frac{r}{R_0} \right] [p_3(z,t) + p_4(z,t)] \right\} \qquad \text{(III-35)}$$

$$\xi(z,t) = \frac{1}{\rho \omega^2 R_0} \left\{ [p_1(z,t) + p_2(z,t)] M_1 e^{i\phi_1} \right.$$

$$\left. + [p_3(z,t) + p_4(z,t)] M_2 e^{i\phi_2} \right\} \qquad \text{(III-36)}$$

$$\zeta(z,t) = \frac{1}{\rho \omega^2 R_0} \left\{ [p_1(z,t) - p_2(z,t)] M_3 e^{i\phi_3} \right.$$

$$\left. + [p_3(z,t) - p_4(z,t)] M_4 e^{i\phi_4} \right\} \qquad \text{(III-37)}$$

$$Q'(z,t) = \frac{R_0}{\omega} \left\{ [p_1(z,t) - p_2(z,t)] M_5 e^{i\phi_5} \right.$$

$$\left. + [p_3(z,t) - p_4(z,t)] M_6 e^{i\phi_6} \right\} \qquad \text{(III-38)}$$

$$w'(0,z,t) = \frac{1}{\rho \omega R_0} \left\{ [p_1(z,t) - p_2(z,t)] M_7 e^{i\phi_7} \right.$$

$$\left. + [p_3(z,t) - p_4(z,t)] M_8 e^{i\phi_8} \right\} \qquad \text{(III-30)}$$

where

$$M_1 e^{i\phi_1} = - \frac{B_1}{S_1} \left[\frac{S_1}{2} - \frac{i^{-3/2}}{\alpha} J_1(i^{3/2}\alpha) \right] \qquad \text{(III-40)}$$

$$M_2 e^{i\phi_2} = -\frac{B_2}{S_2}\left[\frac{S_2}{2} - \frac{i^{-3/2}}{\alpha} J_1(i^{3/2}\alpha)\right] \qquad \text{(III-41)}$$

$$M_3 e^{i\phi_3} = -\frac{\sqrt{B_1}}{S_1}\left[S_1 - J_0(i^{3/2}\alpha)\right] \qquad \text{(III-42)}$$

$$M_4 e^{i\phi_4} = -\frac{\sqrt{B_2}}{S_2}\left[S_2 - J_0(i^{3/2}\alpha)\right] \qquad \text{(III-43)}$$

$$M_5 e^{i\phi_5} = -2\pi\frac{i\sqrt{B_1}}{S_1}\left[\frac{S_1}{2} - \frac{i^{-3/2}}{\alpha} J_1(i^{3/2}\alpha)\right] \qquad \text{(III-44)}$$

$$M_6 e^{i\phi_6} = -2\pi\frac{i\sqrt{B_2}}{S_2}\left[\frac{S_2}{2} - \frac{i^{-3/2}}{\alpha} J_1(i^{3/2}\alpha)\right] \qquad \text{(III-45)}$$

$$M_7 e^{i\phi_7} = -i\frac{\sqrt{B_1}}{S_1}(S_1 - 1) \qquad \text{(III-46)}$$

$$M_8 e^{i\phi_8} = -i\frac{\sqrt{B_2}}{S_2}(S_2 - 1) \qquad \text{(III-47)}$$

Equations (III-31) and (III-34) to (III-47) are the solution for fluid velocity, wall displacement, fluid mass flow and fluid velocity on the axis as a function of time and position with six parameters (σ, β_1, β_2, α, Γ_1, and Γ_2) and four arbitrary constants (P_1, P_2, P_3 and P_4). This solution predicts four waves travelling in the axial direction. These four waves actually constitute two different types of waves each with a transmitted wave (wave moving in the $+z$ direction) and a reflected wave (wave moving in the $-z$ direction). The waves of the same type are identical except for the direction of propagation. The four arbitrary constants determine the strength of the four waves.

The parameters σ and β_1 are functions only of physical and geometric properties of the fluid and the wall. The parameters β_2 and α are functions of the physical and geometric properties and of the frequency. The external constraint parameters Γ_1 and Γ_2 reflect the character of the external constraints.

It is important to note that α has the form of the square root of an unsteady Reynolds number or

22

$$\alpha^2 = \frac{\omega}{\nu} R_o^2 = \frac{\rho(R_o \omega) R_o}{\nu} \equiv R_e \qquad \text{(III-48)}$$

The Reynolds number referred to hereafter is the one defined by (III-48).

The wave speeds (C_1/C_o and C_2/C_o), attenuation factors (δ_1 and δ_2) and the mode shapes as given by the magnitudes (M_1 to M_8) and phase angles (ϕ_1 to ϕ_8) are of course functions only of the six parameters (σ, β_1 , β_2 , α or R_e , Γ_1 , and Γ_2). However, the functional relationships are complex and a parametric study is necessary to illustrate them. The range of physical and geometric properties that determine σ and β_1 are known. The range for β_2 and α should be as broad as possible but consistent with the long wave length approximation which arises by applying (II-3) to wave motion.

$$\frac{\lambda_i}{R_o} = 2\pi \beta_2 \frac{C_i}{C_o} >> 1 \qquad \text{where} \quad i = 1 \text{ or } 2 \qquad \text{(III-49)}$$

Since the constraint parameters, Γ_1 and Γ_2 , have not yet been determined, it is important to know what range of these parameters significantly affect the solution. Considerable insight into the effects of change in Γ_1 and Γ_2 can be obtained from the various limiting forms of the solution including those corresponding to small and large Reynolds number.

B. **Solution for Limiting Values of Reynolds Number or Large Constraint Parameters**
  1. **Motivation for the Limiting Cases of Solution**
      The general solution is complicated by the occurrence of Bessel functions with their argument proportional to the square root of Reynolds number. It can, however, be simplified considerably for limiting values of Reynolds number by retaining only the first few terms of the series and asymptotic expansions of the Bessel functions for small and large Reynolds numbers respectively and other simplified forms of the general solution can be given for limiting large values of the constraint parameters.
  2. **Solutions for Large and Small Reynolds Number**
      For large Reynolds number, α is large and the modulus and phase for the Kelvin functions

23

$$J_\nu(i^{3/2}\alpha) = BER_\nu(\alpha) + i\,BEI_\nu(\alpha) = M'_{\nu'}\,e^{i\Theta'_{\nu'}} \qquad \text{(III-50)}$$

have the asymptotic forms[16)]

$$M'_{\nu'}(\alpha) = \frac{1}{\sqrt{2\pi\alpha}}\;e^{\alpha/\sqrt{2}}\left[1 - \frac{4\nu^2-1}{8\sqrt{2}}\frac{1}{\alpha} + \cdots\right] \qquad \text{(III-51)}$$

$$\Theta'_{\nu'}(\alpha) = \frac{\alpha}{2} + \left(\frac{\nu'}{2} - \frac{1}{8}\right)\pi + \cdots \qquad \text{(III-52)}$$

Substitution of (III-51) and (III-52) into (III-17) to (III-47) and retention of only the terms of order 1 and $1/\alpha$ yields

$$\sqrt{B_1} = \left[-\frac{1}{2K'_1}\left(\sqrt{K_3} + \frac{K'_2}{(1-\sigma/2)}\right)\right]^{1/2}\left[1 + \frac{1}{\sqrt{i}\,\alpha}\,\frac{K_7}{2}\right] \qquad \text{(III-53)}$$

$$\sqrt{B_2} = \left[-\frac{1}{2K'_1}\left(\frac{K'_2}{(1-\sigma/2)} - \sqrt{K_3}\right)\right]^{1/2}\left[1 + \frac{1}{\sqrt{i}\,\alpha}\,\frac{K_8}{2}\right] \qquad \text{(III-54)}$$

$$M_1 e^{i\phi_1} = \frac{1}{4K'_1}\left[\frac{K'_2}{(1-\sigma/2)} + \sqrt{K_3}\right]\left\{1 + \frac{1}{\sqrt{i}\,\alpha}\left(K_7 - \frac{2}{K_5}\right)\right\} \qquad \text{(III-55)}$$

$$M_2 e^{i\phi_2} = \frac{1}{4K'_1}\left[\frac{K'_2}{(1-\sigma/2)} - \sqrt{K_3}\right]\left\{1 + \frac{1}{\sqrt{i}\,\alpha}\left(K_8 - \frac{2}{K_9}\right)\right\} \qquad \text{(III-56)}$$

$$M_3 e^{i\phi_3} = -i\left(\frac{K_5-1}{K_5}\right)\left[\frac{1}{2K'_1}\left(\frac{K'_2}{(1-\sigma/2)} + \sqrt{K_3}\right)\right]^{1/2}\left\{1 + \frac{1}{\sqrt{i}\,\alpha}\left[\frac{K_7}{2} + \frac{K_6}{K_5(K_5-1)}\right]\right\} \qquad \text{(III-57)}$$

$$M_4 e^{i\phi_4} = -i\left(\frac{K_9-1}{K_9}\right)\left[\frac{1}{2K'_1}\left(\frac{K'_2}{(1-\sigma/2)} - \sqrt{K_3}\right)\right]^{1/2}\left\{1 + \frac{1}{\sqrt{i}\,\alpha}\left[\frac{K_8}{2} + \frac{K_{10}}{K_{10}(K_{10}-1)}\right]\right\} \qquad \text{(III-58)}$$

$$M_5 e^{i\phi_5} = \pi\left[\frac{1}{2K'_1}\left(\frac{K'_2}{(1-\sigma/2)} + \sqrt{K_3}\right)\right]^{1/2}\left\{1 + \frac{1}{\sqrt{i}\,\alpha}\left(\frac{K_7}{2} - \frac{2}{K_5}\right)\right\} \qquad \text{(III-59)}$$

24

$$M_6 \, e^{i\phi_6} = \pi\left[\frac{1}{2K_1'}\left(\frac{K_2'}{1-\sigma/2} - \sqrt{K_3}\right)\right]^{1/2}\left\{1 + \frac{1}{i\sqrt{\alpha}}\left(\frac{K_6}{2} - \frac{2}{K_9}\right)\right\} \qquad \text{(III-60)}$$

$$M_7 \, e^{i\phi_7} = \left[\frac{1}{2K_1'}\left(\frac{K_2'}{1-\sigma/2} + \sqrt{K_3}\right)\right]^{1/2}\left\{1 + \frac{1}{i\sqrt{\alpha}}\frac{K_7}{2}\right\} \qquad \text{(III-61)}$$

$$M_8 \, e^{i\phi_8} = \left[\frac{1}{2K_1'}\left(\frac{K_2'}{1-\sigma/2} - \sqrt{K_3}\right)\right]^{1/2}\left\{1 + \frac{1}{i\sqrt{\alpha}}\frac{K_8}{2}\right\} \qquad \text{(III-62)}$$

where

$$K_1' = \beta_3\sigma - \frac{A_4}{1-\sigma/2} \quad, \quad K_2' = \beta_1 + (1-\Gamma_2)\left(\frac{1}{2} - \frac{1-\Gamma_1}{2\beta_3}\right) \qquad \text{(III-63)}$$

$$K_3 = \left(\frac{K_2'}{1-\sigma/2}\right)^2 - \frac{4K_1'\beta_1(1-\Gamma_2)}{\beta_3(1-\sigma/2)} \quad, \quad C_2' = \beta_1\left(\frac{5}{2} - \sigma - \frac{1-\Gamma_1}{2\beta_3}\right) \qquad \text{(III-64)}$$

$$K_4 = 4\left(\frac{K_2'}{1-\sigma/2}\right)^2\left(\frac{C_2'}{2K_2'} - 1\right) - \frac{4K_1'\beta_1}{\beta_3(1-\sigma/2)}\left[\beta_1 - 2(1-\Gamma_2)\right] \qquad \text{(III-65)}$$

$$K_5 = \frac{1}{A_5}\left[\frac{K_2'}{2(1-\sigma/2)} + \frac{1}{2}\sqrt{K_3} + \frac{A_4(1-\Gamma_2)}{\beta_3(1-\sigma/2)}\right] \qquad \text{(III-66)}$$

$$K_6 = \frac{1}{A_5}\left[\left(\frac{K_2'}{1-\sigma/2}\right)\left(\frac{C_2'}{2K_2'} - 1\right) + \frac{K_4}{4\sqrt{K_3}} + \frac{\beta_1 A_4}{\beta_3(1-\sigma/2)}\right] \qquad \text{(III-67)}$$

$$K_7 = \left[\frac{C_2'}{1-\sigma/2} + \frac{K_4}{2\sqrt{K_2}} + 2\sqrt{K_3}\right] \bigg/ \left[\sqrt{K_3} + \frac{K_2'}{1-\sigma/2}\right] \qquad \text{(III-68)}$$

25

$$K_8 = \left[\frac{C_2'}{1-\sigma/2} - \frac{K_4}{2\sqrt{K_3}} - 2\sqrt{K_3} \right] \Big/ \left[\frac{K_2'}{1-\sigma/2} - \sqrt{K_3} \right] \qquad \text{(III-69)}$$

$$K_9 = \frac{1}{A_5} \left[\frac{K_2'}{2(1-\sigma/2)} - \frac{1}{2}\sqrt{K_3} + \frac{A_4(1-\Gamma_2)}{\beta_3(1-\sigma/2)} \right] \qquad \text{(III-70)}$$

$$K_{10} = \frac{1}{A_5} \left[\left(\frac{K_2'}{1-\sigma/2} \right)\left(\frac{C_2'}{2K_2'} - 1 \right) - \frac{K_4}{4\sqrt{K_3}} + \frac{\beta_1 A_4}{\beta_3(1-\sigma/2)} \right] \qquad \text{(III-71)}$$

A_4 and A_5 are defined by (III-20) and (III-22). Note that the expansions for the second type of wave are not valid whenever $(K_2'/(1-\sigma/2)) \approx K_3$ since in such cases the terms of order 1 may be smaller than the terms of order $1/\alpha$.

For small Reynolds numbers, which correspond to small values of α, the first three terms in the ascending series for $J_m(z)$ are retained:

$$J_m(z) = \left(\frac{z}{2} \right)^m \left\{ \frac{1}{m!} - \frac{1}{4}\frac{z^2}{(m+1)!} + \frac{z^4}{32(m+2)!} + \cdots \right\} \text{ FOR SMALL } |z| \qquad \text{(III-72)}$$

Substitution of (III-72) into (III-17) to (III-47) yields

$$\sqrt{B_1} = \frac{z}{\alpha}\sqrt{\frac{2iC_2'}{C_1'}} \left\{ 1 + \frac{i\alpha^2}{4}\left[\frac{C_3'}{4C_2'} - \frac{1}{6} - \frac{\beta_1 C_1'(1-\Gamma_2+\beta_1/2)}{\beta_3 C_2'^2} \right] \right\} \qquad \text{(III-73)}$$

$$\sqrt{B_2} = \left[-\frac{2\beta_1(1-\Gamma_2+\beta_1/2)}{\beta_3 C_2'} \right]^{1/2} \left\{ 1 + \frac{i\alpha^2}{4}\left[-\frac{C_3'}{4C_2'} + \right.\right.$$

$$\left.\left. + \frac{1}{2}\frac{(1-\Gamma_2+\beta_1/4)}{(1-\Gamma_2+\beta_1/2)} - \frac{\beta_1 C_1'(1-\Gamma_2+\beta_1/2)}{2\beta_3 C_2'^2} \right] \right\} \qquad \text{(III-74)}$$

$$M_1 e^{i\phi_1} = \frac{C_2'}{C_1'}\left(C_4' - \frac{1}{2} \right)\left\{ 1 + \frac{i\alpha^2}{4}\left[\frac{C_3'}{2C_2'} - \frac{1}{3} - \frac{\beta_1 C_1'(1-\Gamma_2+\frac{\beta_1}{2})}{\beta_3 C_2'^2} - \frac{\frac{C_4'}{4}+C_4'-\frac{5}{12}}{C_4'-\frac{1}{2}} \right] \right\} \qquad \text{(III-75)}$$

$$M_2 e^{i\phi_2} = \frac{\beta_1\left(1-\Gamma_2+\frac{\beta_1}{2}\right)}{\beta_3\left[C_2'-2A_5(1-\sigma/2)\right]} \left\{ 1 + \frac{i\alpha^2}{4}\left[-\frac{C_3'}{2C_2'} \right.\right.$$

$$\left. + \frac{1-\Gamma_2+\beta_1/4}{1-\Gamma_2+\beta_1/2} - \frac{\beta_1 C_1'\left(1-\Gamma_2+\beta_1/2\right)}{\beta_3 C_2'} \right.$$

$$\left.\left. -\frac{2A_5 C_6'(1-\sigma/2)}{2A_5 C_6'(1-\sigma/2)-C_2'} - \left(C_6'-\frac{1}{2}\right)\frac{2A_5(1-\sigma/2)}{C_2'} \right] \right\} \qquad \text{(III-76)}$$

$$M_3 e^{i\phi_3} = -\frac{i\alpha}{2}\sqrt{\frac{2i\,C_2'}{C_1'}}\left(C_4'-1\right) \qquad \text{(III-77)}$$

$$M_4 e^{i\phi_4} = \left[\frac{2\beta_1\left(1-\Gamma_2+\beta_1/2\right)}{\beta_3 C_2'}\right]^{1/2}\frac{C_2'}{2A_5(1-\sigma/2)-C_2'}\left\{ 1 + \right.$$

$$\left. +\frac{i\alpha^2}{4}\left[-\frac{2A_5 C_6'(1-\sigma/2)}{2A_5 C_6'(1-\sigma/2)-C_2'} - \left(C_6'-1\right)\frac{2A_5(1-\sigma/2)}{C_2'} \right.\right.$$

$$\left.\left. -\frac{C_3'}{4C_2'} +\frac{1}{2}\frac{1-\Gamma_2+\beta_1/4}{1-\Gamma_2+\beta_1/2} - \frac{\beta_1 C_1'\left(1-\Gamma_2+\beta_1/2\right)}{2\beta_3 C_2'^2} \right] \right\} \qquad \text{(III-78)}$$

$$M_5 e^{i\phi_5} = \alpha\frac{\pi}{2}\sqrt{\frac{2i\,C_2'}{C_1'}}\left(C_4'-\frac{1}{2}\right) \qquad \text{(III-79)}$$

$$M_6 e^{i\phi_6} = \pi\left[\frac{2\beta_1\left(1-\Gamma_2+\beta_1/2\right)}{\beta_3 C_2'}\right]^{1/2}\frac{C_2'}{C_2'-2A_5(1-\sigma/2)}\left\{ 1 + \right.$$

$$\left. +\frac{i\alpha^2}{4}\left[-\frac{C_3'}{4C_2'} +\frac{1}{2}\frac{1-\Gamma_2+\beta_1/4}{1-\Gamma_2+\beta_1/2} - \frac{\beta_1 C_1'\left(1-\Gamma_2+\beta_1/2\right)}{2\beta_3 C_2'} \right.\right.$$

$$\left.\left. -\frac{2A_5 C_6'(1-\sigma/2)}{2A_5(1-\sigma/2)-C_2'} - \left(C_6'-\frac{1}{2}\right)\frac{2A_5(1-\sigma/2)}{C_2'} \right] \right\} \qquad \text{(III-80)}$$

$$M_7 e^{i\phi_7} = \frac{\alpha}{2}\sqrt{\frac{2i\,C_2'}{C_1'}}\left(C_4'-1\right) \qquad \text{(III-81)}$$

27

$$M_8 e^{i\phi_8} = -\left[\frac{2\beta_1(1-\Gamma_2+\beta_1/2)}{\beta_3 C_2'}\right]\frac{C_2'}{2A_5(1-\sigma/2)-C_2'}\left\{1+\right.$$

$$+\frac{i\alpha^2}{4}\left[-\frac{2A_5 C_6'(1-\sigma/2)}{C_2'}-\frac{2A_5 C_6'(1-\sigma/2)}{2A_5(1-\sigma/2)-C_2'}-\frac{C_3'}{4C_2'}\right.$$

$$\left.\left.+\frac{1}{2}\frac{1-\Gamma_2+\beta_1/4}{1-\Gamma_2+\beta_1/2}-\frac{\beta_1 C_1'(1-\Gamma_2+\beta_1/2)}{2\beta_3 C_2'^2}\right]\right\} \qquad \text{(III-82)}$$

where

$$C_1'=\beta_3(1-\sigma^2)-(1-\Gamma_1) \quad,\quad C_2'=\beta_1\left(\frac{5}{2}-2\sigma-\frac{1-\Gamma_1}{2\beta_3}\right) \qquad \text{(III-83)}$$

$$C_3'=-\frac{(1-\Gamma_1)(1-\Gamma_2)}{\beta_3}-\frac{\beta_1(1-\Gamma_1)}{2\beta_3}+\beta_1\left(\frac{9}{2}-2\sigma\right)+(1-\Gamma_2) \qquad \text{(III-84)}$$

$$C_4'=\frac{1}{A_5(1-\sigma/2)}\left[\frac{C_3'}{4}-\frac{\beta_1 C_1'(1-\Gamma_2+\beta_1/2)}{2\beta_3 C_2'}+(1-\Gamma_2+\frac{\beta_1}{4})\left(\frac{1-\Gamma_1}{2\beta_3}-\frac{1}{2}+\sigma\right)\right] \qquad \text{(III-85)}$$

$$C_5'=\frac{1}{A_5(1-\sigma/2)}\left[\frac{C_2'}{6}-\frac{C_3'}{3}+\frac{\beta_1 C_1'[16(1-\Gamma_2)+\beta_1]}{6\beta_3 C_2'}-\frac{C_3'}{C_2'}\frac{\beta_1 C_1'(1-\Gamma_2+\frac{\beta_1}{2})}{\beta_3 C_2'}\right.$$

$$\left.-\frac{2\beta_1^2 C_1'^2(1-\Gamma_2+\frac{\beta_1}{2})^2}{\beta_3^2 C_2'^2}+(1-\Gamma_2+\frac{\beta_1}{6})\left(\frac{1-\Gamma_1}{2\beta_3}-\frac{1}{2}+\sigma\right)\right] \qquad \text{(III-86)}$$

$$C_6'=\left[\frac{1-\Gamma_2+\beta_1/4}{A_5(1-\sigma/2)}\left(\frac{1-\Gamma_1}{2\beta_3}-\frac{1}{2}+\sigma\right)+\frac{1}{A_5}\frac{\beta_1 C_1'(1-\Gamma_2+\beta_1/2)}{2\beta_3 C_2'(1-\sigma/2)}\right] \qquad \text{(III-87)}$$

Again, A_4 and A_5 are defined by (III-20) and (III-22).

To obtain the wave speeds and attenuation factors one merely has to substitute the forms for $\sqrt{B_1}$ and $\sqrt{B_2}$ into (III-33). For small α, the wave speed for the first type of waves is directly proportional to α. Then, for zero α or zero Reynolds number, this wave speed is zero and the wave is completely attenuated for all values of the remaining parameters provided $(C_2'/C_1')\neq 0$. For large Reynolds numbers, the variation of the wave speed and attenuation with β_1, β_2, Γ_1, Γ_2 and σ is still complicated in spite of the restriction to large values of α. The significance of the constraint parameters Γ_1 and Γ_2, is demonstrated below for $\sigma=0.5$, $\beta_1=10$, $\beta_2=100$ representing a set of physiologically meaningful values. Figures 2 and 3 show the variation of the wave speeds with Γ_1 for $\Gamma_2=0$. Neither wave speed varies significantly with Γ_1 for $\Gamma_1<10^4$. They increase rapidly with increasing radial constraint within the range $10^4<\Gamma_1<10^7$. However, for $\Gamma_1>10^7$, the wave speed for the first

type of waves becomes relatively independent of Γ_1' , while the wave speed for
the second type of waves continues to increase.

Figure 4 and 5 show the variation of the wave speeds with the axial constraint parameter, Γ_2 , for the case of no radial constraint ($\Gamma_1 = 0$). The wave speed of the first type of waves is quite insensitive to axial constraint with its most significant variation occurring for $1 < \Gamma_2 < 10^3$. The wave speed for the second type of waves, however, is highly sensitive to axial constraint. It increases rapidly with increasing axial constraint. Furthermore, from (III-54) and (III-74), it follows that the wave speed of the second type of waves becomes infinite for

$$\Gamma_2 \geqslant 1 \quad \text{for the large Reynolds number limit} \ (\alpha \to \infty) \qquad \text{(III-88)}$$

and

$$\Gamma_2 \geqslant \left(1 + \frac{\beta_1}{2}\right) \quad \text{for the small Reynolds number limit} \ (\alpha = 0) \qquad \text{(III-89)}$$

For $\sigma = 1/2$, $\beta_1 = 10$, $\beta_2 = 100$, $\Gamma_1 = 0$, $\Gamma_2 = 1$ and infinite Reynolds number, this analysis predicts no motion of the tube wall or the fluid for the second type of waves. Therefore the pressure wave merely travels through a stationary, inviscid, incompressible fluid with infinite speed. Since the speed of propagation of disturbances in such a fluid is known to be infinite, this type of wave is as physically admissible as the model of the system permits. However, the prediction of an infinite wave speed for the second type of waves in the large Reynolds number limit lead the authors of Reference 9 to the erroneous conclusion that this type of wave is physically inadmissible. Their analysis neglected the inertia terms due to wall mass as well as the effects of external constraint, which corresponds to the case $\Gamma_2 = 1$ in the present analysis.

Two observations from the above results are most important. Both types of waves do exist in the large Reynolds number limit. Also, variations of both wave speeds with variation in Reynolds number and external constraint between their limiting values are very large.

The results for the large Reynolds number limit $((1/\alpha) = 0)$ with $\sigma = 0.5$, $\beta_1 = 10$, $\Gamma_1 = 0 = \Gamma_2$ and β_2 varying over a wide range are shown on Figures 6 to 8. The wave speed for the second type of waves is much larger and exhibits

an insignificant dependence upon β_2. The speed of the first type of waves is also constant for large values of β_2 and decreases with decreasing β_2. From Figure 7, the wave length parameter is proportional to β_2 for the second type of waves over the entire range of β_2 considered here and also for the first type of waves if $\beta_2 > 1$ or $(\lambda/R_o) > 2\pi$. Furthermore, $(\lambda_1/R_o) = 1$ for $\beta_2 \simeq 0.28$ and $(\lambda_2/R_o) = 1$ for $\beta_3 \simeq 0.031$. Figure 8 shows that the modulii M_1 to M_8 are essentially exponential functions of β_2 over that range of β_2 for which the long wave length approximation applies. M_1 and M_2 are inversely proportional to β_2^2 while M_3 to M_8 are inversely proportional to β_2. For all β_2 values considered, the phase angles are given by

$$\phi_1 = \phi_2 = \phi_5 = 0 = \phi_6 = \phi_7 = \phi_8 \quad , \quad -\phi_3 = 90° = \phi_4$$

Therefore, the radial wall displacement, the fluid flow rate and the fluid velocity along the axis are all in phase with the pressure for both types of waves. Axial wall displacement lags the pressure by 90° for the first type of waves and leads the pressure by 90° for the second type. Attenuation is, of course, not present because the inviscid limit is also an infinite Reynolds number limit. These results for the inviscid limit are in good agreement with the results for Type I and III axially symmetric waves in the inviscid analysis of Reference 3 for the range of β_2 where $(\lambda/R_o) > 1$.

3. Infinite Radial and Axial Constraint

For limiting radial and axial constraint, $\Gamma_1 = \Gamma_2 \Rightarrow \infty$, (III-23) reduces to

$$Z''(z) = 0$$

and has a solution of the form

$$Z(z) = D_1 \frac{z}{R_o} + D_2 \tag{III-90}$$

No waves are generated in this case. Substitution of (III-90) into (III-21) and performing the limit process, $\Gamma_1 = \Gamma_2 \Rightarrow \infty$, yields

$$\frac{i\omega}{b} F(z) = -D_1 \left[1 - J_o\left(i^{3/2}\alpha\right)\right] \frac{z}{R_o} + D_3 \tag{III-91}$$

From (III- 6), (III-8) to (III-11), (III-90) and (III-91), one obtains

$$p'(z,t) = \frac{\mu}{b}\left[D_1 \; J_0(i^{3/2}\alpha)\frac{z}{R_0} + (D_2 + D_3 + F_2)\right]e^{i\omega t} \tag{III-92}$$

$$u'(r,z,t) = 0 = \xi(z,t) = \zeta(z,t) \tag{III-93}$$

$$w'(r,z,t) = \frac{i}{\rho\omega}\left[1 - \frac{J_0(i^{3/2}\alpha\frac{r}{R_0})}{J_0(i^{3/2}\alpha)}\right]\frac{\partial p'}{\partial z} \tag{III-94}$$

$$Q'(z,t) = i\,\frac{2\pi R_0^2}{\omega}\,M_A\,e^{i\phi_A}\,\frac{\partial p'}{\partial z} \tag{III-95}$$

where

$$M_A\,e^{i\phi_A} = \frac{1}{2} - \frac{i^{-3/2}}{\alpha}J_1(i^{3/2}\alpha)\Big/J_0(i^{3/2}\alpha) \tag{III-96}$$

M_A and ϕ_A are plotted in Figures 9 and 10.

Therefore, in the presence of very large radial and axial constraints the solution predicts a harmonic oscillation with an amplitude that varies linearly with the axial coordinate. As expected from the nature of the constraints, the wall displacements and radial fluid velocity are zero. The axial fluid velocity and mass flow are only related to the pressure variation in the tube.

4. Infinite Radial Constraint

For infinite radial constraints ($\Gamma_1 \to \infty$) and finite axial constraint, (III-23) reduces to

$$\left[R_0^2\frac{d^2}{dz^2} - B_j\right]R_0^2\frac{d^2 z}{dz^2} = 0 \tag{III-97}$$

where

$$B_j = -\frac{1}{\beta_3}\left[(1 - \Gamma_z) - \frac{\beta_1}{2}(1 - \frac{1}{2}\frac{e^{i\phi_A}}{M_A})\right] \tag{III-98}$$

with the index j defined by

31

$$\text{Im}\left(\frac{\Gamma_1 A_9}{A_8}\right)\Bigg|_{\Gamma_1 \to \infty} = \text{Im}\left\{\frac{\beta_1}{\beta_3 \beta_j^2}\left[(1-\Gamma_2 + \frac{\beta_1}{2})\frac{e^{-i\phi_A}}{M_A} - \beta_1\right]\right\} = \begin{cases} >0, j=1 \\ <0, j=2 \end{cases} \tag{III-99}$$

The index j determines the type of waves. Integrating (III-97), one obtains

$$Z_j(z) = D_1 e^{-\sqrt{B_j}\frac{z}{R_0}} + D_2 e^{\sqrt{B_j}\frac{z}{R_0}} + D_3 \frac{z}{R_0} + D_4 \tag{III-100}$$

Substitution of (III-100) into (III-21) and taking $\Gamma_1 \to \infty$ leads to

$$\frac{i\omega}{b}F(z) = \left[\frac{i^{-3/2}}{\alpha}J_1(i^{3/2}\alpha) - z\right]\left[D_1 e^{-\sqrt{B_j}\frac{z}{R_0}}\right.$$

$$+ D_2 e^{\sqrt{B_j}z/R_0}\Big] + \left[\frac{\beta_1}{1-\Gamma_2}\frac{i^{-3/2}}{\alpha}J_1(i^{3/2}\alpha) - 1\right.$$

$$+ J_0(i^{3/2}\alpha)\Big](D_3\frac{z}{R_0} + D_4) + F_3 \tag{III-101}$$

Finally, substitution of (III-100) and (III-101) into (III-6) and (III-8) to (III-11) yields the relations:

$$\rho'(z,t) = \frac{\mu}{b}\left\{z\frac{i^{-3/2}}{\alpha}J_1(i^{3/2}\alpha)\left[D_1 e^{i\omega(t-\frac{z}{\xi_j})}e^{-\delta_j z/R_0}\right.\right.$$

$$\left. + D_2 e^{i\omega(t+\frac{z}{\xi_j})}e^{+\delta_j z/R_0}\right] + (D_3\frac{z}{R_0} + D_4)\left[\frac{\beta_1}{1-\Gamma_2}\frac{i^{-3/2}}{\alpha}J_1(i^{3/2}\alpha)\right. +$$

$$+ J_0(i^{3/2}\alpha)\Big]e^{i\omega t} + (F_2 + F_3)e^{i\omega t}\Big\} \tag{III-102}$$

$$u'(r,z,t) = \frac{1}{\rho\omega R_0}\frac{i}{J_1(i^{3/2}\alpha)}\left\{J_1(i^{3/2}\alpha\frac{r}{R_0}) - \frac{r}{R_0}J_1(i^{3/2}\alpha)\right\}\frac{\partial^2\rho'}{\partial z^2} \tag{III-103}$$

$$w'(r,z,t) = \frac{i}{\rho\omega}\left[1 - \frac{1}{2}i^{3/2}\alpha\frac{J_0(i^{3/2}\alpha\frac{r}{R_0})}{J_0(i^{3/2}\alpha)}\right]\frac{\partial\rho'}{\partial z} + D_3\frac{b}{R_0}\{[z - $$

$$- J_0(i^{3/2}\alpha) - z\frac{i^{-3/2}}{\alpha}J_1(i^{3/2}\alpha)]/[1 - $$

$$- \frac{1}{2}\frac{e^{i\phi_A}}{M_A}] - \frac{\beta_1}{2(1-\Gamma_1)}\left[\frac{i^{-3/2}}{\alpha}J_1(i^{3/2}\alpha) - J_0(i^{3/2}\alpha\frac{r}{R_0})\right]\} \tag{III-104}$$

$$\xi(z,t) = 0, \quad \varsigma(z,t) = \frac{1}{\rho \omega^2}\left\{ 1 - \frac{i^{3/2}\alpha\, J_0(i^{3/2}\alpha)}{J_1(i^{3/2}\alpha)}\right\}^{-1}\frac{\partial \rho'}{\partial z}$$

$$+ \frac{D_3}{R_0}\frac{b}{i\omega}\left\{\frac{\beta_1}{2(1-\Gamma_1)}\left[1 - \frac{1}{2}\frac{e^{-i\phi_A}}{M_A}\right]\right\}J_0(i^{3/2}\alpha)\, e^{i\omega t} \qquad \text{(III-105)}$$

$$Q'(z,t) = 2\pi R_0^2\, \rho b\,\frac{D_3}{R_0}\left[M_A e^{i\phi_A} + \right.$$

$$\left. + \frac{\beta_2}{2(1-\Gamma_2)}\frac{i^{-3/2}}{\alpha}J_1(i^{3/2}\alpha)\Big/ J_0(i^{3/2}\alpha)\right]J_0(i^{3/2}\alpha)\, e^{i\omega t} \qquad \text{(III-106)}$$

where

$$\frac{C_0}{C_j} = \beta_2\,\text{Im}(\sqrt{B_j}) \quad , \quad S_j = \text{Re}(\sqrt{B_j}) \qquad \text{(III-107)}$$

From these equations it follows that only one type of pressure wave can occur, for $\Gamma_1 \rightarrow \infty$. These waves all have the property that the total instantaneous mass flow at any cross section is zero at all times. In accordance with the constraint they also have no radial wall displacements. Besides this, the solution allows for a harmonic pressure fluctuation whose amplitude varies linearly with the axial coordinate and that exhibits an axial wall displacement.

5. Infinite Axial Constraint

For infinite axial constraint ($\Gamma_2 \rightarrow \infty$) with infinite radial constraint, (III-23) reduces to

$$R_0^2\, Z''(z) - \frac{\beta_1}{1-\Gamma_1-\beta_3}\frac{e^{-i\phi_A}}{M_A}Z(z) = \frac{\beta_1(F_2+F_3)e^{-i\phi_A}}{J_0(i^{3/2}\alpha)(1-\Gamma_1-\beta_3)M_A} \qquad \text{(III-108)}$$

and has the general solution

$$Z(z) = D_1 e^{-\sqrt{B_j}\, z/R_0} + D_2 e^{\sqrt{B_j}\, z/R_0} - \frac{F_2+F_3}{J_0(i^{3/2}\alpha)}, \quad B_j = \frac{\beta_1}{1-\Gamma_1-\beta_3}\frac{e^{-i\phi_A}}{M_A} \qquad \text{(III-109)}$$

In this case, the type of waves present is determined by

$$\text{Im}\left(\frac{\Gamma_z A_9}{A_8}\right)\Bigg|_{\Gamma_z \to \infty} = \text{Im}\left[B_j \frac{(1-\Gamma_1-\beta_3)+\beta_3\sigma^2}{1-\Gamma_1-\beta_3}\right] = \begin{cases} >0 & , j=1 \\ <0 & , j=2 \end{cases} \qquad \text{(III-110)}$$

Substitution of (III-109) into (III-21) and application of the limiting process, $\Gamma_z \to \infty$, yields

$$\frac{i\omega}{b}F(z)=\frac{A_6 B_j - A_7}{A_5}\left[D_1 e^{-\sqrt{B_j}\, z/R_0}+D_2 e^{\sqrt{B_j}\, z/R_0}\right]+\frac{A_7}{A_5}\frac{F_2+F_3}{J_0(i^{3/2}\alpha)}+F_3 \qquad \text{(III-111)}$$

From (III-6), (III-8) to (III-11), (III-109) and (III-111), one obtains

$$\rho'(z,t)=\frac{\mu}{b}\left[D_1 e^{i\omega(t-\frac{z}{c_j})}e^{-\delta_j\, z/R_0}+D_2 e^{i\omega(t+\frac{z}{c_j})}e^{\delta_j\, z/R_0}\right] \qquad \text{(III-112)}$$

$$u'(n,z,t)=\frac{R_0}{\rho\omega}\frac{i}{J_0(i^{3/2}\alpha)}\left[\frac{i^{-3/2}}{\alpha}J_1(i^{3/2}\alpha)-\frac{1}{2}\frac{n}{R_0}J_0(i^{3/2}\alpha)\right]\frac{\partial^2\rho'}{\partial z^2} \qquad \text{(III-113)}$$

$$w'(n,z,t)=\frac{1}{\rho\omega}\frac{i}{J_0(i^{3/2}\alpha)}\left[J_0(i^{3/2}\alpha)-J_0(i^{3/2}\alpha\frac{n}{R_0})\right]\frac{\partial\rho'}{\partial z} \qquad \text{(III-114)}$$

$$\xi(z,t)=-\frac{R_0}{\rho\omega^2}M_A e^{i\phi_A}\frac{\partial^2\rho'}{\partial z^2} \quad , \quad \zeta(z,t)=0 \qquad \text{(III-115)}$$

$$Q'(z,t)=2\pi\frac{R_0^2}{\omega}M_A e^{i(\phi_A+\frac{\pi}{2})}\frac{\partial\rho'}{\partial z} \qquad \text{(III-116)}$$

where

$$\frac{c_0}{c_j}=\beta_z\,\text{Im}(\sqrt{B_j}) \quad , \quad \delta_j=\text{Re}(\sqrt{B_j})$$

and M_A and ϕ_A are given by (III-96).

These equations imply that only one type of waves can exist and that these waves have no axial wall displacements. In contrast to the previous limiting cases, this solution does not predict a nonpropagating, harmonic pressure fluctuation.

34

IV. NUMERICAL RESULTS FROM THE GENERAL SOLUTION

A. A Parametric Analysis

Various solutions for limiting values of the constraints and Reynolds number were described in the previous section and are illustrated in Figures 2 to 8. These solutions show that the ranges of Γ_1, Γ_2, and β_2 for which the speed of waves with a long wave length vary significantly are defined by

$$10^4 < \Gamma_1 < 10^7 \quad , \quad \Gamma_2 < 6. \quad , \quad \beta_2 > 1 \tag{IV-1}$$

For the cardiovascular system, the geometric and physical parameters may be limited to

$$0.25 \leq \sigma \leq 0.5 \quad , \quad 5 \leq \beta_1 \leq 20 \tag{IV-2}$$

At the fundamental pulse frequency, β_2 is of the order 10^2. Since biological material is nearly incompressible, Poisson's ratio, σ, may be taken as 0.5. As a representative value for β_1, one may choose $\beta_1 = 10$. Therefore, the basic parameter values in the parametric analysis were

$$\sigma = 0.5 \quad , \quad \beta_1 = 10 \quad , \quad \beta_2 = 10^2 \quad , \quad \Gamma_1 = 0 = \Gamma_2 \tag{IV-3}$$

The constraint parameters, Γ_1 and Γ_2, were modified for this parametric study to reflect only the physical parameters of the system:

$$\kappa_1 = \frac{\Gamma_1}{\beta_1^2} = \frac{k_1 c_o^2}{\rho_w \lambda_h R_o^2} \quad , \quad \kappa_2 = \frac{\Gamma_2}{\beta_2^2} = \frac{k_2 c_o^2}{\rho_w \lambda_h R_o^2} \tag{IV-4}$$

In terms of these new constraint parameters, the basic parameter values defined by (IV-3) can now be given as

$$\sigma = 0.5 \quad , \quad \beta_1 = 10 \quad , \quad \beta_2 = 10^2 \quad , \quad \kappa_1 = 0, \quad \kappa_2 = 0 \tag{IV-5}$$

and the most significant ranges for κ_1 and κ_2 for $\beta_2 = 10^2$ are

$$1 < \kappa_1 < 10^3 \quad , \quad \kappa_2 < 6 \times 10^{-4} \tag{IV-6}$$

Figures 11 to 22 give the results of the parametric analysis in terms of wave speeds, attenuation coefficients and transmission factors. The transmission

factor is defined as $\exp(-\delta\lambda/R_o)$ which represents the ratio of the amplitude of a sinusoidal wave propagating over a distance of one wavelength to its initial value. Results for infinite constraints corresponding to the limiting solutions given in the previous section are also shown for comparison.

In general, the wave speed for the first type of waves increases monotonically with α from a small value at low Reynolds numbers and approaches a finite limiting value. For weak radial constraint, it is relatively constant for $R_e > 9$ and $\alpha > 3$. Whenever the condition $(\lambda_1/R_o) = 2\beta_2\pi(C_1/C_o) >> 1$ is satisfied, the parameters β_1 and β_2 have little effect on this wave speed, and a change in Poisson's ratio, σ, has no significant effect at large Reynolds numbers. Conditions (III-99) and (III-110) indicate that only the first type of waves exists for infinite values of either constraint. For arbitrary values of K_z within the complete range of axial constraint ($0 \leq K_z \leq \infty$), the solution deviates at most by 15% from that corresponding to the basic values at all Reynolds numbers. However, variations in the radial constraint K_1 produce marked changes particularly in the range $1 \leq K_1 \leq 10^3$.

Except for cases with large radial constraints, the wave speed for the second type of waves is relatively constant at low Reynolds numbers and increases monotonically with increasing Reynolds number. However, changes in Poisson's ratio or β_1 produce much larger effects on the speed of this type of wave, while a variation in β_2 again has a negligible effect. The speed approaches infinity as either constraint parameter becomes unbounded, moreover in the presence of a radial constraint with $K_1 > 10^3$ the wave speed is virtually independent of the Reynolds number.

The attenuation coefficient for the first type of waves, δ_1, decreases monotonically with increasing Reynolds number and consequently the transmission factor $\exp(-\delta_1\lambda_1/R_o)$, increases monotonically. A change in Reynolds number may cause very large variations in both quantities. The parameter β_1 has no effect on either quantity but a variation in Poisson's ratio produces a larger relative change (up to 35%) in δ_1 and in the transmission factor. Over the entire Reynolds number range δ_1 is inversely proportional to β_2 while the transmission factor is independent of β_2. At this point it should be recalled that according to Eq. (III-49) the wave length is proportional to β_2 since the wave speed C_1 is independent of β_2. This implies that the transmission factor is not affected by β_2. Variations in the radial constraint ($0 \leq K_1 \leq \infty$) may change δ_1 and the transmission factor by an order of magnitude. For high Reynolds number a change in the

36

axial constraint $(0 \leqslant K_2 \leqslant \infty)$ can alter δ_1 by as much as 50%, while for low Reynolds numbers no noticable effect is produced.

For all cases with weak constraints the attenuation factor for the second type of waves, δ_2 , first increases with increasing Reynolds number, attains a maximum for $\alpha \approx 2.8$ or $R_e \approx 8$ and then decreases monotonically. Except for very low Reynolds numbers, β_1 can have a significant effect on the transmission factor. Again, the attenuation coefficient is inversely proportional to β_2 while the transmission factor has a negligible dependence on β_2 . At low Reynolds numbers, δ_2 decreases and the transmission factor increases with increasing radial constraint. For very strong radial constraints this behavior is predicted for the entire Reynolds number range. With increasing K_2 the attenuation coefficient increases and the transmission factor decreases. For $K_2 \geqslant 5 \times 10^{-4}$, the transmission factor becomes negligible.

Results for the mode shape parameters, M_1 to M_8, are shown on Figures 23 to 38. M_1 , the mode shape parameter for the radial displacement of the first type of waves, exhibits only a mild dependence upon the Reynolds number, Poisson's ratio and β_1 . Furthermore it is inversely proportional to the square of β_2 . M_2 , the mode shape parameter for the radial displacement for the second type of waves first decreases rapidly, attains a minimum and then increases with increasing Reynolds number. This parameter varies significantly with Poisson's ratio for all Reynolds numbers. It changes noticeably with β_1 at high Reynolds numbers, and is inversely proportional to the square of β_2 for the entire Reynolds number range. In the absence of radial and axial constraints, M_2 is larger than M_1 at small Reynolds numbers, but the reverse is true at larger Reynolds numbers. With increasing K_1 , M_1 decreases rapidly irrespective of the Reynolds number, while M_2 decreases rapidly first only at low Reynolds numbers and for all Reynolds numbers when $K_1 \geqslant 10^3$. With increasing axial constraint, M_1 decreases at large Reynolds number and approaches asymptotically a finite limit value while at large Reynolds number, M_2 first decreases with K_2 , obtains a minimum and then increases.

The mode shape parameters for axial displacement, M_3 for waves of the first type and M_4 for waves of the second type exhibit completely different parametric variations. At low Reynolds number, M_3 increases rapidly while M_4 decreases (for $\sigma = 0.5$) rapidly with increasing Reynolds number. At larger Reynolds number both are relatively independent of the Reynolds number,

however, M_4 is in general much larger than M_3. β_1 has no significant effect on M_3 but M_4 shows a relatively large increase with β_1 at large Reynolds number. Both M_3 and M_4 are inversely proportional to β_2 wherever $\lambda/R_0 >> 1$. M_3 increases rapidly with decreasing Poisson's ratio at low Reynolds numbers and conversely decreases with decreasing Poisson's ratio at large Reynolds numbers. M_4 shows exactly the opposite behavior with Poisson's ratio. An increase in κ_1 produces a rapid increase in M_3 at low Reynolds number while for large Reynolds numbers M_3 first decreases and then increases at higher values for κ_1. On the other hand an increase in κ_1 causes a decrease in M_4 for all Reynolds numbers and an increase in κ_2 produces an increase in M_4 at low Reynolds numbers, but for large Reynolds numbers M_4 first increases and then decreases. M_3 decreases with κ_2 for the entire range of Reynolds numbers.

The mode shape parameters for fluid flow rate, M_5 for waves of the first type and M_6 for waves of the second type, also show markedly different behavior. M_5 has no noticeable dependence on β_1 or Poisson's ratio. But with increasing Reynolds number M_5 first noticeably increases and then approaches asymptotically a limit value. M_5 is inversely proportional to β_2. The trends of M_6 with β_1, σ and β_2 are identical to those of M_4. While M_5 is smaller than M_6 for small Reynolds numbers the reverse is true at large Reynolds numbers. The axial constraint has no effect on M_5 but produces effects on M_6 which are similar to the effects on M_4. An increase in κ_1 causes a decrease of M_5 and also a decrease of M_6 at low Reynolds numbers. However, for large radial constraints, M_6 decreases with κ_1 but is virtually independent of the Reynolds numbers.

The mode shape parameters for axial fluid velocity on the axis, M_7 for waves of the first type and M_8 for waves of the second type, have the same trends as the corresponding mode shape parameters for the fluid rate M_5 and M_6. The only exception is the occurrence of a relative maximum-minima at moderate Reynolds numbers.

Figures 39 to 42 illustrate parametric variations of the phase angles between radial wall displacement and pressure, ϕ_1 for waves of the first type and ϕ_2 for waves of the second type. With increasing Reynolds numbers, Figures 39 demonstrates that ϕ_1 increases from zero, assumes a maximum for $\alpha \approx 2.5$, and then decreases. β_2 has no apparent effect on ϕ_1, while β_1 and particularly a change in Poisson's ratio can produce large relative variations.

However, in the absence of constraints, ϕ_1 is small. As can be seen from Figure 40, ϕ_1 approaches zero with increasing axial constraint for all Reynolds numbers, but with increasing radial constraint, the maximum of ϕ_1 increases slightly and shifts to larger Reynolds numbers. For large radial constraints the small phase lead becomes a phase lag with a pronounced minimum at larger Reynolds numbers.

The phase angle ϕ_2 displayed in Figures 41 and 42 is very sensitive to all parameters. In general, ϕ_2 increases, assumes a maximum, and when K_2 is small decreases to zero as R_e increases. As shown in Figure 41, large variations in ϕ_2 are predicted for changes in β_2 at low Reynolds numbers and for changes in β_1 at high Reynolds numbers. Also, a change in Poisson's ratio produces large variations in ϕ_2 for all Reynolds numbers but the most interesting effect is the shift from $\phi_2 = 90^0$ to $\phi_2 = 0^0$ at low Reynold's numbers for all values of Poisson's ratio except those near 0.5. According to Figure 42 an increase of K_2 causes a marked increase of ϕ_2 that is particularly noticeable at large Reynolds numbers. An increase in K_1 generally produces a decrease in ϕ_2.

The graphs in Figures 43 to 46 portray phase angles between axial wall displacement and pressure, ϕ_3 for the first type of waves and ϕ_4 for the second type. Except for the case of large radial constraints and small β_2 (for which $\lambda_1 / R_0 \leqslant 1$), ϕ_3 decreases in Figures 43 and 44 monotonically to -90^0 with increasing R_e. The changes in σ considered in Figure 43 produce large variations in ϕ_3 and shifts the low Reynolds number value from $\phi_3 = 45^0$ to 135°. Figure 44 demonstrates that an increase in K_2 has little effect on ϕ_3 while minute changes in K_1 cause a large shift in ϕ_3 at low Reynolds numbers.

From Figures 45 and 46 it follows that, except for large radial constraints or small β_2, ϕ_4 generally increases. As can be seen in Figure 45, ϕ_4 becomes independent of β_1 at large Reynolds numbers. However β_2 affects ϕ_4 significantly when β_2 and R_e are small. Changes in σ from 0.5 to 0.25 shift the low Reynolds number values from $\phi_4 = 0$ to $\phi_4 = -90^\circ$ and produce significant variations in ϕ_4 for all but very large Reynolds numbers. The graphs in Figure 46 demonstrate that an increase in K_2 produces an increase in ϕ_4, particularly at large Reynolds numbers. Likewise, K_1 can alter ϕ_4 markedly.

The phase angles between fluid flow rate and pressure, ϕ_5 for waves of the first type and ϕ_6 for waves of the

second type, are shown on Figures 47 to 50. Without external constraint, ϕ_5 decreases in Figure 47 from 45° to 0° with increasing R_e; while β_1 and β_2 have no apparent effect on ϕ_5 and Poisson's ratio produces only a small change in ϕ_5. From Figure 48 it follows that an arbitrary variation in K_2 alters ϕ_5 less than 15%. Also, an increase in K_1 produces little effect on ϕ_5 at low Reynolds number, but a significant increase for moderate R_e values and a large decrease in ϕ_5 at large Reynolds numbers. The plots of ϕ_6 in Figures 49 and 50 exhibit the same trends as those for ϕ_2 in Figures 41 and 42. This implies that for the second type of waves the phase angles between fluid flow rate and pressure show a similar parametric dependence as the phase angles between the radial displacement and the pressure.

Figures 51 to 54 display the phase angles between axial fluid velocity on the axis and pressure, ϕ_7 for waves of the first type and ϕ_8 for waves of the second type. According to the graphs in Figure 51 ϕ_7 decreases generally from 45° with increasing R_e attains a minimum for $\alpha \approx 6$ and then approaches gradually to zero. Variations in β_1 and β_2 have no apparent effect on ϕ_7 but a decrease in σ produces a decrease in ϕ_7 at moderate R_e. As shown in Figure 52 an increase in K_2 causes a minute decrease in ϕ_7 near the minimum while an increase in K_1 shifts the minimum to smaller values of ϕ_7 and to slightly larger Reynolds numbers.

From Figure 53 it follows that for the basic parametric case, ϕ_8 decreases from 90°, attains a minimum for $\alpha \approx 7$ or $R_e \approx 49$, a maximum for $\alpha \approx 10$ or $R_e \approx 10^2$, another minimum for $\alpha \approx 15$ or $R_e \approx 225$, and finally approaches zero for very large Reynolds numbers. Changes in β_1 produce large relative variations in ϕ_8 at large Reynolds numbers. For small R_e a decrease in β_2 causes a significant increase in ϕ_8 but this effect is somewhat weaker when $(\lambda_2/R_0) \gg 1$. A decrease in σ again shifts the low Reynolds value from 90° to 0° and produces a significant variation in ϕ_8 except for $\alpha > 10$. According to Figure 54 ϕ_8 is strongly dependent on K_2 for $\alpha > 1$ and on K_1 for $\alpha < 10$.

The first type of waves has larger axial displacements for the parametric values defining the basic parametric case. However, from the results in Figures 8, 23 and 27 it follows that M_1 is inversely proportional to β_2^2 and M_3 is inversely proportional to β_2. Therefore, the ratio of the radial displacement to the axial displacement, (M_1/M_3), must become greater than one at a certain value of β_2. This change in the character of the mode shape is also observed in the inviscid limit and since β_2 is inversely proportional to the frequency, it implies

that the first type of waves exhibit predominantly axial displacements at low frequencies (large β_z) and predominantly radial displacements at high frequencies (small β_z). The same behavior was predicted for inviscid fluids by Maxwell[3].

For a given pressure variation the constraints may cause some interesting effects. With an increasing radial constraint the wave speed, attenuation, and axial displacements for the first type of waves are generally increasing while radial displacements, mass flow rate and axial fluid veclocity decrease. On the other hand, the second type of waves exhibit an increase in wave speed and a decrease in attenuation, wall displacement, fluid mass flow, and axial fluid velocity on the axis with increasing radial constraint. An increase in axial constraint causes an increase in speed and attenuation up to limiting values and a decrease in radial displacement, fluid mass flow and axial fluid velocity on the axis and axial displacement for the first type of waves. For the second type of waves the wave speed and attenuation increase.

B. **Fluid Velocity Profiles**

If only the incident wave of the first type occurs, then according to (III-34) and (III-35)

$$
w_1'(\kappa, z, t) = -\frac{i}{\rho \omega R_0} \frac{\sqrt{B_1}}{S_1} \left[S_1 - J_0 \left(i^{3/2} \alpha \frac{\kappa}{R_0} \right) \right] p(z,t)
$$

$$
u_1'(\kappa, z, t) = \frac{i}{\rho \omega R_0} \frac{B_1}{S_1} \left[\frac{i^{3/2}}{\alpha} J_1 \left(i^{3/2} \alpha \frac{\kappa}{R_0} \right) - \frac{S_1}{2} \frac{\kappa}{R_0} \right] p(z,t)
$$

These two equations can also be written in the form

$$
\frac{w_1'(\kappa, z, t)}{w_1'(0, z, t)} = \left[J_0 \left(i^{3/2} \alpha \frac{\kappa}{R_0} \right) - S_1 \right] / (1 - S_1) \tag{IV-7}
$$

$$
\frac{u_1'(\kappa, z, t)}{w_1'(0, z, t)} = \sqrt{B_1} \left[\frac{i^{-3/2}}{\alpha} J_1 \left(i^{3/2} \alpha \frac{\kappa}{R_0} \right) - \frac{S_1}{2} \frac{\kappa}{R_0} \right] / (1 - S_1) \tag{IV-8}
$$

Likewise, if only the incident wave of the second type occurs,

$$
w_2'(\kappa, z, t) = -\frac{i}{\rho \omega R_0} \frac{\sqrt{B_2}}{S_2} \left[S_2 - J_0 \left(i^{3/2} \alpha \frac{\kappa}{R_0} \right) \right] p(z,t)
$$

41

$$u_z'(\hbar, z, t) = \frac{i}{\rho \omega R_0} \frac{B_z}{S_z} \left[\frac{i^{-3/2}}{\alpha} J_1(i^{3/2}\alpha \frac{\hbar}{R_0}) - \frac{S_z}{2} \frac{\hbar}{R_0} \right] p(z, t)$$

or

$$\frac{w_z'(\hbar, z, t)}{w_z'(0, z, t)} = \left[J_0(i^{3/2}\alpha \frac{\hbar}{R_0}) - S_z \right] / (1 - S_z) \qquad \text{(IV-9)}$$

$$\frac{u_z'(\hbar, z, t)}{w_z'(0, z, t)} = \sqrt{B_z} \left[\frac{i^{-3/2}}{\alpha} J_1(i^{3/2}\alpha \frac{\hbar}{R_0}) - \frac{S_z}{2} \frac{\hbar}{R_0} \right] / (1 - S_z) \qquad \text{(IV-10)}$$

For these simple waves, the expressions (IV-7) to (IV-8) are plotted in Figures 55 to 58 for the basic case in the parametric analysis ($\sigma = 0.5$, $\beta_1 = 10$, $\beta_2 = 10^2$, $\kappa_1 = 0 = \kappa_2$) and three different values for α which range from very small Reynolds numbers to relatively large Reynolds numbers. The axial velocity for the waves of the first type is generally largest in the center of the tube but the difference between the magnitudes of the axial velcoity on the axis and that on the wall decreases with increasing Reynolds number. The magnitude of the radial velocity for the waves of the first type is largest near the tube wall, and its variations with $\hbar$ is greatest for low Reynolds numbers. With increasing Reynolds number the phase difference between the axial velocity at the tube wall and that on the tube axis decreases.

The most significant observation for the waves of the second type is that the change in magnitude and phase of the axial velocity across the tube is negligible at low Reynolds numbers. This absence of an appreciable relative velocity or shear at low Reynolds numbers accounts for the small attenuation of waves of the second type at low Reynolds numbers. At higher Reynolds numbers, the magnitude of the axial velocity at the tube wall is larger than at the axis. The difference in magnitude and phase for the axial velocity on the tube axis and on the tube wall increases with increasing Reynolds number. For the radial velocity the variation in the magnitude across the tube is greatest and the difference in phase is least at low Reynolds numbers.

C. Significance of the Constraint Parameters

Some information regarding the order of magnitude of the external constraint parameters for the cariovascular system can be obtained by considering the surrounding medium to be isotropic, perfectly elastic and incompressible. In such a case the stresses acting on the external surface of the artery can be approximated by the relations

42

$$K_1 \, \xi \approx \tau_{\lambda\lambda} = E_m \frac{\partial \xi}{\partial \lambda}$$

$$K_2 \, \varsigma \approx \tau_{\lambda z} = \frac{1}{2} E_m \left(\frac{\partial \xi}{\partial z} + \frac{\partial \varsigma}{\partial z} \right)$$

in which the orders of magnitude of the derivatives are given by

$$\frac{\partial \xi}{\partial \lambda} = O\left(\frac{\xi}{R_o}\right), \quad \frac{\partial \varsigma}{\partial \lambda} = O\left(\frac{\varsigma}{R_o}\right), \quad \frac{\partial \xi}{\partial z} = O\left(\frac{\xi}{\lambda}\right)$$

Therefore,

$$K_1 = O\left(E_m / R_o\right)$$

and

$$K_2 = O\left(\frac{E_m}{2R_o} \frac{\xi}{\varsigma} + \frac{E_m}{2R_o}\right) = O\left[\frac{E_m}{2R_o}\left(\frac{\xi}{\varsigma} + 1\right)\right]$$

With these results and the definitions of Γ_1, Γ_2, $\mathcal{K}_1$, and $\mathcal{K}_2$, one can write

$$\Gamma_1 = O\left(2 \frac{\rho_w}{\rho} \frac{E_m}{E} \beta_1^2 \beta_2^2\right)$$

$$\Gamma_2 = O\left[\frac{\rho_w}{\rho} \frac{E_m}{E} \beta_1^2 \beta_2^2 \left(\frac{\xi}{\varsigma} + 1\right)\right]$$

$$\mathcal{K}_1 = O\left(2 \frac{\rho_w}{\rho} \frac{E_m}{E} \beta_1^2\right)$$

$$\mathcal{K}_2 = O\left[\frac{\rho_w}{\rho} \frac{E_m}{E} \beta_1^2 \left(\frac{\xi}{\varsigma} + 1\right)\right]$$

The lowest order for Γ_2 and $\mathcal{K}_2$ is obtained for $(\xi/\varsigma) \ll 1$ and

$$(\Gamma_2)_{L.O.} = O\left(\frac{\rho_w}{\rho} \frac{E_m}{E} \beta_1^2 \beta_2^2\right), \quad (\mathcal{K}_2)_{L.O.} = O\left(\frac{\rho_w}{\rho} \frac{E_m}{E} \beta_1^2\right)$$

It has been shown that the minimum value for β_2 at long wave lengths is of order 1. Besides this, $(\rho_w/\rho) = O(1)$ and $\beta_1 = O(10)$ and, therefore, the lowest order of magnitude for the constraint parameter is

$$(\Gamma_1)_{L.O.} = O\left(200 \frac{E_m}{E}\right) = (\mathcal{K}_1)_{L.O.}, \quad (\Gamma_2)_{L.O.} = O\left(100 \frac{E_m}{E}\right) = (\mathcal{K}_2)_{L.O.}$$

In the parametric analysis for the inviscid limit ($\alpha \to \infty$) and for the very viscous fluid limit ($\alpha \to 0$), it was found that $\Gamma_2 = O(1)$ can cause dramatic

43

changes in the propagation characteristics of the second type of wave while $\Gamma_2' = O(1)$ has little effect upon waves of the first type. Also, it was shown that radial constraints only affected either type of waves when $\Gamma_1 \gg O(10^4)$.

For $(E_m/E) << 10^{-3}$, $(\mathcal{K}_1)_{L.O.} = (\Gamma_1)_{L.O.} << O(0.2)$, and $(\mathcal{K}_2)_{L.O.} = (\Gamma_2)_{L.O.} << O(0.1)$ waves of the first and second type should not be significantly affected. With $(E_m/E) > 10^{-2}$, $(\mathcal{K}_1)_{L.O.} = (\Gamma_1)_{L.O.} > O(2)$, and $(\mathcal{K}_2)_{L.O.} = (\Gamma_2)_{L.O.} > O(1)$ the waves of the second type should be rapidly attenuated. Likewise, waves of the first type are unaffected unless $(E_m/E) \gtrsim O(10^2)$. Therefore, with such a surrounding medium, the modulus of elasticity must be at least three orders of magnitude less than that of the vessel wall in order to produce negligible constraint effects, and it must be at least two orders of magnitude greater than that of the vessel wall in order to effect significantly the waves of the first type.

D. Application of this Analysis

1) General Comments

To apply the analysis presented in the preceeding sections to specific cases, the independent parameters α, β_1, β_2, σ, $\mathcal{K}_1$ and $\mathcal{K}_2$ must be prescribed. The wave propagation characteristics (wave speeds, attenuation factors, and mode shapes) can then be determined from the results given in the parametric analysis. The four arbitrary constants P_1, P_2, P_3, and P_4 appearing in the general solution are determined by satisfying four prescribed linear conditions imposed on the dependent variables.

In the past many analyses have considered only the first type of waves using the solution given by Womersley[10] The analysis presented in this report allows for a separate study of each type of waves as well as for the general solution involving both types of waves. Besides this, it takes into account the effects of a distributed radial constraint in addition to those of a distributed axial constraint introduced by Womersley[10].

This section will illustrate the possible errors induced by considering merely one type of waves and by neglecting reflected waves in the solution of a realistic problem. To this end the solutions corresponding to each type of waves will be examined separately and then compared with that involving both types of waves.

By considering only the first or radial type of waves $(P_{3_R} = 0 = P_{4_R})$,

44

Equations (III-31) and (III-34) to (III-39) reduce to

$$P_R(z,t) = P_{1R} e^{i\omega(t-\frac{z}{c_1})} e^{-\delta_1 z/R_0} + P_{2R} e^{i\omega(t+\frac{z}{c_1})} e^{\delta_1 z/R_0} \qquad \text{(IV-11)}$$

$$Q_R(z,t) = \frac{R_0}{\omega} M_5 e^{i\phi_5} \left[P_{1R} e^{i\omega(t-\frac{z}{c_1})} e^{-\delta_1 z/R_0} - P_{2R} e^{i\omega(t+\frac{z}{c_1})} e^{\delta_1 z/R_0} \right] \qquad \text{(IV-12)}$$

$$\xi_R(z,t) = \frac{M_1 e^{i\phi_1}}{\rho\omega^2 R_0} P_R(z,t) \quad , \quad \varsigma_R(z,t) = \frac{1}{\rho\omega^2 R_0^2} \frac{M_3}{M_5} e^{i(\phi_3-\phi_5)} Q_R(z,t) \qquad \text{(IV-13)}$$

$$w_R(0,z,t) = \frac{1}{\rho R_0^2} \frac{M_7}{M_5} e^{i(\phi_7-\phi_5)} Q_R(z,t) \qquad \text{(IV-14)}$$

The same equations yield for the second type of waves $(P_{1A} = 0 = P_{2A})$:

$$P_A(z,t) = P_{3A} e^{i\omega(t-\frac{z}{c_2})} e^{-\delta_2 z/R_0} + P_{4A} e^{i\omega(t+\frac{z}{c_2})} e^{\delta_2 z/R_0} \qquad \text{(IV-15)}$$

$$Q_A(z,t) = \frac{R_0}{\omega} M_6 e^{i\phi_6} \left[P_{3A} e^{i\omega(t-\frac{z}{c_2})} e^{-\delta_2 z/R_0} - P_{4A} e^{i\omega(t+\frac{z}{c_2})} e^{\delta_2 \frac{z}{R_0}} \right] \qquad \text{(IV-16)}$$

$$\xi_A(z,t) = \frac{M_2 e^{i\phi_2}}{\rho\omega^2 R_0} P_A(z,t) \quad , \quad \varsigma_A(z,t) = \frac{1}{\rho\omega R_0^2} \frac{M_4}{M_6} e^{i(\phi_4-\phi_6)} Q_A(z,t) \qquad \text{(IV-17)}$$

$$w_A(0,z,t) = \frac{1}{\rho R_0^2} \frac{M_8}{M_6} e^{i(\phi_8-\phi_6)} Q_A(z,t) \qquad \text{(IV-18)}$$

For each type of waves these results show that the radial wall displacement is proportional to the pressure and that the axial wall displacement and fluid velocity on the axis are both proportional to the instantaneous mass flow. Therefore, when only one type of waves and their reflections are admitted to the solution, one may not prescribe independent conditions on pressure and on the radial wall displacements at the same axial location. Similarly it is not

45

permissible to introduce independent conditions on the instantaneous mass flow, the axial wall displacement and the fluid velocity on the axis at a given axial location. For the solutions given above [Equations (IV-11) to (IV-14) or (IV-15) to (IV-18)] , only two conditions are necessary to specify the arbitrary constants.

Further specialization to only one wave of the first type leads to $P_1 = P_3 = P_4 = 0$ for a wave travelling in the $- z$ direction and $P_2 = P_3 = P_4 = 0$ for a wave travelling in the $+ z$ direction. Similarly a restriction to one wave of the second type implies $P_1 = P_2 = P_3 = 0$ for a wave travelling in the $- z$ direction and $P_1 = P_2 = P_4 = 0$ for a wave travelling in the $+ z$ direction. For such single wave solution the instantaneous mass flow, the wall displacements and the fluid velocity on the axis are all proportional to the pressure and, therefore, only one boundary condition is necessary to determine the motion of the system.

It is important to note that in the past all experimental investigations have attempted to interpret data in terms of only the first type of waves and in most cases the reflected waves (waves travelling in the $- z$ direction) were also neglected. However, in several of these investigations, the experimental apparatus described introduces incompatibilities with the solution that were considered for the wave motion. For example, an electromagnetic flowmeter restricts the radial wall displacement and according to (IV-13) and (IV-17) the pressure at that location will be affected.

The parametric analysis demonstrated that the wave propagation characteristics of the second type of waves are more sensitive to physical and geometric system parameters than those of the first type of waves. Therefore, it is particularly desirable to acquire experimental data on the second type of waves if the physical parameters are to be determined from wave transmission characteristics.

In order to document these comments, four sample calculations are given. The first three are intended to illustrate the possible errors that may evolve by interpreting data for pressure and instantaneous mass flow in terms of only the first type of waves. The imtention of the last sample calculation is to investigate the possibility of using simple constraints to excite the second type of waves.

2) Sample Calculation 1

As mentioned previously, in several experiments, the motion of the system at an arbitrary axial station is calculated from measurements of pressure and possibly fluid instantaneous mass flow at a given location, defined here by $z = 0$, using only the first type of waves. The pressure and instantaneous mass flow at $z = 0$ represent boundary conditions which can be written in the form $P_R(0,t) = P(0,t)$ and $Q_R(0,t) = Q(0,t)$. Utilizing those boundary conditions in (IV-11) and (IV-12) to evaluate the arbitrary constants P_{1R} and P_{2R} one obtains

$$\frac{2 P_R(z,t)}{e^{-i\omega t} P(0,t)} = \left[1 + \frac{\omega}{R_0 M_s} e^{-i\phi_s} \frac{Q(0,t)}{P(0,t)}\right] e^{i\omega\left(t - \frac{z}{c_1}\right)} e^{-S_1 z/R_0}$$

$$+ \left[1 - \frac{\omega}{R_0 M_s} e^{-i\phi_s} \frac{Q(0,t)}{P(0,t)}\right] e^{i\omega\left(t + \frac{z}{c_1}\right)} e^{S_1 z/R_0} \qquad \text{(IV-19)}$$

$$\frac{2 Q_R(z,t)}{e^{-i\omega t} Q(0,t)} = \left\{\left[1 + \frac{\omega}{R_0 M_s} e^{-i\phi_s} \frac{Q(0,t)}{P(0,t)}\right] e^{i\omega\left(t - \frac{z}{c_1}\right)} e^{-S_1 z/R_0}\right.$$

$$\left. - \left[1 - \frac{\omega}{R_0 M_s} e^{-i\phi_s} \frac{Q(0,t)}{P(0,t)}\right] e^{i\omega\left(t + \frac{z}{c_1}\right)} e^{S_1 z}\right\} \frac{P(0,t)}{Q(0,t)} \frac{R_0}{\omega} M_s e^{i\phi_s} \quad \text{(IV-20)}$$

From these relations it follows that the presence of merely one wave travelling in the $+z$ direction (incident wave) is only possible if the measured mass flow and pressure satisfy the condition $Q(0,t) = \frac{R_0}{\omega} M_s e^{i\phi_s} P(0,t)$ in which M_s and ϕ_s are exclusively defined by the system parameters and frequency through σ, β_1, β_2, Γ_1 or K_1 and Γ_2 or K_2. Likewise, there can only be a single wave travelling in the $-z$ direction (reflected wave) if $Q(0,t) = -\frac{R_0}{\omega} M_s e^{i\phi_s} P(0,t)$. For all other values of $Q(0,t)/P(0,t)$ both incident and reflected waves must be present.

When only waves of the second or axial type are present, Equations (IV-15) and (IV 16) together with the boundary conditions $P_A(o,t) = p(o,t)$ and $Q_A(o,t) = Q(o,t)$ yield

$$\frac{2 P_A(z,t)}{e^{-iwt} p(o,t)} = \left[1 + \frac{\omega e^{-i\phi_L}}{R_o M_L} \frac{Q(o,t)}{p(o,t)} \right] e^{iw\left(t - \frac{z}{C_z}\right)} e^{-\delta_z z/R_o}$$

$$+ \left[1 - \frac{\omega e^{-i\phi_L}}{R_o M_L} \frac{Q(o,t)}{p(o,t)} \right] e^{iw\left(t + \frac{z}{C_z}\right)} e^{\delta_z z/R_o} \qquad \text{(IV-21)}$$

$$\frac{2 Q_A(z,t)}{e^{-iwt} Q(o,t)} = \left\{ \left[1 + \frac{\omega e^{-i\phi_L}}{R_o M_L} \frac{Q(o,t)}{p(o,t)} \right] e^{iw\left(t - \frac{z}{C_z}\right)} e^{-\delta_z z/R_o} \right.$$

$$\left. - \left[1 - \frac{\omega e^{-i\phi_L}}{R_o M_L} \frac{Q(o,t)}{p(o,t)} \right] e^{iw\left(t + \frac{z}{C_z}\right)} e^{\delta_z z/R_o} \right\} \frac{p(o,t)}{Q(o,t)} \frac{R_o}{\omega} M_L e^{i\phi_L} \qquad \text{(IV-22)}$$

In this case only the incident wave is present if $Q(o,t)/p(o,t) = \frac{R_o}{\omega} M_L e^{i\phi_L}$ and only the reflected wave if $Q(o,t)/p(o,t) = -\frac{R_o}{\omega} M_L e^{i\phi_L}$. For all other values of $Q(o,t)/p(o,t)$ both waves must be present. (Note that M_L and ϕ_L are determined by the system parameters and the frequency).

3) Sample Calculation 2

In this sample calculation it will be shown that there can be an appreciable difference between the values for the pressure at a given axial location as predicted by the solution representing only the first type of waves and by the general solution if a discrete axial and/or radial displacement constraint is imposed on the vessel. The pressure and fluid flow rate at $z = o$ are assumed to be the same in both solutions. Then, the pressure and motion of the system are given by (IV-13), (IV-14), (IV-19) and (IV-20) when only the first type of waves is assumed to be present. At $z = o$ the following arbitrary and independent displacement constraints are applied:

48

$$\xi(o,t) / \xi_R(o,t) = \pi_1 \quad , \quad \zeta(o,t) / \zeta_R(o,t) = \pi_2 \qquad \text{(IV-23)}$$

where π_1 and π_2 are arbitrary constants.

With (IV-23) and the conditions on pressure and fluid flow rate at $z=0$ one obtains from (III-31) and (III-36) to (III 38)

$$P_1 = \tfrac{1}{2} p(o,t) \left\{ \left(1 - \frac{1-\pi_1}{1-S_1'}\right) + \left(1 - \frac{1-\pi_2}{S_2'-S_3'} S_2'\right) \frac{\omega e^{-i\phi_s}}{R_0 M_s} \frac{Q(o,t)}{p(o,t)} \right\} \qquad \text{(IV-24)}$$

$$P_2 = \tfrac{1}{2} p(o,t) \left\{ \left(1 - \frac{1-\pi_1}{1-S_1'}\right) - \left(1 - \frac{1-\pi_2}{S_2'-S_3'} S_2'\right) \frac{\omega e^{-i\phi_s}}{R_0 M_s} \frac{Q(o,t)}{p(o,t)} \right\} \qquad \text{(IV-25)}$$

$$P_3 = \tfrac{1}{2} p(o,t) \left\{ \frac{1-\pi_1}{1-S_1'} + \frac{1-\pi_2}{S_2'-S_3'} \frac{\omega e^{-i\phi_s}}{R_0 M_s} \frac{Q(o,t)}{p(o,t)} \right\} \qquad \text{(IV-26)}$$

$$P_4 = \tfrac{1}{2} p(o,t) \left\{ \frac{1-\pi_1}{1-S_1'} - \frac{1-\pi_2}{S_2'-S_3'} \frac{\omega e^{-i\phi_s}}{R_0 M_s} \frac{Q(o,t)}{p(o,t)} \right\} \qquad \text{(IV-27)}$$

where $\quad S_1' = \frac{M_2}{M_1} e^{i(\phi_2-\phi_1)} \quad , \quad S_2' = \frac{M_6}{M_s} e^{i(\phi_6-\phi_s)} \quad , \quad S_3' = \frac{M_4}{M_3} e^{i(\phi_4-\phi_3)} \quad$ (IV-28)

It should be noted that with $\pi_1 = 1 = \pi_2$ these constants P_1 to P_4 reduce to the values corresponding to the first type of waves. Also, for $\pi_1 = 0$, there is no radial displacement possible at $z=0$ and, for $\pi_2 = 0$, no axial displacement can develop at $z=0$.

For the parameter values

49

$$\sigma = 0.5 \quad , \quad \beta_1 = 10 \quad , \quad \beta_2 = 10^2, \quad \mathcal{K}_1 = 0 = \mathcal{K}_2 \quad , \quad \alpha = 4$$

and
$$\frac{\omega e^{-i\phi_s}}{R_o M_s} \frac{Q(o,t)}{\mathcal{P}(o,t)} = 1 \qquad \text{(IV-29)}$$

as a condition for only one radial wave travelling in the $+z$ direction, the constants P_1 to P_4 as defined by Equations (IV-24) to (IV-28) were evaluated and substituted into the expressions (III 31) and (III-38) for the pressure and mass flow described by the general solution. The pressure and mass flow for the corresponding radial wave were obtained from (IV-19) and (IV-20). The results are given in the form of the relative errors $(P-P_R)/P_R$ and $(Q-Q_R)/Q_R$ and are plotted in Figures 59 and 60 for various values of π_1 and π_2 . From Figure 59 it follows that a rigid displacement constraint produces an error in the magnitude of the mass flow which increases with z and is of the order of 20% at $z = 20 R_o$. The magnitude of the relative error in the mass flow is more significant than that for the pressure when only a radial constraint is present. However, in either case, the radial constraint has a more pronounced effect.

4) <u>Sample Calculation 3</u>

In the previous example both discrete displacement constraints were applied at the axial location where also the pressure and mass flow were prescribed. Often the vessel segment of interest is subjected to constraints at more than one location. For example, one may have electromagnetic flow meters at both ends of the segment exerting radial constraints. To simulate such a situation, a model is considered in which the pressure and mass flow at the upstream end of the tube are prescribed, and radial constraints are applied at both ends of the tube. The constraints are again expressed in the form:

$$\xi(o,t) / \xi_R(o,t) = \pi_3 = \xi(L,t) / \xi_R(L,t) \qquad \text{(IV-30)}$$

By specifying the pressure and mass flow at $z = 0$, one obtains from (IV-19) and (IV-20)

$$\frac{P_R(L,t)}{P(0,t)} e^{iwL/c_1} e^{\delta_1 L/R_0} = 1 +$$
$$+ \frac{1}{2}\left[e^{2iwL/c_1} e^{2\delta_1 L/R_0} - 1\right]\left[1 - \frac{we^{-i\phi_s}}{R_0 M_s} \frac{Q(0,t)}{P(0,t)}\right] \tag{IV-31}$$

$$\frac{Q_R(L,t)}{Q(0,t)} \frac{w}{R_0} \frac{Q(0,t)}{P(0,t)} e^{iwL/c_1} e^{\delta_1 L/R_0} = 1 - e^{i2wL/c_1} e^{2\delta_1 L/R_0}$$
$$+ \frac{1}{2}\left[3 - e^{i2wL/c_1} e^{2\delta_1 L/R_0}\right] \frac{we^{-i\phi_s}}{R_0 M_s} \frac{Q(0,t)}{P(0,t)} \tag{IV-32}$$

and with (IV-30) the general solution for pressure and mass flow can also be determined. The relative error for pressure and mass flow in this case are given by

$$\left[P(L,t) - P_R(L,t)\right]/\left[P(0,t)(1-\pi_3) e^{-iwL/c_1} e^{-\delta_1 L/R_0}\right] = P_1'$$
$$+ P_2' e^{i2wL/c_1} e^{2\delta_1 L/R_0} + e^{iw(\frac{L}{c_1} - \frac{L}{c_2})} e^{(\delta_1 - \delta_2)\frac{L}{R_0}}\left[P_3'\right.$$
$$\left. + P_4' e^{i2wL/c_1} e^{2\delta_1 L/R_0}\right] \tag{IV-33}$$

$$\left[Q(L,t) - Q_R(L,t)\right]/\left[\frac{R_0}{w} P(0,t)(1-\pi_3) e^{-iwL/c_1} e^{-\delta_1 L/R_0}\right] = P_1'$$
$$- P_2' e^{i2wL/c_1} e^{2\delta_1 L/R_0} + e^{iw(\frac{L}{c_1} - \frac{L}{c_2})} e^{(\delta_1 - \delta_2)\frac{L}{R_0}}\left[P_3' - \right.$$
$$\left. - P_4' e^{i2wL/c_1} e^{2\delta_1 L/R_0}\right]\frac{M_6}{M_s} e^{i(\phi_6 - \phi_s)} \tag{IV-34}$$

where
$$P_1' = P_{11} + P_{12} \frac{\omega e^{-i\phi_5}}{R_0 M_5} \frac{Q(0,t)}{p(0,t)} \tag{IV-35}$$

$$P_2' = P_{21} + P_{22} \frac{\omega e^{-i\phi_5}}{R_0 M_5} \frac{Q(0,t)}{p(0,t)} \tag{IV-36}$$

$$P_3' = P_{31} + P_{32} \frac{\omega e^{-i\phi_5}}{R_0 M_5} \frac{Q(0,t)}{p(0,t)} \tag{IV-37}$$

$$P_4' = P_{41} + P_{42} \frac{\omega e^{-i\phi_5}}{R_0 M_5} \frac{Q(0,t)}{p(0,t)} \tag{IV-38}$$

$$P_{12} = -\frac{1}{2}\Big\{ 1 - \big[e^{i2\omega L/c_2} e^{2\delta_2 L/R_0} -$$
$$- 1\big] e^{i\omega(\frac{L}{c_1} - \frac{L}{c_2})} e^{(\delta_1 - \delta_2)\frac{L}{R_0}} \frac{M_2 M_6}{M_1 M_5} e^{i(\phi_2 - \phi_1 + \phi_6 - \phi_5)} \big[e^{i2\omega L/c_1} e^{2\delta_1 L/R_0}$$
$$- 1\big]^{-1} \Big\}^{-1} \tag{IV-39}$$

$$P_{11} = -2 P_{12}\Big\{ -\frac{1}{2} + \big[\frac{1}{2}(e^{i2\omega L/c_2} e^{2\delta_2 L/R_0} - 1) e^{i\omega(\frac{L}{c_1} - \frac{L}{c_2})} (\frac{M_5}{M_6} e^{i(\phi_5 - \phi_6)}$$
$$- 1) e^{(\delta_1 - \delta_2)\frac{L}{R_0}} + e^{i\omega(\frac{L}{c_1} + \frac{L}{c_1})} e^{(\delta_1 + \delta_2)\frac{L}{R_0}} -$$
$$- e^{i2\omega L/c_1} e^{2\delta_1 L/R_0} \Big\} / \big[(\frac{M_1}{M_2} e^{i(\phi_1 - \phi_2)} - 1)(e^{i2\omega L/c_1} e^{2\delta_1 L/R_0} - 1) \big] \tag{IV 40}$$

$$P_{21} = -P_{11} - \big[1 - \frac{M_2}{M_1} e^{i(\phi_2 - \phi_1)} \big]^{-1} \tag{IV-41}$$

52

$$P_{32} = -P_{12} \quad , \quad P_{32} = -P_{12} \frac{M_s}{M_6} e^{i(\phi_s - \phi_6)} = -P_{42} \qquad \text{(IV-42)}$$

$$P_{31} = -\left\{ P_{11} + \frac{1}{2} \left[1 - \frac{M_6}{M_s} e^{i(\phi_6 - \phi_s)} \right] \Big/ \left[1 - \frac{M_2}{M_1} e^{i(\phi_2 - \phi_1)} \right] \right\} \frac{M_s}{M_6} e^{i(\phi_s - \phi_6)} \qquad \text{(IV-43)}$$

$$P_{41} = -P_{31} + \left[1 - \frac{M_2}{M_1} e^{i(\phi_2 - \phi_1)} \right]^{-1} \qquad \text{(IV-44)}$$

Results for

$$\alpha = 4 \, , \ \beta_1 = 10 \, , \ \beta_2 = 10^2 \, , \ K_1 = 0 = K_2 \quad , \ \sigma = 0.5 \qquad \text{(IV 45)}$$

and
$$\frac{Q(0,t)}{P(0,t)} = a e^{i\beta} \, , \ \frac{\omega a}{R_0 M_s} = 1 \, , \ \beta - \phi_s = 0 \ \text{AND} \ 180^\circ \qquad \text{(IV-46)}$$

are shown on Figures 61 and 62. Note that with $\beta - \phi_s = 0$ and $\frac{\omega a}{R_0 M_s} = 1$, equations (IV-31) and (IV-32) predict the first type travelling in the $+z$ direction, while $\beta - \phi_s = 180^\circ$ gives a wave travelling in the $-z$ direction. The results in Figures 61 and 62 display the relative errors for pressure and mass flow. The phase of these errors is in the neighborhood of 90°. It is apparent that in this case the relative errors are much larger than in Sample Calculation 2.

A comparison of the variations of pressure and mass flow at an axial location as predicted by the first type of wave in the absence of axial constraints with those obtained from the general solution satisfying the radial constraints is also of interest. Figure 63 shows the results for

53

$$P_R(L,t)/A_p \quad , \quad p(L,t)/A_p \quad , \quad \frac{\omega\, Q_R(L,t)}{R_o\, M_s\, A_p} \quad , \text{ AND } \quad \frac{\omega\, Q(L,t)}{R_o\, M_s\, A_p}$$

calculated from (IV-31) to (IV-34) by using the parameters given in (IV-45) together with

$$\frac{L}{R_o} = 30 \, , \quad p(o,t) = A_p e^{i\omega t} \, , \quad \frac{\omega a}{R_o M_s} = 1 \, , \quad \beta - \phi_s = 0 \, , \quad \pi_3 = 0$$

It is evident that the approximate solution in the form of the first type of waves has the same basic pattern as the general solution. However, there is a considerable phase difference between them. Also, the approximate solution overestimates the magnitude of the mass flow by about 12%.

5) Sample Calculation 4

The purpose of this example is to investigate the generation of waves of the second type by simple discrete displacement constraints applied to a tube of given length. The results in the previous two examples showed that discrete radial constraints could produce significant changes in pressure and mass flow as predicted by the terms of only the first type of waves. Therefore, the type of constraints introduced in Sample Calculation 3 may be considered a device to generate waves of the second type. A reasonable measure for the effectiveness of exciting the second type of waves is the difference in the arbitrary constants P_1 , P_2 , P_3 , P_4 , as defined by the general solution satisfying all four boundary conditions and those corresponding to the approximate solution involving only the second type of waves and complying with the pressure and mass flow boundary condition at $z = o$.

The solution in terms of the second type of waves is given by (IV-15) to (IV-18), (IV-21) and (IV-22), where the constants in (IV-15) and (IV-16) are

$$P_{1A} = 0, \quad P_{3A} = \tfrac{1}{2} e^{-i\omega t} p(o,t) \left[1 + \frac{\omega}{R_o} \frac{e^{-i\phi_6}}{M_6} \frac{Q(o,t)}{p(o,t)} \right] \qquad \text{(IV-47)}$$

$$P_{2A} = 0, \quad P_{4A} = \tfrac{1}{2} e^{-i\omega t} p(o,t) \left[1 - \frac{\omega}{R_o} \frac{e^{-i\phi_6}}{M_6} \frac{Q(o,t)}{p(o,t)} \right] \qquad \text{(IV-48)}$$

54

Substituting the pressure and mass flow conditions at $z=0$ together with

$$\frac{\xi(0,t)}{\xi_A(0,t)} = \pi_1 = \text{CONSTANT} \qquad \text{and} \qquad \frac{\xi(L,t)}{\xi_A(L,t)} = \pi_3 = \text{CONSTANT} \qquad \text{(IV 49)}$$

into (III-31), (III-36) and (III-38) one obtains

$$\frac{P_1 - P_{1A}}{e^{-i\omega t} p(0,t)} = (1-\pi_1)P_{11} + (1-\pi_3)\left[P_{12} + P_{13}\frac{\omega}{R_0}\frac{e^{-i\phi_6}}{M_6}\frac{Q(0,t)}{p(0,t)}\right] \qquad \text{(IV-50)}$$

$$\frac{P_2 - P_{2A}}{e^{-i\omega t} p(0,t)} = (1-\pi_1)P_{21} - (1-\pi_3)\left[P_{12} + P_{13}\frac{\omega}{R_0}\frac{e^{-i\phi_6}}{M_6}\frac{Q(0,t)}{p(0,t)}\right] \qquad \text{(IV-51)}$$

$$\frac{P_3 - P_{3A}}{e^{-i\omega t} p(0,t)} = (1-\pi_1)P_{31} - (1-\pi_3)\left[P_{32} + P_{33}\frac{\omega}{R_0}\frac{e^{-i\phi_6}}{M_6}\frac{Q(0,t)}{p(0,t)}\right] \qquad \text{(IV 52)}$$

$$\frac{P_4 - P_{4A}}{e^{-i\omega t} p(0,t)} = (1-\pi_1)P_{41} + (1-\pi_3)\left[P_{32} + P_{33}\frac{\omega}{R_0}\frac{e^{-i\phi_6}}{M_6}\frac{Q(0,t)}{p(0,t)}\right] \qquad \text{(IV-53)}$$

where

$$P_{11} = \left[\frac{M_1}{M_2}e^{i(\phi_1-\phi_2)}e^{i\omega(\frac{L}{C_1}+\frac{L}{C_2})}e^{(S_1+S_2)\frac{L}{R_0}} + \frac{1}{2}\left(\frac{M_5}{M_6}e^{i(\phi_5-\phi_6)}-\right.\right.$$

$$\left.\left. - 1\right)-\frac{1}{2}e^{i2\omega L/C_2}e^{2S_2 L/R_0}\left(1+\frac{M_5}{M_6}e^{i(\phi_5-\phi_6)}\right)\right]/D_2 \qquad \text{(IV-54)}$$

$$P_{12} = \frac{1}{2}\left[1+ e^{i2\omega L/C_2}e^{2S_2 L/R_0}\right]/D_1 \qquad \text{(IV-55)}$$

55

$$P_{13} = \frac{1}{2}\left[1 - e^{i2\omega L/c_2} e^{2\delta_2 L/R_0} \right] / D_1 \qquad \text{(IV-56)}$$

$$P_{21} = \left[\frac{M_1}{M_2} e^{i(\phi_1-\phi_2)} e^{i\omega(\frac{L}{c_2}-\frac{L}{c_1})} e^{(\delta_2-\delta_1)\frac{L}{R_0}} + \frac{1}{2}\left(1 + \frac{M_5}{M_6} e^{i(\phi_5-\phi_6)} \right) \right.$$
$$\left. + \frac{1}{2} e^{i\omega 2L/c_2} e^{2\delta_2 L/R_0} \left(1 - \frac{M_5}{M_6} e^{i(\phi_5-\phi_6)} \right) \right] / D_2 \qquad \text{(IV-57)}$$

$$D_2 P_{31} = \left\{ \frac{M_5}{M_6} e^{i(\phi_5-\phi_6)} e^{i2\omega L/c_2} e^{2\delta_2 L/R_0} + \frac{1}{2}\frac{M_1}{M_2} e^{i(\phi_1-\phi_2)} e^{i\omega(\frac{L}{c_2}-\frac{L}{c_1})} \left[1 - \right. \right.$$
$$\left. \left. - e^{i2\omega L/c_1} e^{2\delta_1 L/R_0} - \frac{M_5}{M_6} e^{i(\phi_5-\phi_6)} \left(1 + e^{i2\omega L/c_1} e^{2\delta_1 L/R_0} \right) \right] e^{(\delta_2-\delta_1)\frac{L}{R_0}} \right\} \qquad \text{(IV-58)}$$

$$P_{32} = \frac{M_5}{M_6} e^{i(\phi_5-\phi_6)} P_{12} \qquad \text{(IV-59)}$$

$$P_{33} = \frac{M_5}{M_6} e^{i(\phi_5-\phi_6)} P_{13} \qquad \text{(IV-60)}$$

$$P_{41} = \left\{ -\frac{M_5}{M_6} e^{i(\phi_5-\phi_6)} + \frac{1}{2}\frac{M_1}{M_2} e^{i(\phi_1-\phi_2)} e^{i\omega(\frac{L}{c_2}-\frac{L}{c_1})} e^{(\delta_2-\delta_1)\frac{L}{R_0}} \left[1 - \right. \right.$$
$$\left. \left. - e^{i2\omega\frac{L}{c_1}} e^{2\delta_1\frac{L}{R_0}} + \frac{M_5}{M_6} e^{i(\phi_5-\phi_6)} \left(1 + e^{i2\omega L/c_1} e^{2\delta_1\frac{L}{R_0}} \right) \right] \right\} / D_2 \qquad \text{(IV-61)}$$

$$D_1 = \frac{M_5}{M_6} e^{i(\phi_5-\phi_6)} \left(1 - e^{i2\omega L/c_2} e^{2\delta_2 L/R_0} \right) -$$
$$- \frac{M_1}{M_2} e^{i(\phi_1-\phi_2)} e^{i\omega(\frac{L}{c_2}-\frac{L}{c_1})} e^{(\delta_2-\delta_1)\frac{L}{R_0}} \left(1 - e^{i2\omega L/c_1} e^{2\delta_1 L/R_0} \right) \qquad \text{(IV-62)}$$

$$D_2 = \left(1 - \frac{M_1}{M_2} e^{i(\phi_1-\phi_2)} \right) D_1 \qquad \text{(IV-63)}$$

The difference in the arbitrary constraints are nondimensionalized with respect to the magnitude of the pressure at $z=0$ and are given in Figures 64 and 65.

$$\alpha = 4, \quad \sigma = 0.5, \quad \beta_1 = 10, \quad \beta_2 = 10^2, \quad \kappa_1 = 0 = \kappa_2, \quad \pi_1 = \pi_3$$

$$\text{and} \quad \frac{\omega e^{-i\phi_c}}{R_o M_c} \frac{Q(0,t)}{p(0,t)} = \begin{cases} 1 & \text{(axial wave in } + z \text{ dir.)} \\[2mm] 0.847\, e^{-i\,110^\circ} & \text{(radial wave in } + z \text{ dir.)} \\[2mm] 0.847\, e^{i\,70^\circ} & \text{(radial wave in } - z \text{ dir.)} \end{cases}$$

where the comments in parentheses indicate the wave type which would have the corresponding pressure-flow relationship at $z=0$. It is obvious that the differences in the arbitrary constants are zero for $\pi_1 = 1$ which is the condition that the radial displacements at $z=0$ and $z=L$ are those associated with a wave of the second type.

The results of this and the previous two sample calculations demonstrate that any application of discrete constraints induces the second type of waves.

V. COMPARISON OF ANALYSIS WITH EXPERIMENTAL RESULTS

A. Elastic Wall Analytical Results

1) <u>Experimental Results of Van Citters</u>[14]. The experimental results of Van Citters are of particular interest since they corroborate the existence and some of the propagation characteristics of the second type of waves. In these experiments a Penrose tube of 100 cm length was connected to rigid tubing at both ends. The tube was filled with water or glycerin. At one end of the tube a step pressure pulse was produced and near the other end the tube was instrumented to measure pressure and axial and radial wall displacements.

From oscillograph recordings of the disturbances in pressure and wall displacements, Van Citters concluded that two types of waves were generated whose speeds were approximately 6m/sec. and 30 m/sec. when the tube was filled with water. The pressure and radial wall displacement appeared to travel at the lowest speed while the axial wall displacement travelled at the faster speed. On the basis of these observations, it was concluded that two independent waves occur; a longitudinal wave with strong axial displacements and a pressure wave accompanied by large radial wall displacements. Furthermore, it was shown that a manual griping of the tube, which simulated a distributed external constraint, produces essentially a complete attenuation of the longitudinal waves. Besides this the amplitude of the longitudinal waves was reduced considerably by substituting glycerin for water.

The results of the parametric analysis show that the magnitude of the pressure variation associated with the second type of wave is much smaller than that for the first type of wave. Consequently, the step pressure pulse should excite primarily the first type of waves. However, Sample Calculations 2 and 3 demonstrated that the clamps holding the tube onto the rigid tubing will require both types of waves to be generated. The exact character of the clamping was not reported and, therefore, the relative strengths of the two types of waves can not be determined theoretically. But it is apparent from the oscillograph recordings that the pressure fluctuations associated with the second type of waves are much smaller than those for the first type of waves. A comparison of the results on Figures 23 to 30 shows that the magnitude of the axial displacements for the second type of waves can still be much larger than those for the first type of waves, even though the magnitudes of the radial wall displacements and pressure fluctuations are extremely small. The parametric analysis also

demonstrated that the dissipation of the second type of waves is larger and specifically predicts a large increase in the dissipation with a weak distributed constraint (the manual gripping). Finally, the ratio of wave speeds $(c_2/c_1 \approx 5)$ is in agreement with the analytical predictions.

2) <u>Experimental Results of Anliker, et al.</u>[13]. During the past two years wave transmission experiments were conducted on anesthetized dogs. Finite trains of small sinusoidal pressure waves were induced in the thoracic aorta of mature mongrel dogs weighing between 20 and 40 kg. These waves were generated by an electrically driven impactor which produced small indentation of the vessel wall. The pressure signals had amplitudes that were generally less than 5mm. Hg peak to peak. Typical results obtained in these experiments for frequencies between 60 and 200 cps. are illustrated in Figures 66 and 67. From Figure 66 it follows that the thoracic aorta is only mildly dispersive with respect to pressure waves in this frequency range as predicted by the theoretical results given in this analysis. The attenuation of such waves in the form of the amplitude ratio A/A_0 as a function of the propagation distance measured in wave lengths is shown in Figure 67. It was found that

$$\frac{A}{A_0} \approx e^{-0.87 \, z/\lambda} \tag{V-1}$$

independent of frequency. No waves of the second type were observed in these experiments.

For the thoracic aorta and frequency between 60 and 200 cps, $\alpha^2 = \frac{\omega}{\nu} R_0^2$ is a large quantity. Therefore, the experimental results may be compared with the limiting solution for large values of α given in section III. Measurements of the aorta showed that

$$R_0 \approx 4.4 \text{ mm.} \quad , \quad h = 1.25 \text{ mm.}$$

The viscosity coefficient of the blood is assumed to be $\nu = 0.05 \text{ cm}^2/\text{sec}$ and the vessel wall is considered incompressible $, \sigma = 1/2$. As limiting phase velocity for large frequencies the experiments yield

$$C_o \cong 5 \ M/SEC$$

Since the aorta was surgically exposed in this experiment the vessel is not subjected to distributed constraints and, therefore, $\Gamma_1 = 0 = \Gamma_2$. With these values for C_o , R_o , and υ one obtains

$$\beta_2 = \frac{182.5 \ CPS}{F} \quad , \quad \alpha^2 = \frac{F}{0.0416 \ CPS} \tag{V-2}$$

The quantities K_1' , $\sqrt{K_3}$ and K_2' are real and positive in this case and hence (III-33) and (III-53) yield

$$\sqrt{B_1} = i \left[\frac{1}{2K_1'} \left(\sqrt{K_3} + \frac{K_2'}{1 - \sigma/2} \right) \right]^{1/2} \left[1 + \frac{1-i}{\sqrt{2} \ \alpha} \ \frac{K_7}{2} \right]$$

$$\frac{C_o}{C_1} = \beta_2 \left[\frac{1}{2K_1'} \left(\sqrt{K_3} + \frac{K_2'}{1 - \sigma/2} \right) \right]^{1/2} \left[1 + \frac{K_7}{2\sqrt{2} \ \alpha} \right]$$

$$\delta_1 = \left[\frac{1}{2K_1'} \left(\sqrt{K_3} + \frac{K_2'}{1 - \sigma/2} \right) \right]^{1/2} \frac{K_7}{2\sqrt{2} \alpha}$$

$$\delta_1 \frac{\lambda_1}{R_o} = \delta_1 \left(2\pi \ \beta_2 \ \frac{C_1}{C_o} \right) = \frac{\pi \ K_7}{\sqrt{2} \ \alpha}$$

Furthermore, the predicted damping of the sinusoidal waves is given by

$$\frac{A}{A_o} = e^{-\delta_1 z/R_o} = e^{-\delta_1 \frac{\lambda_1}{R_o} \frac{z}{\lambda_1}} = e^{\left(-\frac{\pi K_7}{\sqrt{2} \alpha} \right) \frac{z}{\lambda_1}} \tag{V-3}$$

This implies that A/A_o is an exponential function proportional to z/λ_1 . However, the coefficient of z/λ_1 is not independent of frequency. Also, calculations show that $K_7 \approx 1$ and $\alpha \approx 38.0$ at 60 cps. and, therefore, the coefficient of z/λ_1 is only $\frac{\pi K_7}{\sqrt{2} \alpha} = 0.0615$ for $F = 60$ cps. and decreases as the frequency increases.

From this result one may conclude that the viscosity of the blood can

only account for a small fraction of the attenuation of the sinusoidal pressure waves observed in the thoracic aorta of anesthetized dogs for frequencies between 60 and 200 cps. Also, since the aorta was exposed, any attenuation of the waves due to the radiation of energy into the surrounding medium may be disregarded. Therefore, the strong attenuation of the sinusoidal pressure waves must be attributed to damping mechanisms in the aorta wall.

B. Solution With Viscoelastic Wall and Large Reynolds Number

To account for the high attenuation of the pressure waves observed in the experiments the vessel wall is now assumed to behave like a viscoelastic solid. Moreover, since the frequencies of the sine waves generated in Reference 13 are generally above 20, the corresponding values for α may be considered as large. For comparison, the analysis can, therefore, be restricted to large Reynolds numbers.

According to the correspondence principle, the large Reynolds number solution for viscoelastic walls can be obtained simply by replacing Young's modulus E and Poisson's ratio σ in Equations (III-53) to (III-71) by their complex counterparts

$$E = E_R + i\omega E_V, \quad \sigma = \sigma_R + i\omega\sigma_V, \text{ WHERE } \frac{\omega E_V}{E_R} << 1 >> \omega\sigma_V \quad (V-4)$$

In the resulting relations the quantities $\omega E_V/E_R$, $\omega\sigma_V$ and $1/\alpha$ are considered as small parameters, which allows the solutions for the wave speeds, the attenuation factors, the mode shapes and phase angles to be written as:

$$\frac{C_{oR}}{C_1} = \beta_{2R}\sqrt{A_+}\left(1 + \frac{K_{7R}}{2\sqrt{2}\alpha}\right), \quad \frac{C_{oR}}{C_2} = \beta_{2R}\sqrt{A_-}\left(1 + \frac{K_{8R}}{2\sqrt{2}\alpha}\right) \quad (V-5)$$

$$\delta_1 = \frac{1}{2}\sqrt{A_+}\left\{-\left(B_+ \frac{\omega E_V}{E_R} + C_+ \omega\sigma_V\right) + \frac{K_{7R}}{\sqrt{2}\alpha}\right\} \quad (V-6)$$

$$\delta_2 = \frac{1}{2}\sqrt{A_-}\left\{-\left(B_- \frac{\omega E_V}{E_R} + C_- \omega\sigma_V\right) + \frac{K_{8R}}{\sqrt{2}\alpha}\right\} \quad (V-7)$$

$$\delta_1 \frac{\lambda_1}{R_o} = \pi\left\{-\left(B_+ \frac{\omega E_V}{E_R} + C_+ \omega\sigma_V\right) + \frac{K_{7R}}{\sqrt{2}\alpha}\right\} \quad (V-8)$$

61

$$\delta_2 \, \frac{\lambda_2}{R_o} = \pi \left\{ -\left(B_- \frac{\omega E_V}{E_R} + C_- \omega \sigma_V \right) + \frac{K_{8R}}{\sqrt{2} \, \alpha} \right\} \qquad \text{(V-9)}$$

$$M_1 e^{i\phi_1} = \tfrac{1}{2} A_+ \left\{ 1 + i\left(B_+ \frac{\omega E_V}{E_R} + C_+ \omega \sigma_V \right) + \frac{(1-i)}{\sqrt{2}\,\alpha} \left(K_{7R} - \frac{2}{K_{5R}} \right) \right\} \qquad \text{(V-10)}$$

$$M_2 e^{i\phi_2} = \tfrac{1}{2} A_- \left\{ 1 + i\left(B_- \frac{\omega E_V}{E_R} + C_- \omega \sigma_V \right) + \frac{(1-i)}{\sqrt{2}\,\alpha} \left(K_{8R} - \frac{2}{K_{9R}} \right) \right\} \qquad \text{(V-11)}$$

$$M_3 e^{i\phi_3} = -i \left(\frac{K_{5R}-1}{K_{5R}} \right) \sqrt{A_+} \left\{ 1 + i \left(K_{51} \frac{\omega E_V}{E_R} + K_{52} \omega \sigma_V \right) / (K_{5R}-1) + \right.$$
$$\left. + \frac{i}{2} \left(B_+ \frac{\omega E_V}{E_R} + C_+ \omega \sigma_V \right) + \frac{(1-i)}{\sqrt{2}\,\alpha} \left(\frac{K_{7R}}{2} + \frac{K_{6R}}{K_{5R}(K_{5R}-1)} \right) \right\} \qquad \text{(V-12)}$$

$$M_4 e^{i\phi_4} = -i \left(\frac{K_{9R}-1}{K_{9R}} \right) \sqrt{A_-} \left\{ 1 + i \left(K_{91} \frac{\omega E_V}{E_R} + K_{92} \omega \sigma_V \right) / (K_{9R}-1) + \right.$$
$$\left. + \frac{i}{2} \left(B_- \frac{\omega E_V}{E_R} + C_- \omega \sigma_V \right) + \frac{(1-i)}{\sqrt{2}\,\alpha} \left(\frac{K_{8R}}{2} + \frac{K_{10R}}{K_{10R}(K_{10R}-1)} \right) \right\} \qquad \text{(V-13)}$$

$$M_5 e^{i\phi_5} = \pi \sqrt{A_+} \left\{ 1 + \frac{i}{2} \left(B_+ \frac{\omega E_V}{E_R} + C_+ \omega \sigma_V \right) + \frac{(1-i)}{\sqrt{2}\,\alpha} \left(\frac{K_{7R}}{2} - \frac{2}{K_{5R}} \right) \right\} \qquad \text{(V-14)}$$

$$M_6 e^{i\phi_6} = \pi \sqrt{A_-} \left\{ 1 + \frac{i}{2} \left(B_- \frac{\omega E_V}{E_R} + C_- \omega \sigma_V \right) + \frac{(1-i)}{\sqrt{2}\,\alpha} \left(\frac{K_{6R}}{2} - \frac{2}{K_{9R}} \right) \right\} \qquad \text{(V-15)}$$

$$M_7 e^{i\phi_7} = \sqrt{A_+} \left\{ 1 + \frac{i}{2} \left(B_+ \frac{\omega E_V}{E_R} + C_+ \omega \sigma_V \right) + \frac{(1-i)}{2\sqrt{2}\,\alpha} K_{7R} \right\} \qquad \text{(V-16)}$$

$$M_8 e^{i\phi_8} = \sqrt{A_-} \left\{ 1 + \frac{i}{2} \left(B_- \frac{\omega E_V}{E_R} + C_- \omega \sigma_V \right) + \frac{(1-i)}{2\sqrt{2}\,\alpha} K_{8R} \right\} \qquad \text{(V-17)}$$

$$\text{where} \quad \beta_{2R} = \frac{C_{oR}}{R_o \omega} \, , \quad C_{oR}^2 = \frac{E_R \lambda}{2 \rho R_o} \, , \quad \beta_{3R} = \frac{2\beta_1 \beta_{2R}^2}{1 - \sigma_R^2} \qquad \text{(V-18)}$$

$$A_{\pm} = \frac{1}{2K'_{1R}} \left(\frac{K'_{2R}}{1-\sigma_R/2} \pm \sqrt{K'_{3R}} \right) \tag{V-19}$$

$$B_{\pm} = \left[\frac{(1-\Gamma_1)(1-\Gamma_2)}{2(1-\sigma_R/2)\beta_{3R}} \pm \sqrt{K'_{3R}} \, \frac{K_{31}}{K_{32}} \right] \Big/ \Big(\frac{K'_{2R}}{1-\sigma_R/2}$$
$$\pm \sqrt{K'_{3R}} \Big) - \frac{\beta_{3R}(1-\sigma_R^2)}{2(1-\sigma_R/2)K'_{1R}} \tag{V-20}$$

$$C_{\pm} = \left[\frac{K'_{2R}}{2(1-\sigma_R/2)} + \frac{(1-\Gamma_1)(1-\Gamma_2)\sigma_R}{\beta_{3R}(1-\sigma_R/2)(1-\sigma_R^2)} \pm \sqrt{K'_{3R}} \, \frac{K_{32}}{K_{3R}} \right] \Big/ \Big(\frac{K'_{2R}}{(1-\sigma_R/2)}$$
$$\pm \sqrt{K'_{3R}} \Big) - \frac{1}{2(1-\sigma_R/2)} \tag{V-21}$$

$$K'_{1R} = \beta_{3R}\sigma_R - \left[\tfrac{1}{2}(1-\Gamma_1) - \beta_{3R}(\tfrac{1}{2}-\sigma_R) \right] \Big/ (1-\sigma_R/2) \tag{V-22}$$

$$K'_{2R} = \beta_1 + \frac{1-\Gamma_2}{2} \left(1 - \frac{1-\Gamma_1}{\beta_{3R}} \right) \tag{V-23}$$

$$K'_{3R} = \left(\frac{K'_{2R}}{1-\sigma_R/2} \right)^2 - \frac{4\beta_1(1-\Gamma_2)K'_{1R}}{\beta_{3R}(1-\sigma_R/2)} \tag{V-24}$$

$$K_{31} = \frac{(1-\Gamma_1)(1-\Gamma_2)}{\beta_{3R}(1-\sigma_R/2)^2} \left(K'_{2R} - 2\beta_1 \right) \tag{V-25}$$

$$K_{32} = \left(\frac{K'_{2R}}{1-\sigma_R/2} \right)^2 \frac{1}{(1-\sigma_R/2)} + \left(\frac{K_{2R}}{(1-\sigma_R/2)^2} \right) \frac{(1-\Gamma_1)(1-\Gamma_2)}{\beta_{3R}} \frac{2\sigma_R}{1-\sigma_R^2}$$
$$- \frac{2(\tfrac{1}{2}-\sigma_R)}{(1-\sigma_R^2)} \frac{4\beta_1(1-\Gamma_2)K'_{1R}}{\beta_{3R}(1-\sigma_R/2)^2} \tag{V-26}$$

$$G_{5R} = \frac{K'_{2R}}{2(1-\sigma_R/2)} + \frac{(1-\Gamma_2)}{\beta_{3R}(1-\sigma_R/2)} \left[\tfrac{1}{2}(1-\Gamma_1) - \beta_{3R}(\tfrac{1}{2}-\sigma_R) \right] \tag{V-27}$$

63

$$G_{51} = - \frac{(1-\Gamma_1)(1-\Gamma_2)}{4\beta_{3R}(1-\sigma_R/2)} \tag{V-28}$$

$$G_{52} = \frac{G_{5R}}{2(1-\sigma_R/2)} + \frac{1-\Gamma_2}{1-\sigma_R/2} + \frac{2\sigma_R G_{51}}{1-\sigma_R^2} \tag{V-29}$$

$$K_{5R} = \frac{1}{A_{5R}} \left(G_{5R} + \tfrac{1}{2}\sqrt{K_{3R}} \right) \tag{V-30}$$

$$K_{51} = \frac{G_{51} + \tfrac{1}{4}\sqrt{K_{3R}}\,\frac{K_{31}}{K_{3R}}}{G_{5R} + \tfrac{1}{2}\sqrt{K_{3R}}} - \frac{(1-\Gamma_1)(1-\Gamma_2)}{2\beta_{3R}(1-\sigma_R/2)A_{5R}} \tag{V-31}$$

$$K_{52} = \frac{G_{52} + \tfrac{1}{2}\sqrt{K_{3R}}\,\frac{K_{32}}{K_{3R}}}{G_{5R} + \tfrac{1}{2}\sqrt{K_{3R}}} - \frac{(1-\Gamma_2)(3 + \frac{1-\Gamma_1}{2\beta_{3R}})}{4A_{5R}(1-\sigma_R/2)^2} - \frac{\sigma_R(1-\Gamma_1)(1-\Gamma_2)}{\beta_{3R}A_{5R}(1-\sigma_R/2)(1-\sigma_R^2)} \tag{V-32}$$

$$A_{5R} = \beta_1 - (1-\Gamma_2)\frac{\tfrac{1}{2}-\sigma_R}{1-\sigma_R/2} + \frac{(1-\Gamma_1)(1-\Gamma_2)}{2\beta_{3R}(1-\sigma_R/2)} \tag{V-33}$$

$$K_{9R} = \frac{1}{A_{5R}} \left(G_{5R} - \tfrac{1}{2}\sqrt{K_{3R}} \right) \tag{V-34}$$

$$K_{91} = \frac{G_{51} - \tfrac{1}{4}\sqrt{K_{3R}}\,\frac{K_{31}}{K_{3R}}}{G_{5R} - \tfrac{1}{2}\sqrt{K_{3R}}} - \frac{(1-\Gamma_1)(1-\Gamma_2)}{2A_{5R}\beta_{3R}(1-\sigma_R/2)} \tag{V-35}$$

$$K_{92} = \frac{G_{52} - \tfrac{1}{4}\sqrt{K_{3R}}\,\frac{K_{32}}{K_{3R}}}{G_{5R} - \tfrac{1}{2}\sqrt{K_{3R}}} - \frac{(1-\Gamma_2)(3 + \frac{1-\Gamma_1}{\beta_{3R}})}{4A_{5R}(1-\sigma_R/2)^2} - \frac{(1-\Gamma_1)(1-\Gamma_2)\sigma_R}{A_{5R}\beta_{3R}(1-\sigma_R/2)(1-\sigma_R^2)} \tag{V-36}$$

The remaining constants K_{4R}, K_{7R}, K_{8R}, K_{6R} and K_{10R} are obtained from (III-67) to (III-71) by substituting E_R and σ_R for E and σ.

In many cases the parameter $(1-\Gamma_1)/\beta_{3R}$ is small and the limiting form of the solution defined by (V-4) to (V-36) is nearly unaffected by variations in this parameter. By taking $(1-\Gamma_1)/\beta_{3R} = 0$ the above solution reduces to:

$$A_{\pm} = \frac{(1-\sigma_R/2)^2}{2\beta_1 \beta_{2R}^2 (1-\sigma_R^2)} \left[\frac{(\beta_1 + \frac{1-\Gamma_2}{2})}{(1-\sigma_R/2)} \pm \sqrt{R_{3R}} \right] \quad \text{(V-37)}$$

$$B_{\pm} = -1 \quad \text{(V-38)}$$

$$C_{\pm} = \left[\frac{(\beta_1 + \frac{1-\Gamma_2}{2})}{2(1-\sigma_R/2)^2} \pm \sqrt{R_{3R}} \frac{R_{32}}{2R_{3R}} \right] \Big/ \left[\frac{(\beta_1 + \frac{1-\Gamma_2}{2})}{(1-\sigma_R/2)} \pm \sqrt{R_{3R}} \right]$$
$$- \frac{1}{2(1-\sigma_R/2)} \quad \text{(V-39)}$$

$$R_{3R} = \left[(\beta_1 + \tfrac{1-\Gamma_2}{2})^2 - 2\beta_1 (1-\Gamma_2)(1-\sigma_R^2) \right] \Big/ (1-\sigma_R/2)^2 \quad \text{(V-40)}$$

$$R_{32} = \left[(\beta_1 + \tfrac{1-\Gamma_2}{2})^2 - 4\beta_1 (\tfrac{1}{2}-\sigma_R)(1-\Gamma_2) \right] \Big/ (1-\sigma_R/2)^2 \quad \text{(V-41)}$$

$$R_{4R} = 4\left(\frac{\beta_1 + \frac{1-\Gamma_2}{2}}{1-\sigma_R/2} \right)^2 \left[\frac{\beta_1(\frac{5}{2}-2\sigma_R)}{2(\beta_1 + \frac{1-\Gamma_2}{2})} - 1 \right] - \frac{2\beta_1(1-\sigma_R^2)}{(1-\sigma_R/2)^2} \left[\beta_1 - 2(1-\Gamma_2) \right] \quad \text{(V-42)}$$

$$K_{7R} = \left[\frac{\beta_1(\frac{5}{2}-2\sigma_R)}{(1-\sigma_R/2)} + \frac{R_{4R}}{2\sqrt{R_{3R}}} + 2\sqrt{R_{3R}} \right] \Big/ \left[\frac{(\beta_1 + \frac{1-\Gamma_2}{2})}{(1-\sigma_R/2)} + \sqrt{R_{3R}} \right] \quad \text{(V-43)}$$

$$K_{8R} = \left[\frac{\beta_1(\frac{5}{2}-2\sigma_R)}{(1-\sigma_R/2)} - \left(\frac{R_{4R}}{2\sqrt{R_{3R}}} + 2\sqrt{R_{3R}} \right) \right] \Big/ \left[\frac{(\beta_1 + \frac{1-\Gamma_2}{2})}{(1-\sigma_R/2)} - \sqrt{R_{3R}} \right] \quad \text{(V-44)}$$

$$A_{5R} = \beta_1 - (1-\Gamma_2) \frac{(\frac{1}{2}-\sigma_R)}{(1-\sigma_R/2)} \quad \text{(V-45)}$$

$$G_{5R} = \frac{(\beta_1 + \frac{1-\Gamma_2}{2})}{2(1-\sigma_R/2)} - (1-\Gamma_2) \frac{(\frac{1}{2}-\sigma_R)}{(1-\sigma_R/2)} \quad \text{(V-46)}$$

$$G_{51} = 0 \quad \text{(V-47)}$$

65

$$G_{52} = \left[\left(\beta_1 + \tfrac{1-\Gamma_2}{2} \right) - (1-\Gamma_2)\left(\tfrac{1}{2} - \sigma_R \right) 2 \right] / \left[4\left(1-\sigma_R/2 \right)^2 + \tfrac{1-\Gamma_2}{(1-\sigma_R/2)} \right] \quad \text{(V-48)}$$

$$K_{51} = 0 = K_{91} \quad \text{(V-49)}$$

$$K_{52} = \frac{G_{52} + \tfrac{1}{2}\sqrt{R_{3R}}\,\frac{R_{32}}{R_{3R}}}{G_{5R} + \tfrac{1}{2}\sqrt{R_{3R}}} - \frac{3(1-\Gamma_2)}{4A_{5R}(1-\sigma_R/2)^2} \quad \text{(V-50)}$$

$$K_{92} = \frac{G_{52} - \tfrac{1}{4}\sqrt{R_{3R}}\,\frac{R_{32}}{R_{3R}}}{G_{5R} - \tfrac{1}{2}\sqrt{R_{3R}}} - \frac{3(1-\Gamma_2)}{4A_{5R}(1-\sigma_R/2)^2} \quad \text{(V-51)}$$

where K_{5R} and K_{9R} are given by (V-30) and (V-34). These equations can now be substituted into relations (V-5) to (V-15) to obtain the wave speeds, attenuation, mode shapes and phase angles.

Both limiting solution forms given here exhibit no effects of the visco-elastic properties upon the wave speeds. For elastic walls Womersley's analysis produced the result

$$\frac{C_0}{C_1} = X - iY \quad \text{(V-52)}$$

where the axial and spatial variation of all quantities is given by the function

$$F\left(t - \tfrac{z}{C_1} \right) = e^{i\omega\left(t - \tfrac{z}{C_1} \right)}$$

and X and Y are tabulated in Womersley's report. Then, C_0/C_1 contains both wave speed and attenuation factor. Taylor in Reference 17 has shown that substitution of the relations in (V-4) into Womersley's solution yields

$$\frac{C_{0R}}{C_1} = (X - iY)(1 - i\omega W) \quad \text{WHERE} \quad W = \tfrac{1}{2}\frac{E_V}{E_R} + \tfrac{1}{3}\sigma_V \quad \text{(V-53)}$$

or, in the form of the present analysis,

$$\frac{C_1}{C_{OR}} = \left(\frac{C_1}{C_0}\right)_{ELASTIC} \Big/ \left[1 - \frac{\omega W}{2\pi}\left(\delta_1 \frac{\lambda_1}{R_0}\right)_{ELASTIC}\right] \tag{V-54}$$

$$\delta_1 \frac{\lambda_1}{R_0} = \left[\left(\delta_1 \frac{\lambda_1}{R_0}\right)_{ELASTIC} + 2\pi \omega W\right] \Big/ \left[1 - \frac{\omega W}{2\pi}\left(\delta_1 \frac{\lambda_1}{R_0}\right)_{ELASTIC}\right] \tag{V-55}$$

where $\left(C_1/C_0\right)_{ELASTIC}$ and $\left(\delta_1 \lambda_1/R_0\right)_{ELASTIC}$ are the quantities for elastic walls. For large α, $\left(\delta_1 \lambda_1/R_0\right) \ll 1$, $W \ll 1$ and

$$\frac{C_1}{C_{OR}} = \left(\frac{C_1}{C_0}\right)_{ELASTIC} + \text{TERMS OF ORDER } \frac{\omega W}{2\pi}\left(\delta_1 \frac{\lambda_1}{R_0}\right)_{ELASTIC} \tag{V-56}$$

$$\delta_1 \frac{\lambda_1}{R_0} = \left[\left(\delta_1 \frac{\lambda_1}{R_0}\right)_{ELASTIC} + 2\pi \omega W\right] + \text{TERMS OF ORDER } \left[\omega W\left(\delta_1 \frac{\lambda_1}{R_0}\right)^2_{ELASTIC}\right.$$
$$\text{OR } \left.(\omega W)^2\left(\delta_1 \frac{\lambda_1}{R_0}\right)_{ELASTIC}\right] \tag{V-57}$$

Therefore, Taylor's analysis also shows little dependence of the wave speed on the viscoelastic behaviour of the wall. Also, for large α Taylor's results are of the same form as those given here, except that the coefficients of E_V/E_R and σ_V are constant in Taylor's analysis.

McDonald and Gessner in Reference 5 have shown that the data of Bergel can be presented in a form utilizing the function W defined in (V-53).

$$\frac{\omega E_V}{E_R} = \text{TAN } \phi_B = 2\omega W \tag{V-58}$$

where ϕ_B is the viscoelastic parameter presented as experimental data by Bergel.

C. Comparison of a Viscoelastic Damping Parameter Computed from Anliker's Data with Previous Results

As in the comparison of experimental data with the results of the elastic

67

wall analysis essential geometric and physical quantities are

$$R_0 = 4.4 \text{ MM} \;, \quad h = 1.25 \text{ MM}, \quad \beta_1 = 3.5 \;, \quad \Gamma_1 = 0 = \Gamma_2 \;, \quad \sigma_R = \frac{1}{2}$$

$$C_{0R} = 5 \text{M/SEC} \;, \quad \alpha^2 = \frac{F}{0.0416 \text{ CPS}} \;, \quad \beta_{2R} = \frac{182.5 \text{ CPS}}{F}$$

Since $\beta_{3R} = \frac{28}{5} \beta_{2R}^2 > 7.5$ for frequencies less than 200 cps., the quantity $(1-\Gamma_1)/\beta_{3R}$ is small even for no distributed radial constraint $(\Gamma_1 = 0)$. Making use of this fact in the limiting solution for large α, one obtains

$$\frac{C_1}{C_{0R}} = 0.979 \left(1 - \frac{1}{2\sqrt{2} \alpha} \right) \;, \quad \frac{C_2}{C_{0R}} = 3.15 \left(1 - \frac{4.56}{2\sqrt{2} \alpha} \right) \tag{V-58}$$

$$\delta_1 \frac{\lambda_1}{R_0} = \pi \left\{ -\left(-\frac{\omega E_V}{E_R} + 0.145 \,\omega\, \sigma_V \right) + \frac{1}{\sqrt{2} \alpha} \right\} \tag{V-59}$$

$$\delta_2 \frac{\lambda_2}{R_0} = \pi \left\{ \left(\frac{\omega E_V}{E_R} + 1.5 \,\omega\, \sigma_V \right) + \frac{4.56}{\sqrt{2} \alpha} \right\} \tag{V-60}$$

As shown in (V-3), $\delta_i \lambda_i / R_0$ is the attenuation coefficient, k_i, introduced by Anliker in (V-1). From the experimental data it follows that $k_1 \approx 0.87 = \delta_1 \frac{\lambda_1}{R_0}$. The substitution of this value into (V-59) yields

$$\omega \left(\frac{E_V}{E_R} - 0.145 \,\sigma_V \right) = \frac{0.87}{\pi} - \frac{1}{\sqrt{2} \alpha} \tag{V-61}$$

as the viscoelasticity contribution to the attenuation coefficient, k_1. This contribution can be interpreted as a viscoelastic damping parameter. It is plotted in Figure 68 as a function of frequency together with the experimental data obtained by Anliker et al.[13] and Bergel[4].

According to the data of Bergel, ϕ_B is sufficiently small so that (V-58) can be approximated by

68

$$\omega \mathcal{W} = \frac{1}{2} \text{TAN } \phi_B \approx \frac{1}{2} \phi_B$$

It should be noted that Bergel's results are based on a different viscoelastic model and on measurements conducted in the excised vessels. His viscoelastic attentuation parameter increases with frequency.

For frequencies above 60 cps. the theoretically predicted variation of the viscoelastic attentuation parameter is in good agreement with the experimentally measured attenuation coefficient due to all sources of attenuation. From relation (V-61) it follows that the damping contribution produced by the viscosity of the blood is negligibly small at higher frequencies.

The viscoelastic parameter in (V-61) and the expression for $2\omega \mathcal{W}$ in (V-53) have the same coefficient for E_V/E_R but the coefficients for σ_V are of different sign and magnitude. The terms underlined in Equation (V-21) and (V-39) define the coefficient of σ_V in $\mathcal{W}$. Additional data are necessary to the individual values of E_V, E_R, σ_V and σ_R.

VI. CONCLUSIONS

The general solution of the boundary value problem posed in this analysis produces two types of waves travelling along the axis of the vessel. The first or slower type of waves has been studied extensively by Womersley and others. Recently both types have been investigated by several authors[3),11),15),18)], however, without considering the effects of constraints. The results of Atabek and Lew[11)], Womersley[10)], and the present analysis are in good agreement for corresponding values of the system parameters. The results presented here for the large Reynolds number limit are also in good agreement with those of Maxwell and Anliker[3)] for an inviscid fluid.

In the present analysis as well as in those of Womersley[10)] and Atabek and Lew[11)], the fluid viscosity appears in the solutions only through the non-dimensional parameter $\alpha = R_0 \sqrt{\omega/\nu}$ which is essentially the square root of an unsteady Reynolds number. In the parametric study given here it was shown that a variation in α produces the most significant changes in the wave propagation characteristics for the slow waves when $\alpha < 5$ and for the fast waves when $\alpha > 1$. The frequency appears not only in α, but also in the parameter $(\beta_2 = C_0/(R_0 \omega))$ which plays an important role in determining the propagation characteristics of the fast waves, particularly when the parameter α has a limiting effect.

The wave speed for the first type of waves in the presence of a weak radial constraint increases monotonically with α from zero at $\alpha = 0$ and reaches asymptotically a value which differs by less than twenty per cent from the Moens-Korteweg speed, C_0. For the second type of waves and very small values of α, mild distributed external constraints (axial and/or radial) the wave speed is relatively insensitive to variations in α. Furthermore, it is $1.8\ C_0$ for $\alpha < 1$, and with increasing α it approaches an approximate limit toward value of $5\ C_0$. A distributed radial constraint can produce an order of magnitude variation in the wave speed for the first type of waves while a distributed axial constraint merely produces a variation of less than 15%. However, both a radial or axial constraint can cause an infinite change of the wave speed for the second type of waves.

Regardless of the constraints, the first or slower type of waves are strongly attenuated for $\alpha < 1$ and the attenuation due to the blood viscosity diminishes rapidly with increasing α. In the absence of constraints the waves

70

of the second or faster type exhibit small attenuation due to the viscosity of the blood for $\alpha < .2$ and $\alpha > 100$. It assumes a maximum for $\alpha \approx 2.8$. However, in contrast to the slow waves, the attenuation of the second type of waves is strongly affected by distributed external constraints.

For the first type of waves the wall displacement has a dominant radial component at high frequencies but at low frequencies the axial displacement component dominates. The second type of waves always has a dominant axial displacement component. Both of these statements are true for weak external constraints. With strong constraints, the displacement mode shape can be altered considerably. The wall motions associated with the two types of waves indicate that the faster type of waves involves a strong shearing interaction between the blood and the vessel wall while the slow type of waves should exhibit relatively strong pressure fluctuations, particularly at higher frequencies.

The second type of waves were found to be much more sensitive to variations in the system parameters than the first type of waves. The phase angle between pressure and radial wall displacement for the first type of wave are almost negligible. The investigation of the effects of discrete constraints such as clamps or electromagnetic flow meters on the pressure and instantaneous mass flow has demonstrated that such constraints may produce significant changes.

A comparison of the present analysis with the experimental results obtained by Van Citters from a mechanical model of a blood vessel showed qualitative and some quantitative agreement. In particular Van Citters' results verify the theoretical prediction that weak distributed external constraint can almost completely attenuate the second type of waves. This fact may account for the lack of in vivo evidence of naturally occurring waves of the second type.

The application of the present analysis to the data of Anliker, et al, however, has indicated that the viscosity of the blood does not cause sufficient attenuation nor the proper variation of the attenuation with frequency. Since experimental information is usually obtained only for larger Reynolds numbers, the solution for this limiting case was modified to include wall viscoelasticity, and the resulting system of equations was applied to predict the viscoelastic attenuation parameter for waves of the first type. With one exception[5] this parameter is considerably larger than that previously reported.

For high frequencies the blood viscosity contributed only a few percent

to the attenuation parameters, δ_i λ_i / R_o . However, with frequency extending down to 1 cps. and no external constraints, the viscosity contribution is of the order of 14% for the first type of the order of 65% for the second type of waves.

Two features of the solution are questionable and both are related to limitations of the analysis. First, the limitation to $\lambda/R_o \gg 1$ is required in the linearized equations of motion for the fluid and is also implied in the application of a membrane analysis for the displacements of the vessel wall. Therefore, with a fluid of constant viscosity, the analytical results obtained for large α or equivalently large ω will be questionable unless the wave speed also increases such that $\lambda = c/f$ still satisfies $\frac{\lambda}{R_o} \gg 1$. Second, the limitation $(\frac{\omega T}{L})_1 = \frac{\omega}{c_1} \ll 1$ appears to be unrealistic when α approaches zero since c_1 also approaches zero. Unfortunately no experimental data is available for small value of α . In a more realistic study of the first type of waves with small α the convective terms have to be included in the Navier Stokes equations.

REFERENCES

1. Chien, S., Usami, S., Taylor, M., Lundberg, J.L., and Gregson, M.I., "Effects of Hematocrit and Plasma Proteins of Human Blood Rheology at Low Shear Rates", Journal of Applied Physiology, January 1966, p. 81.

2. McDonald, D.A., Blood Flow in Arteries, Edward Arnold Ltd., London, 1960.

3. Maxwell, J.A. and Anliker, M., "Dispersion and Dissipation of Waves in Blood Vessels", SUDAAR Report No. 312, Stanford University, May 1967. Part I of this report has been published under the title, "The Dispersion of Waves in Blood Vessels" in Biomechanics Symposium, edited by Y.C. Fung, New York, ASME, 1966, pp. 46-67. Part II is currently in press in the Biophysical Journal under the title "The Dissipation and Dispersion of Small Waves in Arteries and Veins with Viscoelastic Wall Properties".

4. Bergel, D.H., "The Dynamic Elastic Properties of the Arterial Wall", J. Physiol., Vol. 156, 1961, pp. 458-469.

5. McDonald, D.A. and Gessner, J., "Wave Attenuation in Viscoelastic Arteries", Proceedings of the First International Conference on Hemorheology, Pergamon Press, Oxford, 1966.

6. Rudinger, G., "Review of Current Mathematical Methods for the Analysis of Blood Flow", Biomedical Fluid Mechanics Symposium, 1966, ASME, New York, pp. 1-33.

7. Skalak, R., "Wave Propagation in Blood Flow", Biomechanics Symposium, edited by Y.C. Fung, New York, ASME, 1966, pp. 20-40.

8. Fung, Y.C., "Biomechanics, Its Scope, History and Some Problems of Continuum Mechanics in Physiology", J. App. Mech. Reviews, Vol. 21, No. 1, Jan. 1968, pp. 1-20.

9. Morgan, G.W. and Kiely, J.P., "Wave Propagation in a Viscous Liquid Contained in a Flexible Tube", The Journal of the Acoustical Society of America, Vol. 25, No. 3, May 1954, p. 323.

10. Womersley, J.R., "An Elastic Tube Theory of Pulse Transmission and Oscillatory Flow in Mammalian Arteries", Wright Air Development Center Technical Report WADC-TR 56-614, 1957.

11. Atabek, H.B. and Lew, H.S., "Wave Propagation Through a Viscous Incompressible Fluid Contained in an Initially Stressed Elastic Tube", Biophysical Journal, Vol. 6, 1966, p. 481.

12. Dick, D., Kendrick, J., Matson, G. and Rideout, V.C., "Measurement of Nonlinearity in the Arterial System of the Dog by a New Method", Circulation Research, Vol. 22, 1968, p. 101.

13. Anliker, M., Histand, M.B. and Ogden, E., "Dispersion and Attenuation of Small Artificial Pressure Waves in the Aorta", SUDAAR Report No. 342, Stanford University, April 1968.

14. Van Citters, R. L., "Longitudinal Waves in the Wall of Fluid-Filled Elastic Tubes", <u>Circulation Research</u>, Vol. VIII, No. 6, Nov. 1960, p. 1145.

15. Anliker, M., Moritz, W. E. and Ogden, E., "Transmission Characteristics of Axial Waves in Blood Vessels", SUDAAR Report No. 343, Stanford University, April 1968.

16. Abramowitz, M. and Stegun, I. A., <u>Handbook of Mathematical Functions with Formulas, Graphs, and Mathematical Tables</u>, National Bureau of Standards Applied Mathematics Series 55, December 1965.

17. Taylor, M. G., "An Experimental Determination of the Propagation of Fluid Oscillations in a Tube with a Visco-elastic Wall", <u>Phys. Med. Biol.</u>, Vol. 4, p. 67.

18. Klip, Willem, "Formulas for Phase Velocity and Damping of Longitudinal Waves in Thick-Walled Viscoelastic Tubes", <u>Journal of Applied Physics</u>, Vol. 38, No. 9, August 1967, pp. 3745-3755.
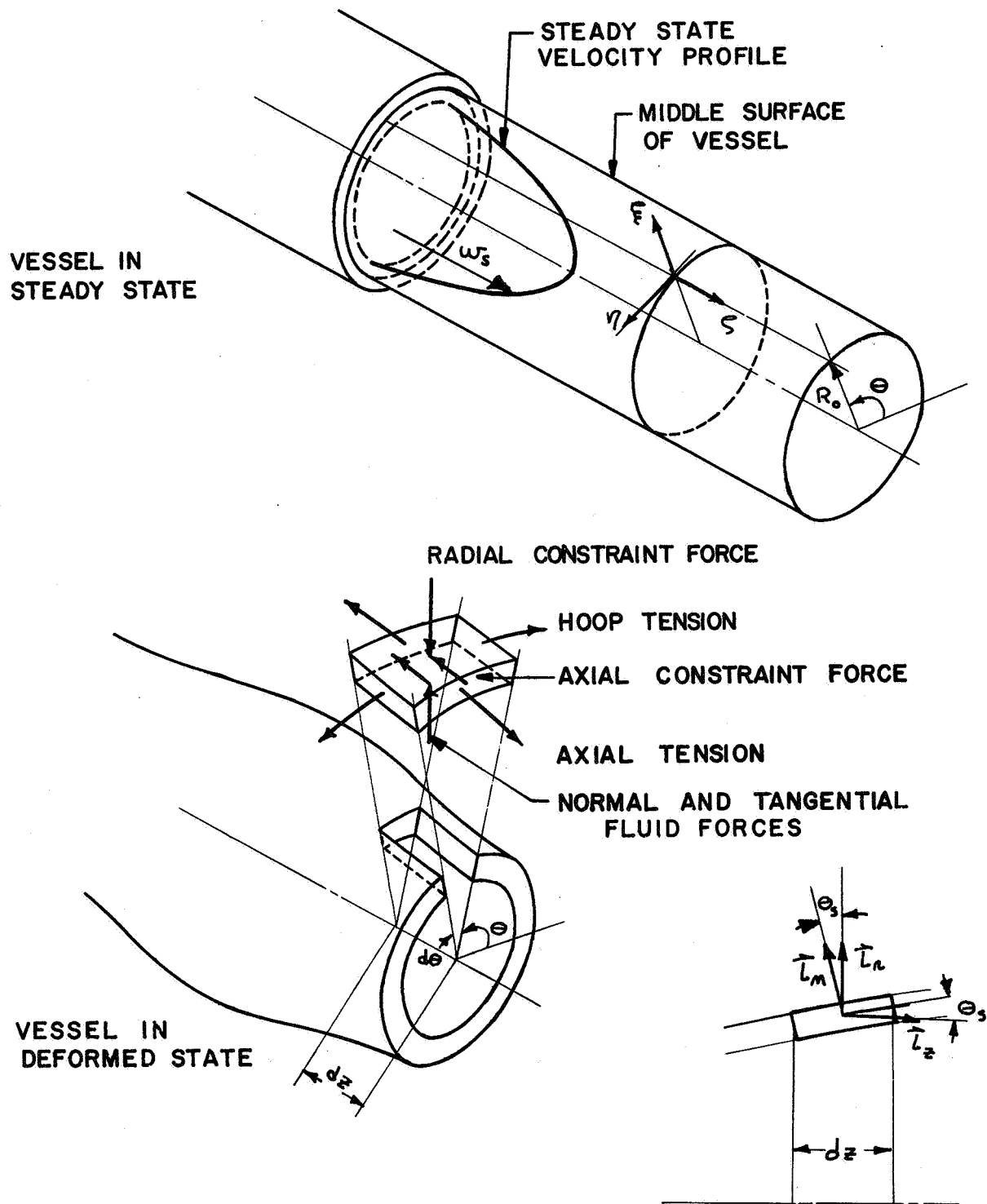
Figure 1. A Membrane Element
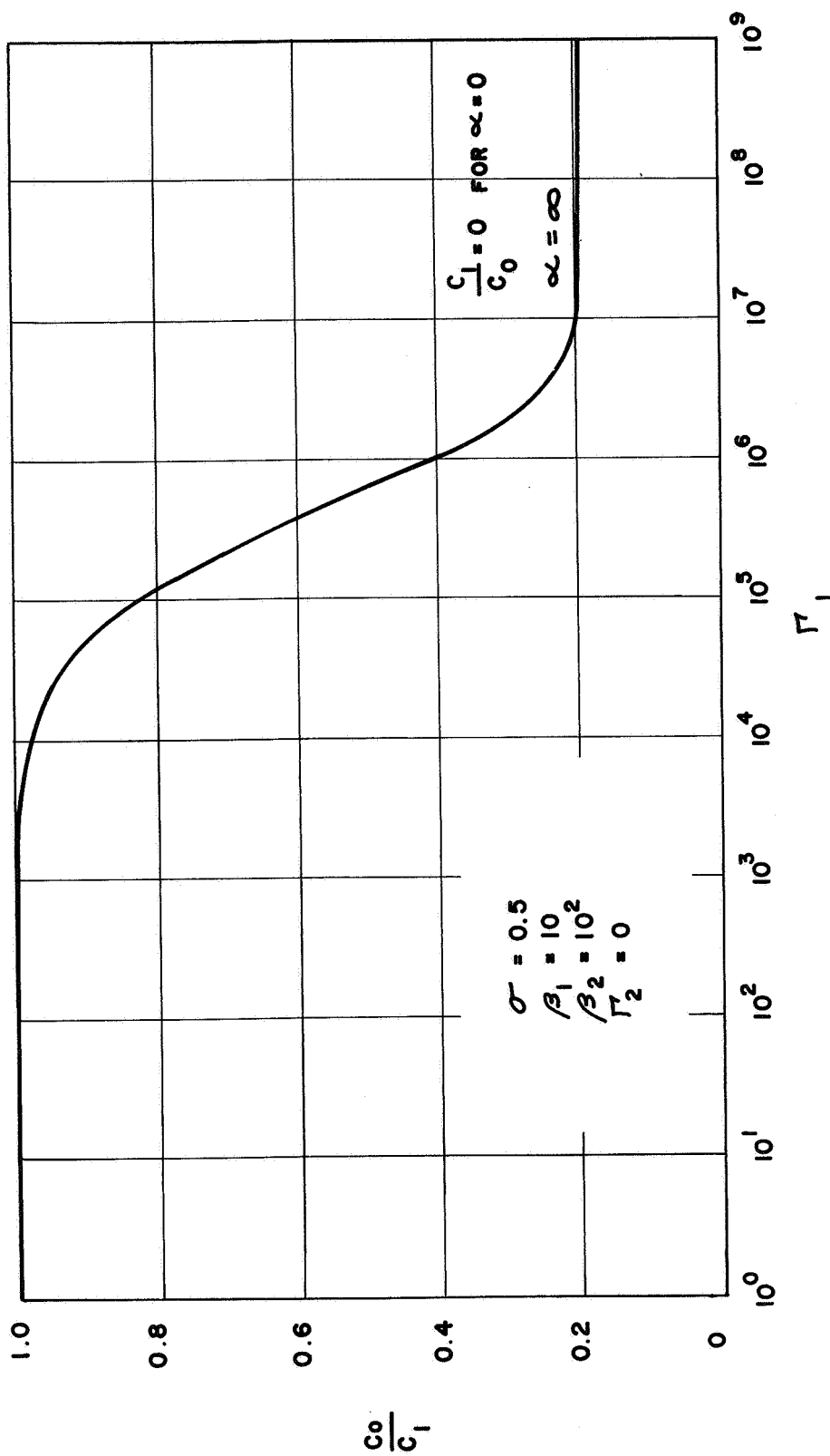
Figure 2. Speed of Waves of the First Type as a Function of the Radial Constraint Parameter
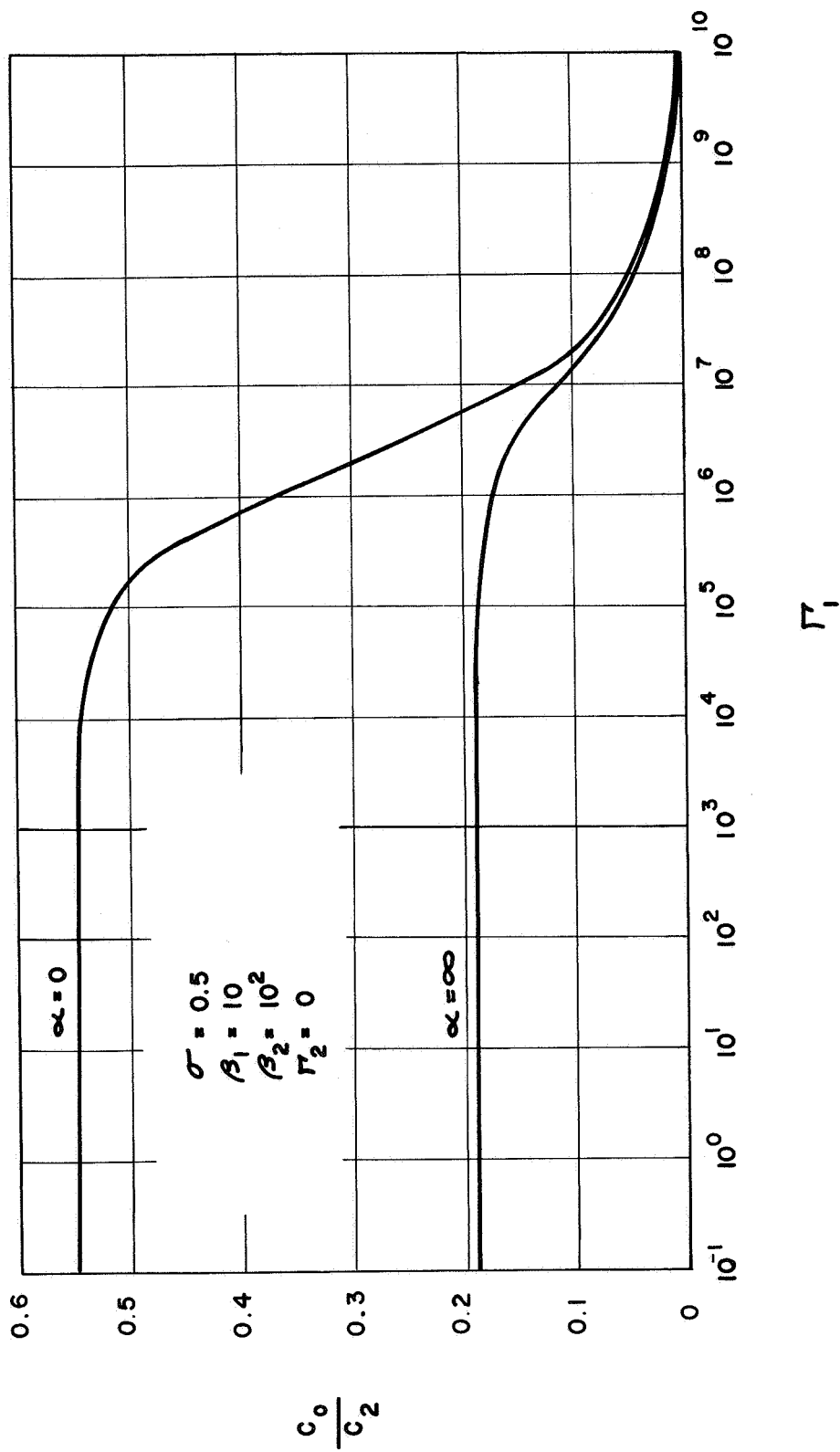
Figure 3. Speed of Waves of the Second Type as a Function of the Radial Constraint Parameter
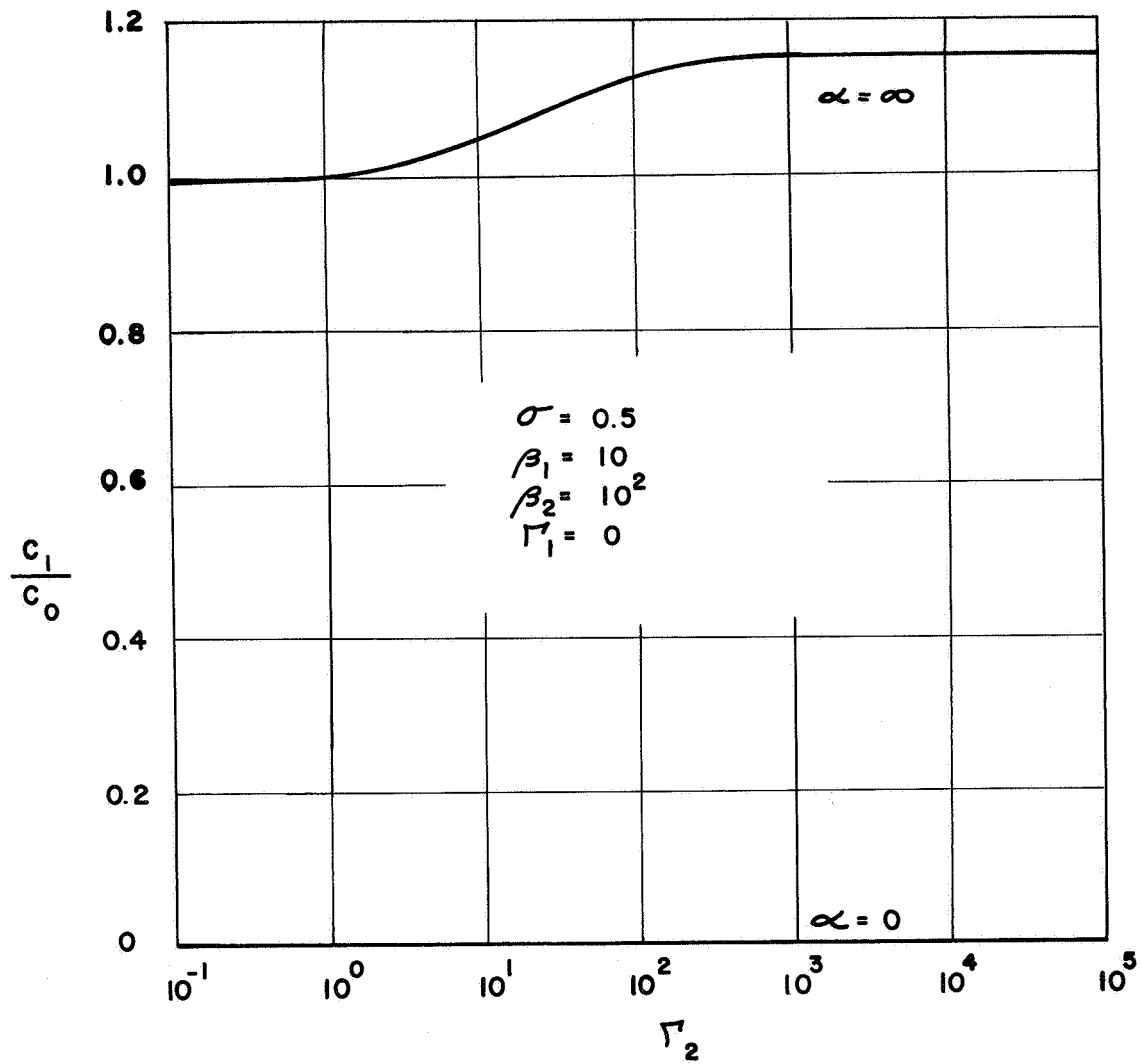
Figure 4. Speed of Waves of the First Type as a Function of the Axial Constraint Parameter

78
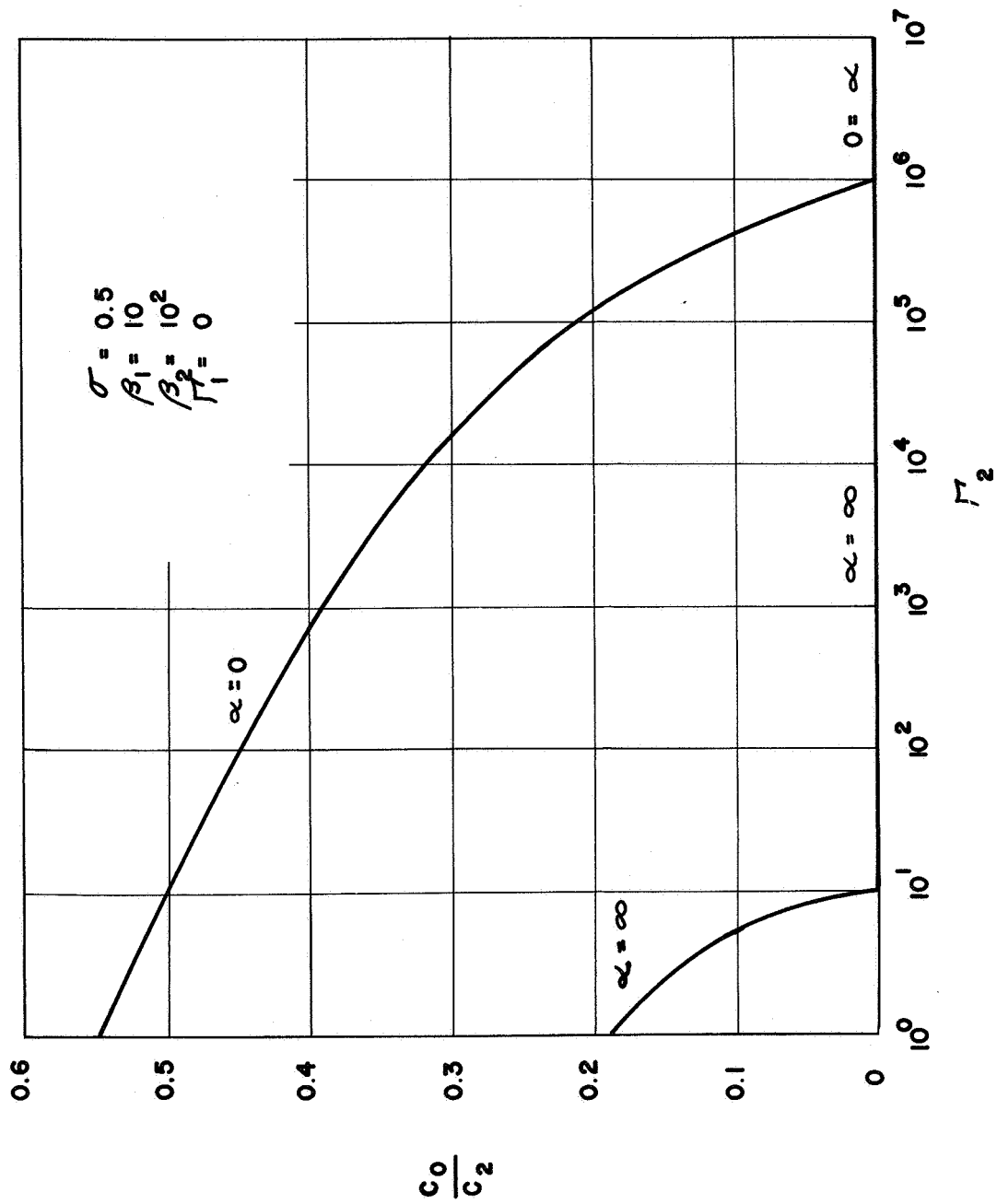
Figure 5. Speed of Waves of the Second Type as a Function of the Axial Constraint Parameter

79
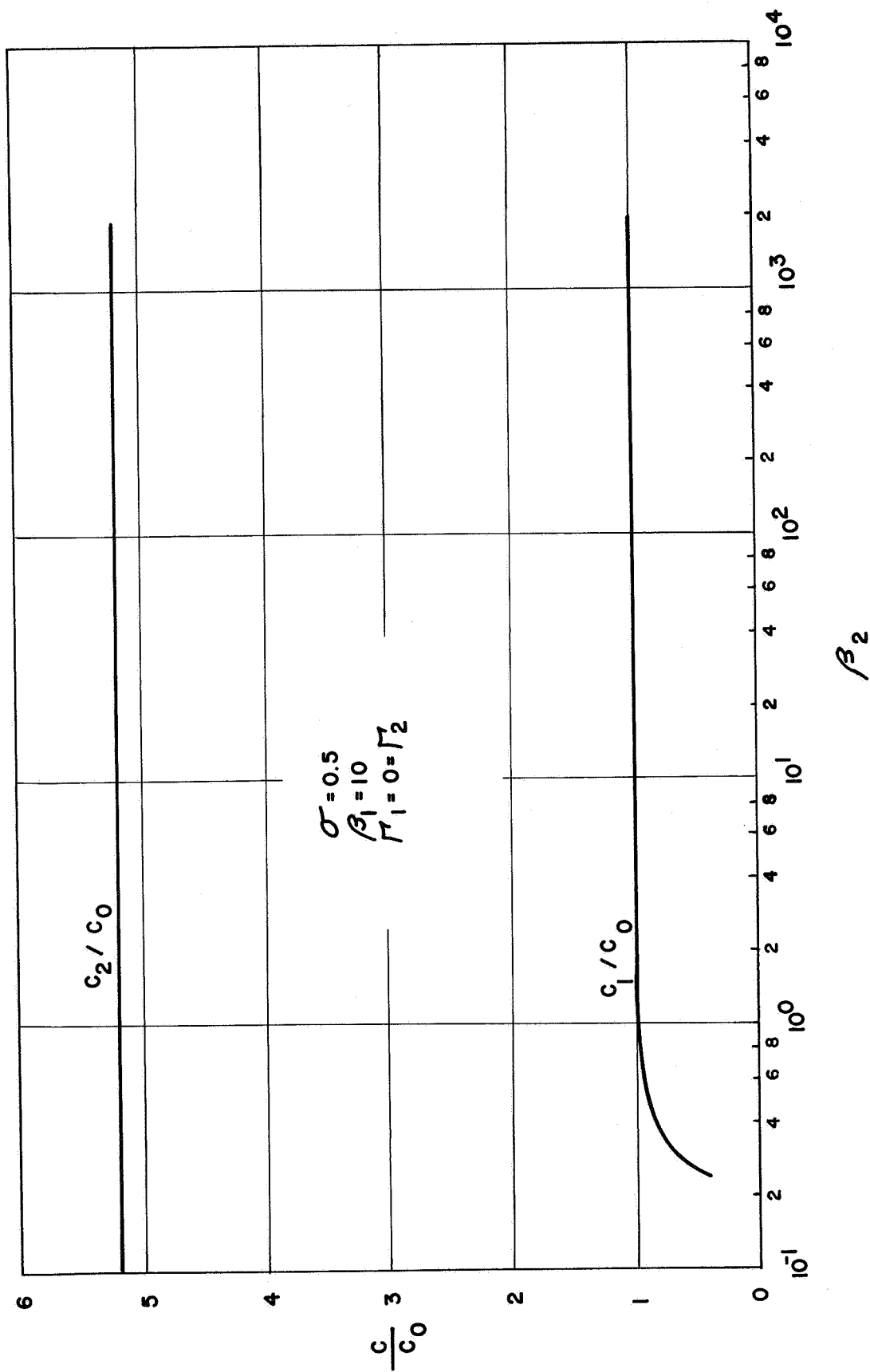
Figure 6. Wave Speeds as a Function of β_2 for the Large Reynolds Number Limit
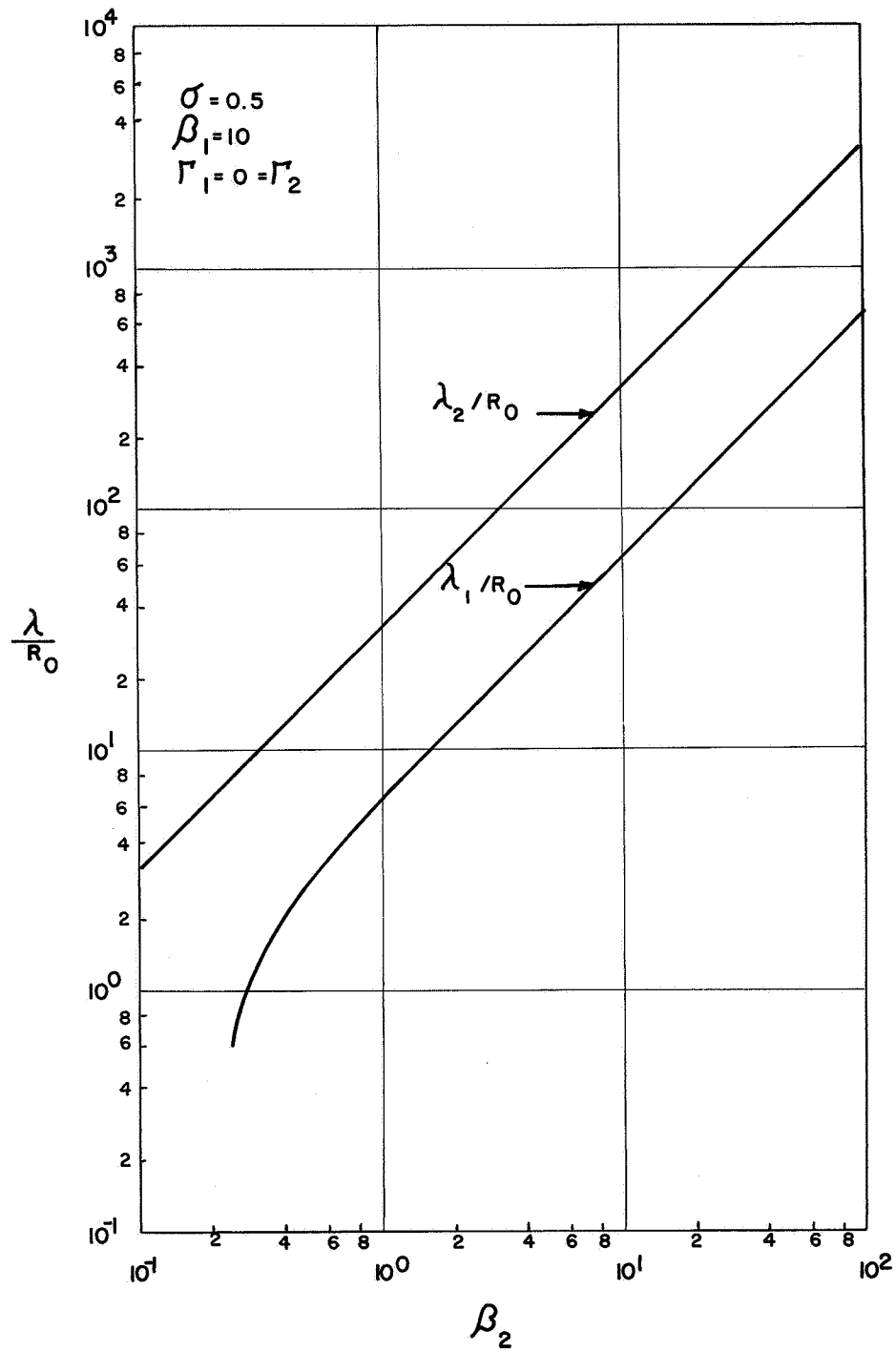
Figure 7. Wave Lengths as a Function of β_2 for the Large Reynolds Number Limit
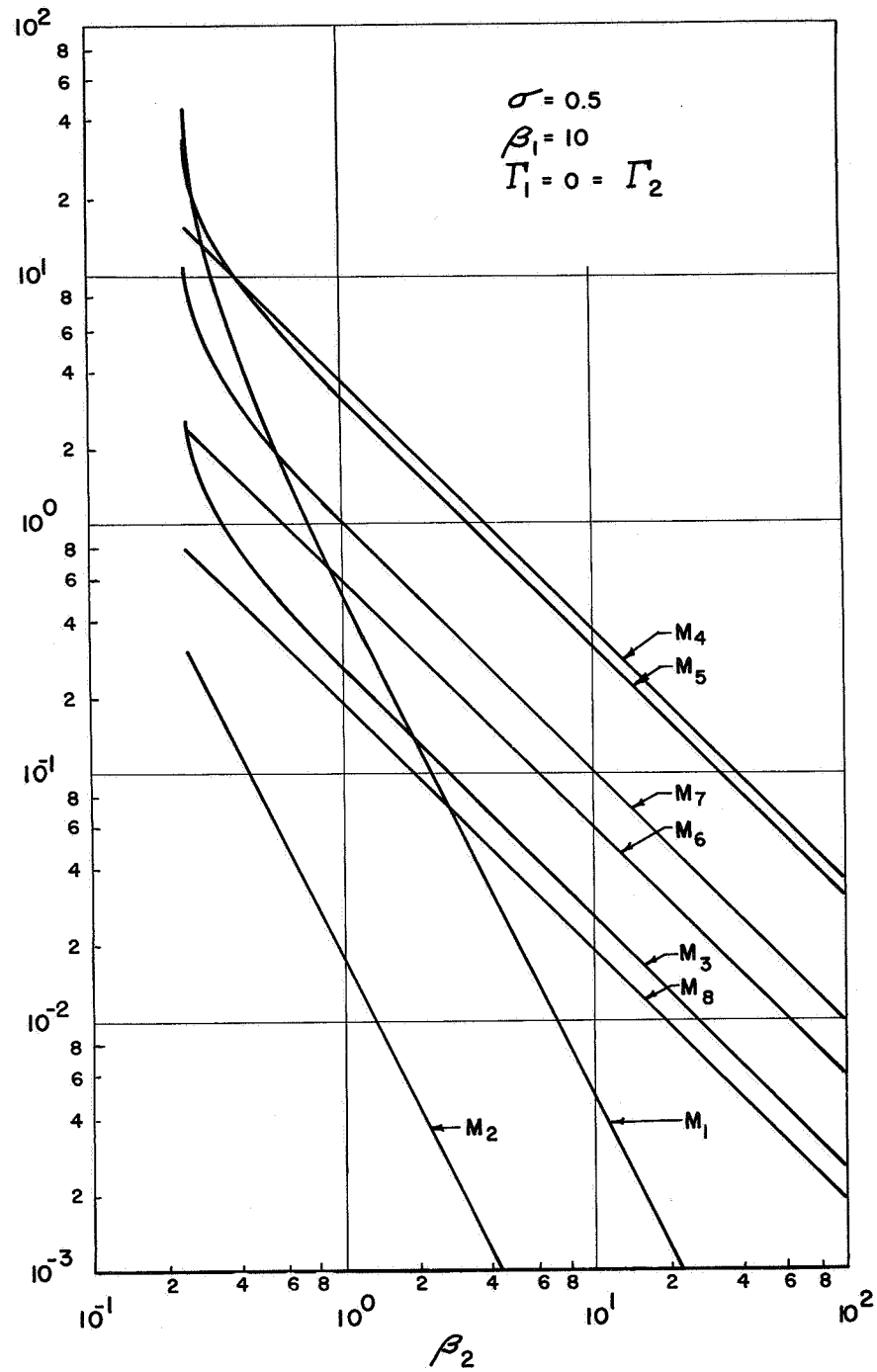
Figure 8. Mode Shape Parameters as a Function of β_2 for the Large Reynolds Number Limit
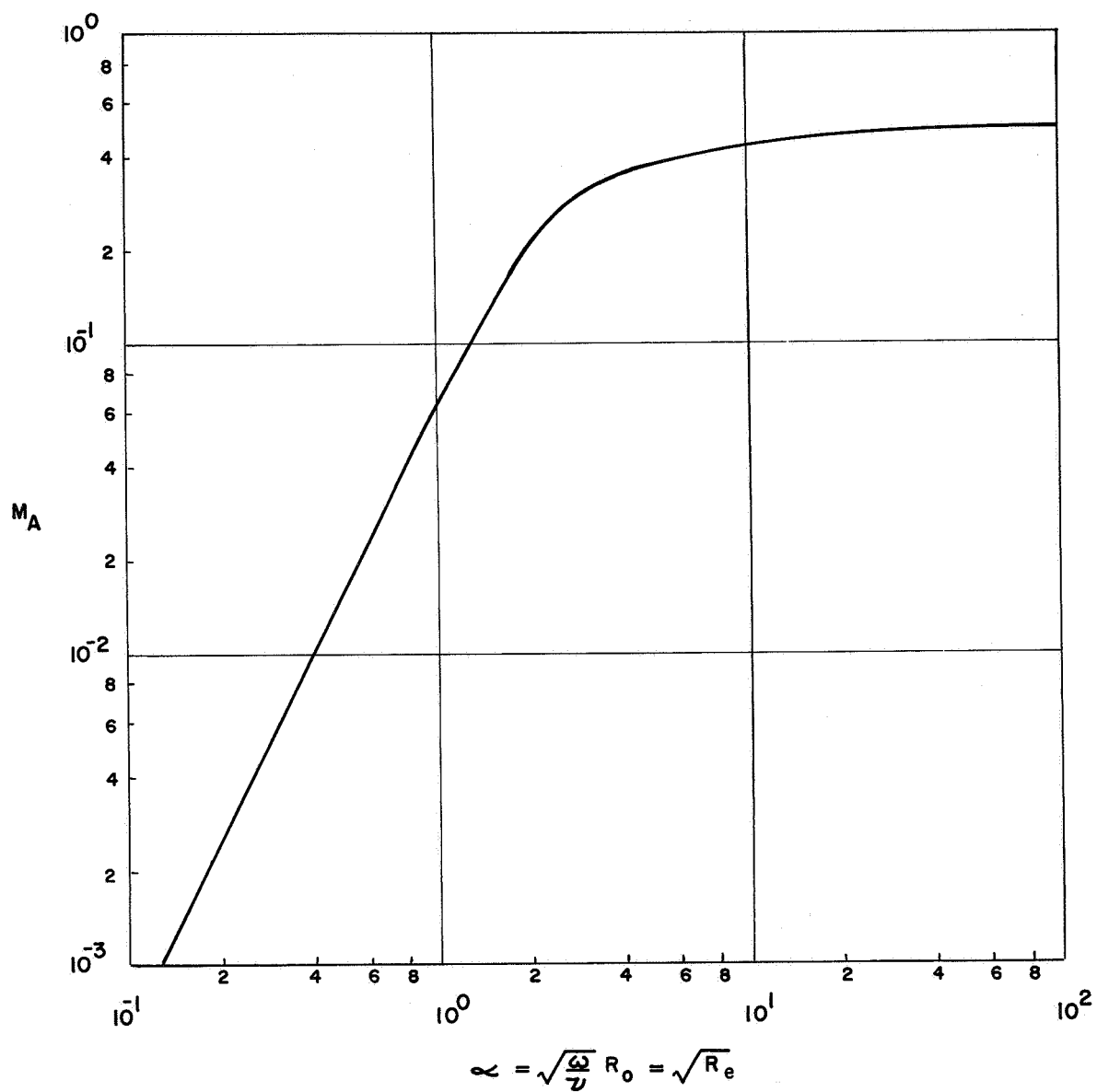
Figure 9.   The Magnitude, M_A, as a Function of Reynolds Number
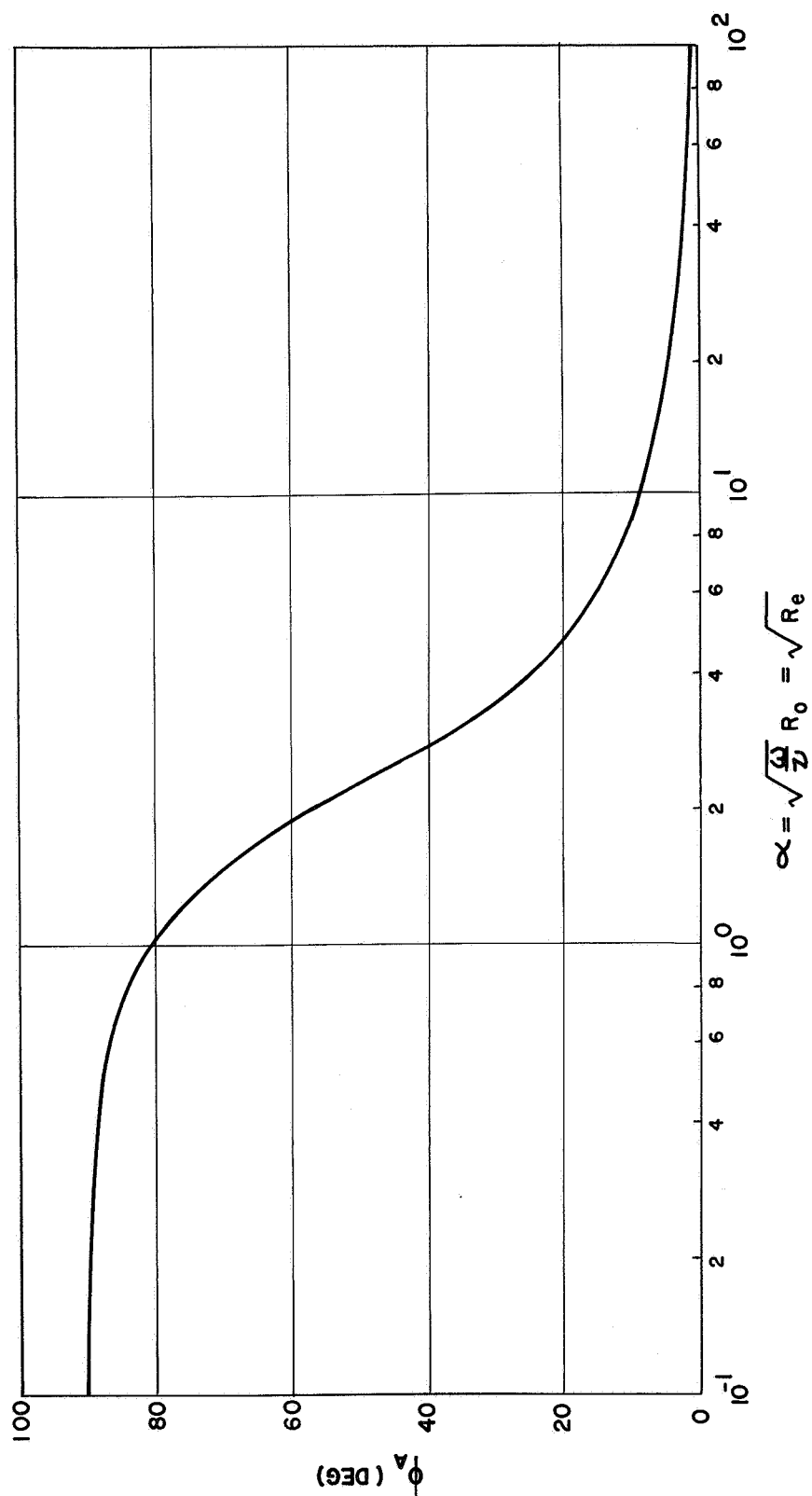
Figure 10. The Angle, ϕ_A, as a Function of Reynolds Number

$\alpha = \sqrt{\dfrac{\omega}{\nu}}\, R_0 = \sqrt{R_e}$

84
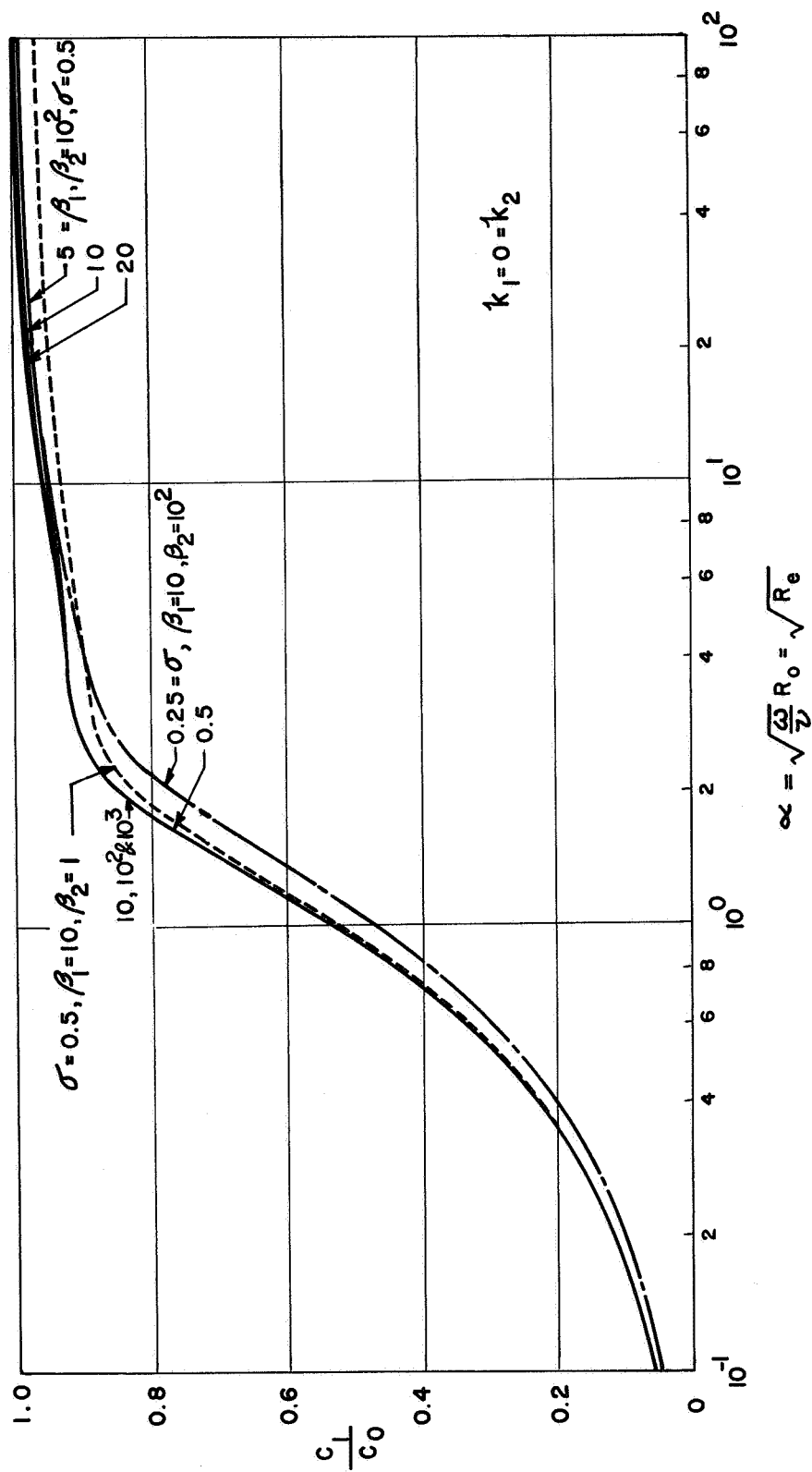
Figure 11. Wave Speed for the First Type of Waves as a Function of Reynolds Number
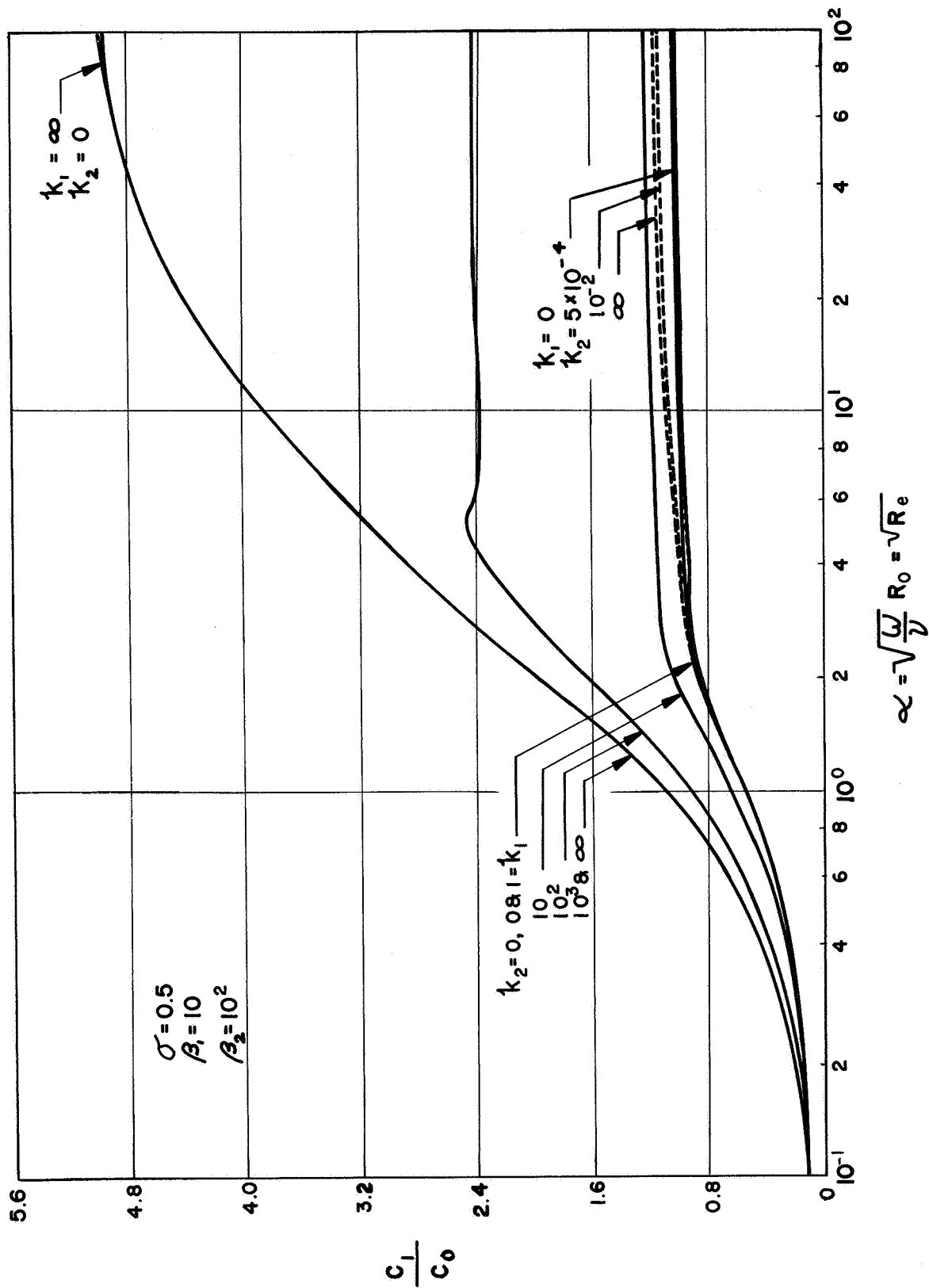
Figure 12. Wave Speed for the First Type of Waves as a Function of Reynolds Number
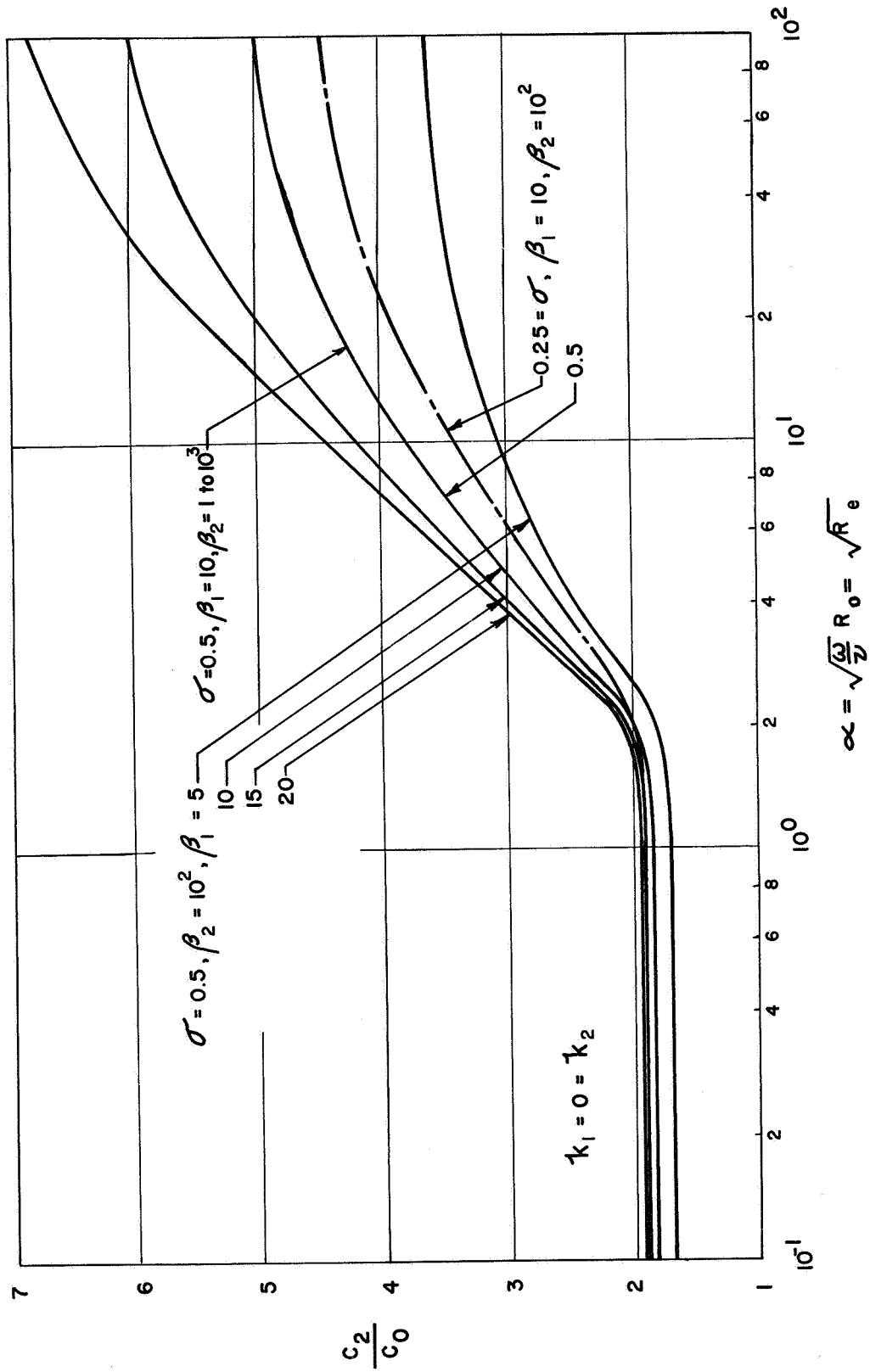
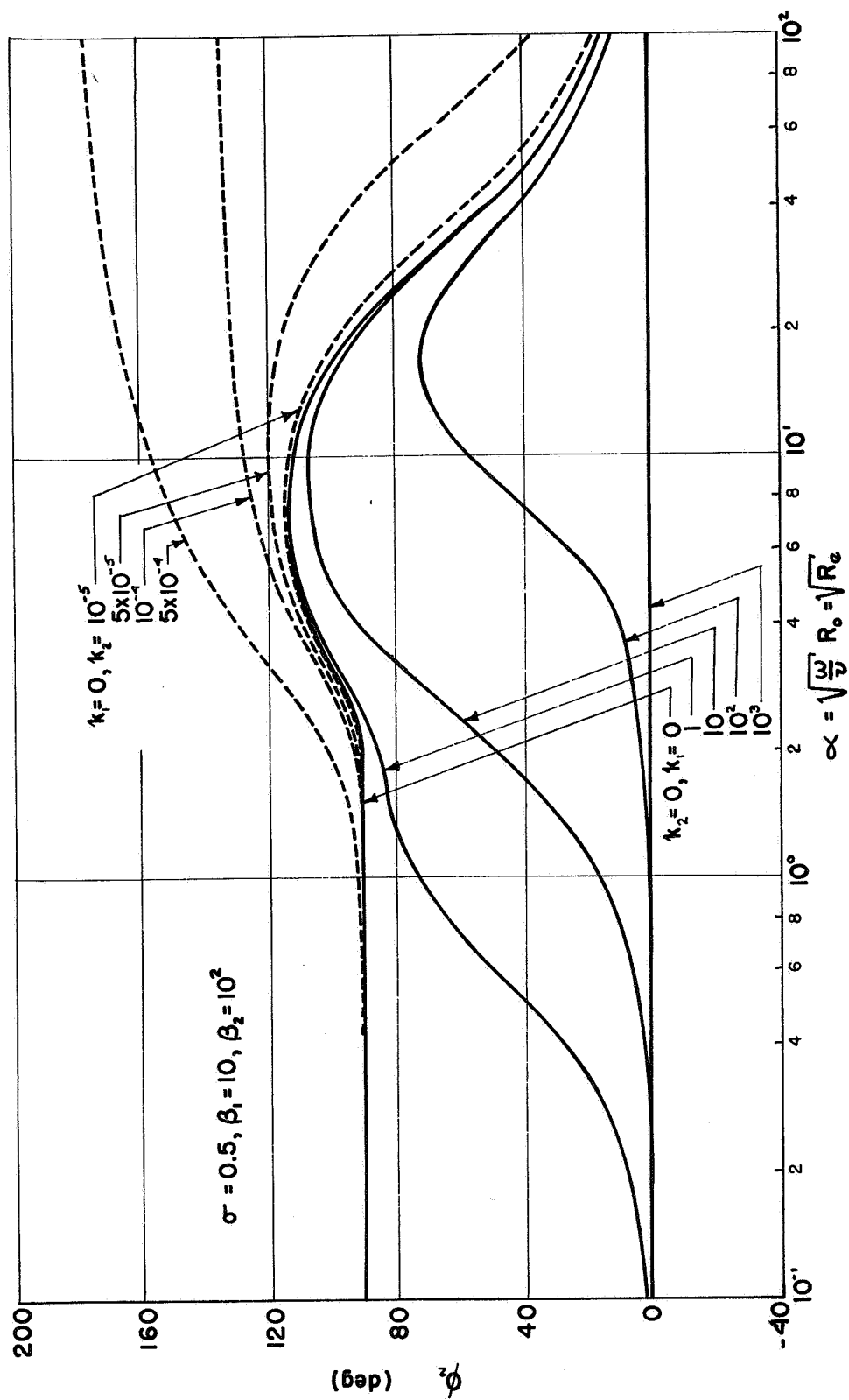Figure 13. Wave Speed for the Second Type of Waves as a Function of Reynolds Number
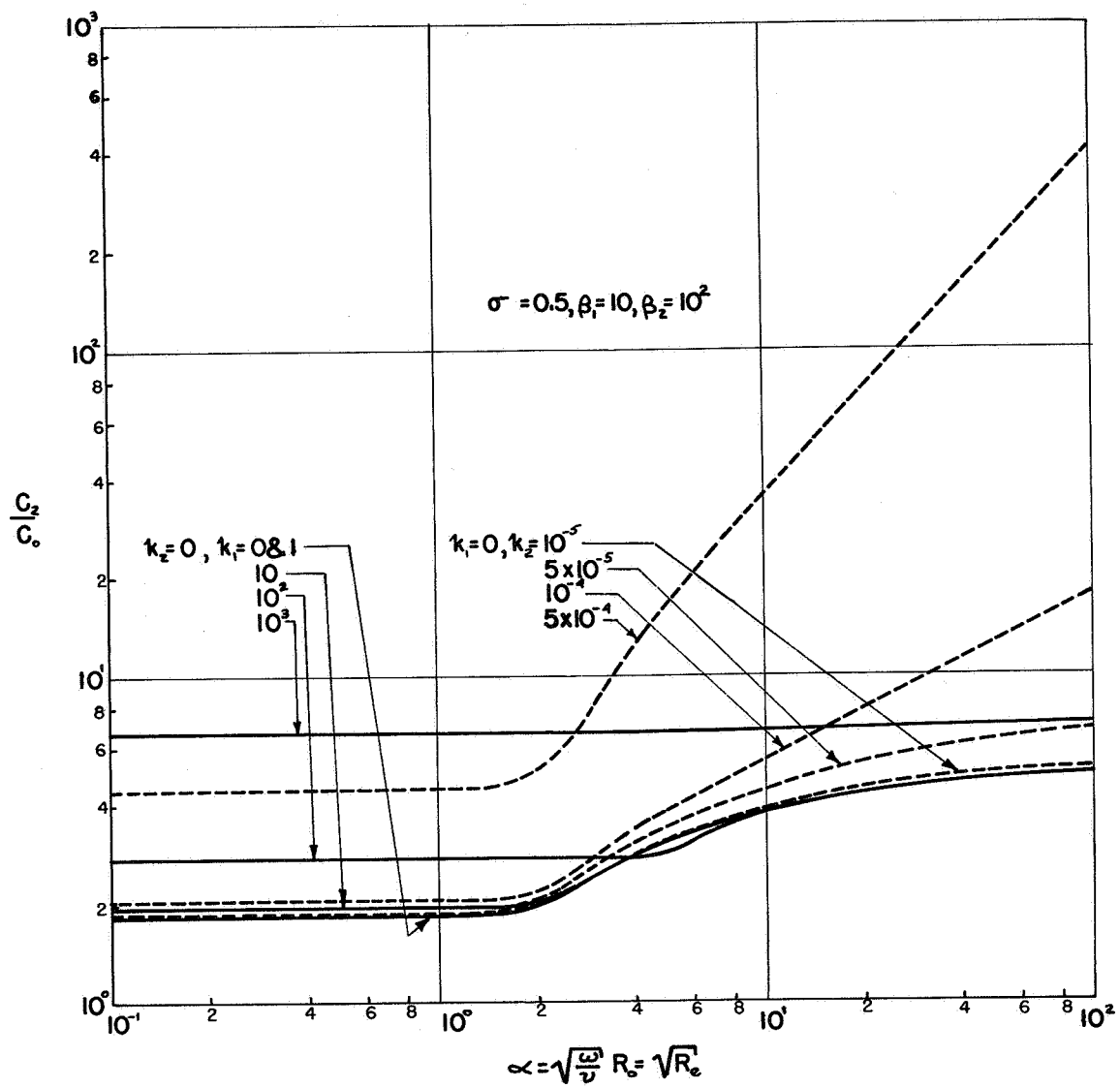
Figure 14. Wave Speed for the Second Type of Waves as a Function of Reynolds Number

88
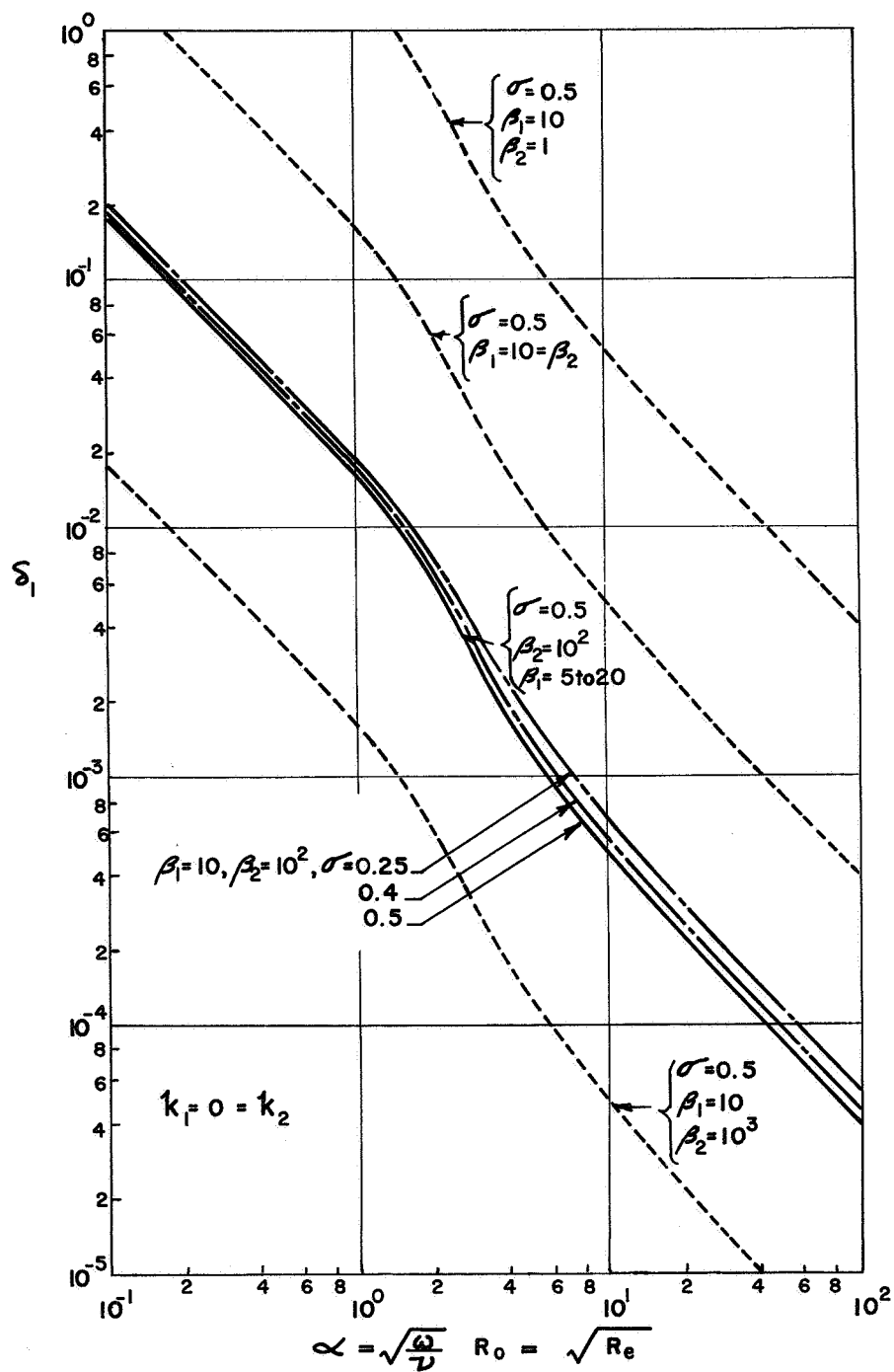
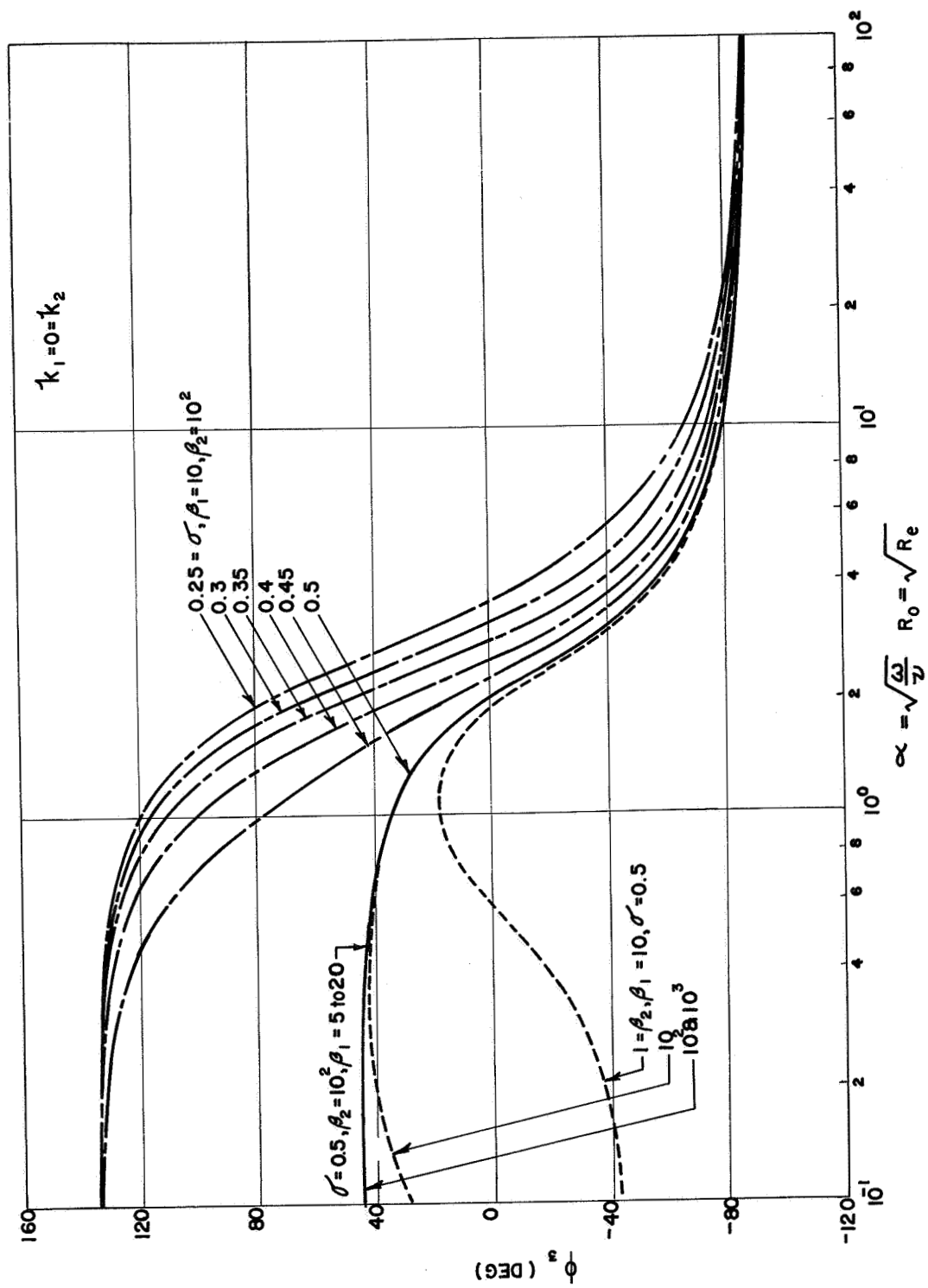Figure 15. Attenuation Coefficient for the First Type of Waves as a Function of Reynolds Number
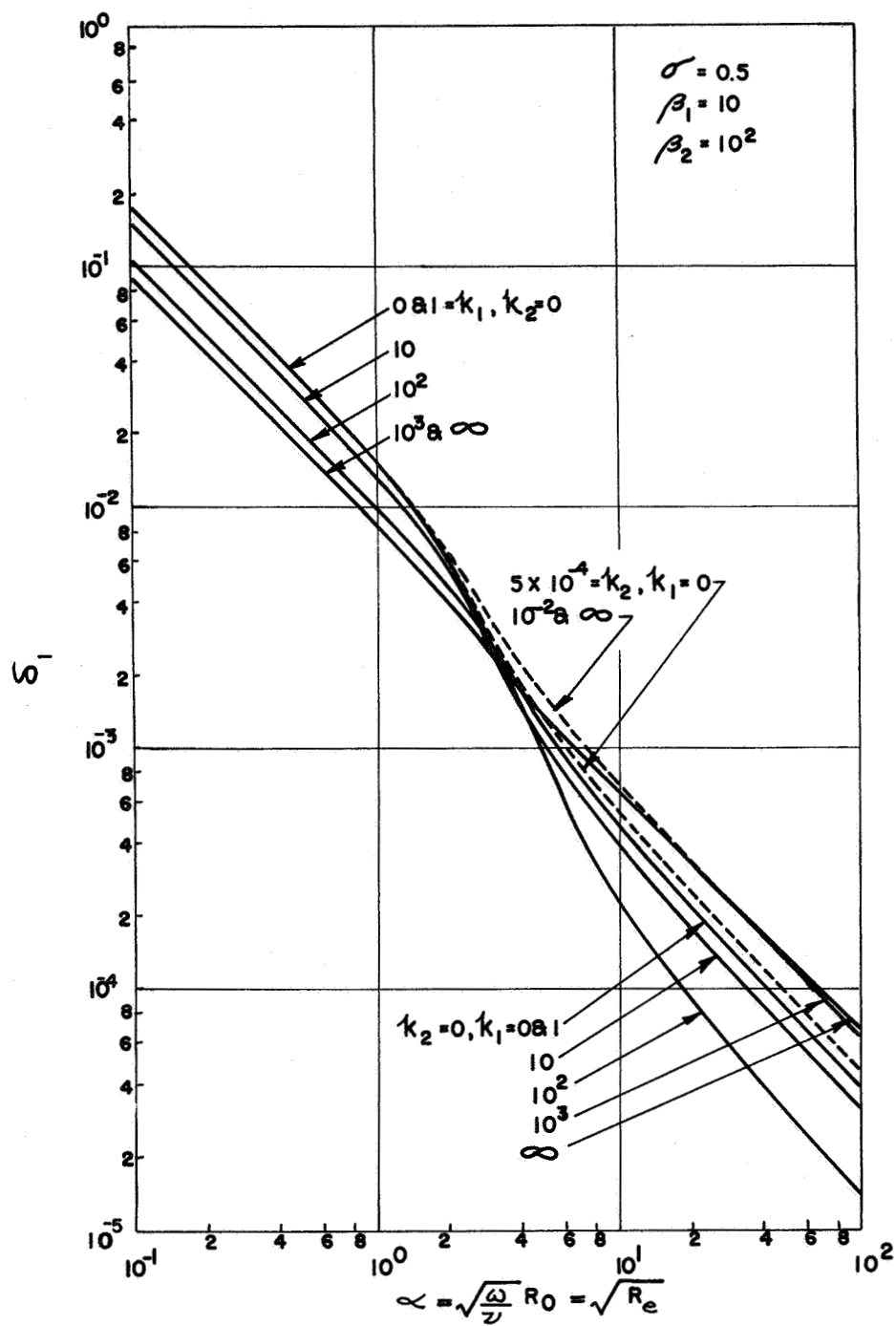
Figure 16. Attenuation Coefficient for the First Type of Waves as a Function of Reynolds Number

90
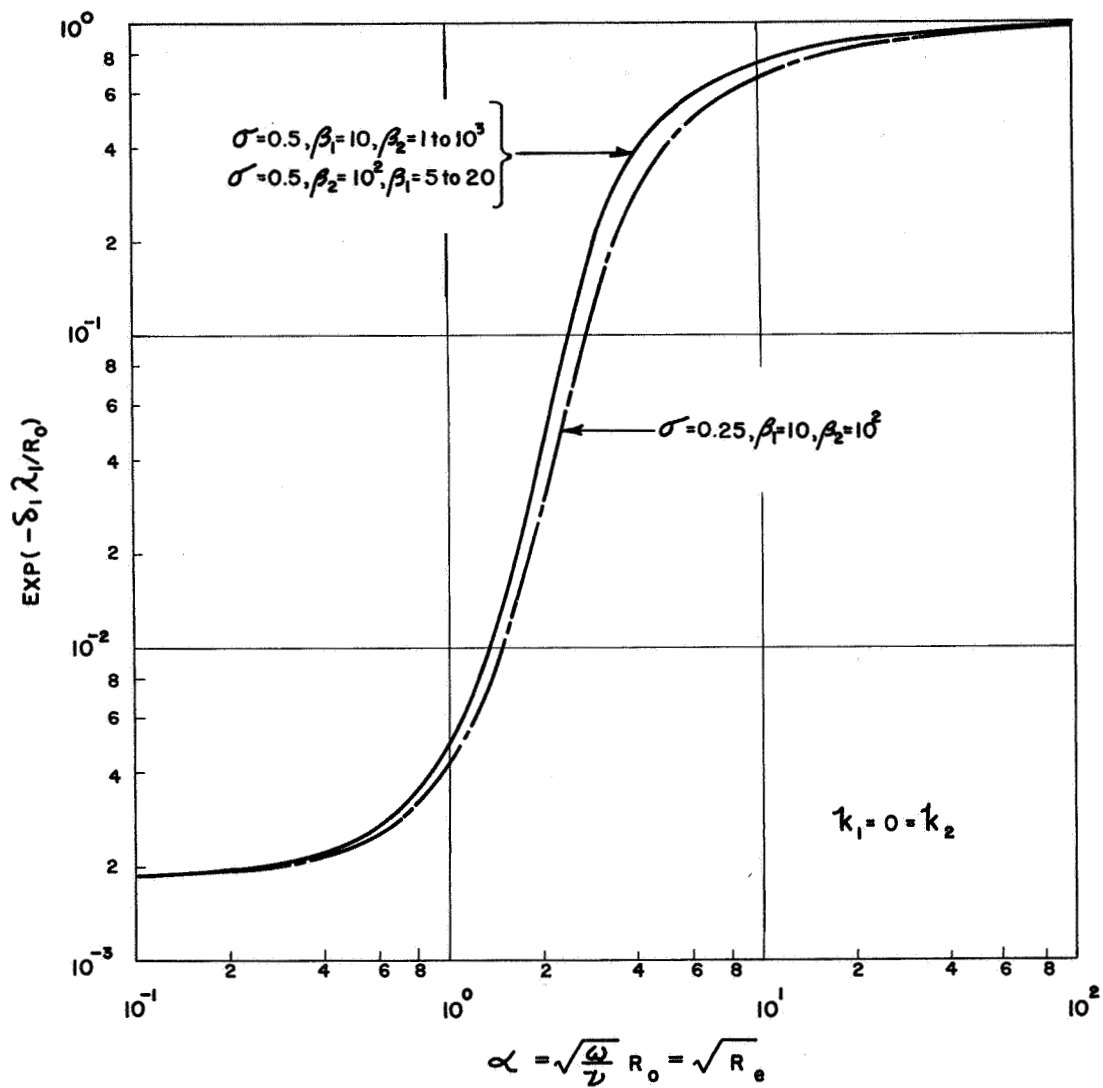
Figure 17. Transmission Factor for the First Type of Waves as a Function
of Reynolds Number

10^0

8
6

$k_1=0, k_2=5\times10^{-4}$

10^{-2}

∞

4

2

10^{-1}

8
6

$\sigma=0.5,\ \beta_1=10,\ \beta_2=10^2$

4

2

10^{-2}

8
6

$0 a_1 = k_1,\ k_2=0$

4

10

10^2

2

10^3 TO ∞

10^{-3}

10^1 2   4   6   8 10^0 2   4   6   8 10^1 2   4   6   8 10^2

$\text{EXP}(-\lambda_1\ \delta_1/R_0)$

$\propto = \sqrt{\dfrac{\omega}{\nu}}\ R_0 = \sqrt{R_e}$
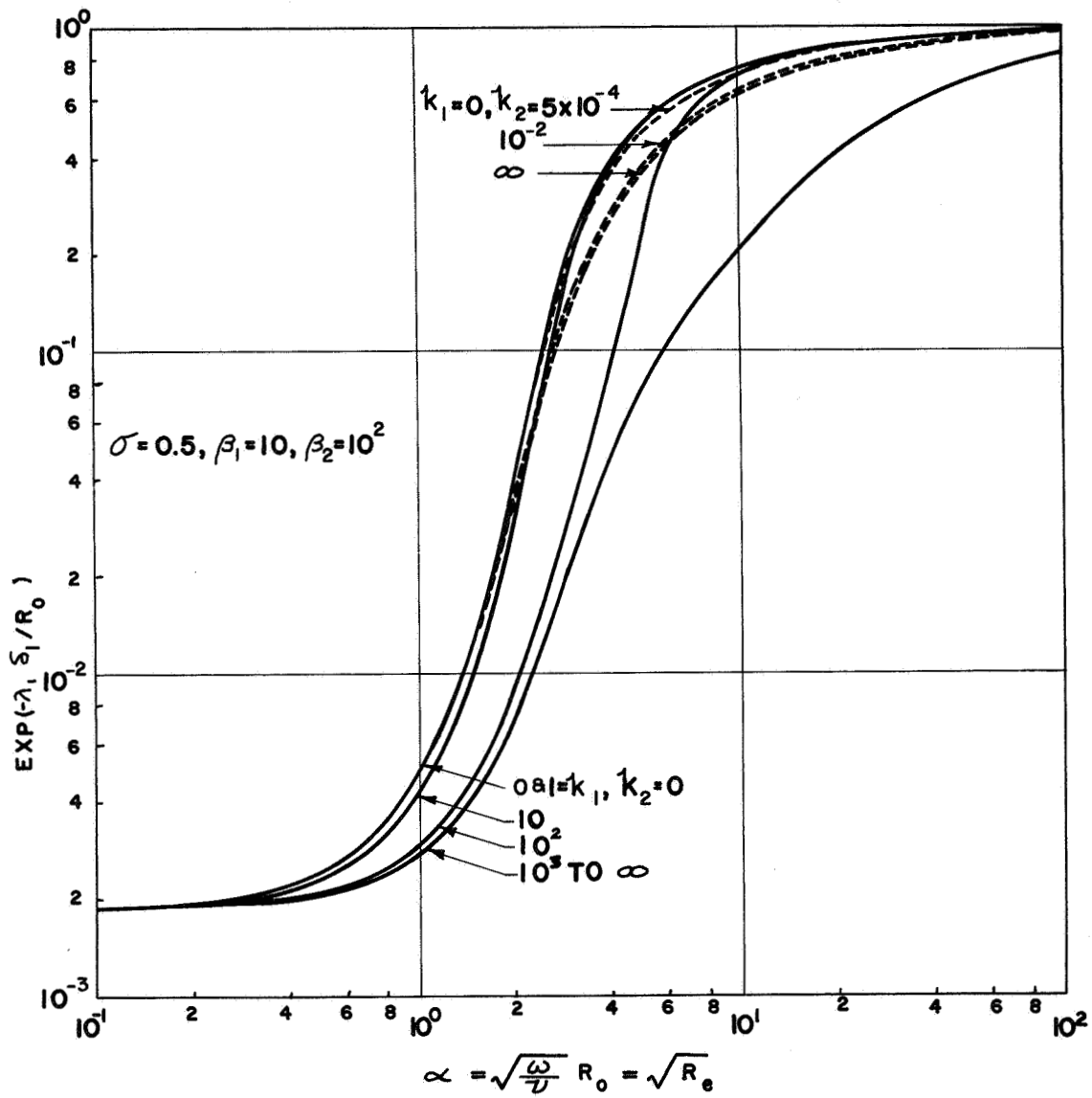
Figure 18. Transmission Factor for the First Type of Waves as a Function of Reynolds Number
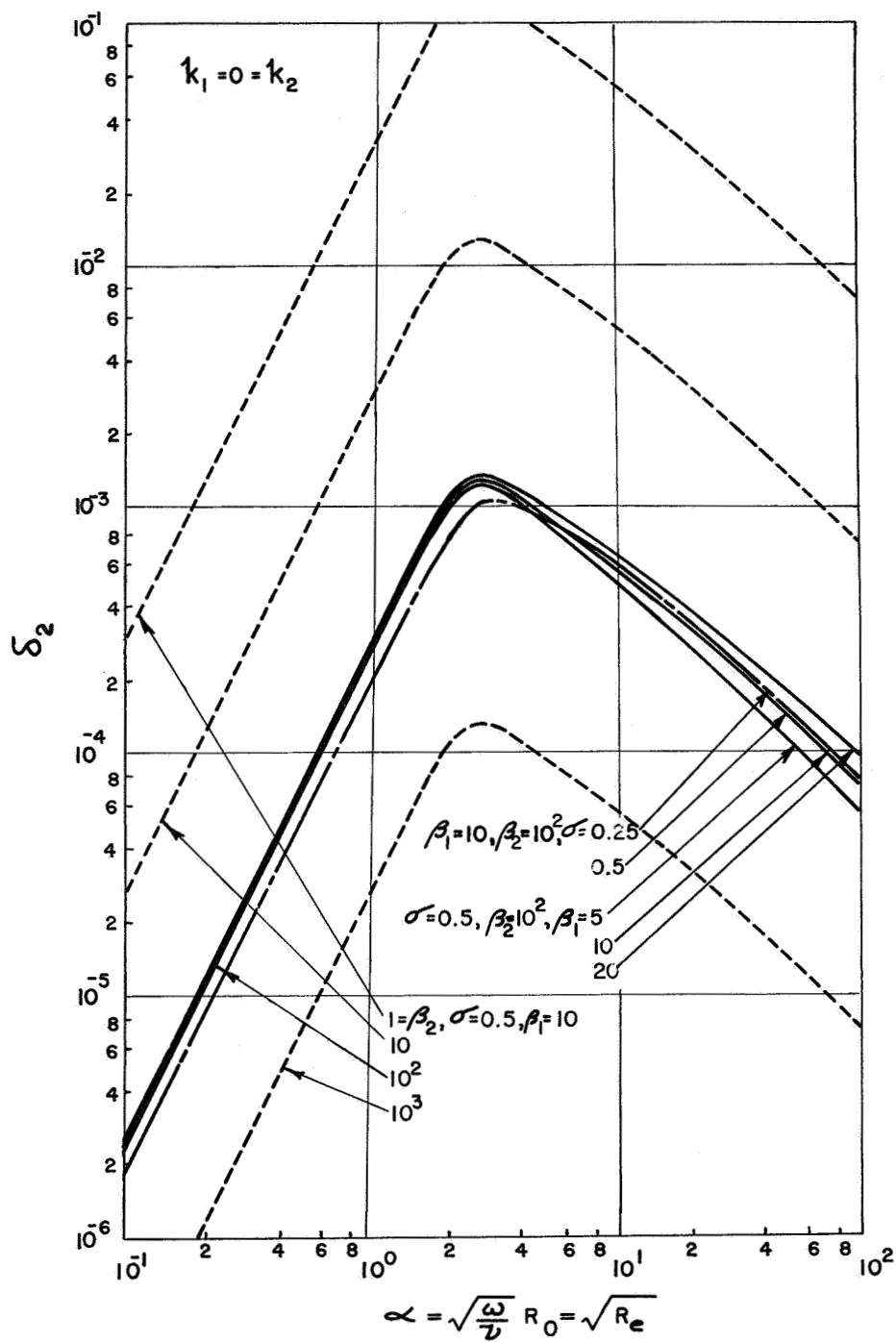
Figure 19. Attenuation Coefficient for the Second Type of Waves as a Function of Reynolds Number

93
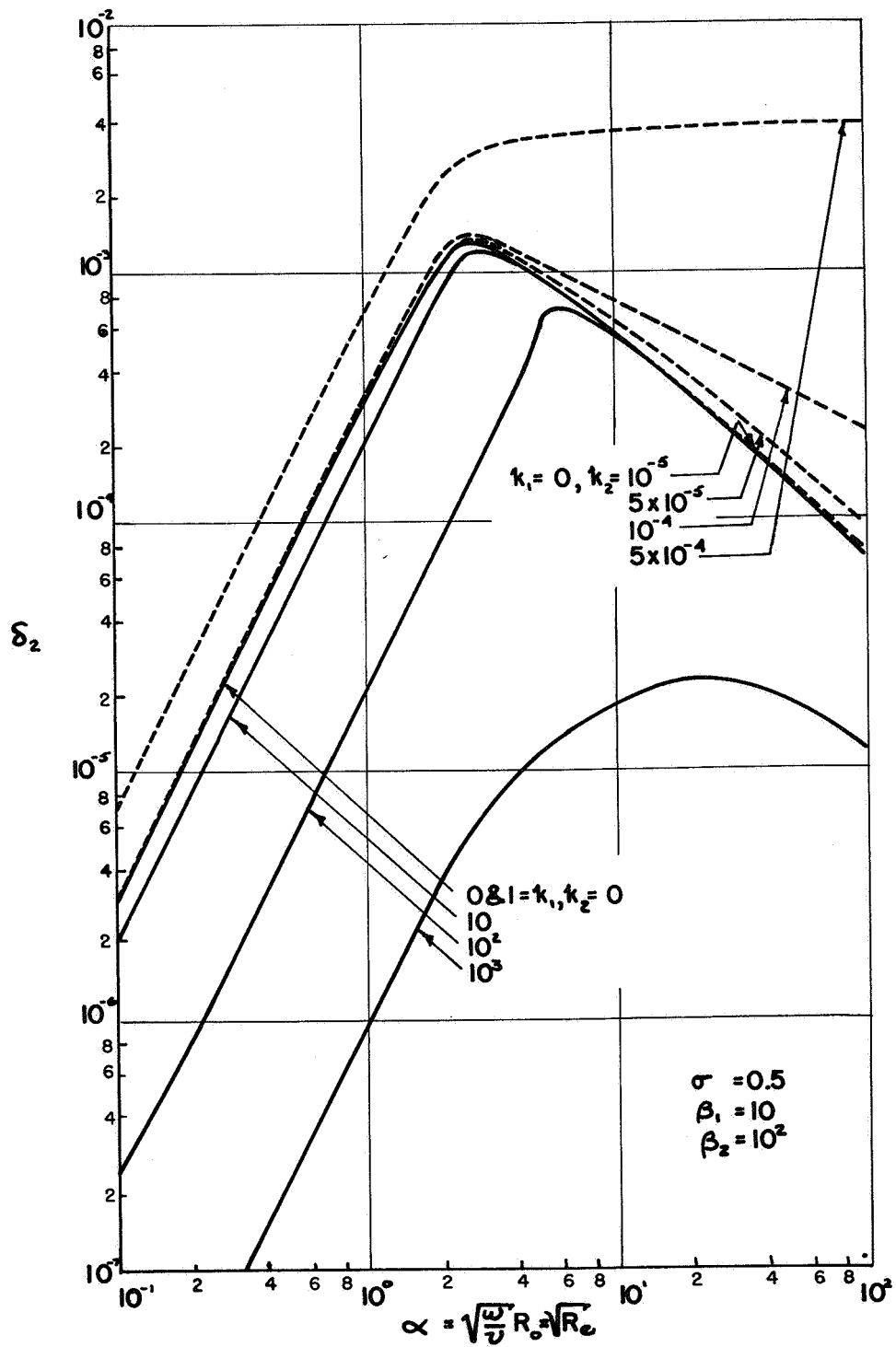
Figure 20. Attenuation Coefficient for the Second Type of Waves as a Function of Reynolds Number

94
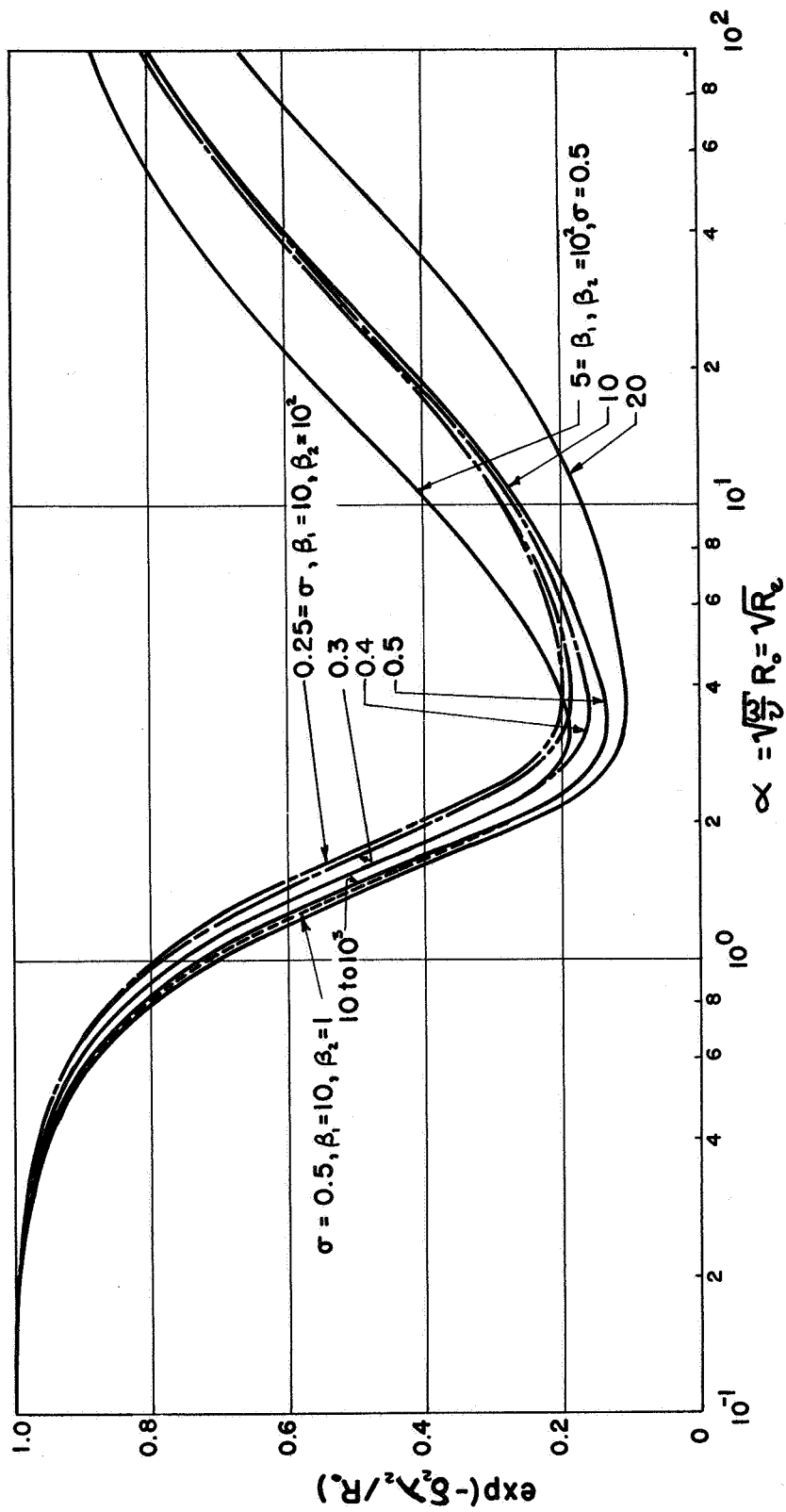
Figure 21. Transmission Factor for the Second Type of Waves as a Function of Reynolds Number

95
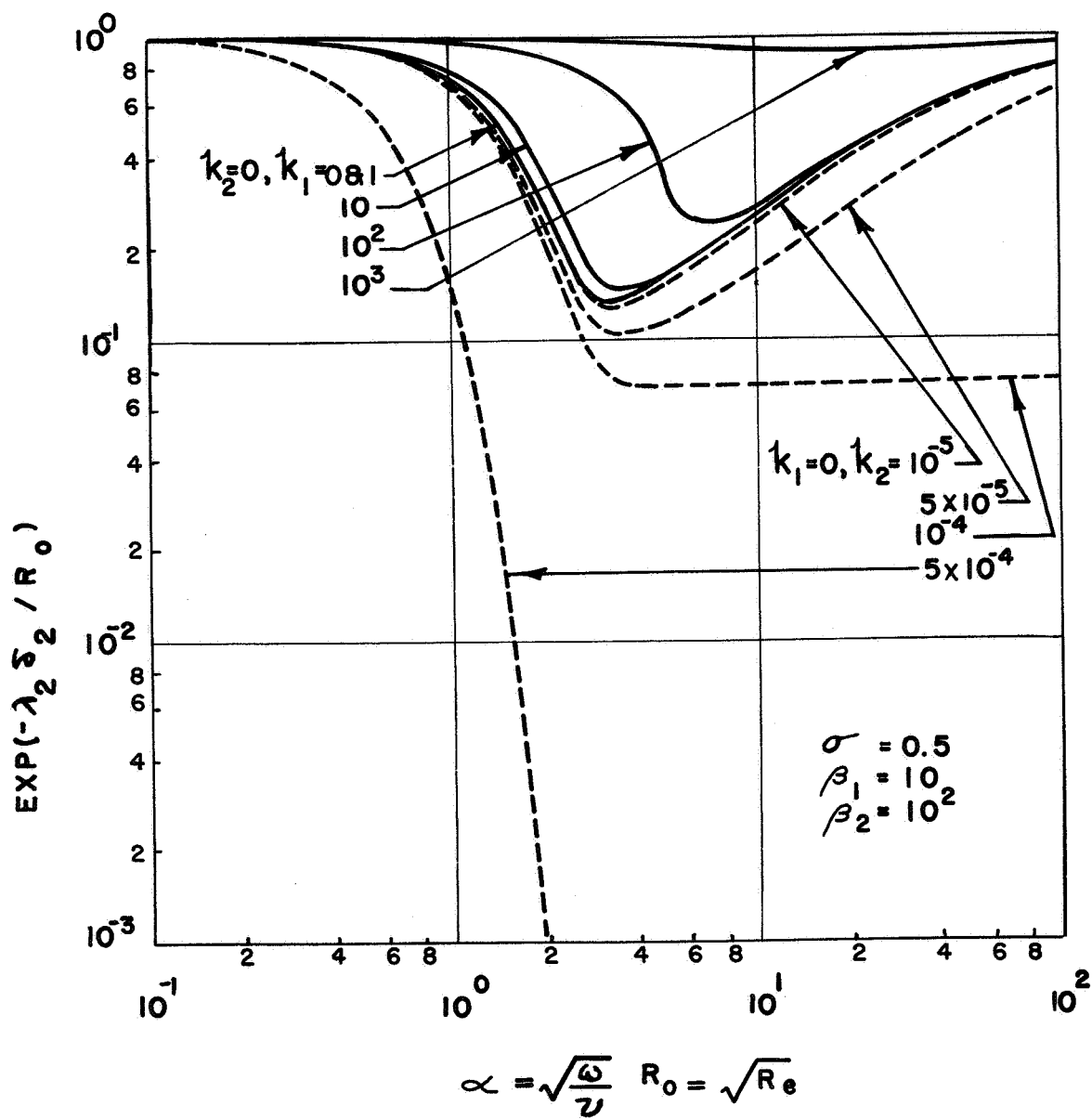
Figure 22. Transmission Factor for the Second Type of Waves as a Function of Reynolds Number
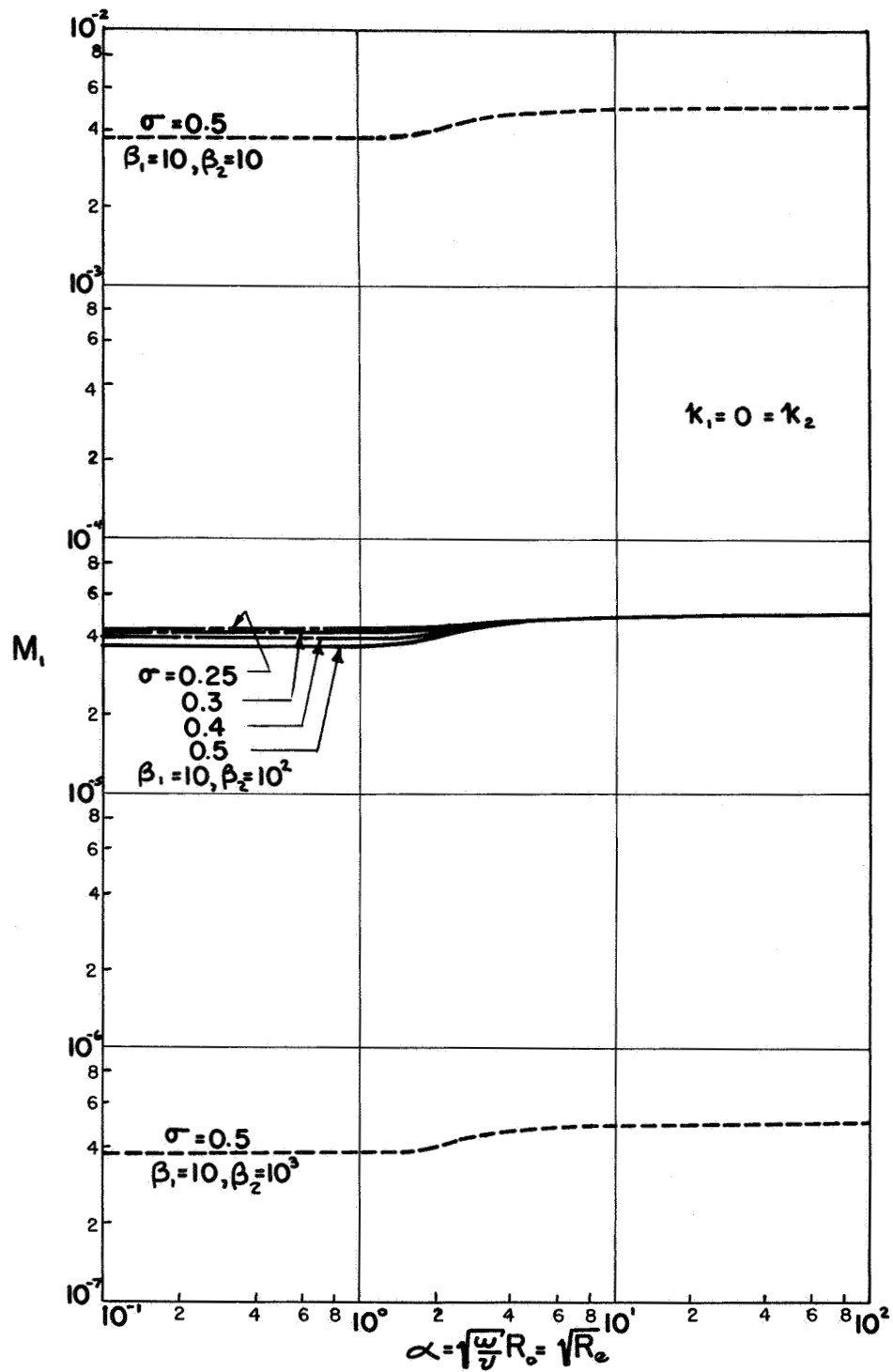
Figure 23. The Mode Shape Parameter for the Radial Displacements of the
First Type of Waves as a Function of Reynolds Number
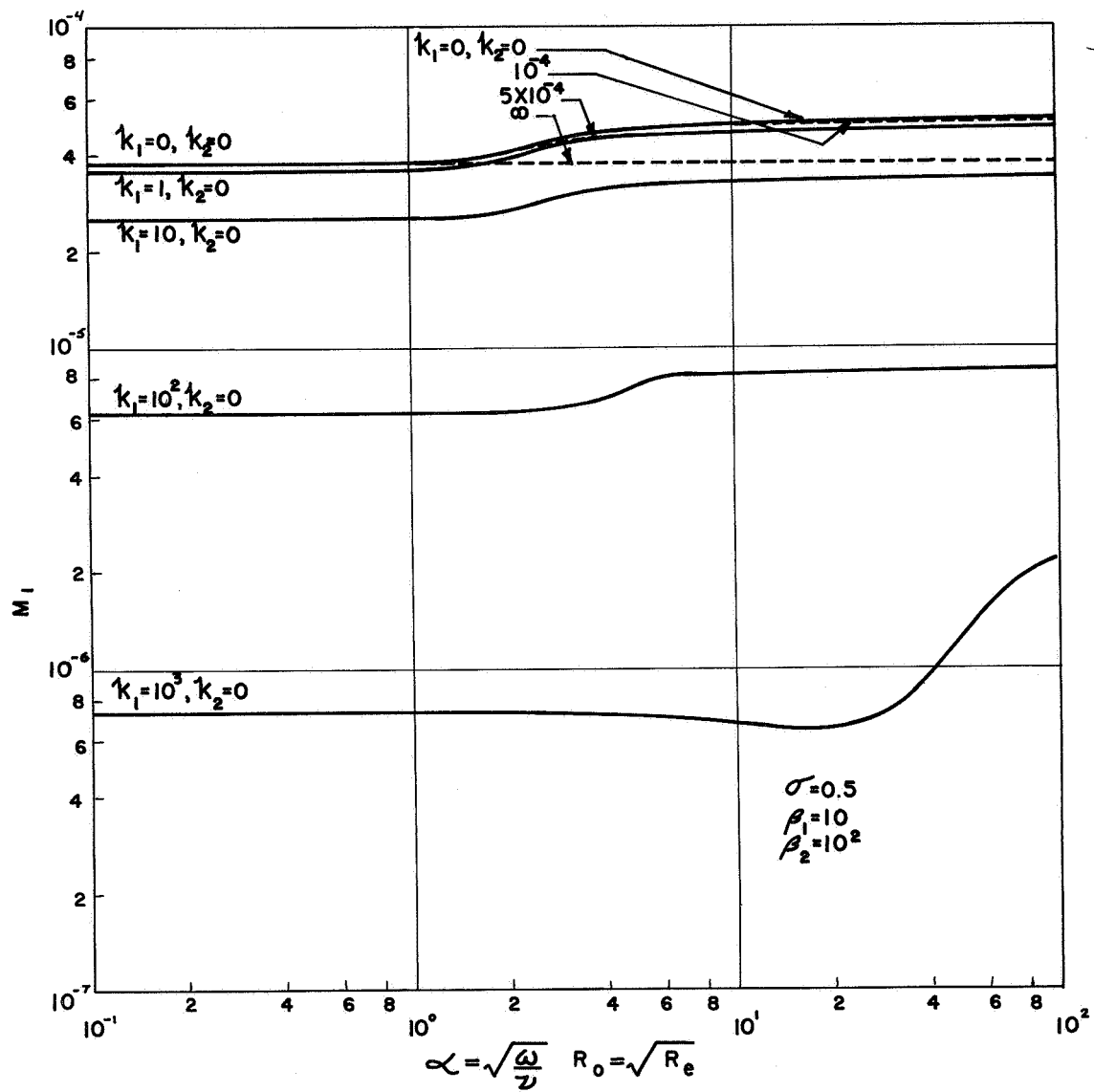
Figure 24. The Mode Shape Parameter for the Radial Displacements of the
First Type of Waves as a Function of Reynolds Number
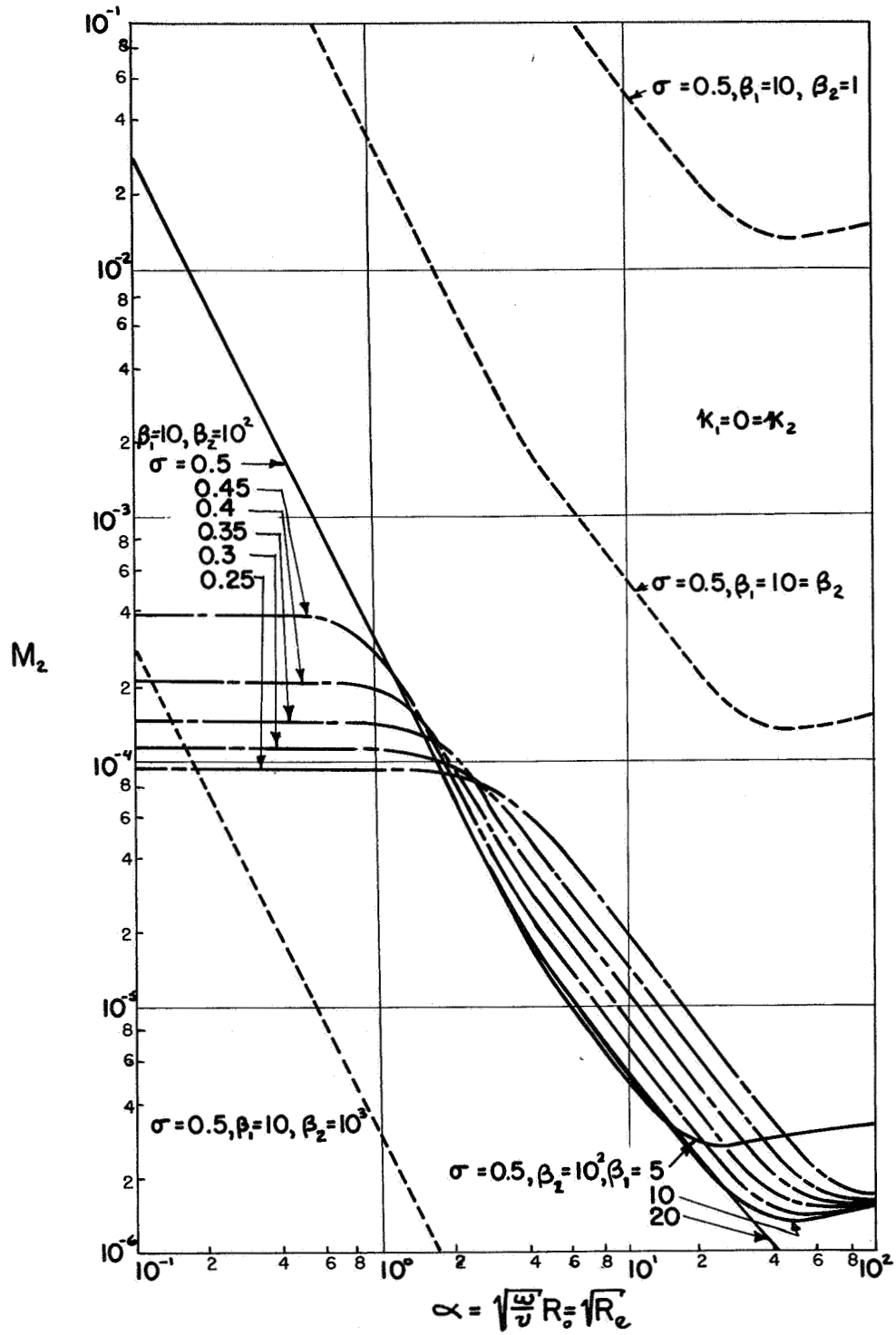
Figure 25. The Mode Shape Parameter for the Radial Displacements of the Second Type of Waves as a Function of Reynolds Number

99
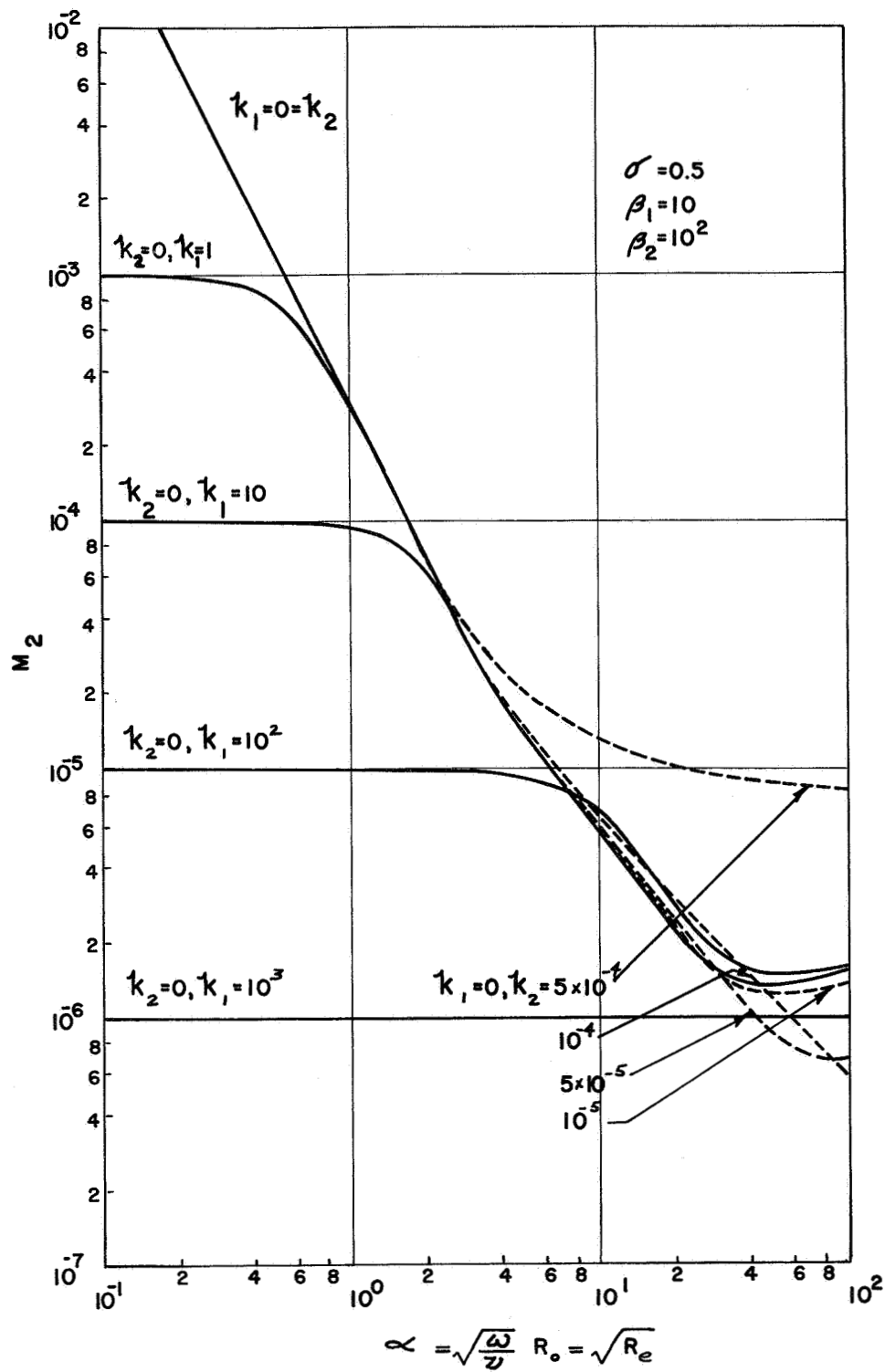
Figure 26. The Mode Shape Parameter for the Radial Displacements of the Second Type of Waves as a Function of Reynolds Number
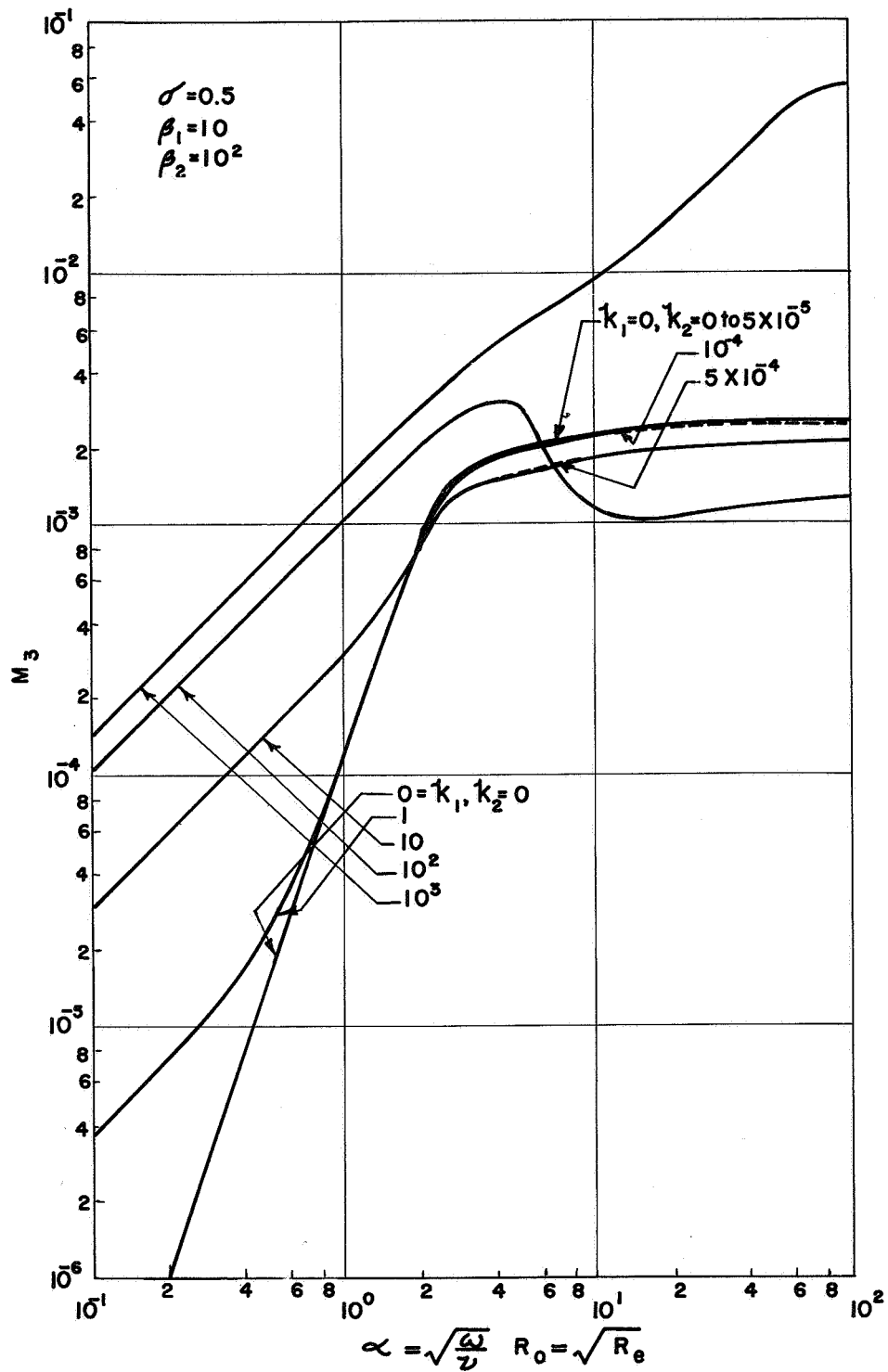
Figure 28. The Mode Shape Parameter for the Axial Displacements of the
First Type of Waves as a Function of Reynolds Number
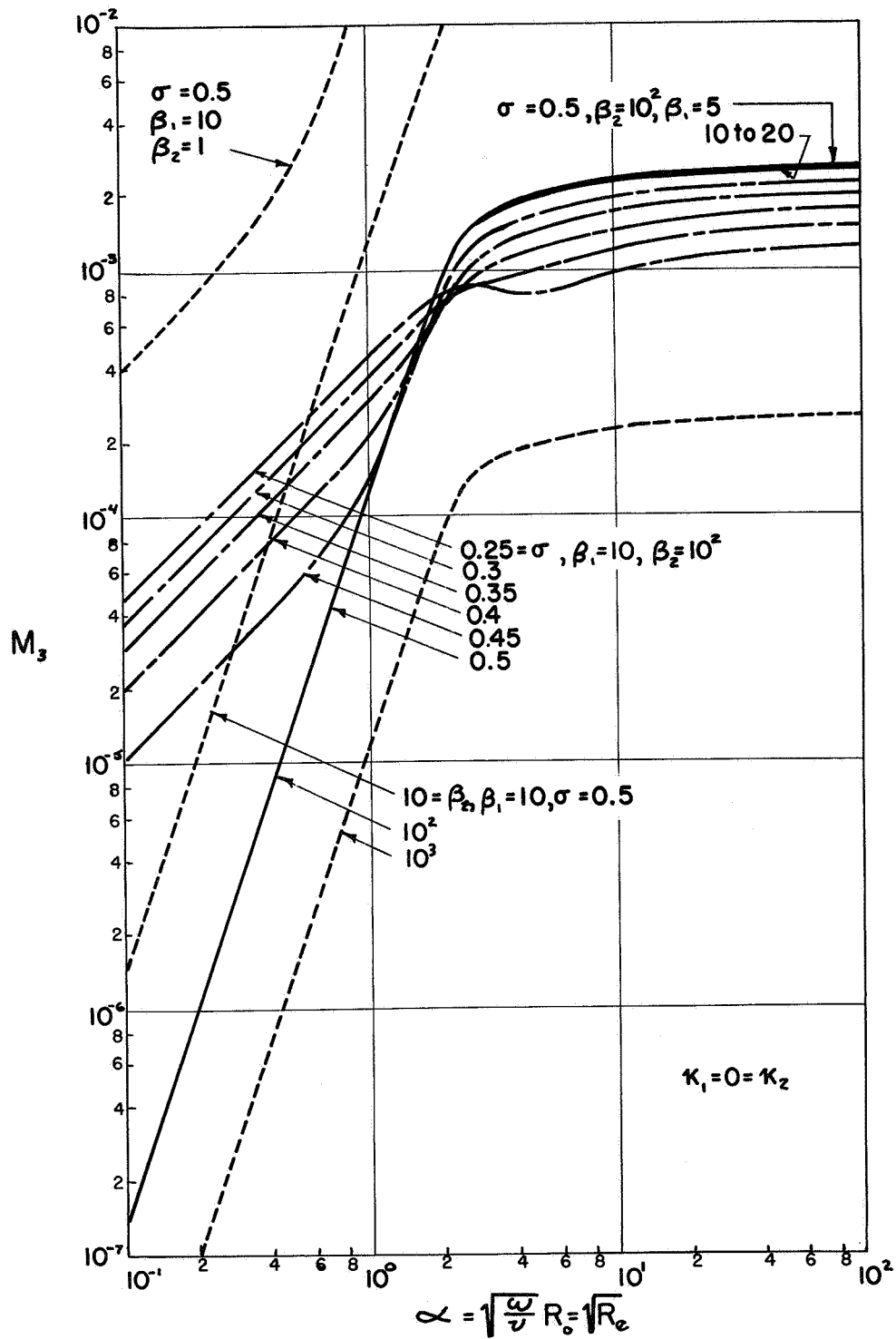
Figure 27. The Mode Shape Parameter for the Axial Displacements of the First Type of Waves as a Function of Reynolds Number

102
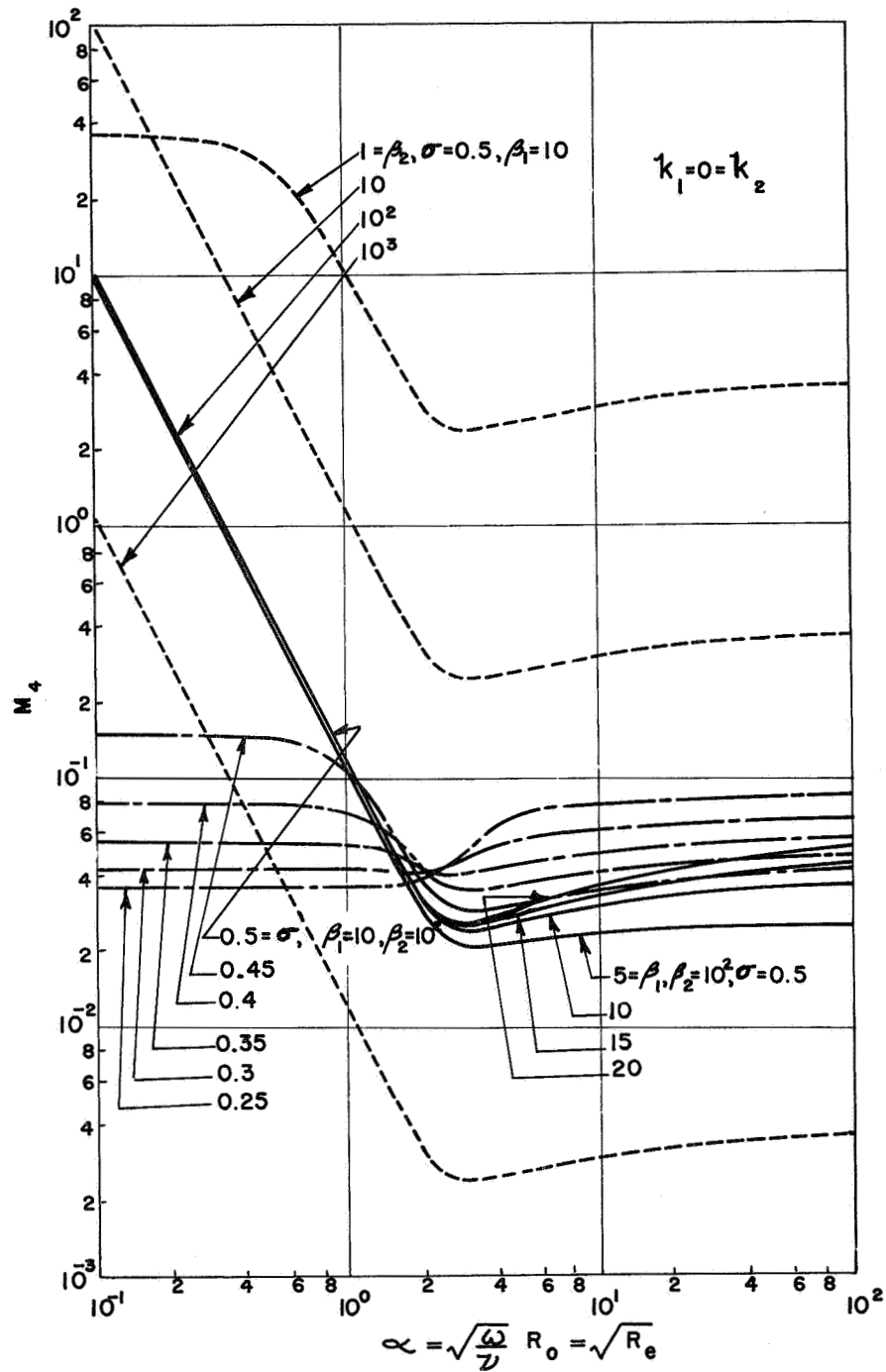
Figure 29. The Mode Shape Parameter for the Axial Displacements of the Second Type of Waves as a Function of Reynolds Number

103
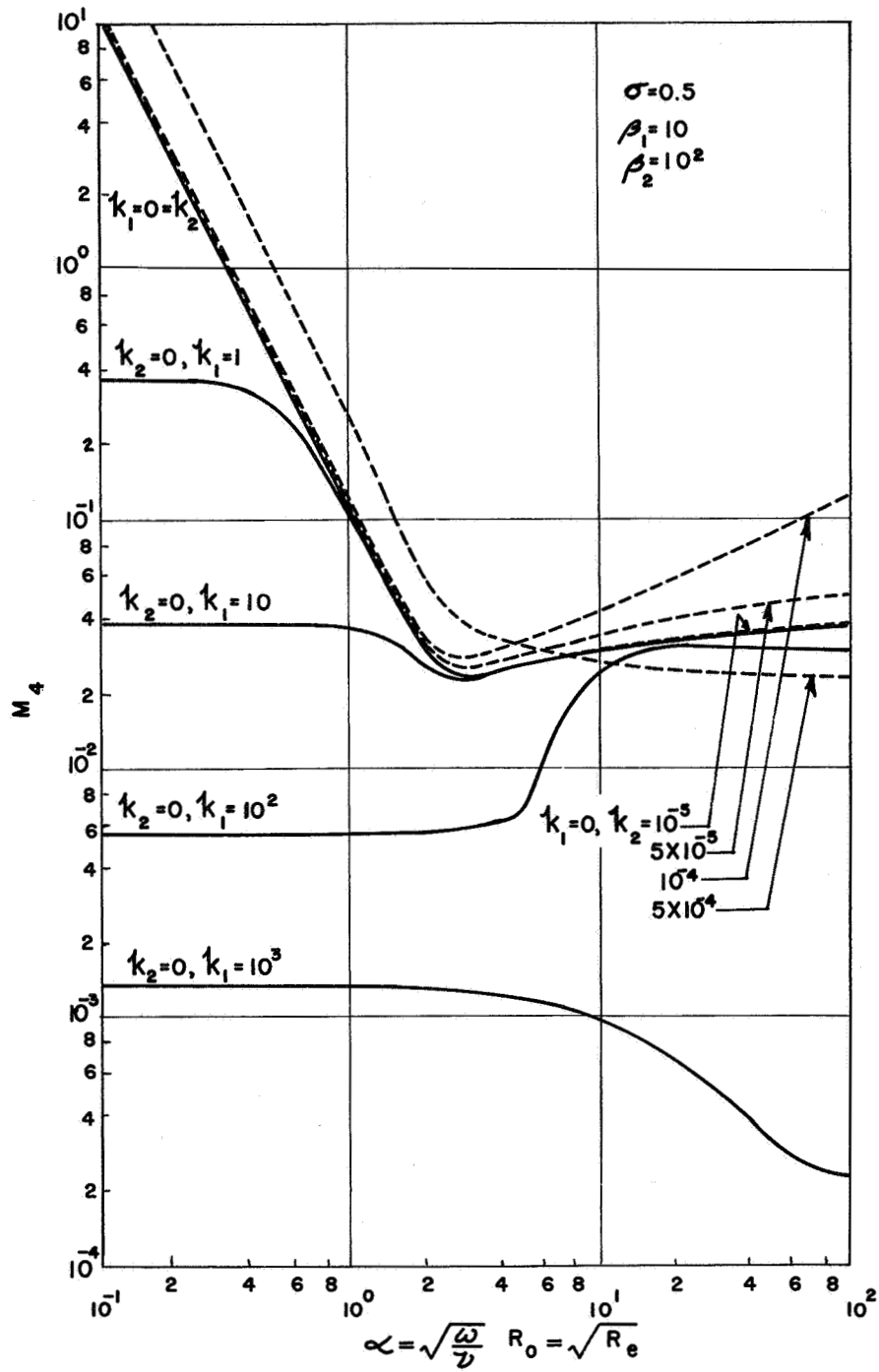
Figure 30. The Mode Shape Parameter for the Axial Displacements of the Second Type of Waves as a Function of Reynolds Number

104
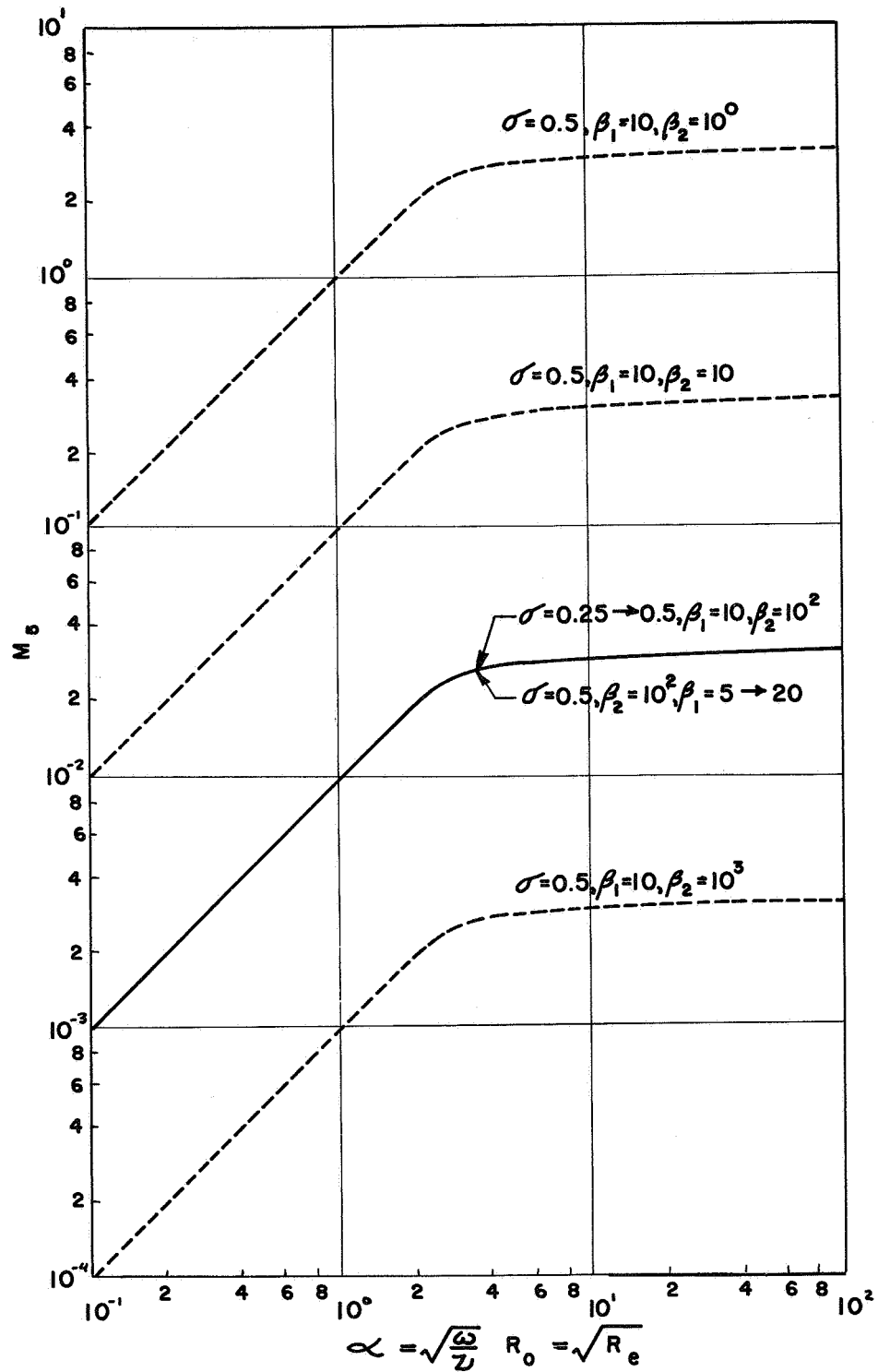
Figure 31. The Mode Shape Parameter for Fluid Mass Flow Rate with the First Type of Waves as a Function of Reynolds Number

105
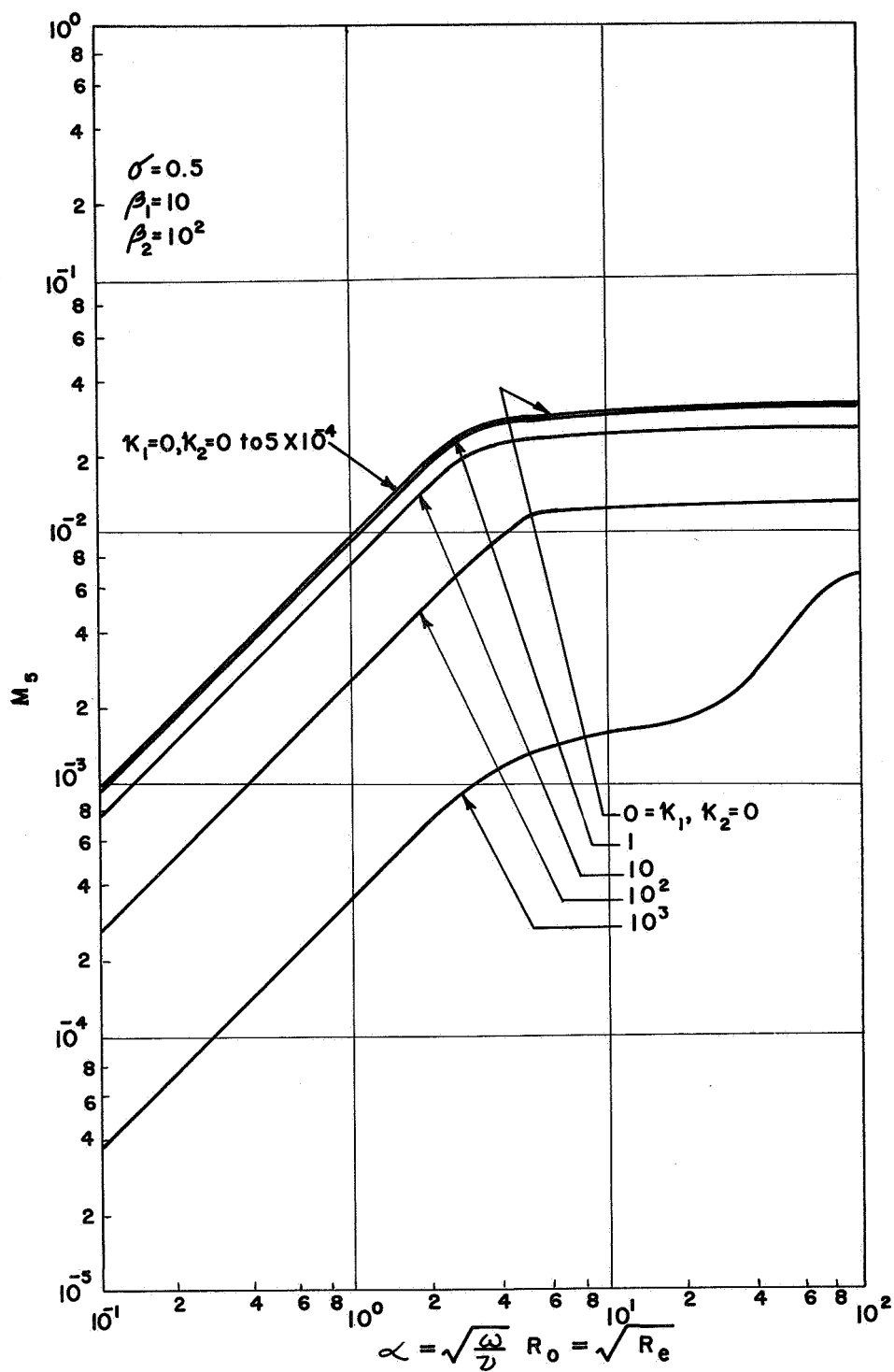
Figure 32. The Mode Shape Parameter for Fluid Mass Flow Rate with the First Type of Waves as a Function of Reynolds Number
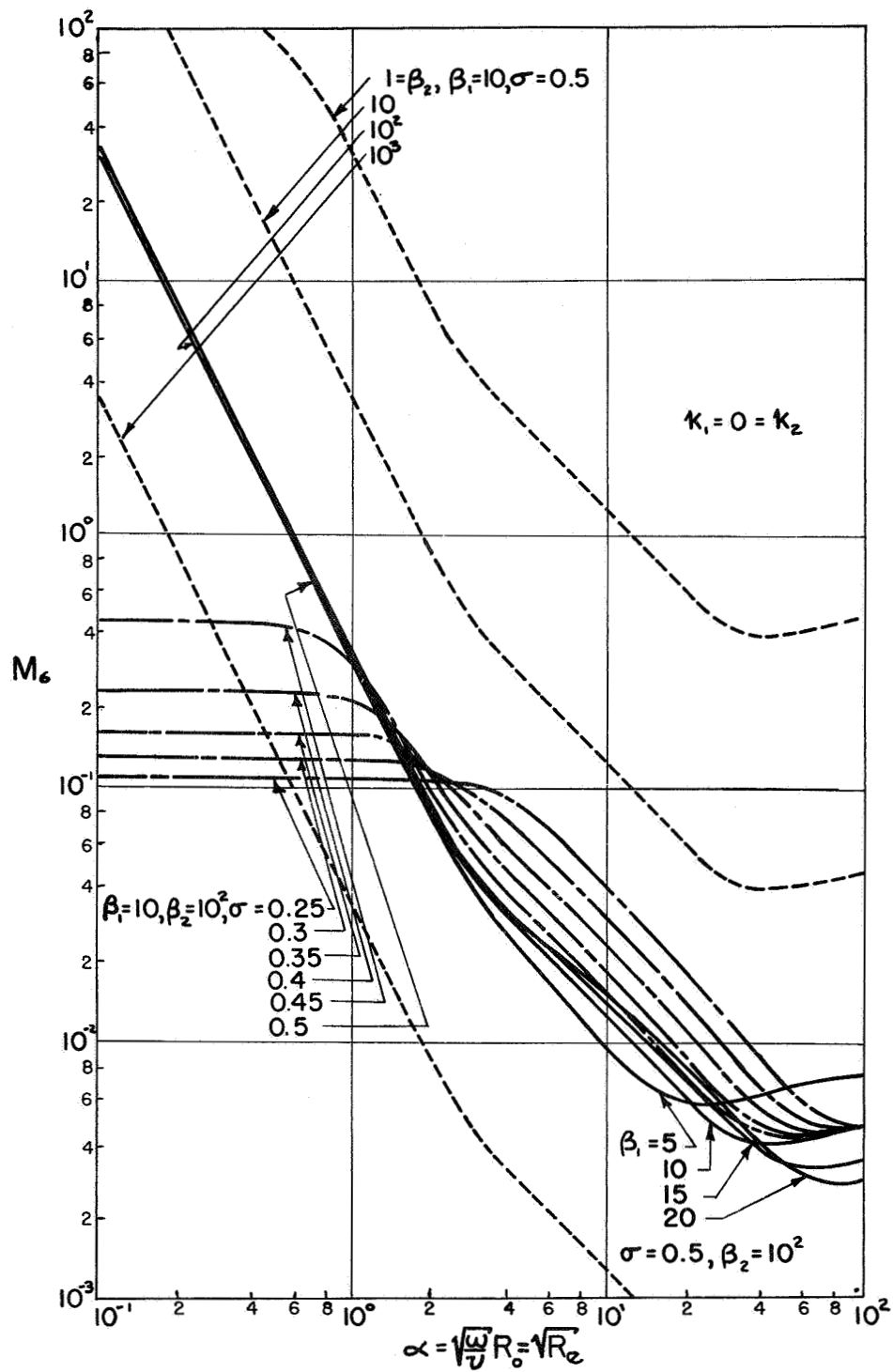
Figure 33. The Mode Shape Parameter for Fluid Mass Flow Rate with the Second Type of Waves as a Function of Reynolds Number
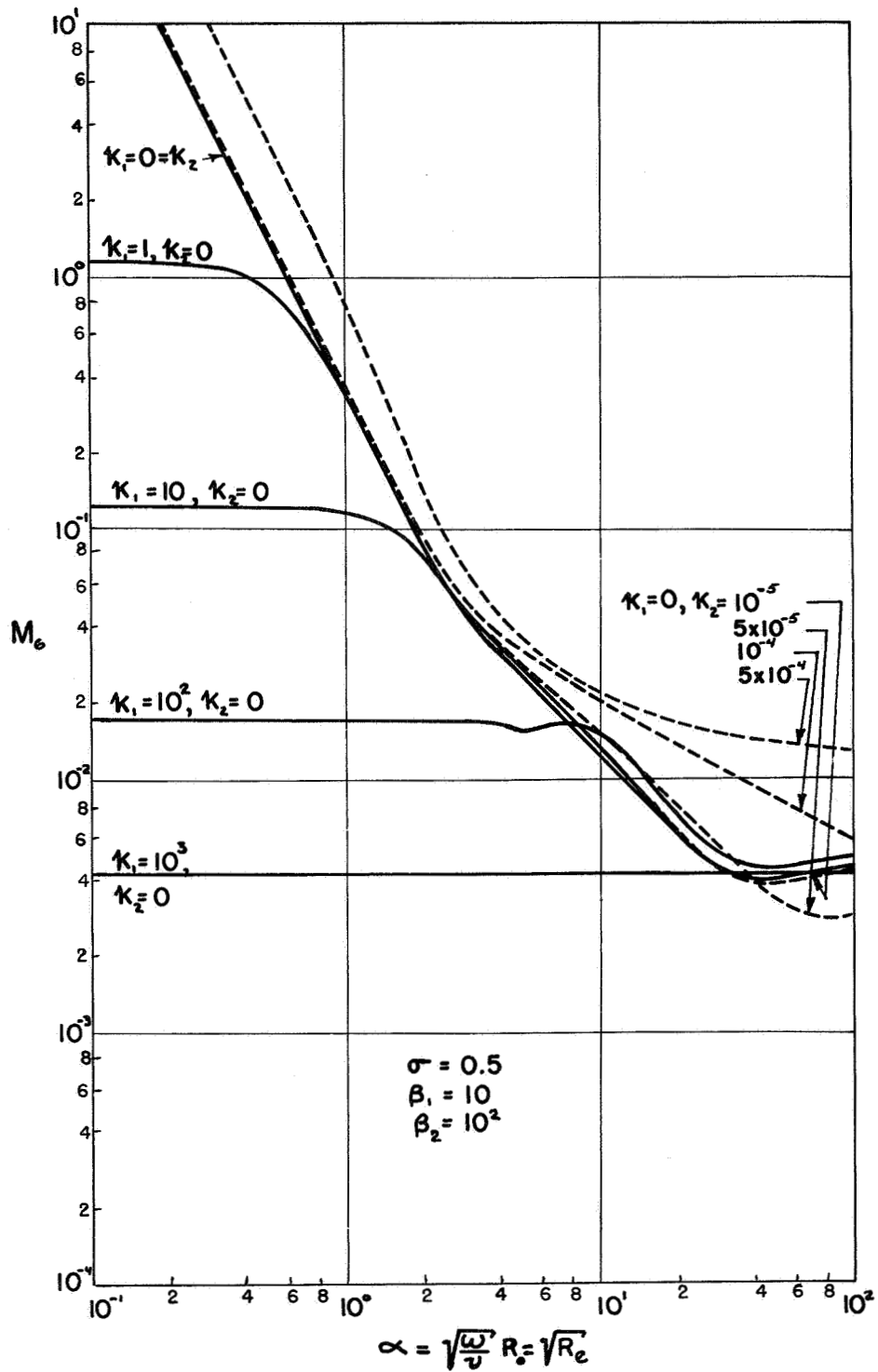
Figure 34. The Mode Shape Parameter for Fluid Mass Flow Rate with the Second Type of Waves as a Function of Reynolds Number
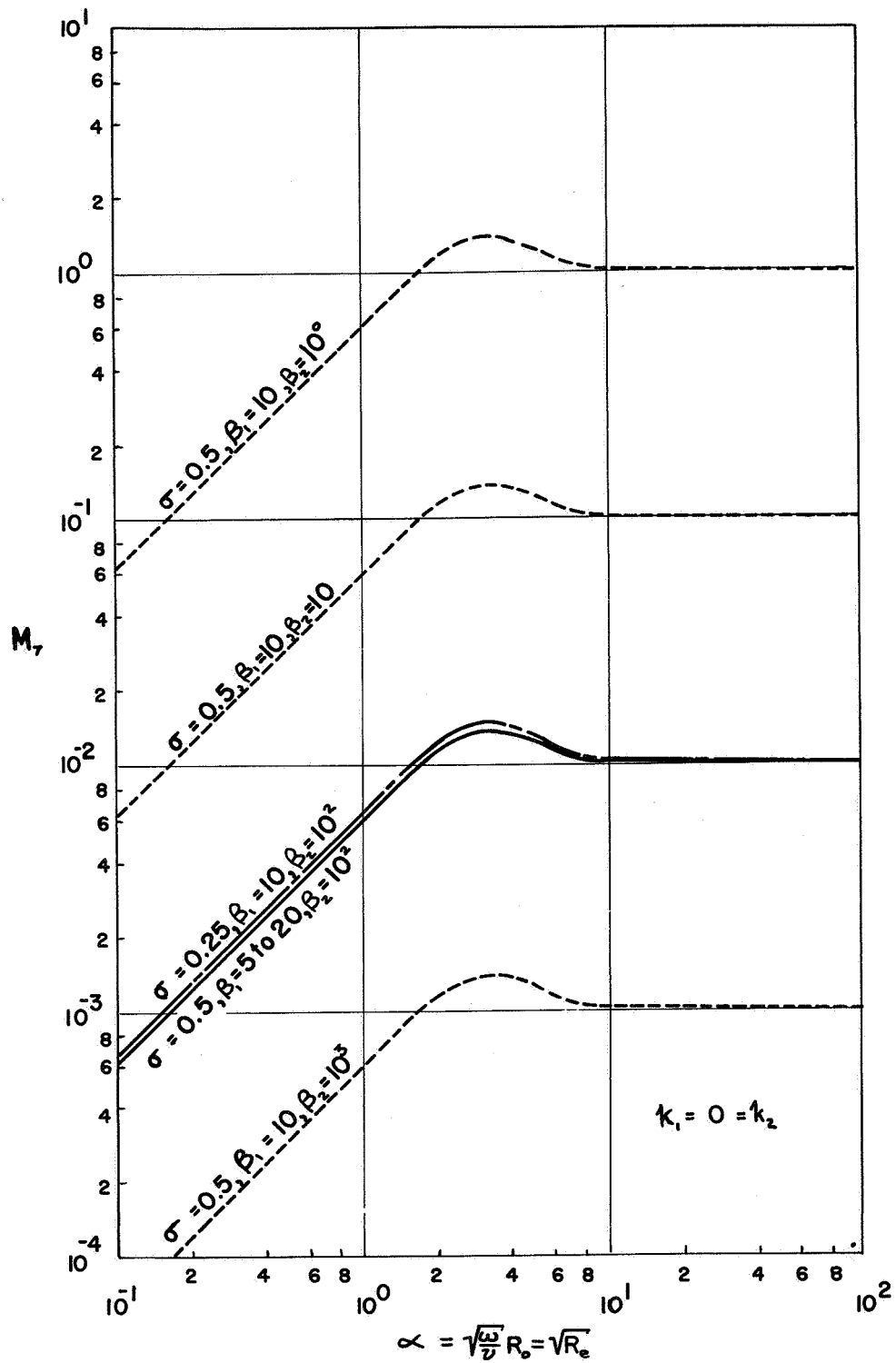
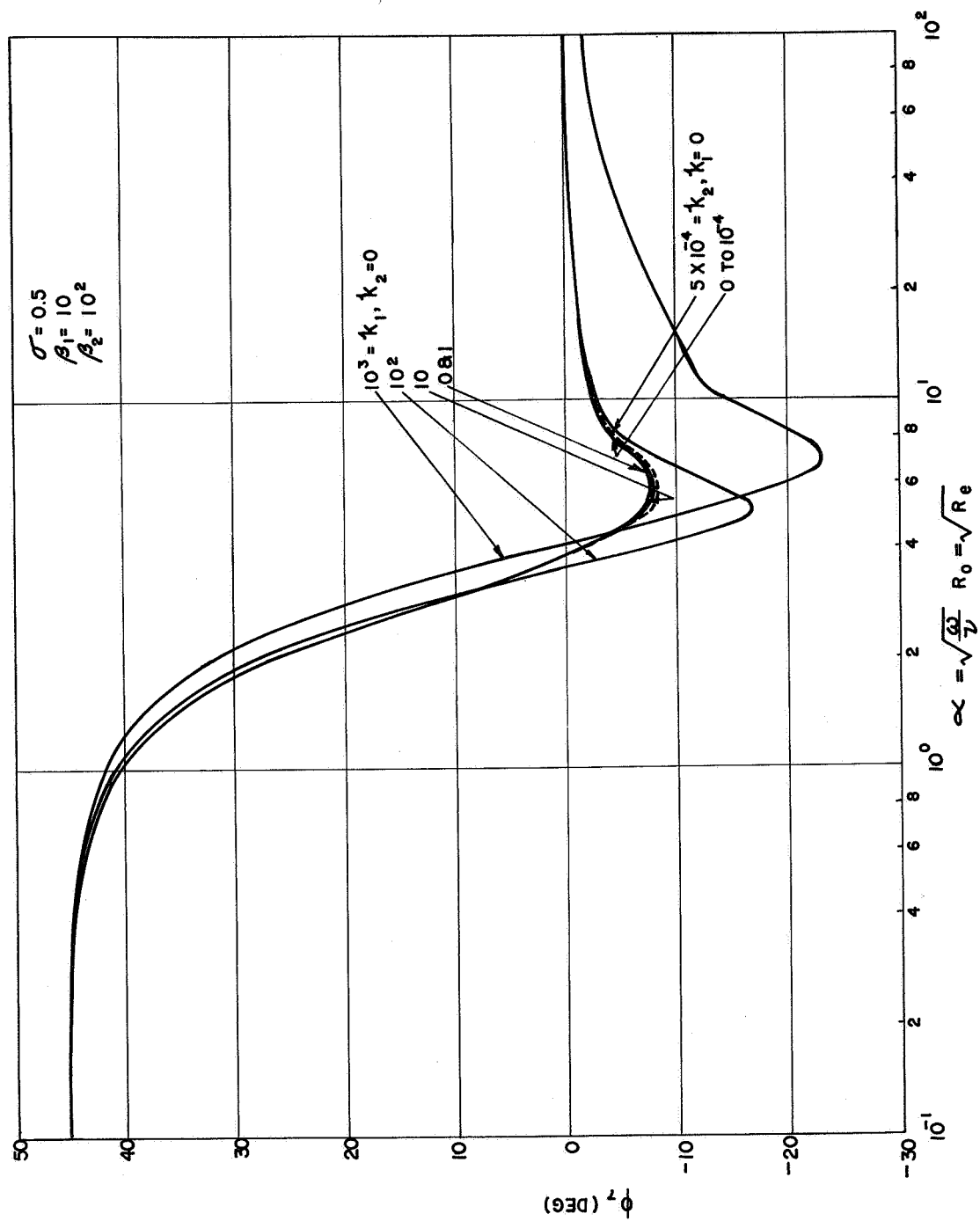Figure 35. The Mode Shape Parameter for Axial Fluid Velocity on the Axis with the First Type of Waves as a Function of Reynolds Number
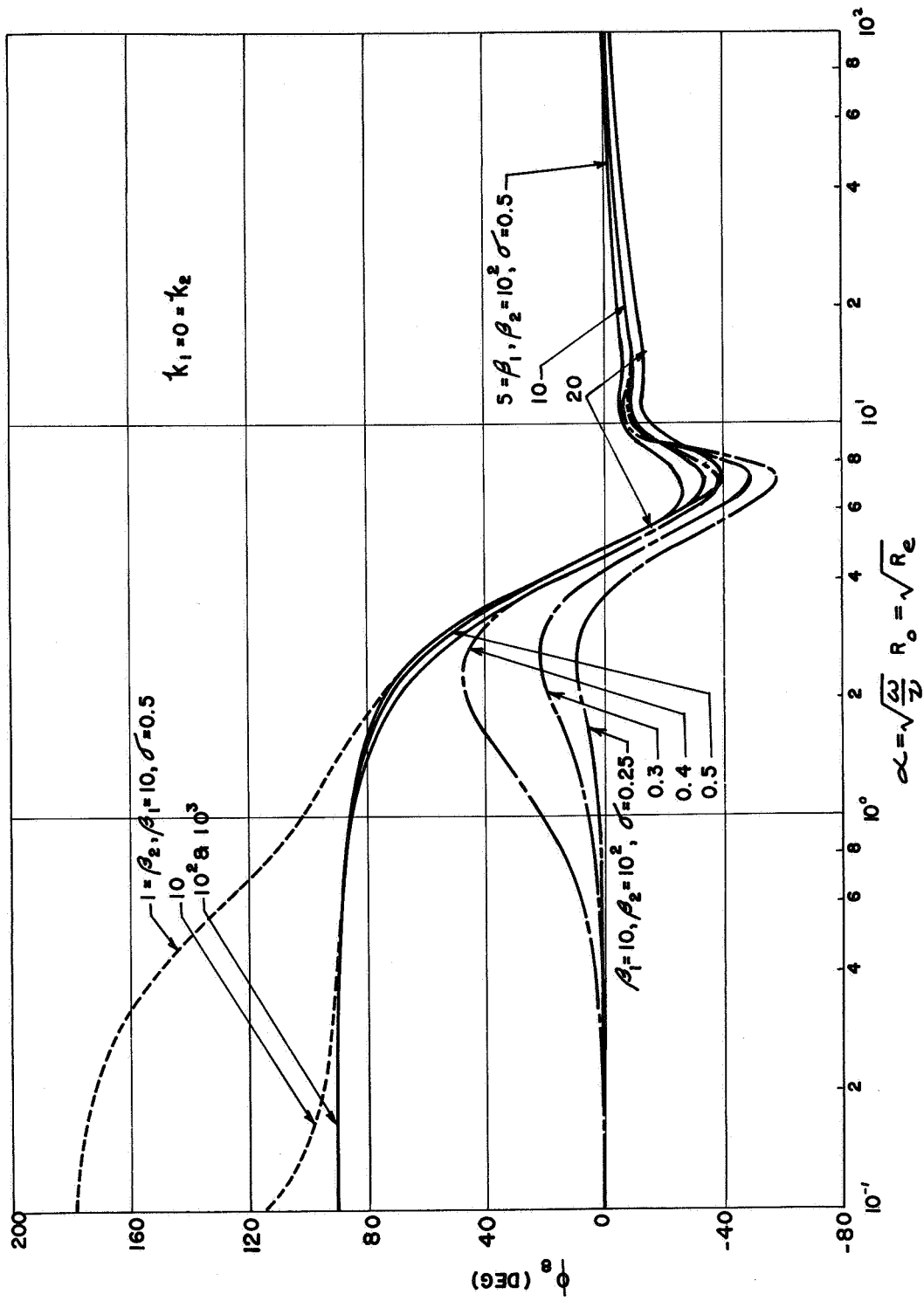
109
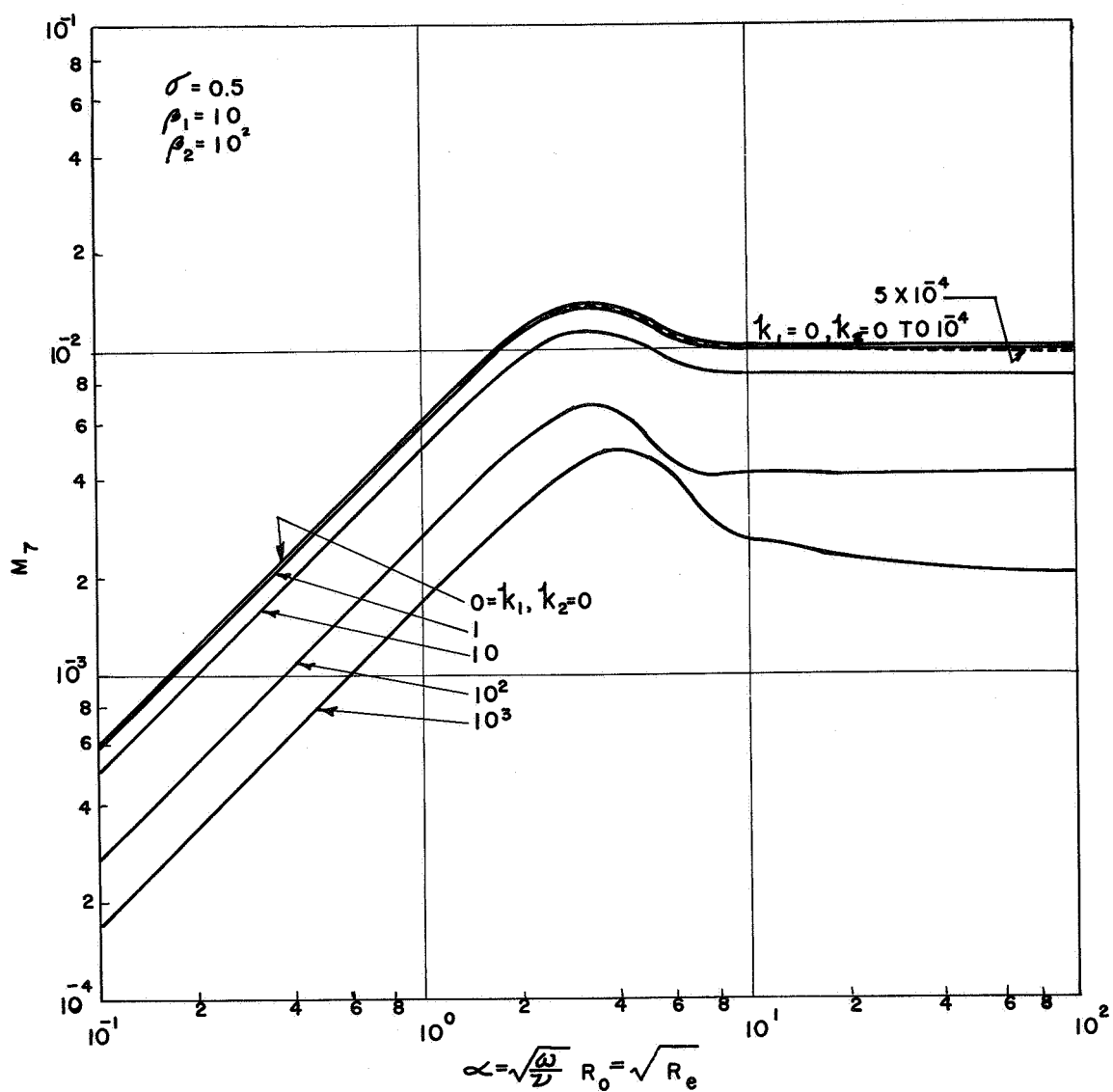
Figure 36. The Mode Shape Parameter for Axial Fluid Velocity on the Axis with the First Type of Waves as a Function of Reynolds Number
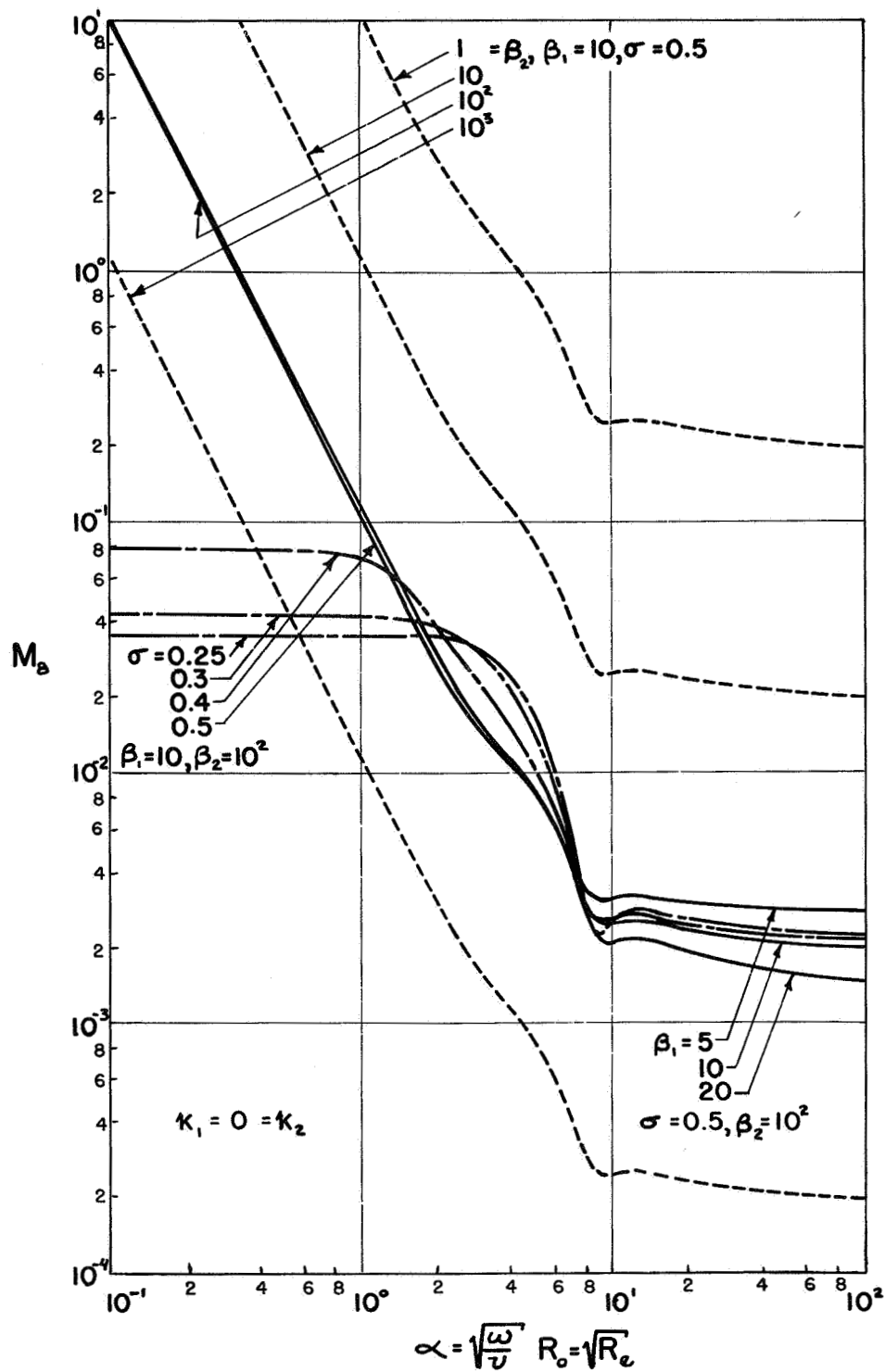
Figure 37. The Mode Shape Parameters for Axial Fluid Velocity on the Axis with the Second Type of Waves as a Function of Reynolds Number
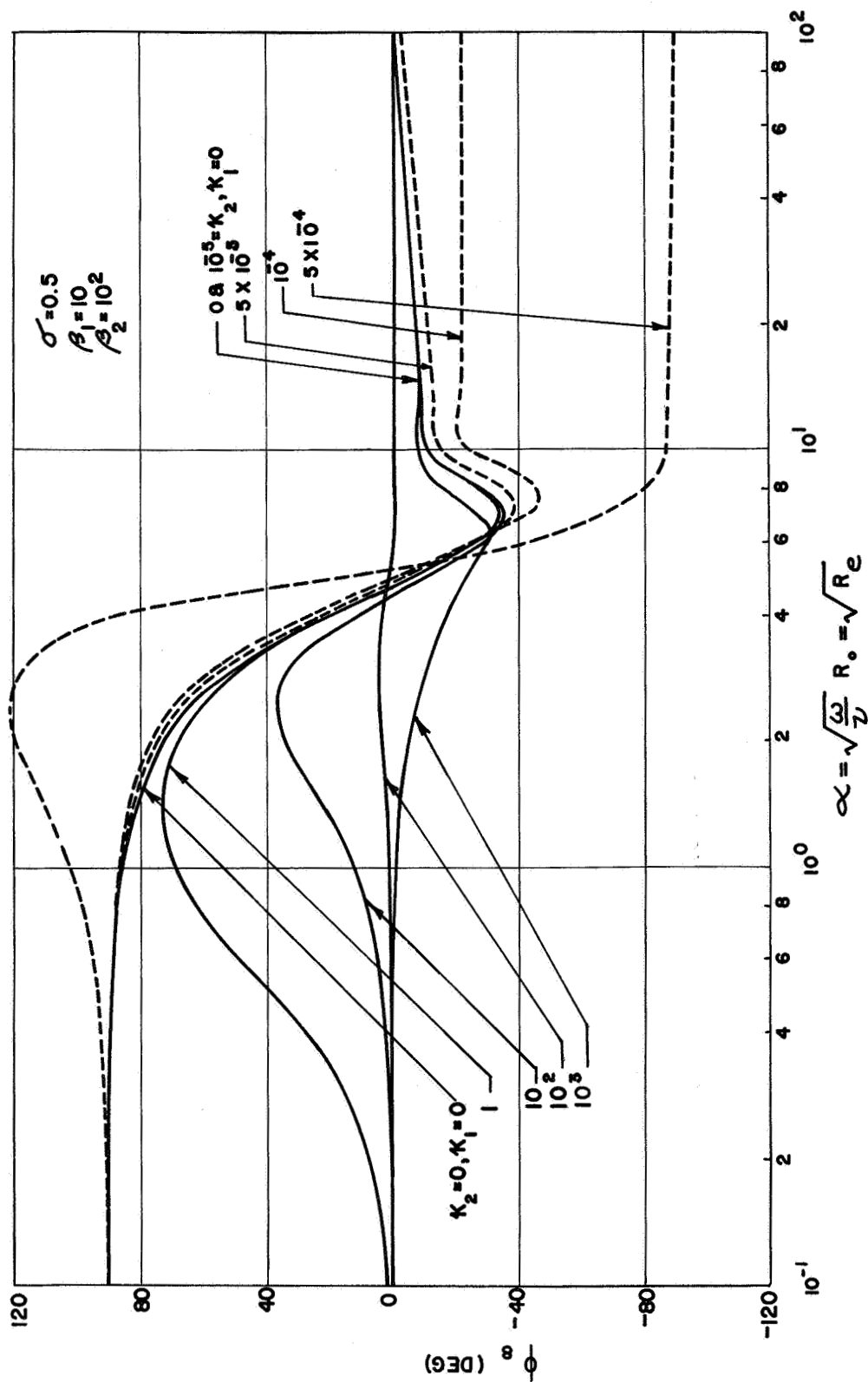
111
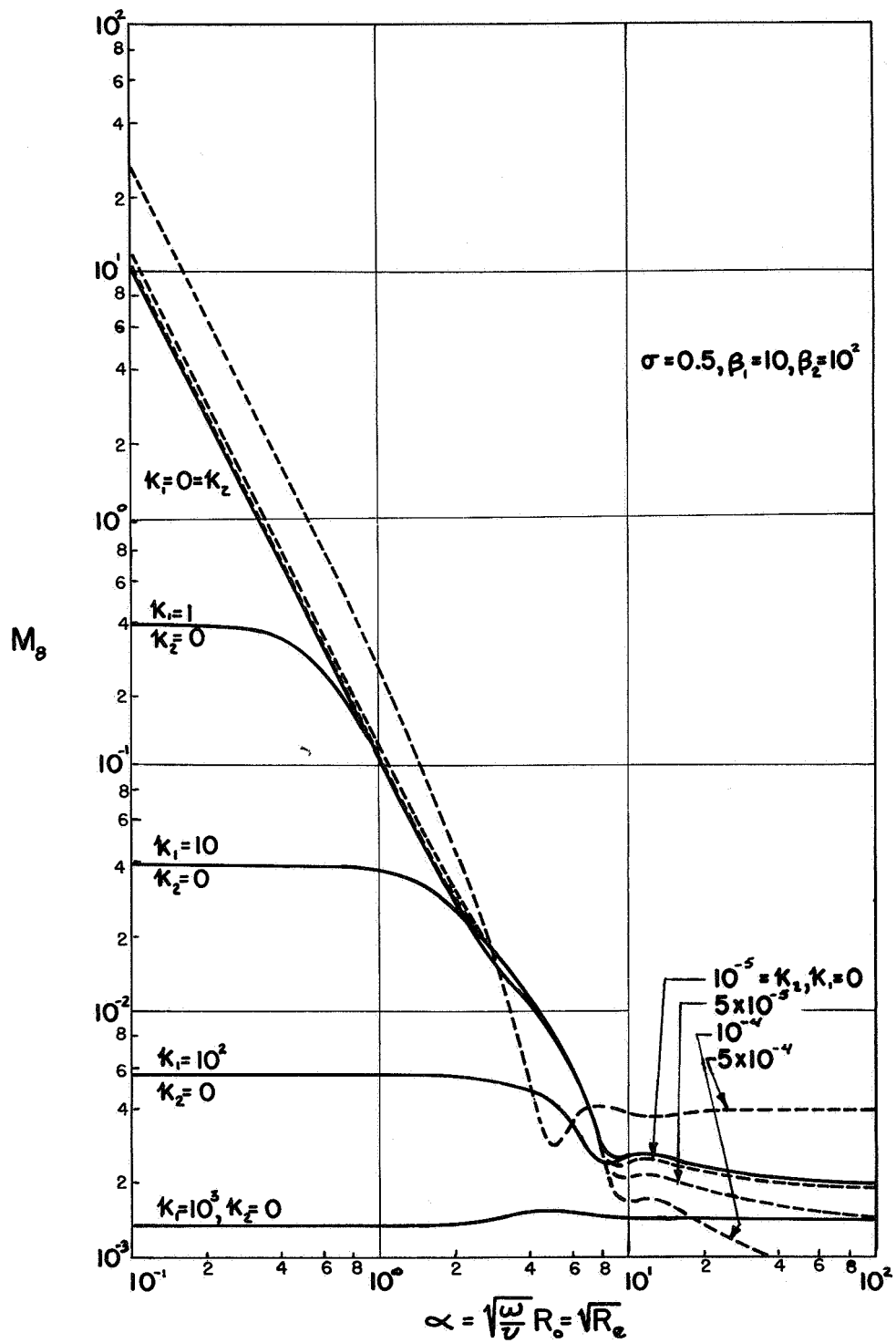
Figure 38. The Mode Shape Parameters for Axial Fluid Velocity on the Axis with the Second Type of Waves as a Function of Reynolds Number

112
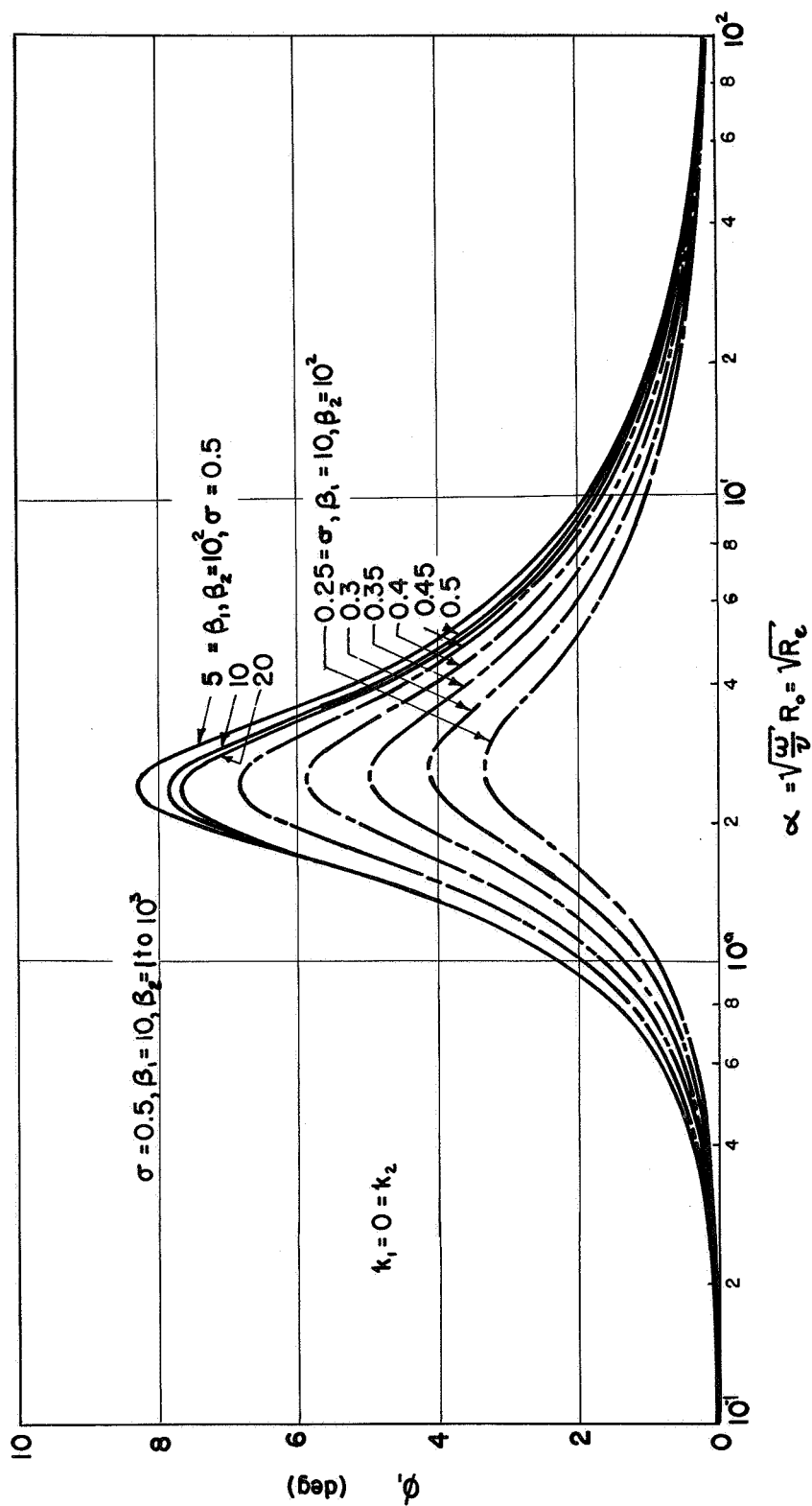
Figure 39. The Phase Angle for Radial Displacement of the First Type of Waves as a Function of Reynolds Number
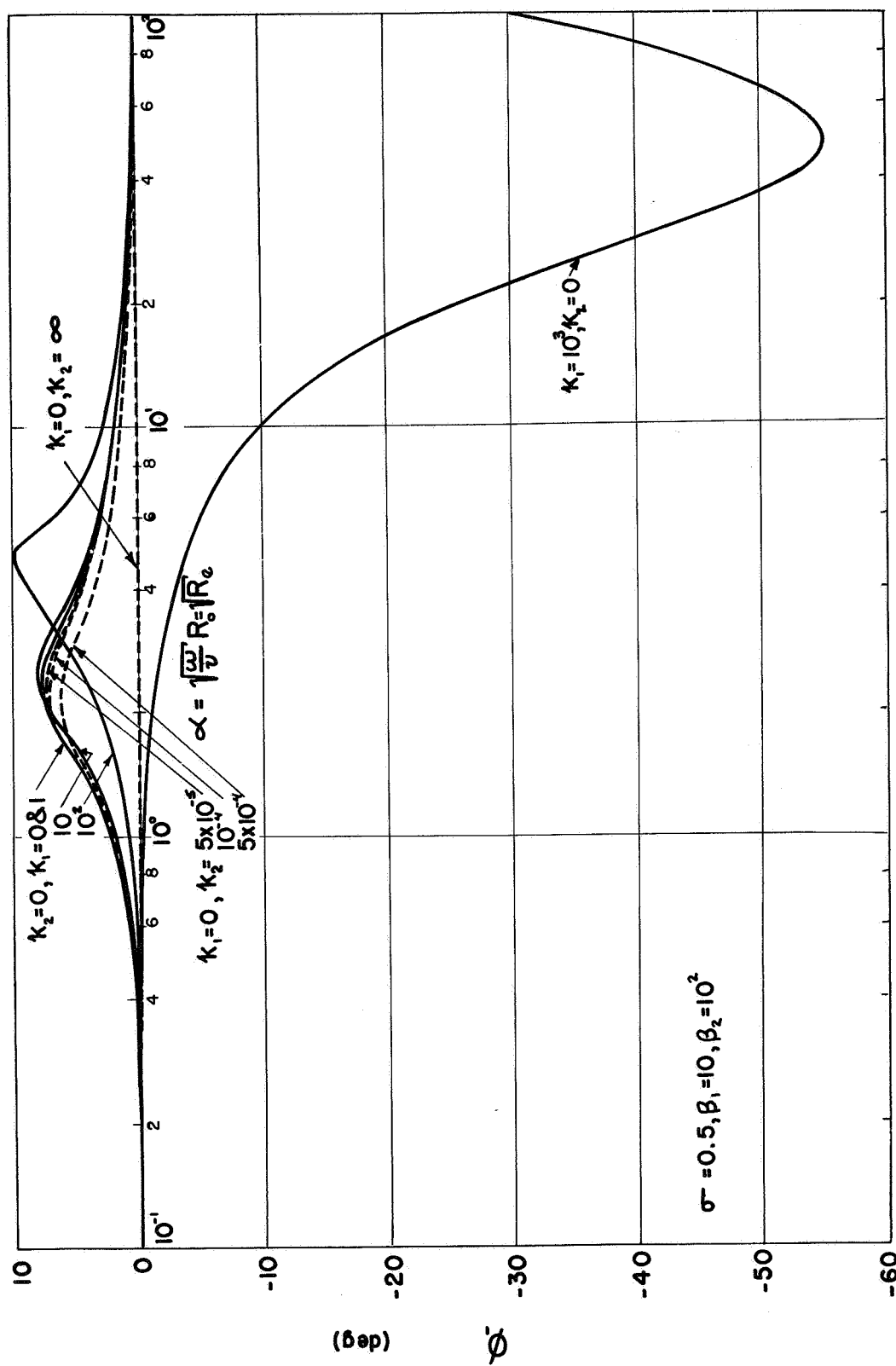
Figure 40. The Phase Angle for Radial Displacement of the First Type of Waves as a Function of Reynolds Number
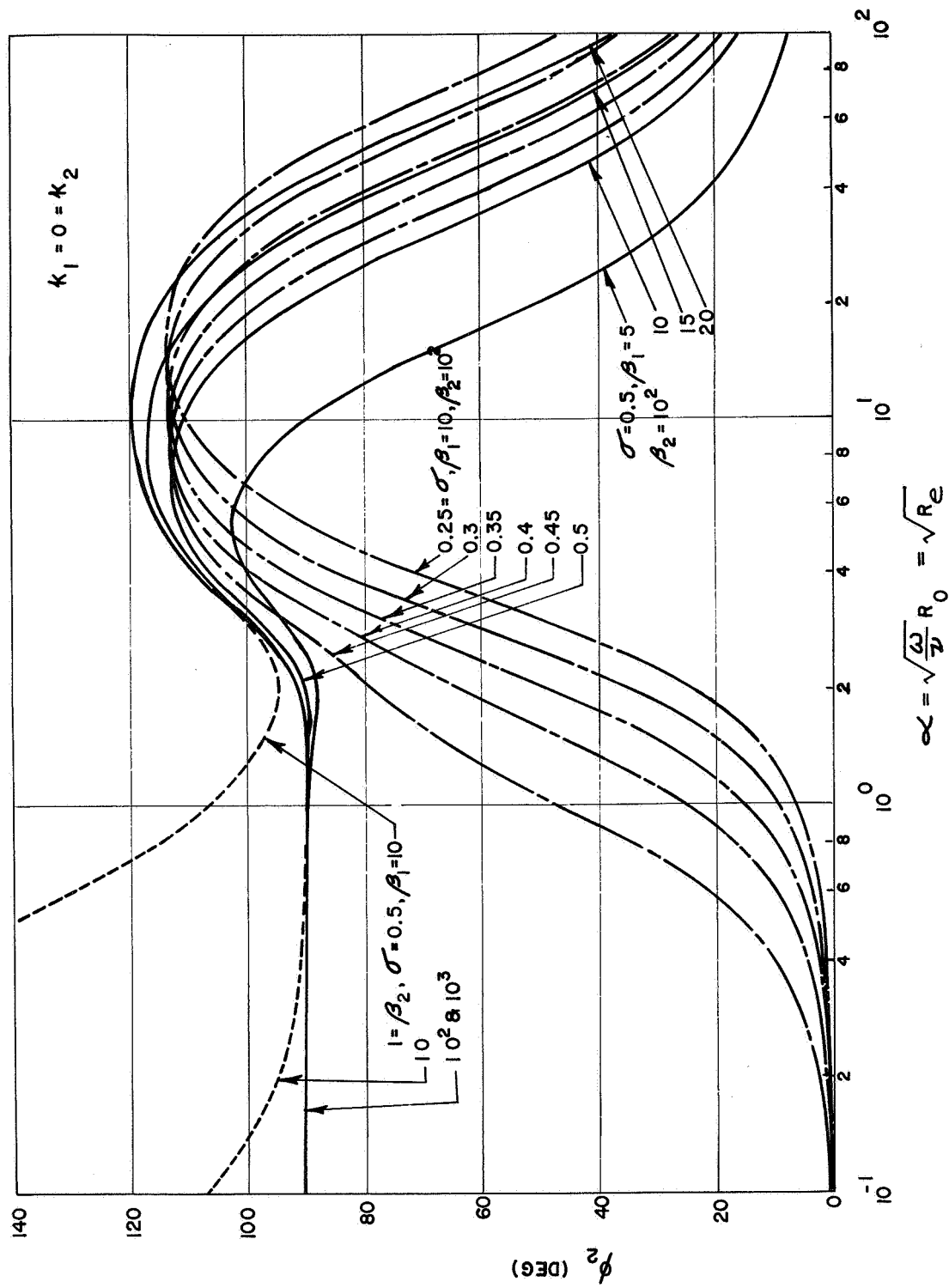
Figure 41. The Phase Angle for Radial Displacement of the Second Type of Waves as a Function of Reynolds Number

115

Figure 42. The Phase Angle for Radial Displacement of the Second Type of Waves as a Function of Reynolds Number

116

Figure 43. The Phase Angle for Axial Displacement of the First Type of Waves as a Function of Reynolds Number

117
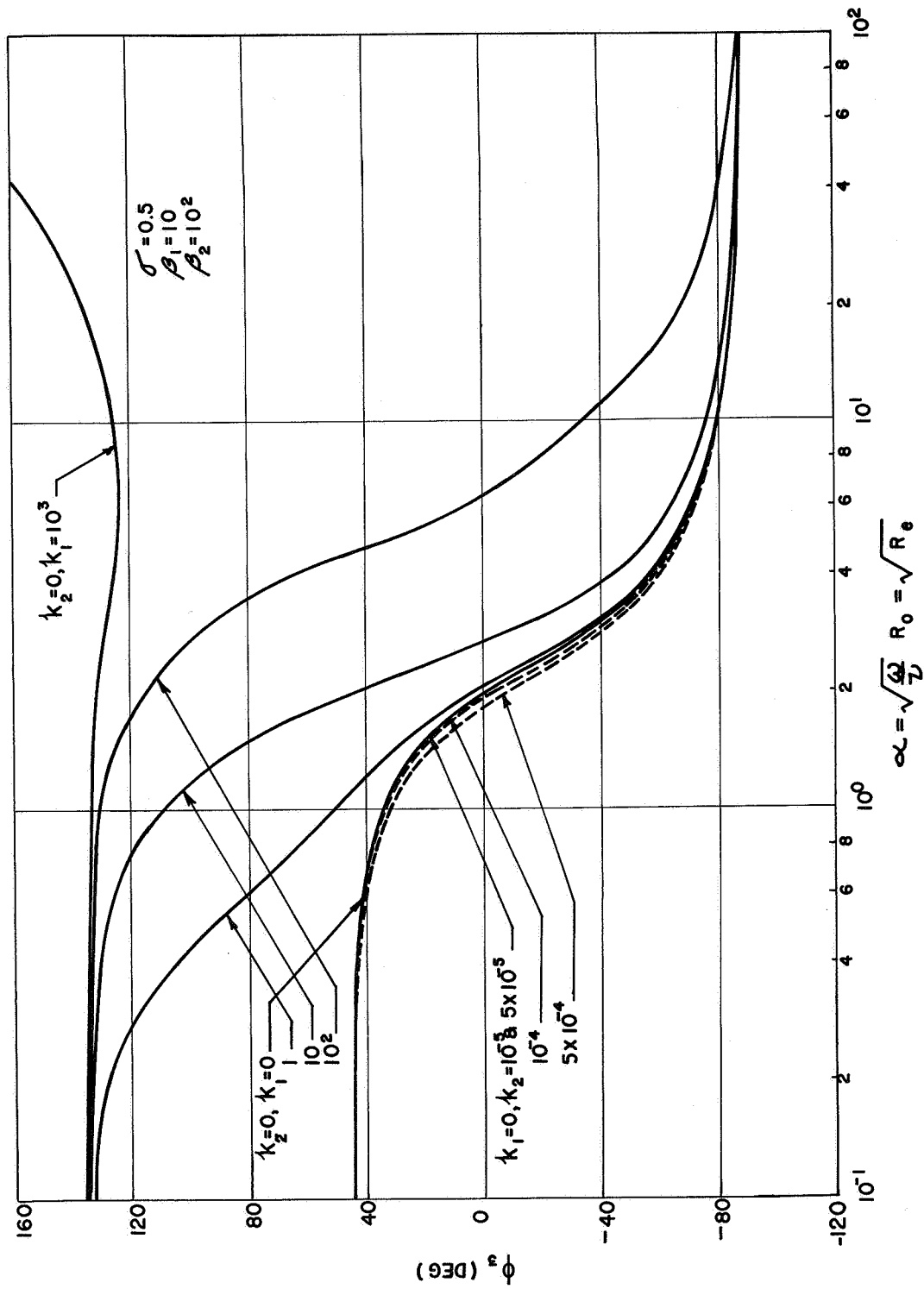
Figure 44. The Phase Angle for Axial Displacement of the First Type of Waves as a Function of Reynolds Number

118
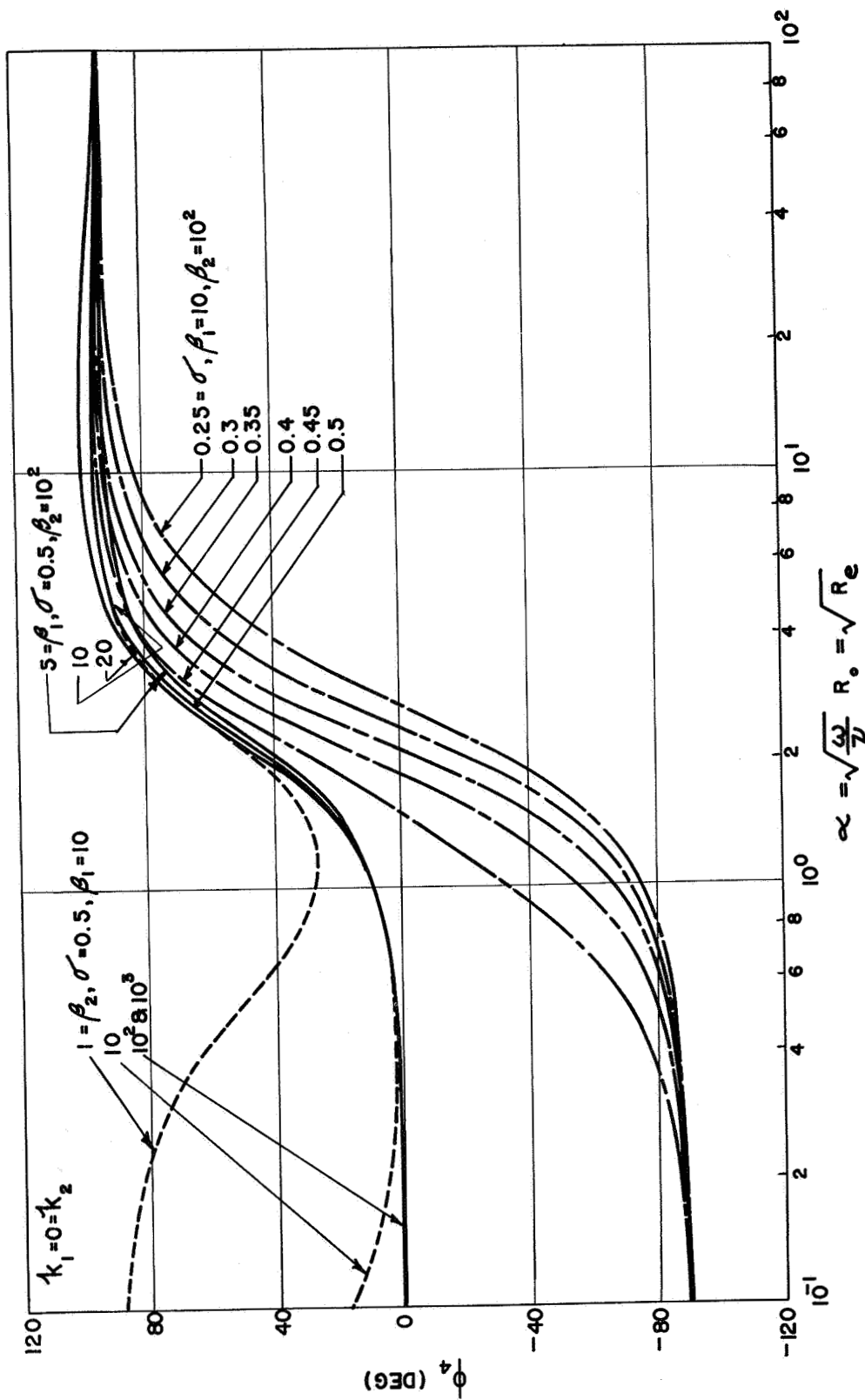
Figure 45.   The Phase Angle for Axial Displacement of the Second Type of Waves as a Function of Reynolds Number

119
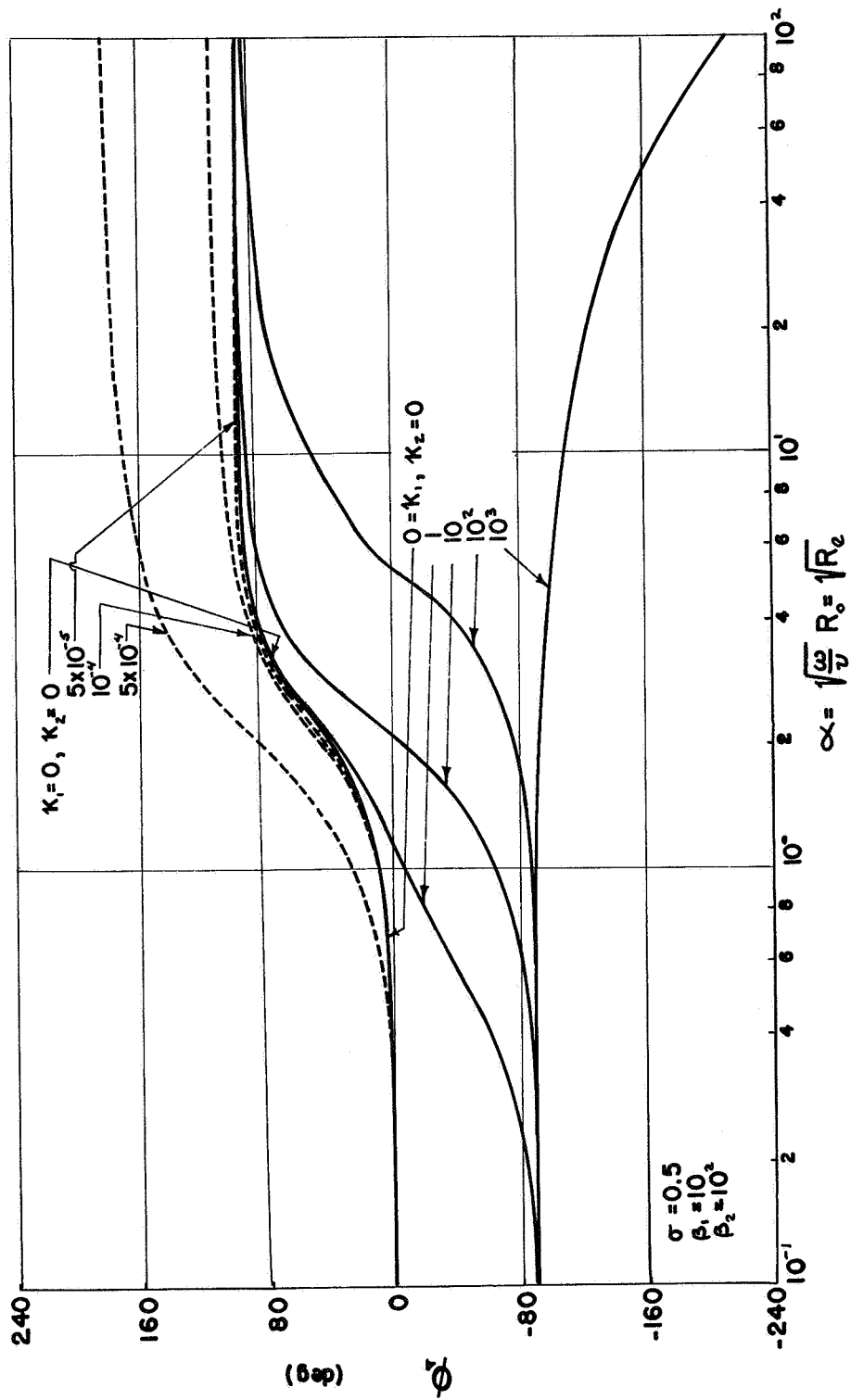
Figure 46. The Phase Angle for Axial Displacement of the Second Type of Waves as a Function of Reynolds Number

120
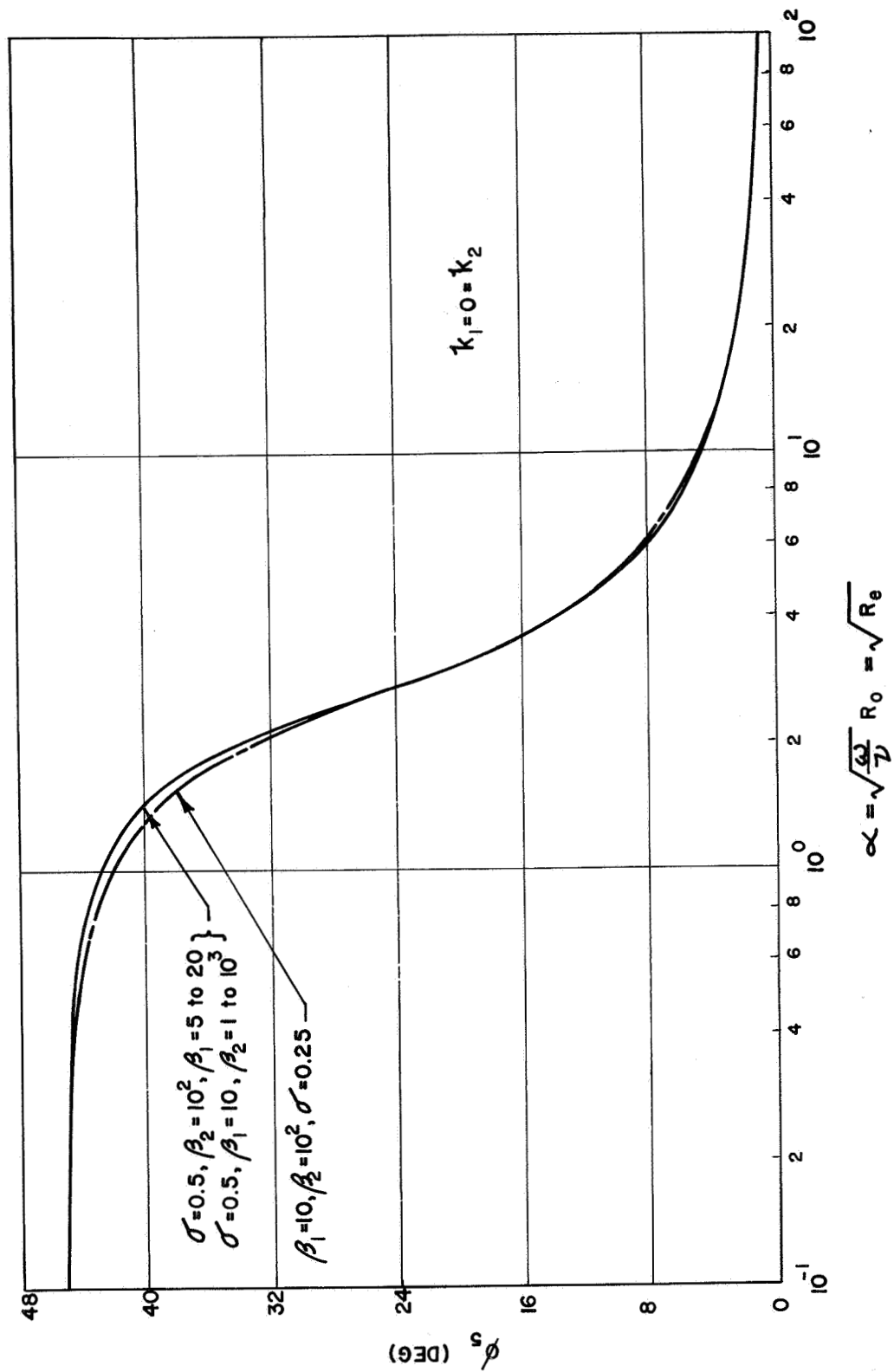
Figure 47.   The Phase Angle for Fluid Mass Flow Rate of the First Type of Waves as a Function of Reynolds Number

121
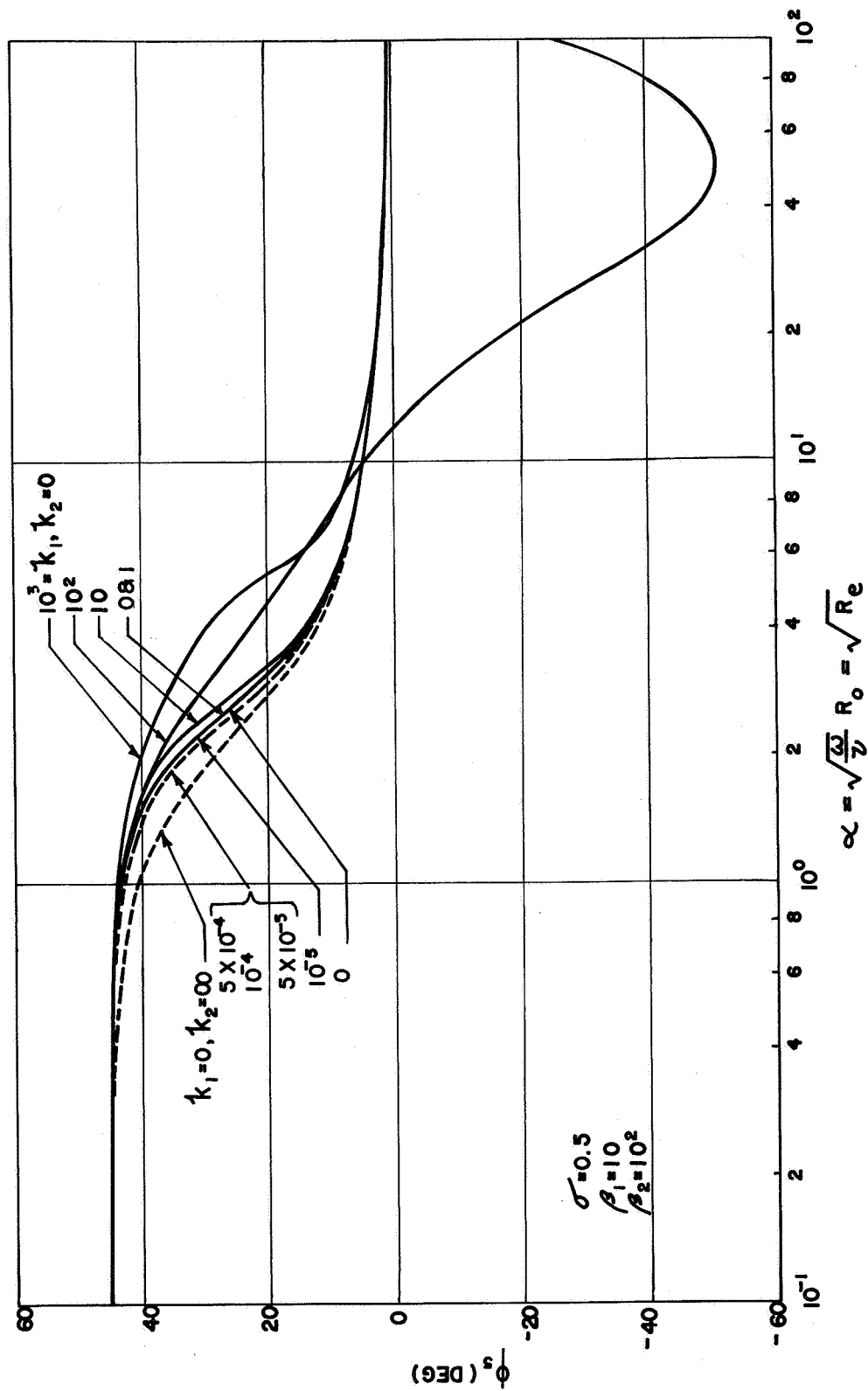
Figure 48. The Phase Angle for Fluid Mass Flow Rate of the First Type of Waves as a Function of Reynolds Number

122
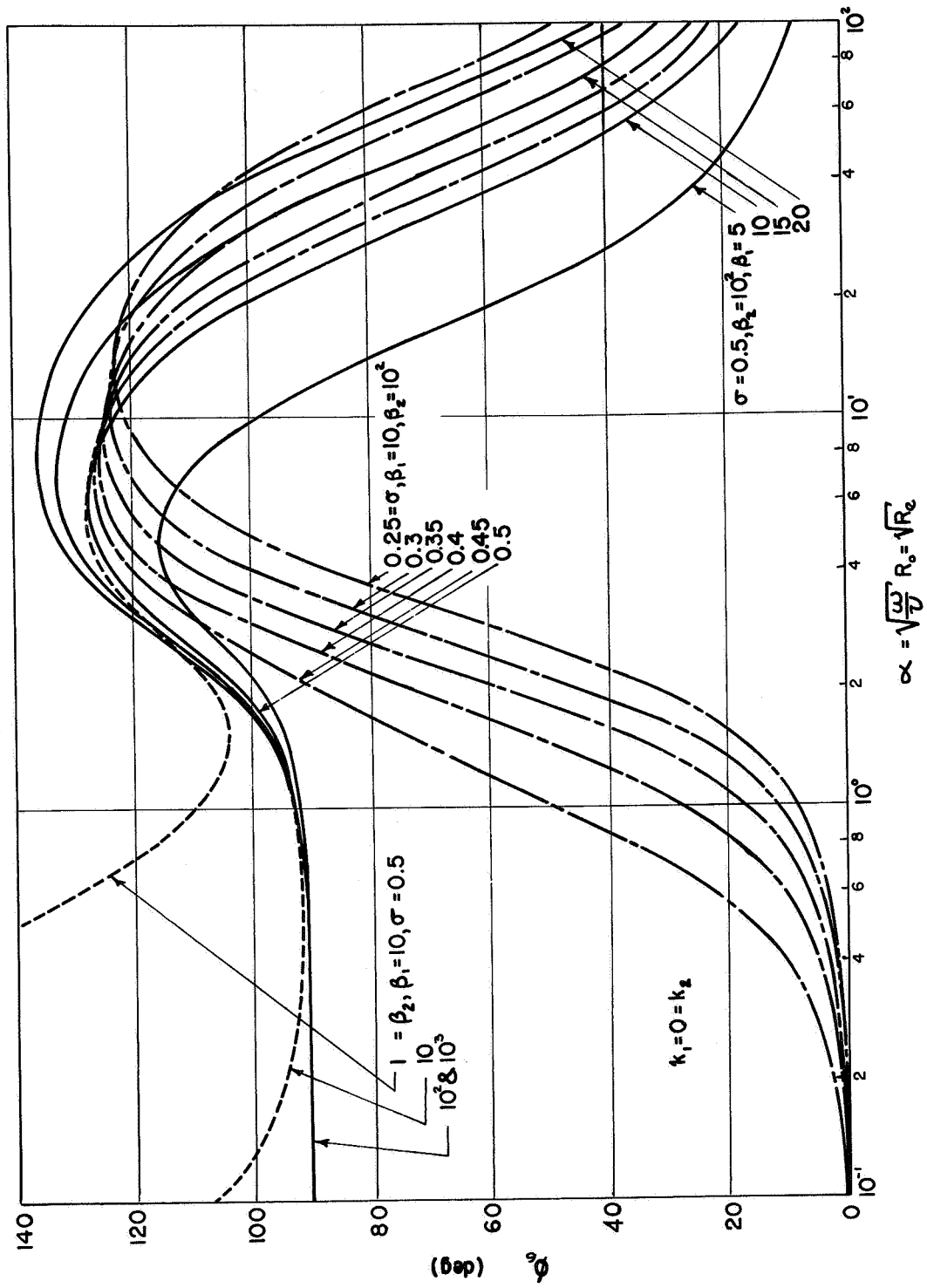
Figure 49. The Phase Angle for Fluid Mass Flow Rate of the Second Type of Waves as a Function of Reynolds Number

123
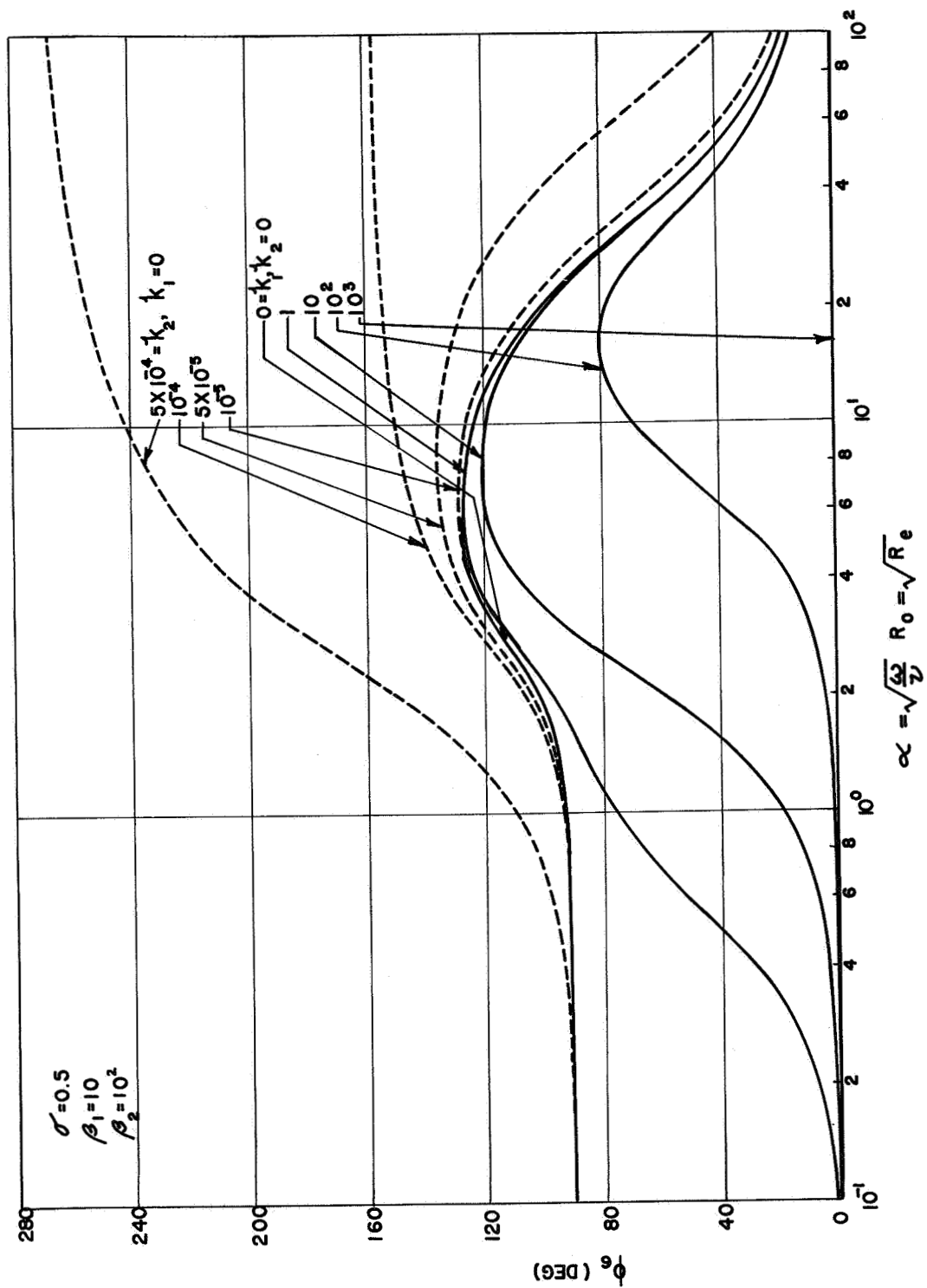
Figure 50. The Phase Angle for Fluid Mass Flow Rate of the Second Type of Waves as a Function of Reynolds Number

124
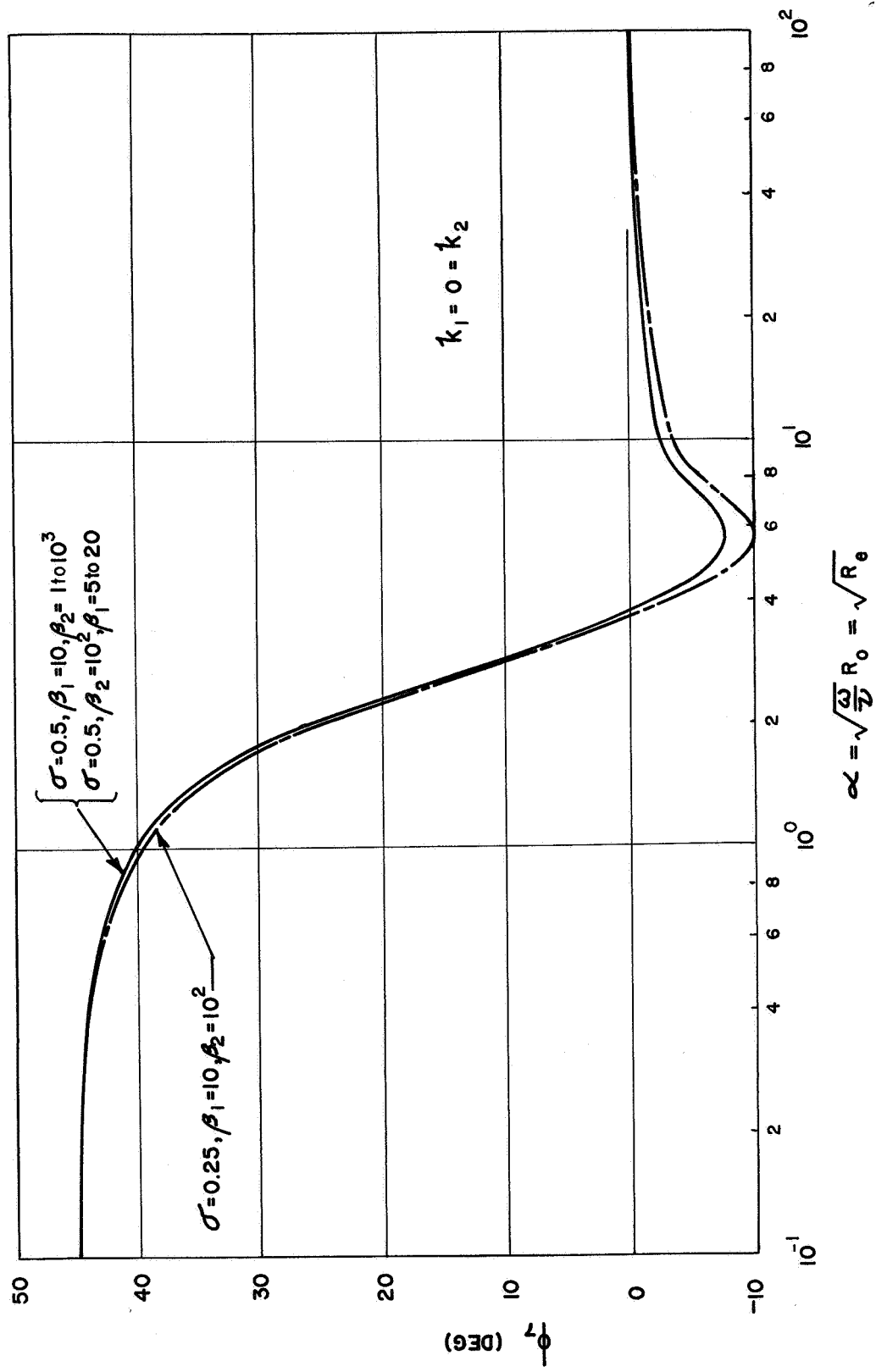
Figure 51. The Phase Angle for Axial Fluid Velocity on the Axis with the First Type of Waves as a Function of Reynolds Number

Figure 52. The Phase Angle for Axial Fluid Velocity on the Axis with the First Type of Waves as a Function of Reynolds Number

Figure 53. The Phase Angle for Axial Fluid Velocity on the Axis with the Second Type of Waves as a Function of Reynolds Number

127

Figure 54. The Phase Angle for Axial Fluid Velocity on the Axis with the Second Type of Waves as a Function of Reynolds Number
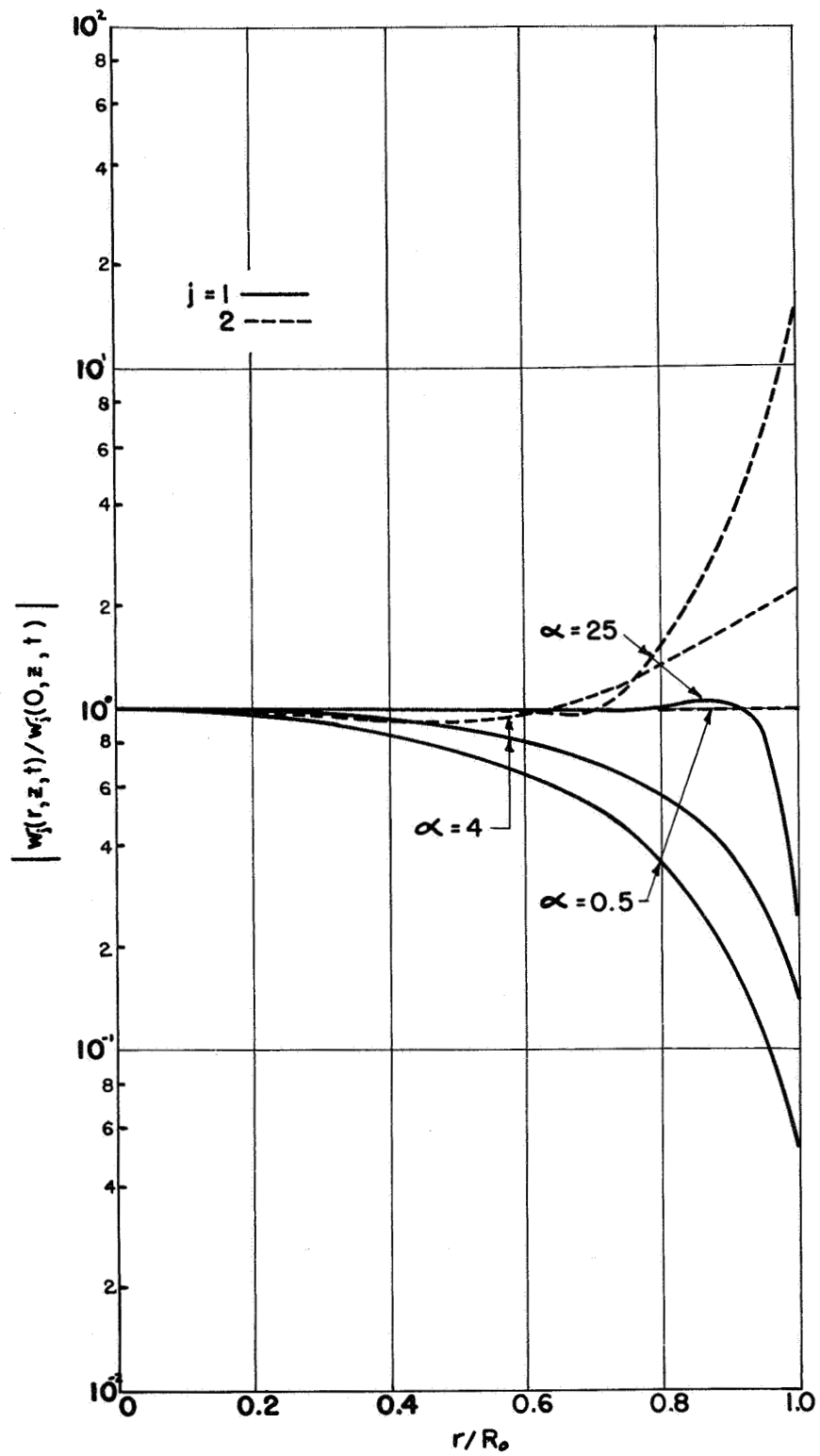
Figure 55. Radial Distribution of the Magnitude of the Axial Velocity

129
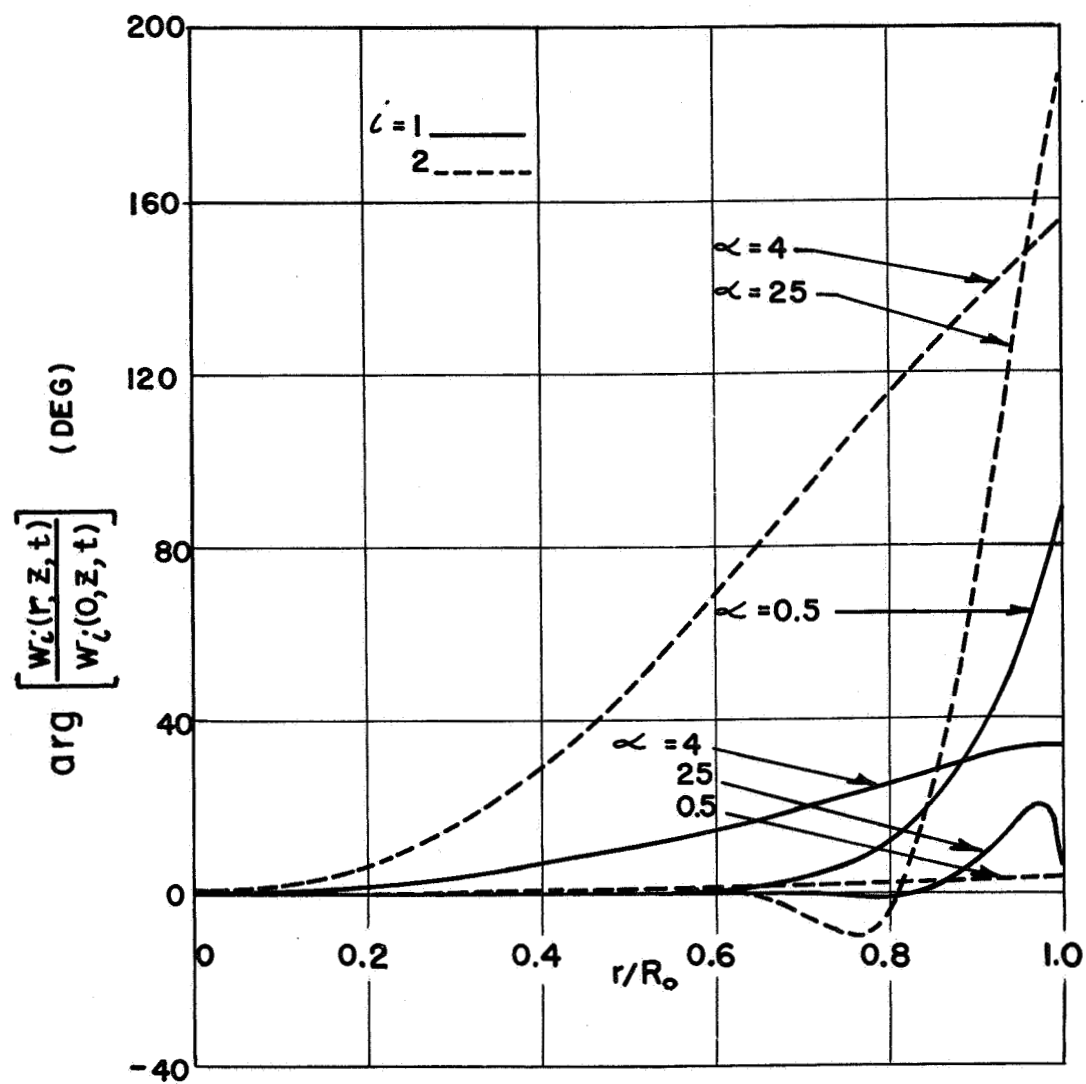
Figure 56. Radial Distribution of the Phase of the Axial Velocity
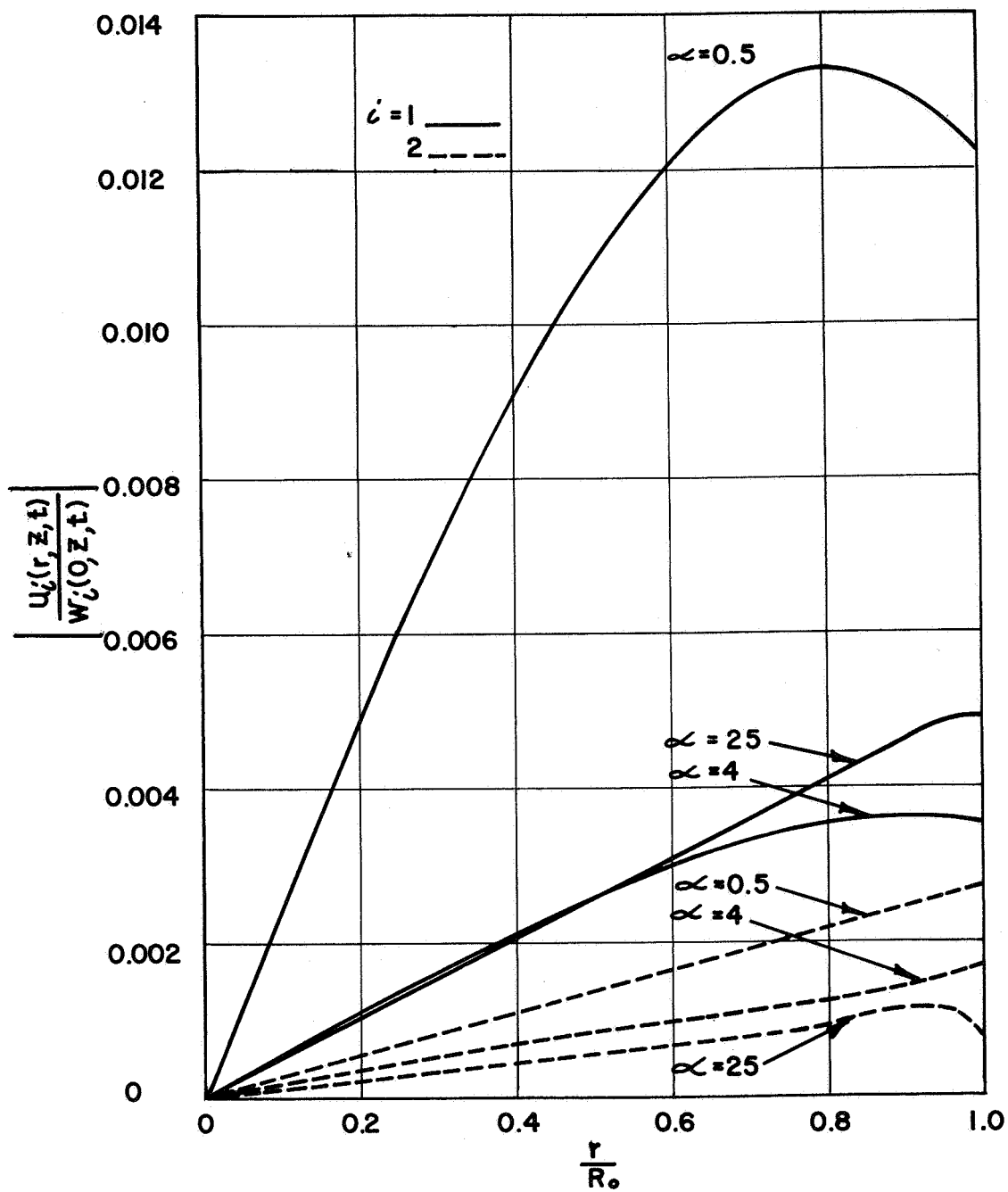
Figure 57. Radial Distribution of the Magnitude of the Radial Velocity

131
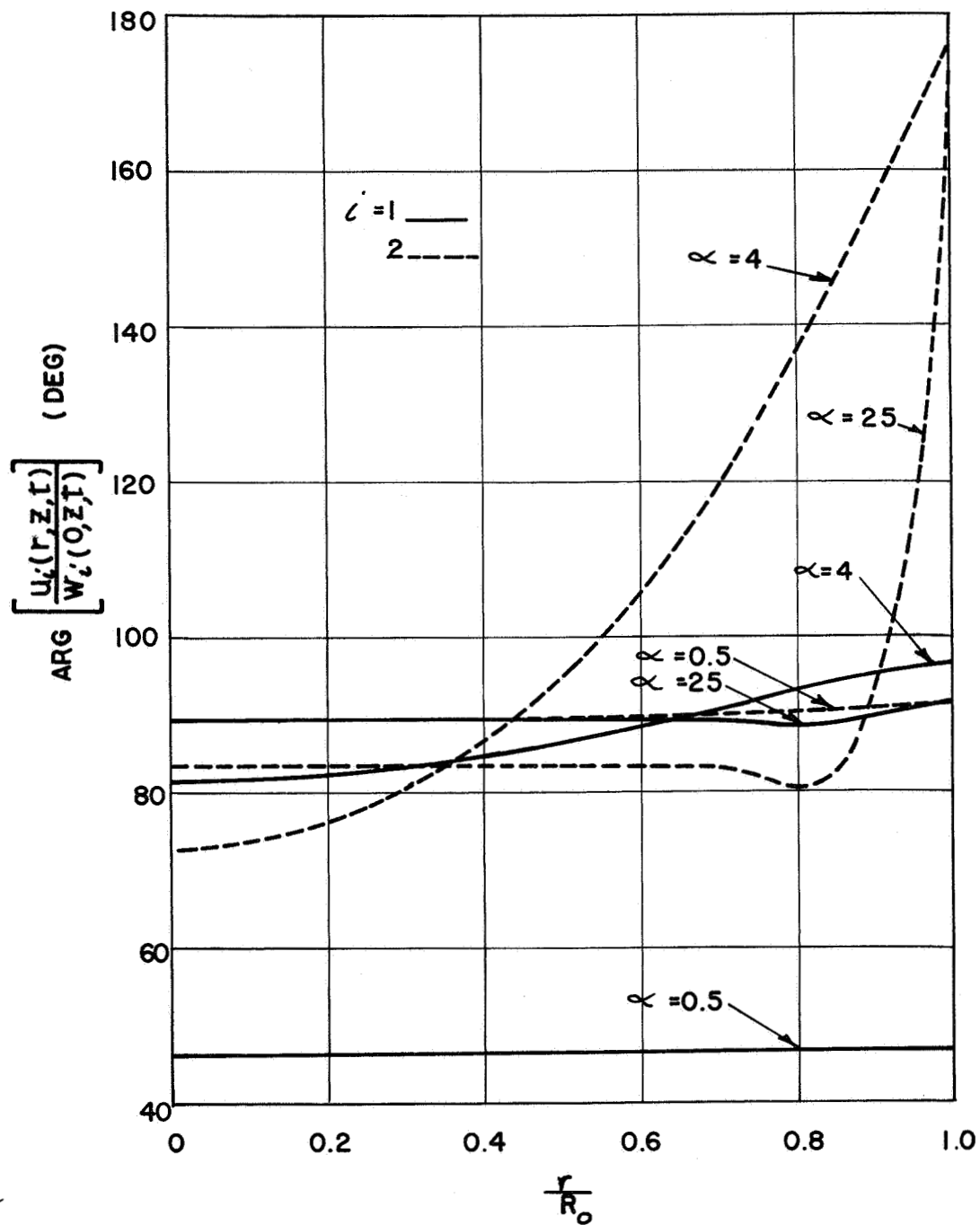
Figure 58. Radial Distribution of the Phase of the Radial Velocity

132
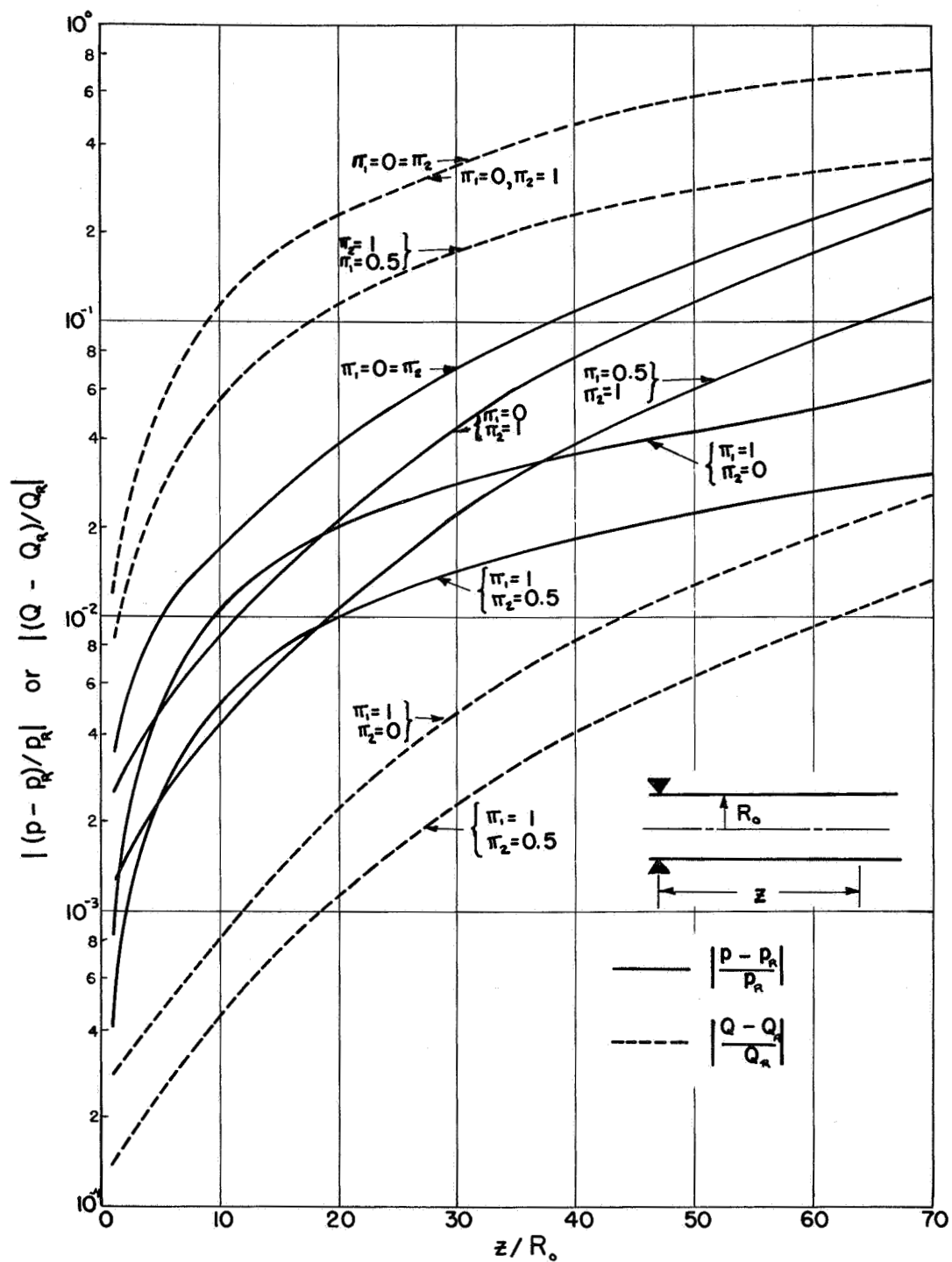
Figure 59. Magnitude of Relative Errors in Pressure and Fluid Mass Flow for Sample Calculation 2
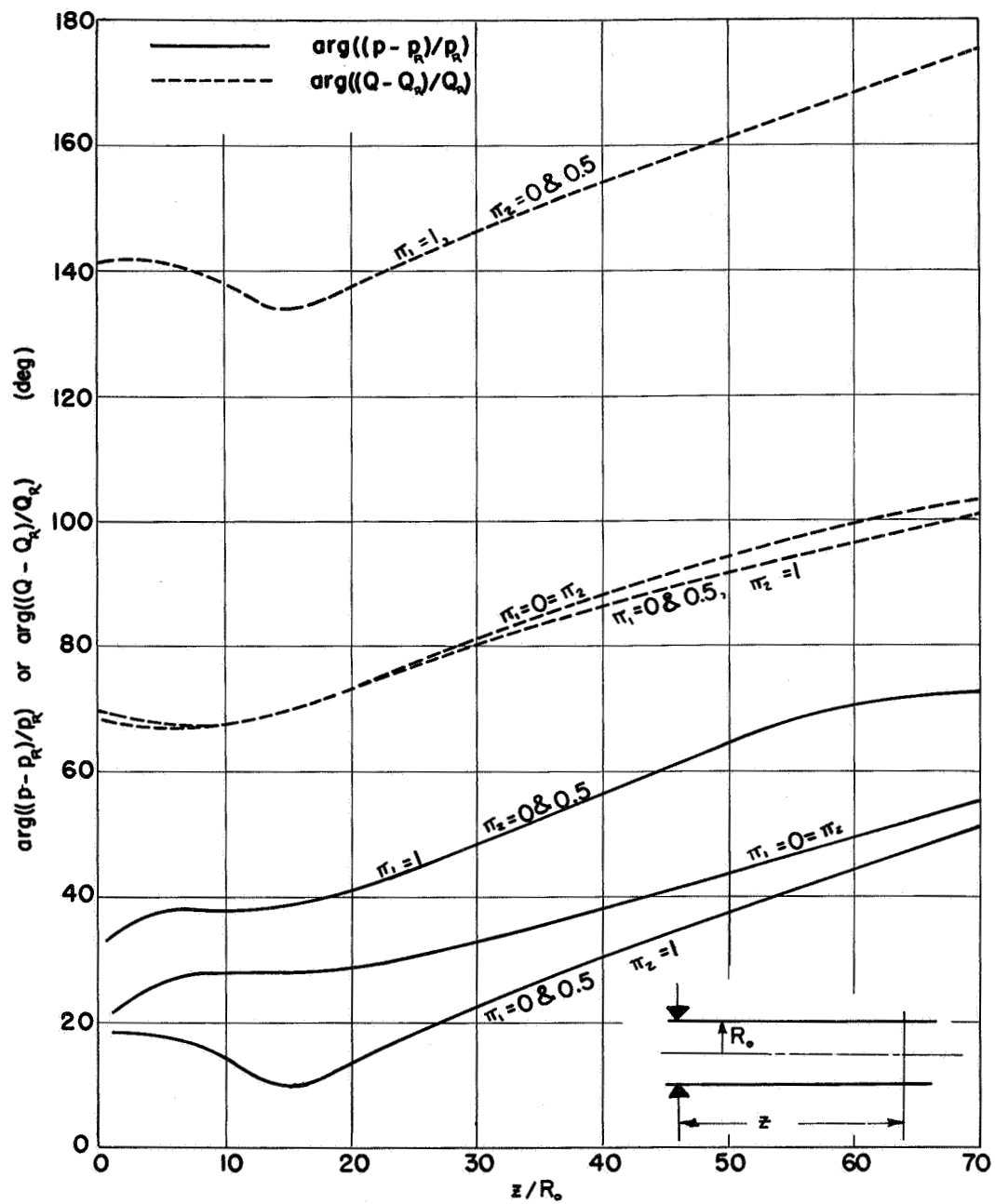
Figure 60. Phase of Relative Errors in Pressure and Fluid Mass Flow for Sample Calculation 2

134
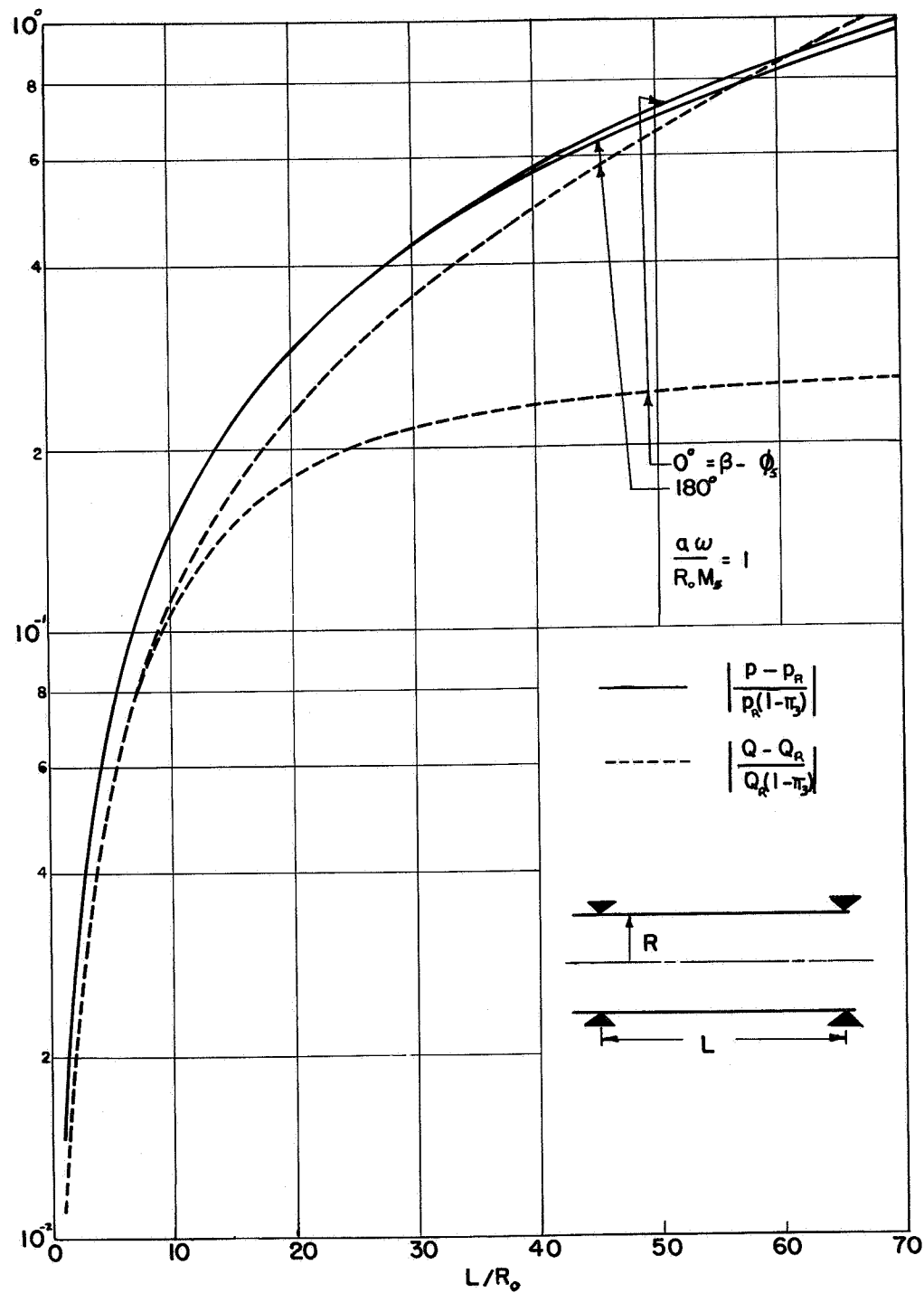
Figure 61. Magnitude of Relative Errors in Pressure and Fluid Mass Flow for Sample Calculation 3
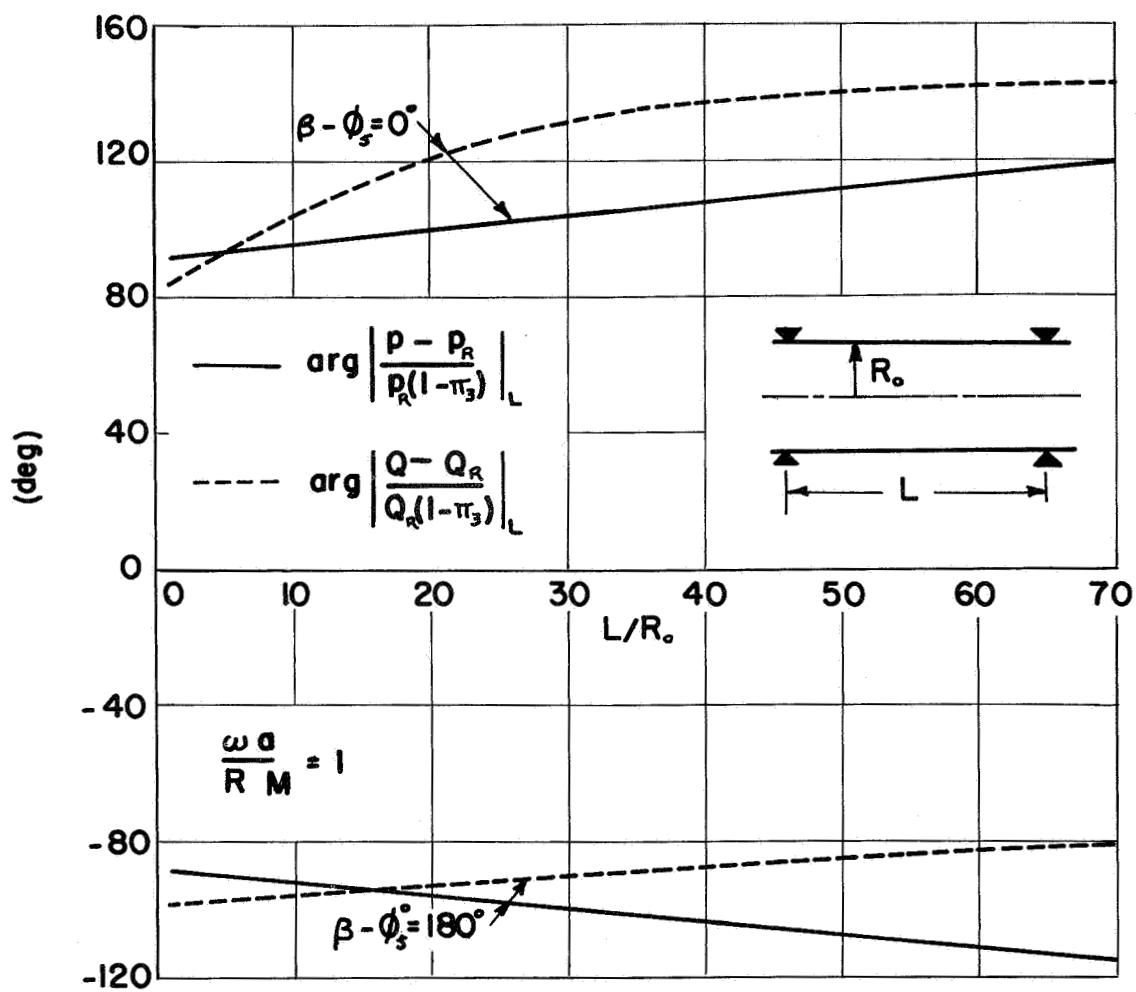
Figure 62. Phase of Relative Errors in Pressure and Fluid Mass Flow for Sample Calculation 3
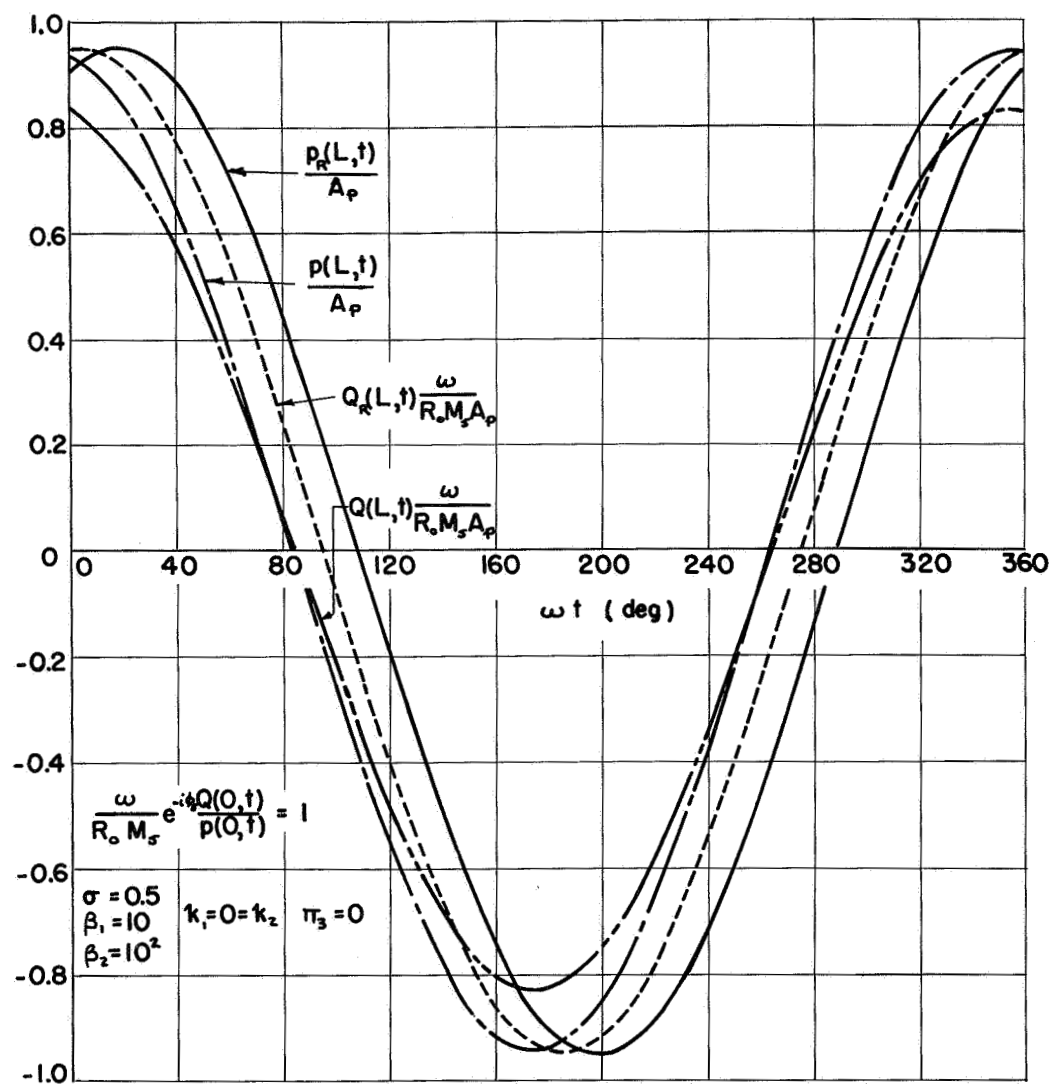
Figure 63. Variation of Pressure and Fluid Mass Flow for Sample Calculation 3

137
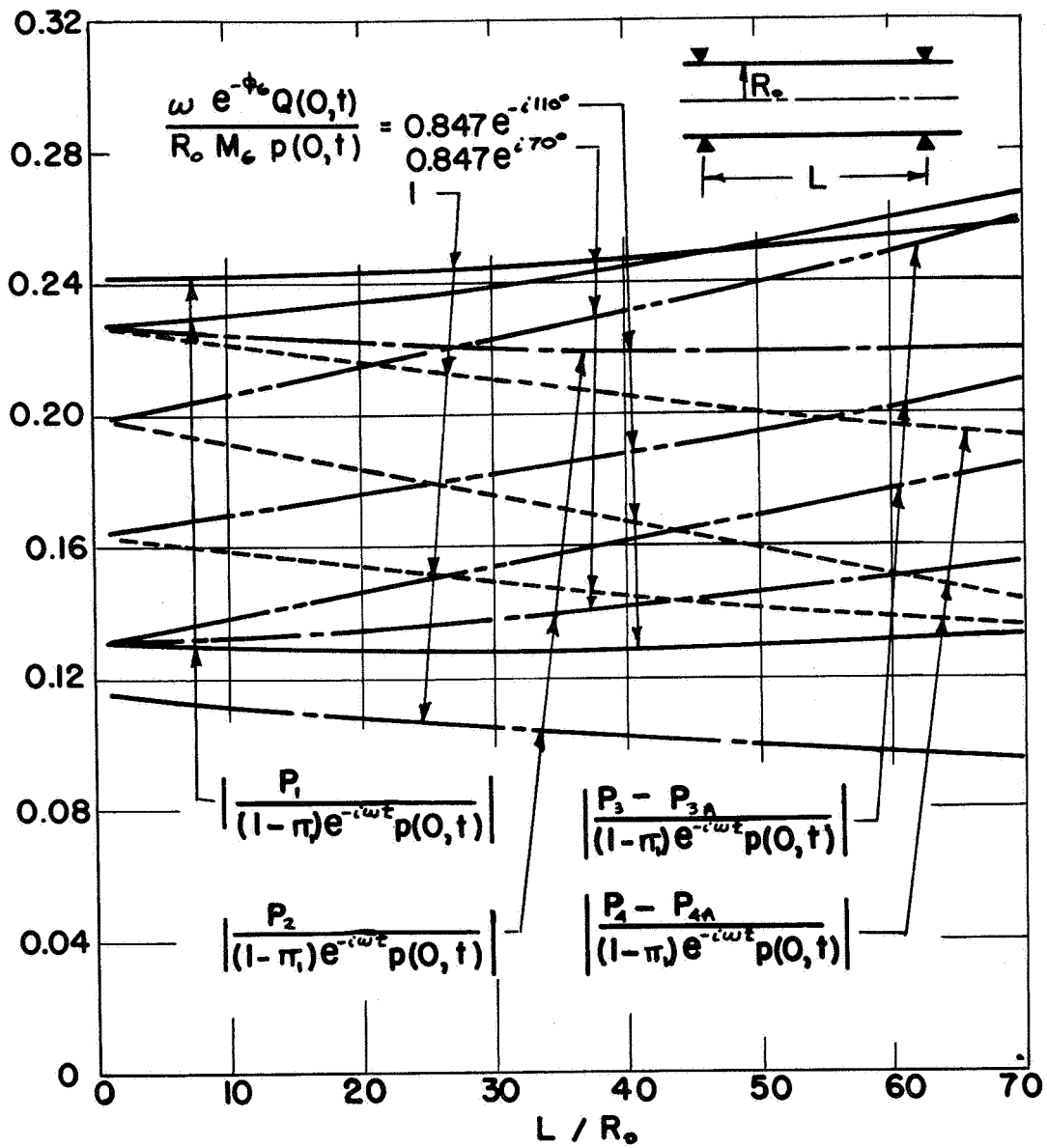
Figure 64. Magnitude of the Relative Error in Arbitrary Coefficients for Sample Calculation 4
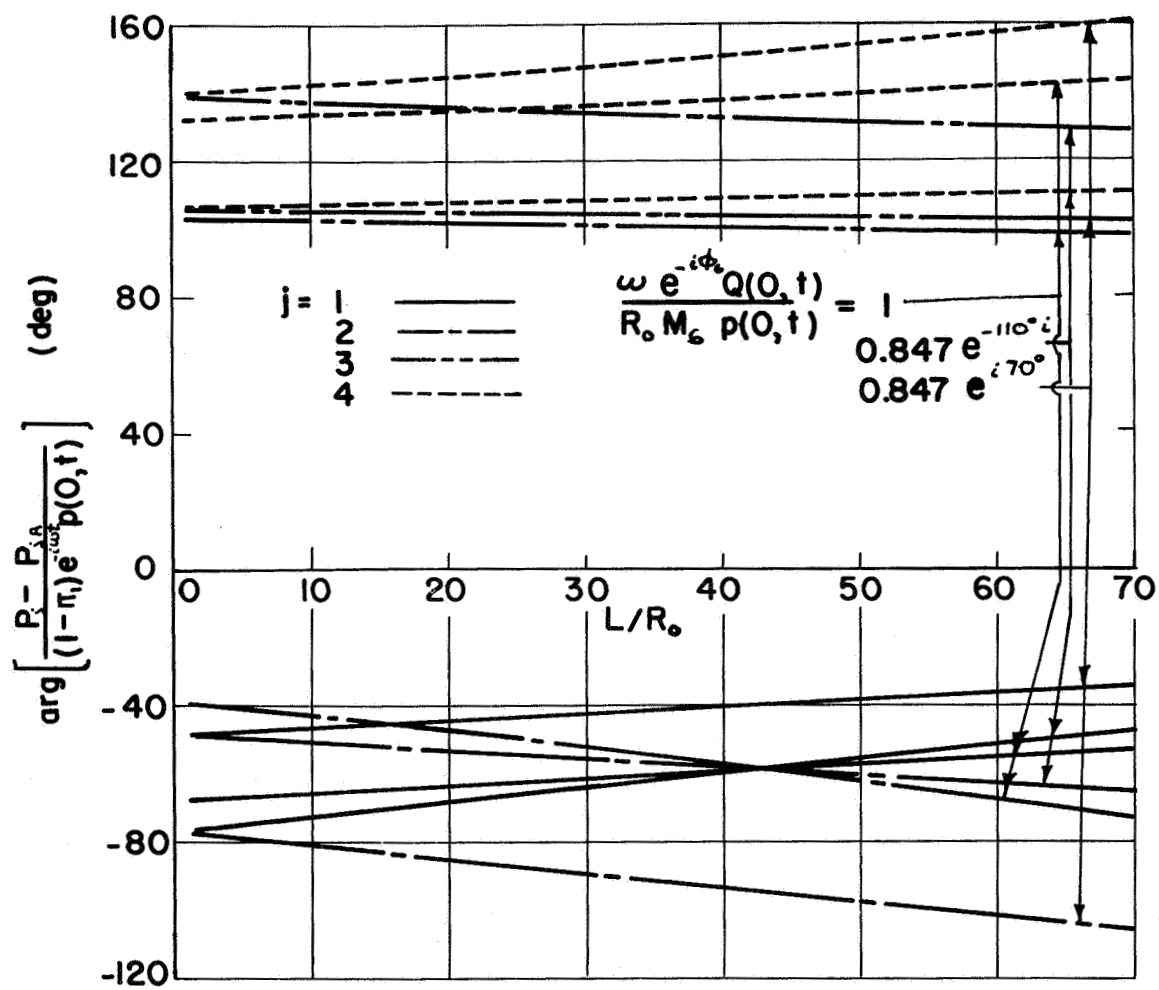
Figure 65. Phase of the Relative Error in Arbitrary Coefficients for Sample
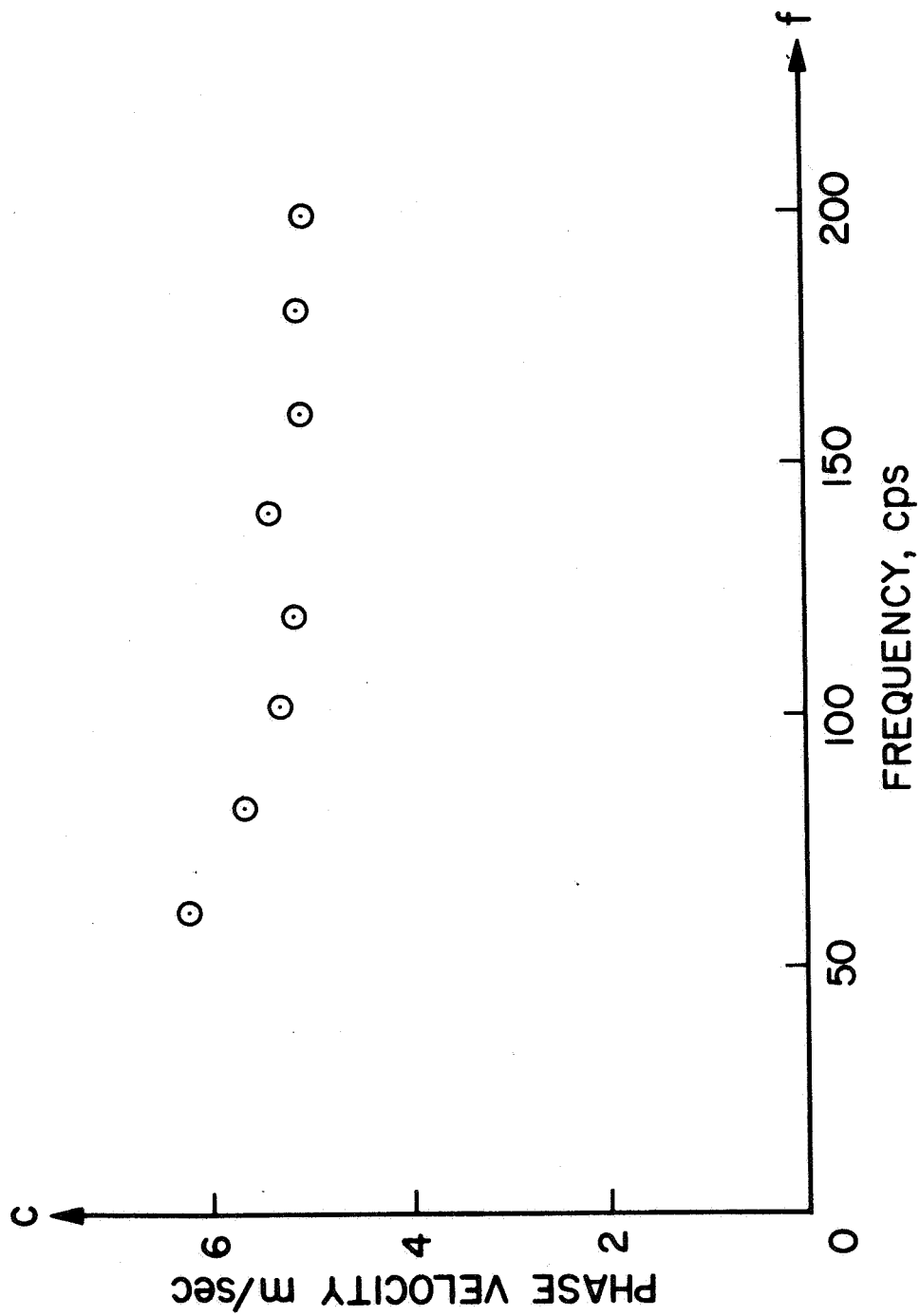Calculation 4

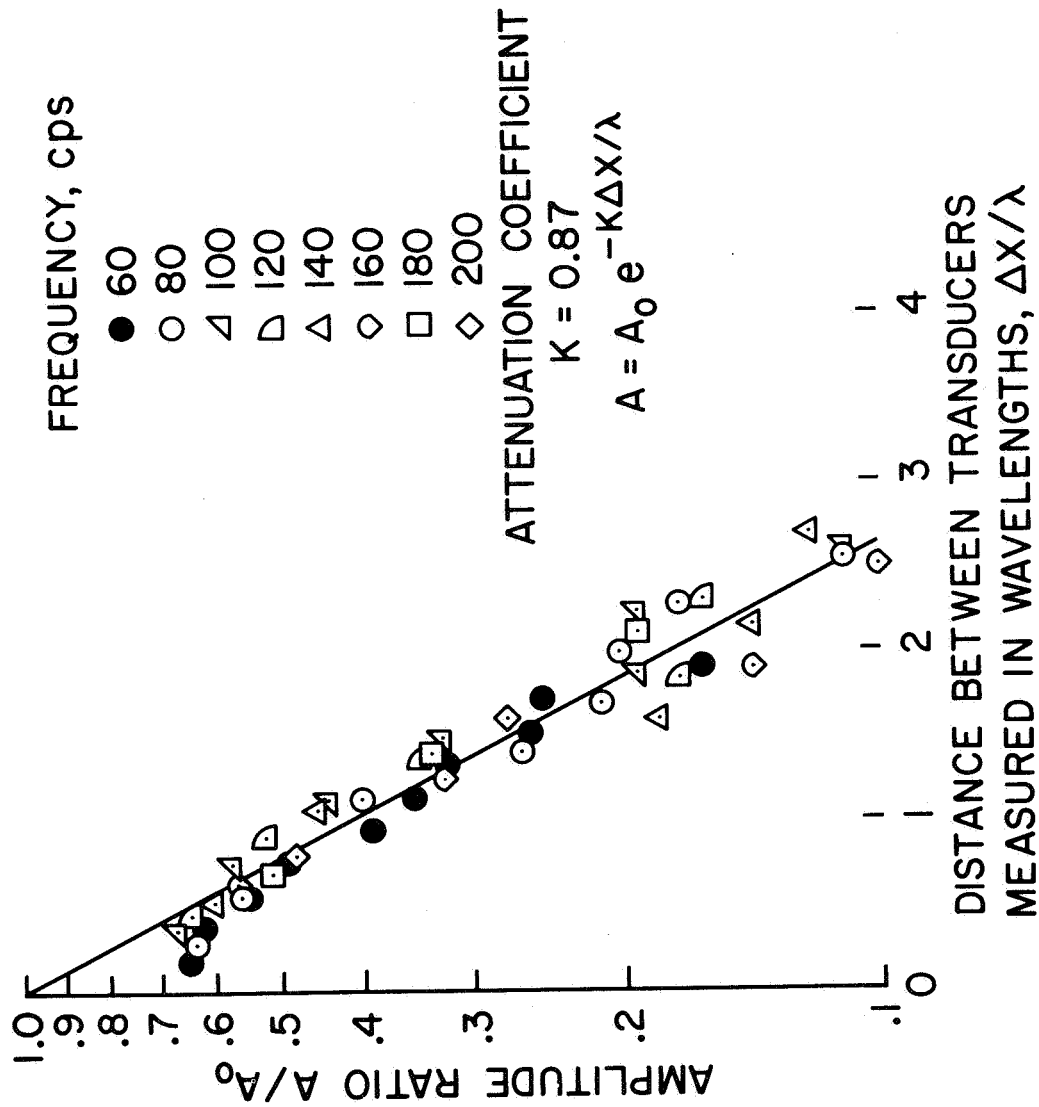Figure 66. Dispersion in a Dog's Aorta from Data of Reference 13

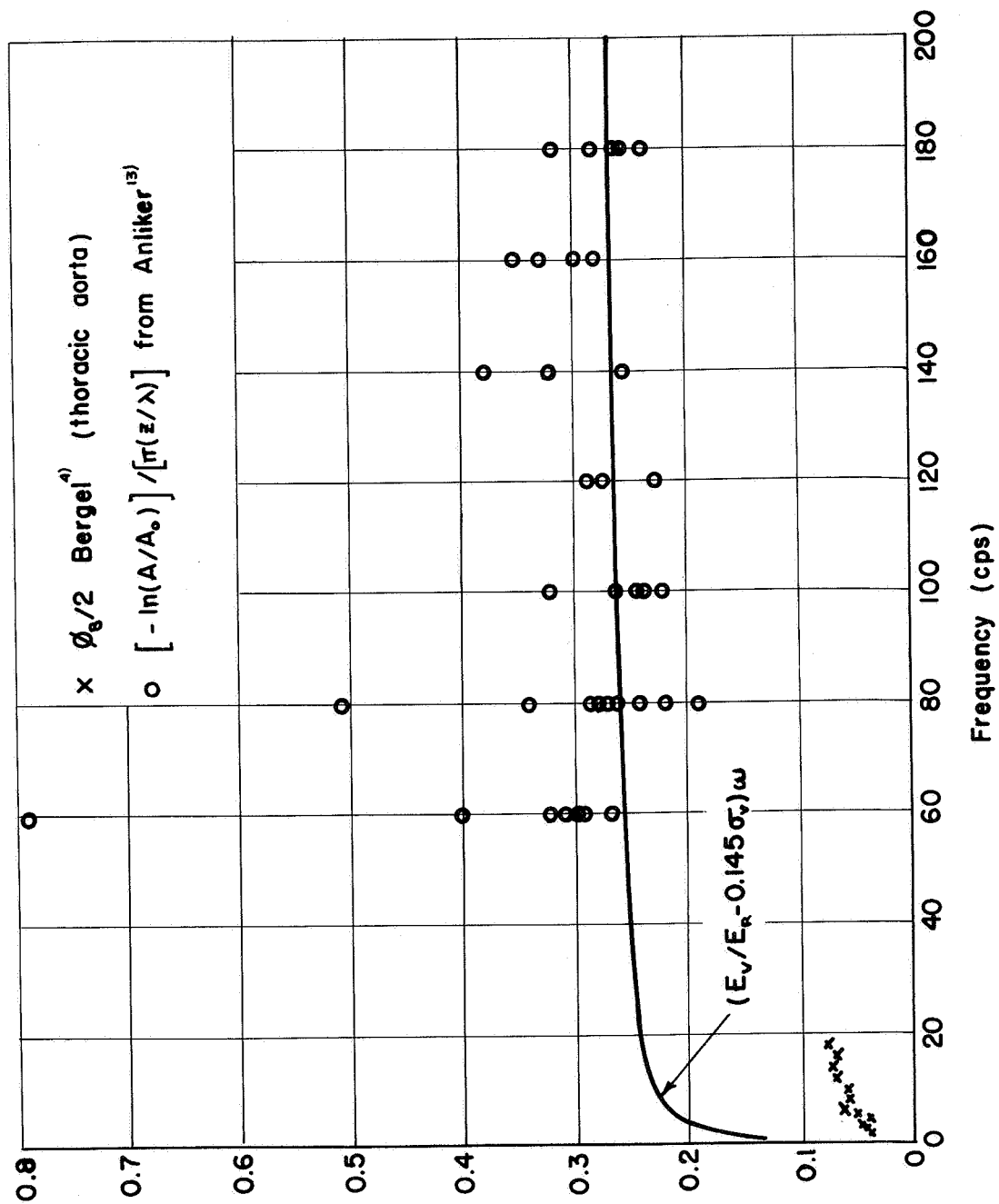Figure 67. Dissipation in a Dog's Aorta from Data of Reference 13

Figure 68. A Viscoelastic Parameter from Data of Reference 13